The Role of Neutralizing Antibodies in HIV-1 infection

David George Bonsall

Imperial College London

Jefferiss Trust Laboratory

Department of Medicine

Thesis submitted for the degree of Ph.D.

2011

The writer has recently (May, 1892) obtained experimental evidence that the blood of vaccinated, and consequently immune, calves contains something which neutralizes the specific virulence of vaccine virus, both bovine and humanized. Four drops of blood serum from a calf, which had been vaccinated two weeks previously, mixed with one drop of liquid lymph recently collected in a capillary tube, after contact for one hour, was used to vaccinate a calf; the same animal was also vaccinated with lymph, preserved on three quills, which was mixed with four drops of serum from the immune calf and left for one hour. The result of these vaccinations was entirely negative, while vaccinations upon the same calf, made with virus from the same source, and mixed with the same amount of blood serum from a non-immune calf, gave a completely successful and typical result.

George Miller Sternberg, 1862
Protective Inoculations in Infectious Diseases

The first recorded evidence for the virus-neutralizing component of serum that we now know to be antibodies.

Declaration

The work described herein is the work of the candidate except where clearly indicated. Cell lines, recombinant proteins and plasmids obtained from collaborators are indicated in Chapter 2, Materials and Methods.

The case study described in Chapter 4 was led by Professor Paul Klenerman (Nuffield Department of Clinical Medicine, Oxford University). The phylogenetic analyses (shown in Figures 4.5-4.7) were carried out by Dr Gary Huang and Dr Aris Katzourakis at Oxford University. The HLA typing and $CD8^+$ T cell functional analysis was conducted by Dr John Frater at Oxford University. All clinical data ($CD4^+$ T cell counts, HIV-1 VL, Hepatitis B VL, immunoglobulin quantification, and liver function tests) were acquired at clinical laboratories at St Mary's Hospital, London.

In Chapter 5, viral load assessments and $CD4^+$ T cell counts were carried out at clinical laboratories affiliated with the following centres: The Mortimer Market Centre (London, UK), St Mary's Hospital (London, UK), Royal Free Hospital (London, UK), St Bartholomew's Hospital (London, UK), Brighton General Hospital (Brighton), San Raffaele Hospital (Milan, Italy), Isipingo Clinic (Durban, South Africa), Verulum Clinic (Durban, South Africa), Botha's Hill Clinic (Durban, South Africa), Umkomaas Clinic (Durban, South Africa), Durban City Hospital, (Durban, South Africa), Taylor Square Clinic (Syndey, Australia), The Centre Clinic (Melbourne, Australia)

David George Bonsall

Abstract

Human immunodeficiency virus type 1 is a major cause of morbidity and mortality worldwide and there is urgent demand for a protective vaccine. A major goal of vaccine development is the elicitation of antibodies capable of neutralizing diverse strains. In order to achieve this goal it is necessary to understand the dynamic relationship between neutralizing antibodies (NAbs) and HIV-1, *in vivo.*

In humans, HIV-1 rapidly escapes from NAbs, confirming that humoral responses inhibit virus replication. However, neutralizing responses are commonly detected in viraemic patients and the clinical impact of NAbs on HIV-1 control is unclear. To investigate this further, viral load (VL) and NAb activity were assessed longitudinally in patients enrolled into a clinical trial of short-course antiretroviral therapy (ART), administered in early infection. The aims of this study were two-fold: i) to understand the importance of VL in the control of NAb responses and ii) to assess whether NAbs contribute to durable control of VL set-point.

A high-throughput pseudovirus neutralization assay was developed, using automated counting procedures to quantify infected TZM-bl reporter cells. The assay was used to assess NAb responses with autologous viruses derived from 22 patients. Seven patients with low VL set-points ($<10^4$ RNA copies/ml) failed to develop neutralizing responses throughout the 48-144 week follow-up period. In contrast, the remaining patients developed progressively-increasing neutralizing plasma titres (IC_{50}) that correlated with the extent and timing of VL rebound after cessation of ART. This suggests that the production of NAbs depends on the duration and extent of viraemia in early infection. Viral load was poorly predictive of neutralizing responses against heterologous isolates assayed in 38 patients, suggesting that other factors are important in the production of antibodies with cross-neutralizing activity.

Depletion of specific immunological compartments can yield crucial information as to their functional importance in vivo. We took advantage of a unique opportunity to investigate the role of NAbs and the consequences of their depletion in an HIV-1 infected human. Three years after cessation of short-course ART, the patient was treated for pre-existing low-grade lymphoplasmacytic lymphoma by antibody-mediated depletion of $CD20^+$ B cells using rituximab. This treatment was followed by a 1.7 $\log_{10}$ rise in HIV-1 VL which spontaneously reversed. Autologous NAb responses decreased as viraemia flared, and recovered as VL was controlled. Antibodies were found to target the CD4 binding site (CD4bs), as shown by competitive-binding assays. Sequence analysis revealed diversification through generation of new variants as NAbs decreased, with subsequent selection of NAb-resistant mutants at sites consistent with the binding data. These data suggest that B cell function contributed to long-term control of VL in this individual and that NAbs may be more important in controlling HIV-1 infection than previously suspected.

Acknowledgements

First and foremost I would like to thank my supervisors, Professor Myra McClure and Professor Andrew George for all the help and support they have provided. I am especially grateful for the time and energy Professor McClure has invested in my academic development.

I take this opportunity to thank Dr Peter Cherepanov and Dr Massimo Pizzato, who were always on hand to answer my questions with excellent advice and practical solutions. I thank all those involved in the SPARTAC clinical trial for providing me with an invaluable and enjoyable experience. In particular, I thank Dr Sarah Fidler and Professor Jonathan Weber for helping me understand the clinical aspects of this project. Thanks also to Dr Kholoud Porter and Dr Katherine Donegan for their help with the statistical analyses described in Chapter 5. Dr Mark Robinson joined the SPARTAC team in late 2009 and I am grateful for the support he has provided.

Thanks must go to Professor Paul Klenerman, Dr Emma Thomson, Dr Graham Cooke and Professor Quentin Sattentau for inviting me to take part in a successful and enjoyable collaboration (Chapter 4). Thanks also to Dr Gary Huang for allowing me to present some of the data he acquired as part of this collaboration.

I thank the Medical Research Council and the Wellcome Trust for funding this project. I am also grateful for the additional support provided by the NIHR Biomedical Research Centre funding scheme.

This project was made possible by the support of my friends and family. I would like to thank all the scientists at the Jefferiss Trust for keeping me close to sanity. Finally, I thank Tony for all his unconditional love and support.

Table of Contents

Declaration……3

Abstract……4

Acknowledgements……6

List of Figure……9

List of Tables……11

List of Abbreviations ……12

Chapter 1: Introduction……15

1.1 Introduction……16
1.2 The origins of the HIV-1 pandemic……18
1.3 HIV-1 genome……19
1.4 Virion structure……23
1.5 The early phase of the HIV-1 life cycle……26
1.6 The late phase of the HIV-1 life cycle……30
1.7 Structural features of the HIV-1 Envelope glycoproteins that facilitate virus entry……31
1.8 Antibody structure and function……35
1.9 The production and function of antibodies are both linked to the same variables functional affinity and antigen concentration……35
1.10 Structural features of Env that limit binding to antibodies and BCRs……38
1.11 Antibodies that circumvent the structural defenses of Env……39
1.12 Mechanisms of virus neutralization……43
1.13 Non-neutralizing roles of antibody in HIV-1 infection……48
1.14 Assays of HIV-1 neutralization……50
1.15 Virological factors that affect neutralization in vitro……51
1.16 Target cell factors that affect neutralization in vitro……53
1.17 The natural course of early HIV-1 infection……55
1.18 The role of cellular immune responses in the control of HIV-1……58
1.19 The role of neutralizing antibodies in the control of viral load. ……60
1.20 The impact of ART on the control of HIV-1 infection……65
1.21 Rationale for administering ART in early infection……66
1.22 Outline of this thesis……68

Chapter 2: Materials and Methods……70

2.1 Mammalian cell lines and tissue culture maintenance……71
2.2 DNA vectors used for cloning, sequencing and pseudovirus construction……71
2.3 Antibodies, plasma and recombinant proteins. ……74
2.4 Clinical assays of HIV-1 viral load……74
2.5 Clinical assays for the quantification of antibodies. ……75
2.6 Extraction of viral RNA from human plasma ……75

2.7 Reverse transcription of viral RNA..... 76
2.8 PCR amplification of full-length HIV-1 envelope for construction of expression plasmids..... 76
2.9 Purification of PCR amplified DNA..... 78
2.10 DNA digestion..... 78
2.10.1 DNA digestion for plasmid construction..... 78
2.10.2 Analytical restriction digest..... 79
2.11 Gel Extraction..... 79
2.12 DNA ligation..... 80
2.13 Production of competent bacteria..... 80
2.14 Transformation of competent E.coli..... 81
2.15 Screening bacterial clones for the intended plasmid construct..... 81
2.16 Monitoring growth of pcDNA.env transformed E.coli..... 83
2.17 Alkaline-lysis mini-preprepartion of plasmid DNA. 83
2.18 Large-scale alkaline-lysis maxi-preparation of DNA plasmids with high copy number..... 84
2.19 Construction of HIV-1 Env-pseudotyped viruses..... 85
2.19.1 Transfection of 293T/17 cells with linear polyethyleneimine..... 85
2.19.2 Transfections with lipofectamine 2000..... 86
2.20 Infectivity screening of HIV-1 Env-pseudotyped virus. 86
2.21 Titration of HIV-1 Env and VSV-G-pseudotyped virus..... 88
2.22 Assessing antibody-mediated neutralization of HIV-1 Env-pseudotyped virus..... 88
2.23 Quantification of pseudovirus infection by luciferase detection..... 89
2.24 Site directed mutagenesis 89
2.25 Quantification of HIV-1 reverse transcriptase activity..... 90
2.26 Competitive binding assays..... 92
2.27 Evolutionary analyses of HIV-1 envelope genes..... 92
2.27.1 PCR amplification of HIV-1 envelope for sequencing reactions..... 92
2.27.2 TOPO TA cloning of HIV-1 envelope genes for sequencing analyses..... 93
2.27.3 Phylogenetic analyses..... 94
2.28 HLA typing..... 94
2.29 IFN-γ ELISPOT assays..... 95

Chapter 3: A high through-put neutralization assay for HIV-1 Env-pseudotyped viruses..... 96
3.1 Introduction..... 97
3.2 Results..... 100
3.2.1 Optimization of molecular cloning to construct HIV-1 Env-expression Cassettes..... 100
3.2.2 MACH-1 strain E.Coli are partially resistant to HIV-envelope toxicity..... 106
3.2.3 Envelopes derived from different HIV-I isolates exhibited variable levels of toxicity in E.coli..... 108
3.2.4 Optimization of 293T/17 cell transfections for the construction of Env-pseudotyped viruses..... 111
3.2.5 Optimization of a high-throughput pseudovirus-microtitration assay..... 114
3.2.6 Validation of the β-Gal neutralization assay. 117

3.3 Discussion..... 119

Chapter 4: B cell depletion in an HIV-1 infected human reveals a role for NAbs in the control of VL.... 122

4.1 Introduction..... 123
4.2 Clinical History..... 125
4.3 Results..... 127
4.3.1 Impact of B cell depletion on plasma antibody concentration..... 127
4.3.2 Neutralizing plasma titres against HIV-I temporarily decreased following rituximab therapy..... 127
4.3.3 Antibody characterization..... 133
4.3.4 Analysis of sequence evolution in HIV-1 envelope over time..... 137
4.3.5 Neutralization susceptibility of mutated Env-pseudotypes to NAbs and patient plasma..... 145
4.3.6 Mutant Env-pseudoviruses exhibited similar levels of infectivity after correction for RT activity..... 147
4.3.7 Analysis of CTL responses prior to Rituximab Therapy..... 153
4.3.8 Impact of rituximab monotherapy on HBV co-infection..... 155

4.4 Discussion..... 157

Chapter 5: The neutralizing response to HIV-1 following short course antiretroviral therapy in PHI..... 164

5.1 Introduction..... 165
5.2 Results..... 167
5.2.1 Patient demographics..... 167
5.2.2 Neutralizing responses were variably detected within 4-12 weeks of stopping ART..... 173
5.2.3 Longitudinal assessment of NAb responses following discontinuation of early ART..... 179
5.2.4 NAb responses were associated with delayed viral rebound after cessation of early ART..... 184
5.2.5 Clade specific differences of VL and NAb response..... 186
5.2.6 Neutralization of heterologous HIV-1 Env-pseudotypes..... 186

5.3 Discussion..... 193

Chapter 6: Conclusions..... 200

6.1 Conclusions..... 201
6.2 Footnotes..... 209

References..... 210

Publications pertaining to this thesis..... 237

A one-step SYBR Green I-based product-enhanced reverse transcriptase assay for the quantitation of retroviruses in cell culture supernatants..... 238

B-cell depletion reveals a role for antibodies in the control of chronic HIV-1 Infection..... 245

List of Figures

Figure 1.1 The percentage of adults (15-49) infected with HIV-1 worldwide..... 17

Figure 1.2 The HIV-1 genome.....22

Figure 1.3 Models of HIV-1 virion structure..... 24

Figure 1.4 Schematic representation of the HIV-1 life cycle.....27

Figure 1.5 Structure of HIV-1 envelope..... 32

Figure 1.6 Models of neutralizing and non-neutralizing antibodies..... 45

Figure 1.7 Effector functions of antibodies that involve Fcγ receptors and cellular immune responses.....49

Figure 2.1 DNA vectors used for HIV-1 envelope cloning..... 72

Figure 2.2 DNA vectors used for pseudovirus construction.....73

Figure 2.3 High throughput colony screening method for the identification of pcDNA.*env* constructs. 82

Figure 3.1 Schematic representation of the HIV-I Env-pseudotype neutralization assay..... 99

Figure 3.2 Isolation of *env* by RT-PCR amplification of viral RNA was variably efficient..... 101

Figure 3.3 Efficiency of ligation reactions used to construct *env* expression plasmids..... 104

Figure 3.4 Toxicity of HIV-1 *env* variants in *E.coli* is associated with transcription-promoters orientated with the *env* ORF. 105

Figure 3.5 Susceptibility to HIV-*env* toxicity is dependent on *E.coli* strain..... 107

Figure 3.6 Envelope clones exhibit variable levels of toxicity in *E.coli*. 110

Figure 3.7 Optimization of pseudovirus production by PEI transfection..... 113

Figure 3.8 Optimized cell-seeding protocol for HIV-1 pseudotype microneutralization assays. 115

Figure 3.9 Comparison of luminometry with automated spot counting for TZM-bl based pseudovirus infectivity assays. 116

Figure 3.10 Validation of the high-throughput microneutralization assay for HIV-Env pseudotypes. 118

Figure 4.1 Clinical course of HIV-1 in relation to rituximab therapy.....126

Figure 4.2 Autologous neutralizing antibody titres assayed over time. 131

Figure 4.3 Antibody binding to HIV-1 envelope decreased following rituximab therapy..... 135

Figure 4.4 Antibody binding to HIV-1 envelope decreased following rituximab therapy.....136

Figure 4.5 Diversification of HIV-1 *env* sequences after rituximab therapy..... 138
Figure 4.6 Ancestral analysis of emerging strains 139
Figure 4.7 Tracking of selected envelope mutants..... 142
Figure 4.8 Locations of selected mutations within HIV-1 envelope. 143
Figure 4.9 Impact of selected mutations on susceptibility of the virus to neutralizing antibodies..... 146
Figure 4.10 Optimization of the SG-PERT assay for the quantification of pseudovirus particles..... 148
Figure 4.11 Impact of selected mutations on pseudovirus infectivity. 152
Figure 4.12 Clinical course of HIV-1, HBV and ALT in relation to Rituximab therapy 156
Figure 5.1 Pre-ART CD4 counts and VLs were not significantly affected by gender or HIV-1 subtype..... 169
Figure 5.2 Men infected with subtype B virus had higher VL set-points than women infected with subtype C virus..... 172
Figure 5.3 VSV-G pseudotyped virus was not neutralized by patient plasma 175
Figure 5.4 VL detected during PHI correlated with chronic VL set-points. 176
Figure 5.5 Neutralizing responses rebounded after cessation of early ART..... 180
Figure 5.6 Rebounding neutralizing responses were associated with high VL set-point 182
Figure 5.7 Neutralizing responses followed rebounding VLs 183
Figure 5.8 Neutralizing responses against autologous-contemperanous Env-pseudovirus were associated with delayed viral rebound. 185
Figure 5.9 Neutralization of Tier 1B heterologous strains weakly correlated with VL and autologous NAb titre..... 191

List of Tables

Table 1.1 Classification and functions of the HIV-1 proteins 20

Table 1.2A Studies that suggest a positive correlation or no correlation between NAb potency and VL..... 63

Table 1.2B Studies that suggest NAb responses are associated with slower rates of disease progression..... 63

Table 2.1 Primers used for PCR amplification, sequencing, mutagenesis and quantitative-RT PCR..... 77

Table 3.1 Identification of samples with low N3VL that underwent ultracentrifugation prior to RT-PCR 102

Table 3.2 Stability of pcDNA.*env* plasmids in transformed MACH-1 *E.coli* 109

Table 4.1 Impact of rituximab on plasma immunoglobulin concentrations..... 128

Table 4.2 Impact of rituximab on neutralizing plasma titres (IC_{50}). 129

Table 4.3 Neutralizing plasma titres against heterologous virus..... 132

Table 4.4 Analysis of CD8+ T cell responses and epitope evolution over time..... 154

Table 5.1 Patient demographics and clinical manifestations during PHI..... 170

Table 5.2 Half maximal neutralizing titres of patient sera tested with autologous Env pseudotypes..... 174

Table 5.3 Breadth and potency of neutralizing responses assayed in chronic infection..... 188

List of Abbreviations

ACD	acid-citrate-dextrose
ADCC	antibody dependent cell mediated cytotoxicity
ADCVI	antibody-dependent cell-mediated virus inhibition
AID	activation-induced cytidine deaminase
AIDS	acquired immunodeficiency virus
ALT	alanine transaminase
ANOVA	analysis of variance
APOBEC3G	apolipoprotein B mRNA editing enzyme catalytic polypeptide 3 G
ART	antiretroviral therapy
BCR	B cell receptor
β–gal	β–galactosidase
BMV	Brome mosaic Virus
CA	capsid proteins (p24)
CCR5	C-C chemokine receptor 5
CD	cluster differential
CD4bs	CD4bs
CD4i	CD4 inducible
cDNA	complementary DNA
C-HR	carboxy-terminal heptad repeats
CMV	cytomegalovirus
CRF	circulating recombinant form
C-terminal	carboxy-terminal
CTL	cytotoxic T cell
CXCR4	CXC chemokine receptor 4
DC	dendritic cell
DC-SIGN	dendritic cell-specific ICAM3 grabbing non-integrin
DEAE-dextran	diethylaminoethyl-dextran
DMEM	Dulbecco's modified eagle's medium
DMSO	dimethyl sulfoxide
DNA	deoxyribosenucleic acid
E.coli	*Escherichia coli*
EC	elite controller
EDTA	ethylenediaminetetraacetic
ELISA	enzyme linked immunosorbant assays
ELISpot	enzyme-linked immunospot assay
Env	envelope
ESCRT-I	endosomal sorting complex required for transport 1
FCS	fetal calf serum
FFU	focus forming units
FP	fusion peptide
GALT	gut-associated lymphoid tissue
gp	glycoprotein
HAART	highly active antiretroviral therapy
HBcAb	hepatitis B virus core antibody

HBsAg	hepatitis B virus surface antigen
HBV	hepatitis B virus
HCDR	heavy chain complementary determining region
HIV-1	human immunodeficiency virus type 1
HIV-2	human immunodeficiency virus type 2
HLA	human leukocyte antigen
HRP	horseradish peroxidase
IC_{50}	half-maximal inhibitory concentration
IC_{90}	90% inhibitory concentration
ICAM	inter-cellular adhesion molecule
IFN	interferon
Ig	immunoglobulin
IL	interleukin
IN	integrase
IQR	inter-quartile range
ITAM	immuno-receptor tyrosine based activation motif
IU	infectious units
kb	kilo base
kDa	kilo Dalton
LB	lysogeny broth (aka Luria-Bertani broth)
LCDR	light chain complementary determining region
LCL	lymphoplasmacytic lymphoma
LEDGF	lens epithelium-derived growth factor
LPS	lipopolysaccharide (Endotoxin)
LTNP	long-term non-progressor
LTR	long-terminal repeat
MA	matrix protein (p17)
MCMC	Markov chain Monte Carlo
MCS	multiple cloning site
MHC	major histocompatibility complex
ML	maximum likelihood
M-MLV	Moloney murine leukemia virus
MPER	membrane proximal external region
mRNA	messenger RNA
NAb	neutralizing antibody
NC	nucleocapsid protein
N_e	effective population size
N-HR	amino terminal heptad repeat
NK cell	natural killer cell
nm	nanometer
NNRTI	non-nucleoside reverse transcriptase inhibitors
NRTI	nucleoside reverse transcriptase inhibitors
N-terminal	amino terminal
PBMC	peripheral blood mononuclear cells
PBS	phosphate buffered saline
PCR	polymerase chain reaction
PEI	polyethylenimine
PERT assay	product-enhanced reverse transcriptase assay

Pfu	*Pyrococcus furiousus*
PHI	primary HIV-I infection
PI	protease inhibitors
PIC	pre-integration complex
pol	polymerase
PP	polypurine tract
PR	protease
R	repeat sequence
RLU	relative light units
RNA	ribonucleic acid
RRE	rev response element
RT	reverse transcriptase
rTth pol	recombinant *Thermus thermophilus* polymerase
SDS	sodium dodecyl sulphate
SG	SYBR green
SHIV	simian human immunodeficiency virus
SIV	simian immunodeficiency virus
SIVcpz	simian immunodeficiency virus chimpanzee strain
SIVgor	simian immunodeficiency virus gorilla strain
SOB	super-optimal broth
SOC	super-optimal broth with catabolite repression
SPARTAC	short-pulse antiretroviral therapy at seroconversion
SV40	simian virus 40
TAE	tris-acetate-EDTA
Taq	*Thermus aquaticus*
TAR	trans-acting responsive element
TCID	tissue culture infectious dose
TCLA	T cell lab adapted
TE	tris-EDTA
TMB	3,3',5,5' - tetramethylbenzidine
TNF	tumour necrosis factor
U3	unique 3-prime domain
U5	unique 5-prime domain
UNAIDS	The United Nations Joint Programmed on HIV/AIDS
UV	ultraviolet
VC	viraemic controllers
VL	viral load
VSV-G	vesicular stomatitis virus G protein
WHO	World Health Organization
WT	wild type
X-gal	bromo-chloro-indolyl-galactopyranoside

Introduction

In June 1981 the Centers for Disease Control (United States of America) reported five unexplained cases of an acquired immunodeficiency syndrome (AIDS) in men co-infected with *Pneumocystis pneumonia* and cytomegalovirus (CMV) (Gottlieb, 2006). Since then more than 25 million people worldwide have died from AIDS-related complications (UNAIDS, epidemic update 2009, www.unaids.org). Despite these harrowing figures, rapid progress has been made towards controlling the AIDS pandemic. Two years after the first diagnoses, human immunodeficiency virus type 1 (HIV-1) was identified as the causative agent of AIDS (Barre-Sinoussi *et al*., 1983, Popovic *et al*., 1984) and by 1985, phase 1 clinical trials had begun on the first drug to treat HIV-1 infection (Fischl *et al*., 1987). Today, rates of AIDS-related mortality are now declining in several countries, which is largely due to the introduction of combination antiretroviral therapy (ART) (Bhaskaran *et al*., 2008, Jahn *et al*., 2008). Nevertheless, approximately 0.8% of the adult population, worldwide, are infected with HIV-1 (UNAIDS, 2008), and the need for a protective vaccine is greater than ever (Figure 1.1).

In HIV-1 infection, T cells that express the CD4 antigen are the principle targets of virus infection, while $CD8^+$ T cells are considered important in controlling viral replication (Carrington and O'Brien, 2003, Crawford *et al*., 2007, Pereyra *et al*., 2008a, Schmitz *et al*., 1999). B cells are the producers of antibodies and are also involved in regulation of T cell responses. For a vaccine to achieve sterilizing immunity to HIV-1 it may be necessary to induce T and B lymphocyte responses, and there has been some success following a vaccination trial that aimed to do this. A randomized, placebo-controlled trial (RV144) conducted on 16,000 participants showed a 31% reduced risk of HIV-1 infection in individuals vaccinated with recombinant-canarypox vector (ALVAC) and recombinant HIV-1 envelope glycoprotein (AIDSVAX) (Rerks-Ngarm *et al*., 2009). Antibodies may have been responsible for this protective effect, as individuals vaccinated with ALVAC/AIDSVAX as part of a previous study produced HIV-1 specific

Figure 1.1 The percentage of adults (15-49) infected with HIV-1 worldwide

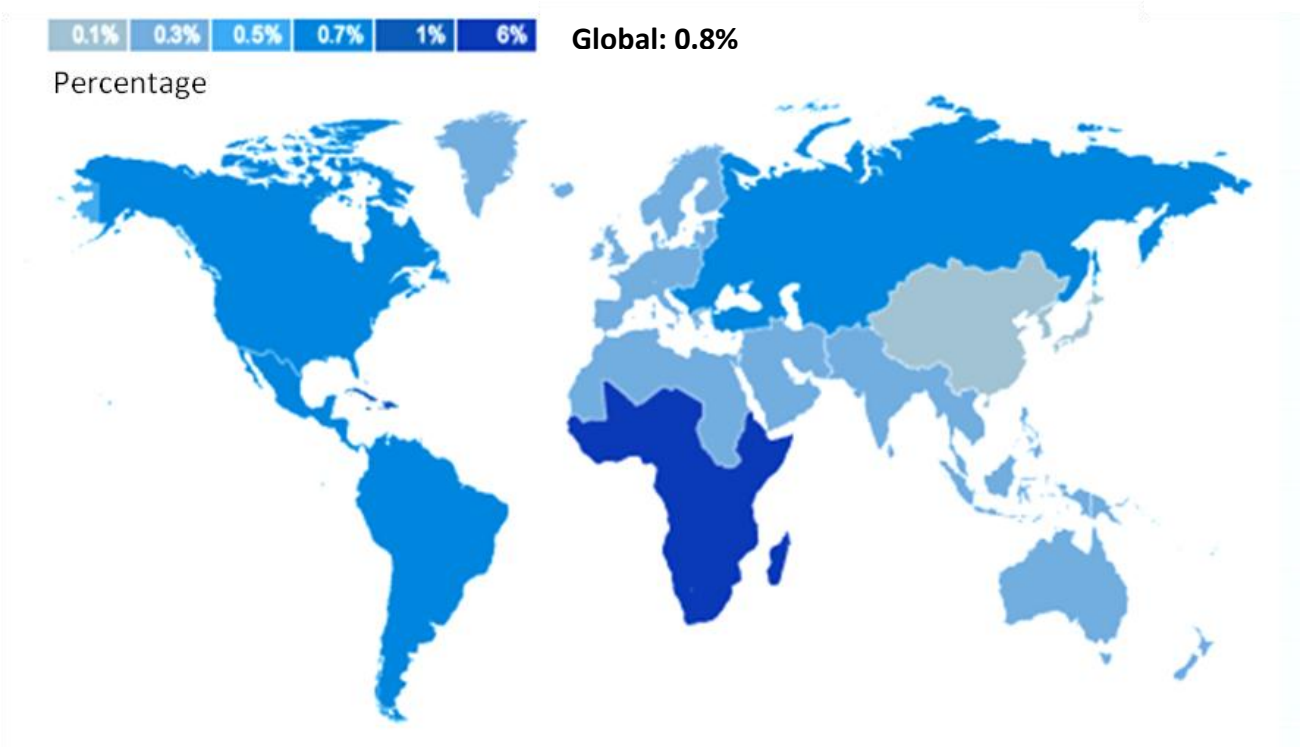


Figure 1.1: The map is colour coordinated to show the prevalence (%) of HIV-1 infections in men and women aged 15-49, per region. Data are taken from the UNAIDS/WHO epidemic update (2008), in accordance with the terms and conditions stated on the web-site (http://unaids.org/en). Epidemiological estimates are based on anonymous monitoring at designated 'sentinel surveillance' sites. These estimates are supported by national surveys conducted in 33 countries.

antibodies that had antiviral effects *in vitro* (Karnasuta *et al*., 2005). Other vaccination trials have been less successful. The phase-2 STEP trial of an adenovirus vector-based vaccine failed to protect against infection despite inducing HIV-1 specific T cell responses (Buchbinder *et al*., 2008). Post-hoc analyses indicated a modest increase in infection rates in uncircumcised vaccine recipients and those with previously acquired immune responses to adenovirus serotype 5 (Robertson, 2008b, Robertson, 2008a, Hutnick *et al*., 2009, Sekaly, 2008). The immunological correlates of these dichotomous clinical outcomes have yet to be determined.

Some HIV-1 infected individuals produce antibodies that neutralize autologous and heterologous strains of HIV-1, *in vitro* (Carotenuto *et al*., 1998b, Deeks *et al*., 2006a, Sather *et al*., 2009). Understanding the mechanisms that control the production of neutralizing responses in these patients, particularly during the early stages of infection, is central to the development of HIV-1 vaccines. Additionally, it is important to understand the role of neutralizing antibodies (NAbs) in established HIV-1 infection as this may identify novel targets for drug interventions that could potentiate protective immunity and delay progression to AIDS.

1.2 The origins of the HIV-1 pandemic

The human immunodeficiency viruses, HIV-1 and HIV-2, are lentiviruses belonging to the family of Retroviridae. Each virus originated from separate zoonotic transmissions from species of African primates infected with simian immunodeficiency virus (SIV). The most likely ancestor of HIV-2 is an SIV strain that infects sooty mangabeys and was probably transmitted to humans in the 1940's (Lemey *et al*., 2003). HIV-2 is endemic in West Africa and is less infectious and less virulent than HIV-1 (Pepin *et al*., 1991). The closest ancestor of HIV-1 is SIVcpz, which infects the common chimpanzee, *Pan troglodytes* (Gao *et al*., 1999). Two separate SIV strains closely resemble distinct parts of the SIVcpz genome, indicating that separate cross-species transmissions produced a hybrid virus capable of infecting humans

in parts of Africa where primates are hunted and eaten (Bailes *et al*., 2003). The earliest confirmed case of HIV-1, for which genetic material has been recovered, dates back to 1957. By comparing differences between this viral genome with those of other early cases, Worobey *et al.* estimated that HIV-1 entered the human population near the beginning of the 20th century (Worobey *et al*., 2008). It is likely that SIV has been transmitted to humans on at least four separate occasions, thus founding four separate HIV-1 lineages: major (M), outlier (O), N and P. An SIV strain that infects gorillas (SIVgor) is the most likely ancestor of HIV-1 groups O and P (Takehisa *et al*., 2009, Plantier *et al*., 2009).

The majority of HIV-1 infections belong to group M, which is sub-divided further into nine distinct subtypes: A, B, C, D, F, G, H, J and K. Viruses from separate clades occasionally recombine within super-infected individuals and, if transmitted, become known as circulating recombinant forms (reviewed in Carr *et al*., 1998). Subtype B infections predominate in Europe and North America, while subtype C infections predominate in Sub-Saharan Africa and are responsible for approximately half of all HIV-1 infections worldwide (Osmanov *et al*., 2002).

1.3 HIV-1 genome

The HIV-1 genome consists of a dimer of single-stranded RNA molecules of approximately 9 kilobases (kb) in length. Each sense-stranded RNA genome contains nine genes that encode fifteen proteins classified as accessory proteins (Vpu, Vpr, Vif, and Nef), regulatory proteins (Tat and Rev) and nine structural proteins cleaved from precursor proteins (Gag, Pol, and Env). (Figure 1.2 and Table 1.1). Because the HIV-1 genome is transcribed by cellular RNA polymerase (pol) II, the 5' terminus is capped via a 5'-5' phosphodiester bond to an M7 GTP group and the 3' terminus ends with approximately 200 adenosine bases (polyA). Immediately internal to the 5' cap and the 3' adenosines are non-coding sequences that play important roles in DNA replication. The organization of these sequences and the protein-coding portions of the genome are shown in Figures 1.2 and 1.4.

Table 1.1 Classification and functions of the HIV-1 proteins

Protein type	Precursor	Viral protein	Other names	Size (kDa)	Localization	Functions and interactions
Structural	Gag Gag-Pol	MA	Matrix	17	Virion	•Anchors Gag and Gag-Pol into the membrane •Interacts with the cytoplasmic tail of gp41
		CA	Core capsid	24	Virion	•Provides structure to the virion core
		NC	Nucleocapsid	7	Virion	•Encapsidates viral RNA
		p6	-	6	Virion	•Binds and incorporates Vpr into virion
	Gag-Pol	PR	Protease	15	Virion	•Cleaves Gag and Gag-Pol precursor proteins
		RT	Reverse Transcriptase	66, 51	Virion	•Reverse transcribes viral RNA
		RNAse H*	-		Virion	•Degrades RNA template
		IN	Integrase	31	Virion	•Integration of DNA provirus
	gp160	gp120	Envelope surface subunit	120	Virion Plasma membrane	•Binds to the host antigen, CD4, and to the chemokine receptors CCR5 and/or CXCR4
		gp41	Envelope transmembrane subunit	41	Virion Plasma membrane	•Mediates virus:cell fusion
Regulatory		Tat		16/14	Nucleus Nucleolus	•Transactivator of HIV-1 gene expression •Binds to the TAR RNA element •Prevents 5' polyadenylation signal from causing premature termination of transcription
		Rev		19	Nucleus Nucleolus Cytoplasm	•Interacts with Rev response element in *env* •Shuttles mRNA from nucleus to cytoplasm
Accessory		Vif	Viral protein F	23	Cytoplasm Membrane Virion	•Promotes virion maturation and infectivity •Promotes polyubiquitination of the antiviral host cell protein, APOBEC 3G, which deaminates viral RNA:DNA heteroduplexes
		Vpr	Viral protein R	10-15	Virion (Nuclear membrane?)	•Promotes nuclear localization of preintegration complex •Inhibits cell division •Induces cell differentiation •Interacts with p6 part of the Gag precursor
		Vpu	Viral protein U	16	Plama membrane	•Enhances virion release by inhibiting host-cell protein, CD134 (tetherin), activity. •Promotes degradation of CD4 in the endoplasmic reticulum •Promotes Env maturation •Increases cell susceptibility to Fas-mediated apoptosis
		Nef	Negative factor	25	Plasma membrane Cytoplasm (Virion?)	•Enhances virion production •Down-regulates CD4 and MHC class I molecules •Interacts with clatherin-dependant protein sorting pathways •Binds to Src kinases and modulates cell signal transduction

Table 1.1 Classification and function of the HIV-1 proteins

The fifteen HIV-1 proteins are divided into three categories: structural proteins, regulatory proteins and accessory proteins. The functions and localization of each protein are shown. Reverse transcriptase is a multifunctional enzyme, which exhibits RNA and DNA dependent polymerase activity and ribonuclease H (RNase H) activity. The active sites of both enzymes are located on the p66 subunit of the p66/p51 heterodimer (*).

Figure 1.2 The HIV-1 genome

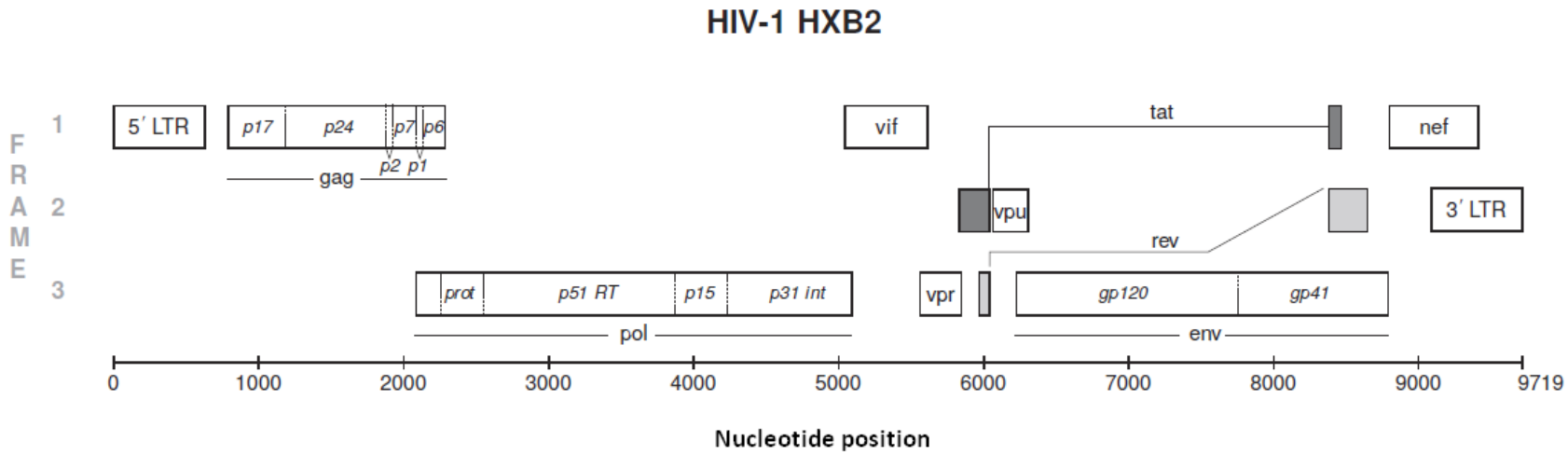


Figure 1.2 shows the positions of the open reading frames (ORFs) and LTRs of the HIV-1 genome. The x-axis indicates the positions of each ORF with reference to HIV-1 strain HXB2CG, which is the numbering system used throughout this thesis. The regulatory proteins, Tat and Rev, are both encoded by two exons shown as shaded rectangles. The diagram has been adapted, with permission, from the Los Alamos sequence compendium (2010) (http://www.hiv.lanl.gov)

1.4 Virion structure

The HIV-1 virion is approximately 100 nm in diameter and is surrounded by a lipid bi-layer, enriched with cholesterol and sphingomyelin (Liao *et al*., 2001). Embedded in the viral membrane are the envelope (Env) glycoproteins that mediate virus entry. The 120 kilo Dalton surface subunit of Env, gp120, is non-covalently attached to the transmembrane subunit, gp41. Both glycoproteins form 7-14 trimers on the virion surface (Chertova *et al*., 2002, Lu *et al*., 1995, Weiss *et al*., 1990, Chan *et al*., 1997). Several host proteins have been detected within the virus envelope, including complement-regulatory proteins CD55 and CD59 that protect against antibody-dependant and antibody-independent mechanisms of viral inactivation (Marschang *et al*., 1995, Saifuddin *et al*., 1997, Saifuddin *et al*., 1995).

Nascent virions are non-infectious due to highly-stable associations between the Gag and Gag-Pol precursors that make up the interior-core structure (Gottlinger *et al*., 1989) (Figure 1.3A). Myristoyl groups at the N-termini of Gag and Gag-Pol interact with the internal leaflet of the lipid envelope. During virion maturation, Gag-Pol precursors dimerize to form the active site of viral protease (PR), which cleaves Gag-Pol to form the HIV-1 enzymes: PR, reverse transcriptase (RT) and integrase (IN). Additionally, PR cleaves Gag to form the membrane-associated matrix protein (MA), capsid (CA), nucleocapsid (NC), C-terminal domain (p6), and two spacer domains (Henderson *et al*., 1992, Mervis *et al*., 1988) (reviewed in (Gottlinger, 2001)). Mature virus particles are recognized by their electron-dense cone-shaped cores, which consist of hexagonal lattices of CA, beneath which resides the dimeric RNA genome, encapsidated by NC (Gelderblom, 1991) (Figure 1.3B).

Figure 1.3 Models of HIV-1 virion structure

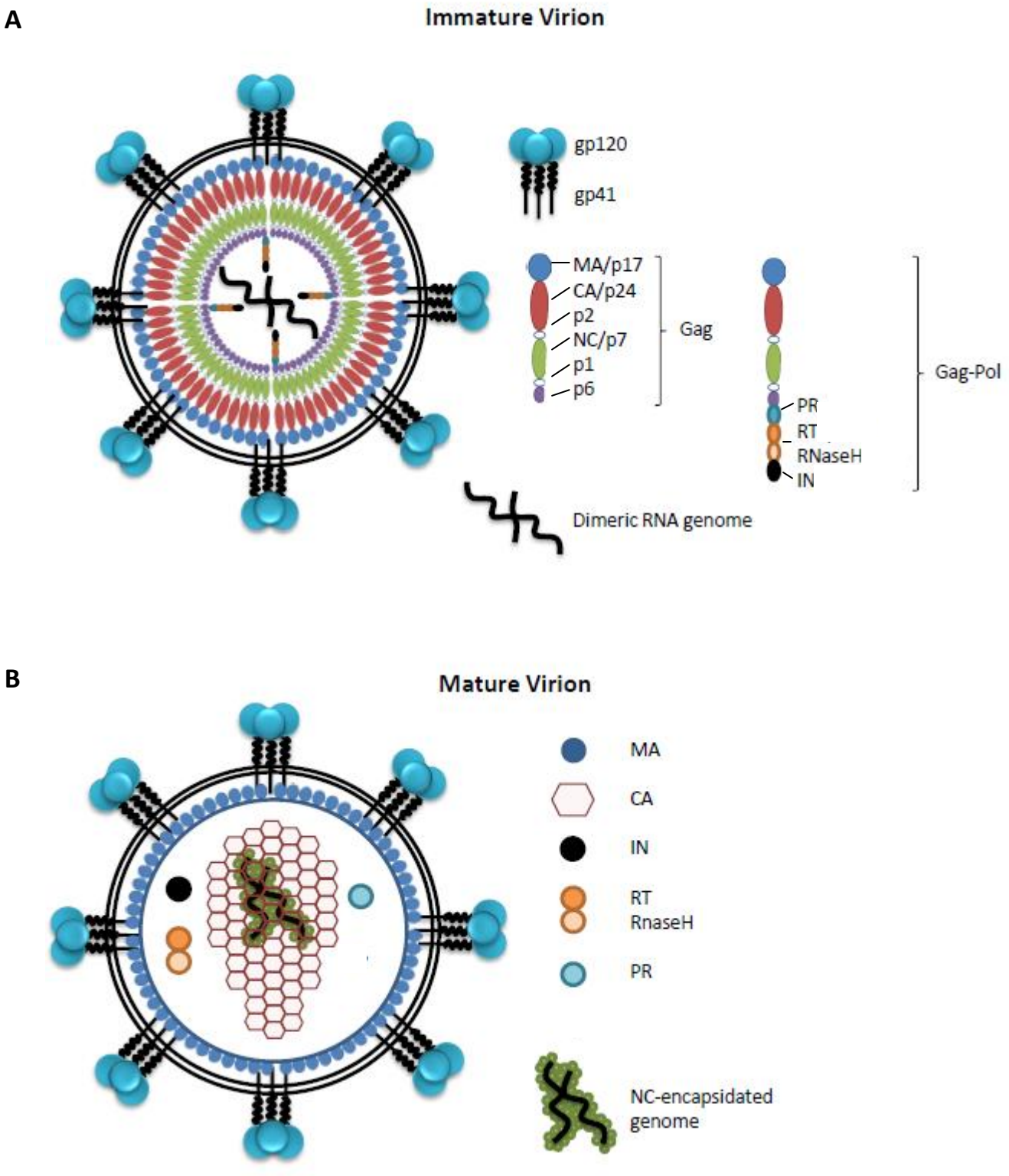


Figure 1.3 Models of HIV-1 virion structure

Figure 1.3 A: The immature HIV-1 virion is shown. The interior-core structure is formed by stable interactions between Gag and Gag-Pol precursors. The different colours show domains that correspond to the mature proteins, formed when PR cleaves these precursors. Trimers of gp120 and gp41 are shown embedded in the lipid membrane

Figure 1.3 B: The mature HIV-1 virion is shown with cleaved Gag and Pol proteins. The conical core is formed from a hexagonal lattice of CA proteins. Beneath the core resides the dimeric-RNA genome, encapsidated by NC. Several viral-accessory proteins have also been detected in the virus core (not shown; see Table 1.1 for details)

1.5 The early phase of the HIV-1 life cycle

The HIV-1 life cycle is divided into early and late phases (Figure 1.4). The early phase begins with virus entry. The mechanism of HIV-1 entry was thought to be independent of pH and and endocytosis (McClure *et al*., 1988). However, recently Miyauchi *et al.* tracked single virus particles using live-cell imaging and showed that HIV enters cells via dynamin-dependent endocytosis prior to fusion (Miyauchi *et al.,* 2010). The majority of virions that attach to the cell membrane are endocytosed, but this generally leads to degradation of the virus by the endocytic pathway (Fredericksen *et al*., 2002, Schwartz *et al*., 1998). Virus attachment may be facilitated by electrostatic interactions between gp120 and cell-surface proteoglycans (Mondor *et al*., 1998, Moulard *et al*., 2000). Additionally, lectin-binding proteins such as dendritic cell-specific ICAM3 grabbing non-integrin (DC-SIGN) bind to mannose type carbohydrates attached to gp120 (ICAM3 stands for intra-cellular adhesion molecule 3) (Geijtenbeek *et al*., 2000). These interactions enhance virus infection *in vitro*, but they are not essential for virus entry.

The primary receptor for HIV-1 entry is CD4, which is expressed on T-helper cells, regulatory-T cells, macrophages and dendritic cells (Klatzmann *et al*., 1984, McDougal *et al*., 1986). Additionally, the seven transmembrane G protein-coupled chemokine receptors, CXCR4 and CCR5, are critical co-factors required for HIV-1 entry (Alkhatib *et al*., 1996, Deng *et al*., 1996, Feng *et al*., 1996). Transmitted viruses are usually CCR5 tropic (R5), while CXCR4-tropic variants (X4) tend to arise later in infection, although subtype C viruses are rarely CXCR4 tropic (Salazar-Gonzalez *et al*., 2009). Variants that enter the cell independently of CD4 have been reported, as have isolates capable of binding to alternative chemokine receptors, *in vitro*, such as CXCR6 and CCR8 (reviewed in (Clapham and McKnight, 2001)). Virus entry is subject to inhibition by NAbs, which are the subject of this thesis. Therefore, structural aspects of virus entry will be described in detail in subsequent sections.

Figure 1.4 Schematic representation of the HIV-1 life cycle

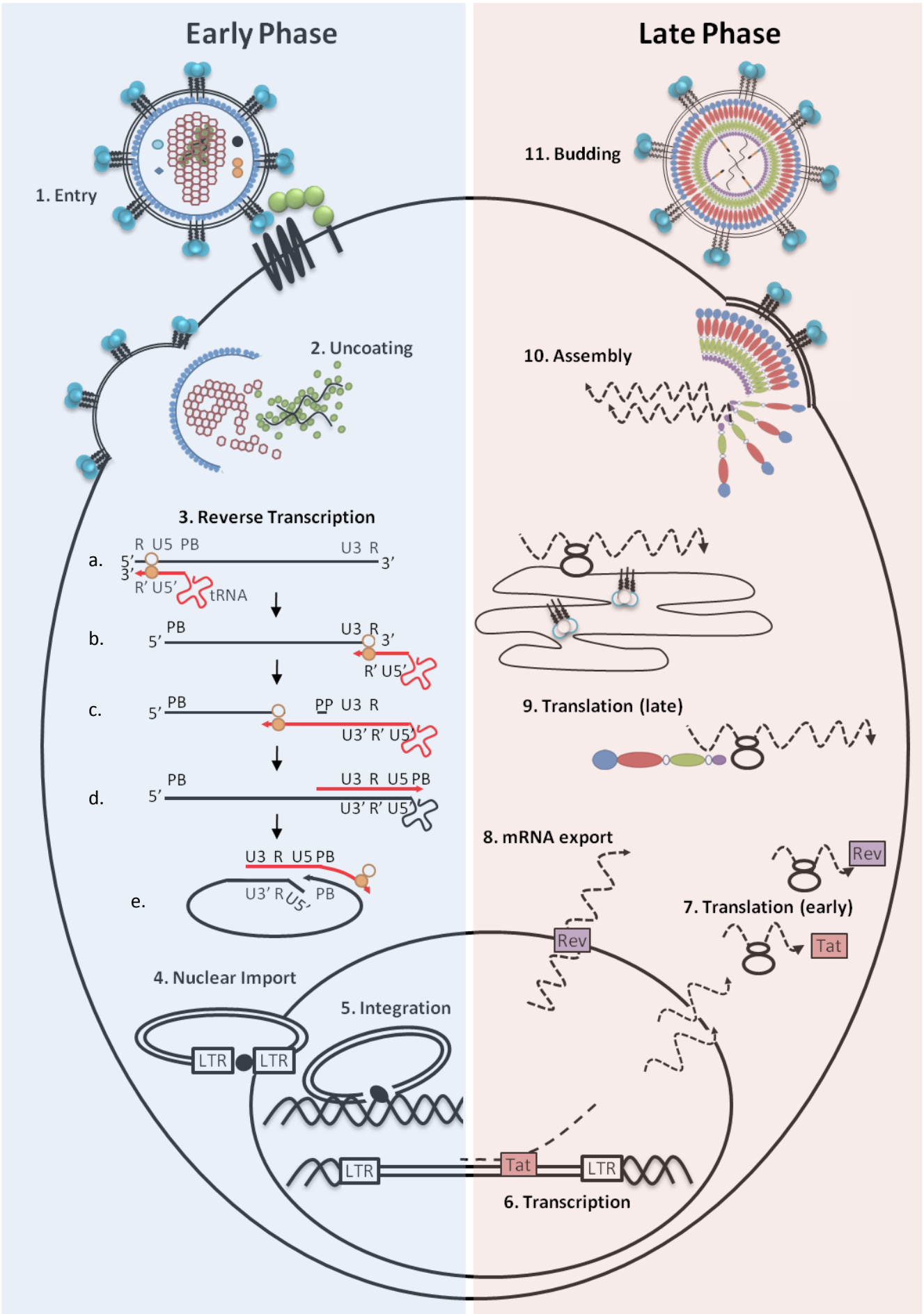


Figure 1.4 Schematic representation of the HIV-1 life cycle

The stages of the HIV-1 replication cycle are shown. The early phase is shaded blue and the late phase is shaded red.

1. The surface subunit of viral Env (gp120) binds to the CD4 host antigen and the CCR5 or CXCR4 chemokine receptor leading to gp41-mediated fusion of virus and cell membranes.
2. The virus core is released into the cytoplasm and MA and CA layers disassemble, releasing the RNA genome.
3. Reverse transcriptase synthesizes DNA while RNase H (also part of RT) digests the RNA template.
    a. tRNA primes transcription of –sssDNA from the 5' PB site
    b. –sssDNA is transported to the 3' PB sequence of viral RNA
    c. Reverse transcription of the full-length minus strand is primed by –sssDNA, while RNAase H degrades the RNA template, sparing the polypurine (PP) tracts.
    d. Plus-strand DNA synthesis is primed from the PP tracts
    e. After removal of all viral RNA and tRNA, the PB sequence of the plus-strand base-pairs with the complementary PB sequence of the minus strand, leading to the synthesis of full-length duplex viral DNA.
4. Viral DNA forms the PIC which is transported into the nucleus through nuclear pores.
5. Viral DNA integrates into the host genome forming the provirus
6. The initial phase of transcription is initiated by host transcription factors (including NFκB)
7. Fully-spliced viral mRNA translocates to the cytoplasm, leading to translation of Tat and Rev
8. Viral Tat is require for transcription of full-length viral RNA, while Rev is required to export mRNA to the cytoplasm
9. Unspliced and partially-spliced viral mRNA is translated to produce Gag, Gag-Pol and gp160
10. The Gag and Gag-Pol precursors assemble around viral RNA. Trimeric gp160 is cleaved by cellular-furin proteases into gp120 and gp41 subunits, which are transported to the plasma membrane. The cytoplasmic tail of gp41 associates with the MA domain of Gag.
11. Immature virus particles bud from the plasma membrane.

Upon fusion with the host cell membrane, MA dissociates and the core of the virion is released into the cytoplasm (Fassati and Goff, 2001, Zhang *et al*., 2000). Metastable interactions between CA proteins allow the core to uncoat by a simple dilution effect and secondary to the pH of the cytoplasm (Briggs *et al*., 2004) and reviewed in (Lehmann-Che and Saib, 2004). The RNA genome is released into the cytoplasm, which leads to the formation of the reverse transcriptase complex (RTC) that consists of viral proteins RT, IN, Vpr and p17 and several host factors (Fassati and Goff, 2001). Reverse transcription is primed by a molecule of transfer RNA (tRNA, lys3) that binds to the primer binding (PB) sequence at the 5' end of the genome (Mak *et al*., 1994). Initially, a short product known as minus-strand strong-stop DNA (-sssDNA) is synthesized by the transcriptase activity of RT, while a second enzyme activity of RT, RNase H, digests the RNA template. Subsequently, -sssDNA is released from the 5'-end of the genome and is transported to a short repeated sequence (R) at the 3' end, where it primes reverse transcription of the full-length minus strand (Ghosh *et al*., 1995, Wohrl and Moelling, 1990, Wang *et al*., 1994, Klarmann *et al*., 1997, Driscoll and Hughes, 2000). Short stretches of purines, called polypurine tracts (PPt), escape degradation by RNase H, and serve as primers for the synthesis of plus-strand DNA (reviewed in Telesnitsky and Goff, 1997).

The final product of reverse transcription is a linear, double-stranded (ds) DNA molecule flanked by sequences called long-terminal repeats (LTRs). The dsDNA genome forms the pre-integration complex (PIC) by binding to several host and viral proteins, including IN (Farnet and Bushman, 1997, Miller *et al*., 1997). The PIC is transported into the nucleus where it interacts with several host proteins including lens-epithelium derived growth factor (LEDGF). Chromatin binds to the PIC through interactions with LEDGF, which results in the targeted integration of the viral genome, usually into active transcription sites of chromosomal DNA (Cherepanov *et al*., 2003, Maertens *et al*., 2003). Integration heralds the end of the early phase of the virus life cycle.

1.6 The late phase of the HIV-1 life cycle

The integrated form of the virus is known as the provirus. The 5' LTR contains elements that bind to cellular transcription factors that promote RNA-pol II dependant transcription, while the 3' LTR overlaps *nef* and is responsible for transcription termination. During the early phase of transcription, fully-spliced viral RNA transcripts translocate from the nucleus to the cytoplasm for expression of Nef, Rev and Tat. An RNA stem loop in the 5' LTR, known as the trans-acting responsive element (TAR), binds to viral Tat protein, which promotes transcription of full-length mRNA (Karn, 1999). Unspliced and partially-spliced mRNA transcripts encoding the structural precursors Env, Gag, and Gag-Pol are transported from the nucleus by Rev, which binds to another RNA stem loop in *env,* known as the Rev-response element (RRE) (Malim *et al*., 1990) (Figure 1.4).

The uncleaved MA domain of Gag binds to phosphatidylinositol-(4,5)-bisphosphate in the plasma membrane. This interaction is thought to expose N-terminal myristate moieties of Gag that anchors the precursor into the phosphor-lipid membrane, specifically within microdomains known as lipid rafts (Saad *et al*., 2006). Viral RNA is encapsidated by Gag through interactions between zinc-finger domains in NC that bind to structurally-conserved RNA stem loops that constitute the psi site (ψ). The process of RNA encapsidation serves as a scaffold for CA-mediated multimerization of Gag and Gag-pol around the dimeric genome (Muriaux *et al*., 2001). Virus assembly ends with budding of the virus particle from the plasma membrane, which is facilitated by host-derived endosomal sorting machinery including the clathirin adapter complex and the endosomal sorting complex required for transport (ESCRT-I), which localize to the site of virus assembly through interactions with p6 and MA, respectively (Camus *et al*., 2007).

Gag alone is sufficient to produce virus particles, but the formation of infectious virions requires the incorporation of Env glycoproteins. Both gp120 and gp41 are cleaved by the cellular protease, furin, from the 160 kDa trimeric-precursor, gp160, which is encoded by HIV-1 *env* and translated on endoplasmic-reticulum-bound polyribosomes (Allan *et al*., 1985, Hallenberger *et al*., 1992, Veronese *et*

al., 1985). Oligosaccharides are attached to gp120 and gp41 by host cellular machinery in the ER and Golgi. Specifically, these are linked to asparagine side chains in amino acid sequences NXS or NXT, where the second residues can be any amino acid except proline. This sequence is known as a glycosylation sequon. In primary $CD4^+$ T cells and macrophages, interactions between the cytoplasmic tail of gp41 and the MA domain of Gag are essential for Env incorporation. However, truncation of the gp41 cytoplasmic domain has little effect on the infectivity of virions produced in some cell lines (eg. HeLa), suggesting that Env may also be incorporated in a non-specific manner. The host factor, TIP47, probably acts as co-factor for Env incorporation, since this protein has been shown to bind gp41 and MA (Lopez-Verges *et al*., 2006).

1.7 Structural features of the HIV-1 Envelope glycoproteins that facilitate virus entry.

Sequence analyses of diverse HIV-1 strains demonstrate that gp120 is divided into five variable regions and five conserved regions (Starcich *et al*., 1986). Kwong *et al.* solved the X-ray crystal structure of the gp120 core in complex with the two N-terminal domains of CD4, which revealed gp120 has two domains linked by a bridging sheet and held together by seven disulphide bridges (Figure 1.5 A). The N-terminus of the inner domain interacts with gp41 (Figure 1.5 B), while the outer domain forms the exposed face of the envelope trimer (Kwong *et al*., 1998) (Figure 1.5 C). The gp41 subunit consists of an N-terminal hydrophobic fusion peptide (FP), two heptad repeats (N-HR and C-HR), a transmembrane domain and a cytoplasmic tail. In solution, peptides consisting of the N-HR and C-HR domains naturally form trimeric structures consisting of coiled coils of alpha-helices known as six-helix bundles. Strong associations between the ectodomains of gp41 are largely responsible for the trimeric arrangement of Env. (Chan *et al*., 1997, Weissenhorn *et al*., 1997). The primary HIV-1 receptor, CD4, consists of four immunoglobulin-

Figure 1.5 Structure of HIV-1 envelope

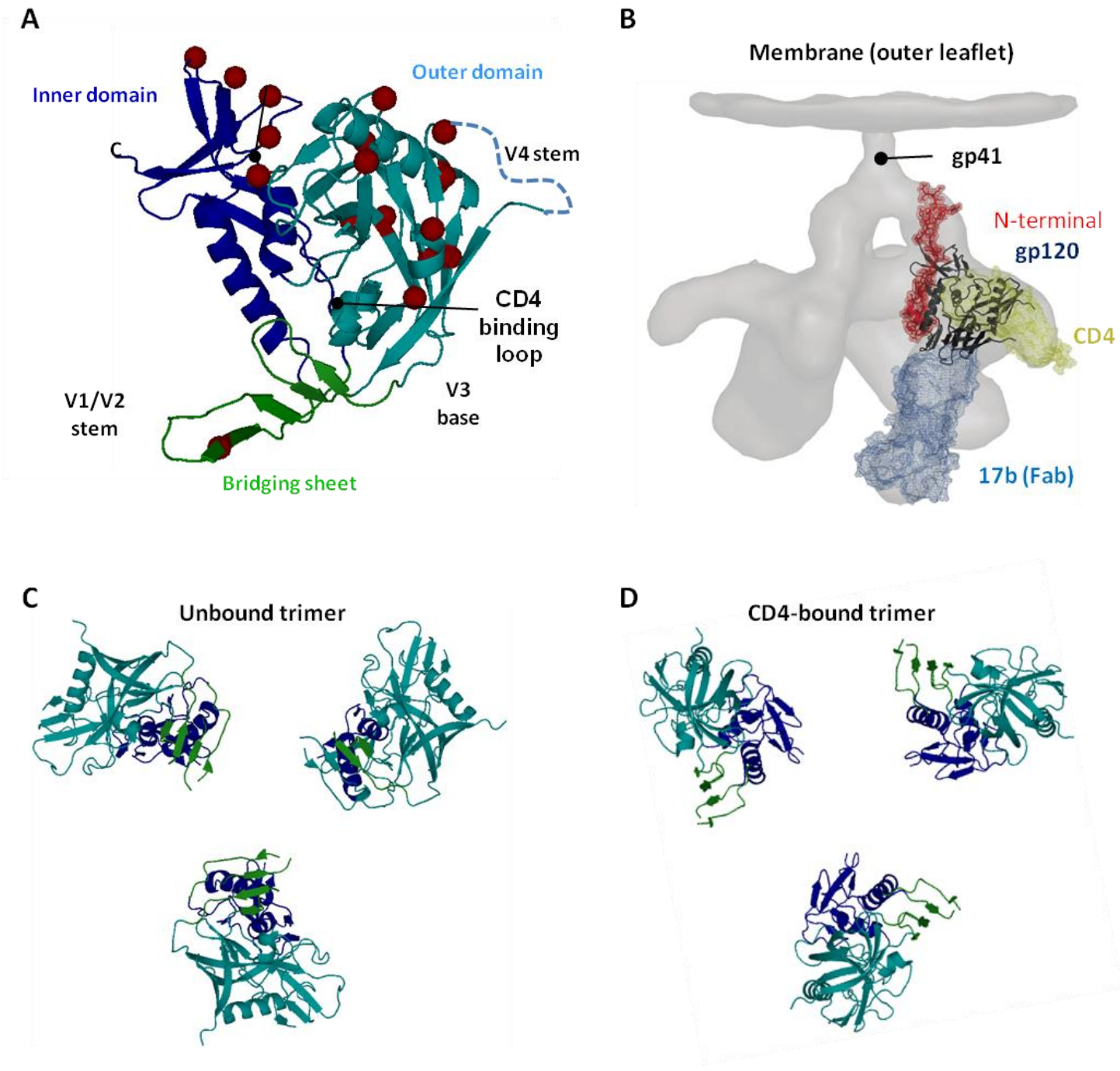


Figure 1.5 Structure of HIV-1 envelope

Figure 1.5 A: The atomic-level crystal structure of the gp120 core is shown (2.5 Å). This structure was solved by Dr Peter Kwong in 1998 (Kwong *et al.*, 1998). The structure was obtained from crystals of gp120, the N-terminal domains of CD4 (D1-D2) and a Fab fragment from neutralizing antibody, 17b. The gp120 core has deletions at the N and C termini and at the V1/V2 and V3 loops. The positions of the N-linked glycans are highlighted with red spheres. The structure was downloaded from the Research Collaboratory for Structural Bioinformatics Protein Data Bank (RCSB PDB) and PyMol software was used to construct ribbon diagrams and highlight domains. Only the gp120 core is shown; the CD4 domains and Fab fragment of 17b are hidden. (PDB ID: 1GC1)

Figure 1.5 B: The crystal structure of the gp120 core bound to CD4 (D1-D2) and the 17b Fab fragment is shown superimposed on a 3 dimensional cryo-electron tomogram, solved by Liu *et al*. (20 Å) (Liu *et al*., 2008). The image is available in the cryo-electron microscopy data bank (EMDB ID: 3DNN).

Figure 1.5 C: The relative positions of each gp120 monomer within an unbound Env trimer are shown. The colour scheme is the same as for Figure 1.5A (PDB ID: 3DNN) (Liu *et al*., 2008).

Figure 1.5 D: The relative positions of each gp120 monomer within a CD4-bound Env trimer are shown. The binding of gp120 to CD4 causes each monomer to rotate by approximately 45°. (PDB ID: 3DNO) (Liu *et al*., 2008).

All structures are taken from the RCSB protein and electron microscopy data banks in accordance with the terms of use stated on the website (www.pdb.org) (Berman *et al*., 2000)

like extracellular domains with a flexible hinge separating domains three and four (Littman *et al*., 1988, Maddon *et al*., 1985, Wu *et al*., 1997)#101}. The amino terminal domain (D1) interacts with the conserved CD4-binding site on gp120, which consists of residues that are discontinuous in the primary amino acid sequence. Part of the CD4-binding site is recessed into the gp120 core, while other parts are more exposed, especially the CD4-binding loop formed from the α-3 helix and the β-15 strand (Figure 1.5 A) (Kwong *et al*., 1998, Chen *et al*., 2005). In its unbound state, the CD4-binding sites are situated on top of the trimer and are protected by the V1/V2 loops and N-linked carbohydrate moieties.

Upon binding to CD4, gp120 undergoes a conformational change in its tertiary structure. Specifically, the β-20 and β-21 strands re-orientate to stabilize the bridging sheet and the CD4-binding loop dislocates to make contact with CD4 (Huang *et al*., 2005, Kwong *et al*., 2000, Kwong *et al*., 1998). Cyro-electron tomography, in conjunction with X-ray crystallography, has shown how CD4 binding affects the quaternary and tertiary conformations of Env trimers. Binding to CD4 causes each gp120 monomer to rotate by approximately 45 degrees which places the gp41 stalk in close proximity to the target cell membrane (Figure 1.5 D). Concomitantly, the V3 loop is repositioned to point directly toward the target cell, readying it for chemokine receptor binding (Liu *et al*., 2008).

Binding of gp120 to CCR5 or CXCR4 transduces a conformational change in gp41 that causes the FP to penetrate the outer leaflet of the target-cell membrane (Liu *et al*., 2008, Dimitrov *et al*., 2005). This results in the formation of a pre-hairpin intermediate, which connects the virus with the target cell. Subsequently, gp41 rearranges to form six-helix bundles that results in the formation of fusion pores and the merger of viral and cellular membranes (Markosyan *et al*., 2003, Melikyan *et al*., 2000).

1.8 Antibody structure and function

Antibodies are immunglobulins that are the secreted form of the B cell receptor (BCR). All immunoglobulins consist of multimeric complexes of two proteins known as the heavy (H) and light (L) chains. There are two types of light chain (κ and λ) and five types of heavy chain (μ, δ, γ, α, and ε) that define the major antibody isotypes (IgM, IgD, IgG, IgA and IgE, respectively) (Edelman, 1991). The IgG isotype has two heavy chains that each consist of an N-terminal variable domain and three constant domains with a flexible hinge linking domains two and three. Disulphide bonds attach each heavy chain to a light chain consisting of one variable and one constant domain. This configuration produces a characteristic Y-shaped antibody molecule. A constant domain consisting of the heavy chains only constitute the Fc portion, while the two arms of the 'Y' shaped molecule are known as the Fab portions.

Loops protruding from the variable domains of each Fab portion form the complementary-determining regions CDR1, CDR2 and CDR3. In total, six CDRs (three from each heavy and light chain) make up the antigen-binding site, or paratope, of each Fab portion (Saphire *et al*., 2001). The chemical composition and electrostatic properties of the paratope determine its specificity for particular epitopes (antigenic determinants) (McCoy *et al*., 1997). Specificity is also a function of "shape complementarity" that defines how well epitope and paratope structures fit together (Lawrence and Colman, 1993) and reviewed in (Epa V.C. and Colman P.M., 2001).

1.9 The production and function of antibodies are both linked to the same variables: functional affinity and antigen concentration

Immature B cells express membrane-bound IgM monomers in complex with invariant Igα and Igβ proteins that together form the B cell receptor complex (BCR). During early B cell development, gene segments encoding the immunoglobulin variable domains (designated V, D and J) undergo somatic recombination involving a complex of enzymes that includes proteins encoded by the recombination

activating genes RAG1 and RAG2 (Agrawal and Schatz, 1997). Consequently, immature B cells carry diverse BCRs that bind differentially to antigens such as HIV-1 Env. Antigen binding cross-links BCR complexes and transduces signals through immuno-receptor tyrosine based activation motifs (ITAM) located on the cytoplasmic tails of Igα and Igβ proteins, which leads to the differentiation of B cells (Cornall *et al*., 2000). Alternative splicing of mRNA results in modifications to the immunoglobulin heavy chain and the synthesis and secretion of soluble IgM, which is the major isotype of primary immune responses. Subsequent differentiation to memory B cells and plasma cells involves further modifications to the H chain that switches protein expression from IgM to IgG; a process that requires direct contact with $CD4^+$ T helper cells (Aruffo *et al*., 1993).

Immunoglobulin variable domains are modified further by a process known as affinity maturation, whereby activation induced cytidine deaminase (AID) introduces mutations that alter the affinities of BCRs. Those B cell clones that express mutated BCRs with high affinity to antigen are selected, while BCRs that lose affinity to antigen cease to transduce survival signals, causing the B cell to die by apoptosis (Clarke *et al*., 1985, Petersen-Mahrt *et al*., 2002). The antigen-dependent stages of B cell maturation occurs at sites in the lymphoid tissue known as germinal centres and involves Follicular dendritic cells (FDCs) and $CD4^+$ T cells (Schwickert *et al*., 2007). Follicular helper T cells (Tfh) that express CD4 and the CXCR5 chemokine receptor play a critical role in forming germinal centres by expressing cytokines IL-4 and IL-21 (Breitfeld *et al*., 2000). Interactions between the BCR and cognate antigen, as well as interactions between the CD40 antigen of B cells and the CD40 ligand of $CD4^+$ T cells, are both required for antibody isotype switching, affinity maturation and B cell proliferation. If either of these interactions is absent the B cell will die by apoptosis. The outcome of affinity maturation is the production of antibodies that bind strongly to antigen.

The strength of association between immunoglobulins and antigen, HIV-1 Env for example, is defined by the intrinsic affinity of monovalent interactions and the avidity of multivalent interactions. The interaction between monovalent antibody paratopes (P) and antigen epitopes (E) that forms epitope-paratope complexes (PE) can be defined by the following equilibrium equation:

1. $$P + E \leftrightharpoons PE$$

At equilibrium the association rate of P and E equals the dissocation rate of PE such that concentrations P, E and PE remain constant. Thus, at equilibrium, concentrations of P, E and PE are related to the association equilibrium constant (Ka), by the Law of Mass Action:

2. $$Ka = \frac{[PE]}{[P][E]}$$

Equation 2 indicates that the concentration of PE at equilibrium is proportional to the concentration of P and E and the affinity of the interaction (reviewed in George *et al*., 1997). Importantly, the Law of Mass Action governs the interactions between viral antigen and BCRs and also the interaction between antibodies and viral antigen. When an immature B cell is exposed to a novel antigen the proportion of BCRs that will become cross-linked will depend on the functional affinity (avidity) of the BCR to the antigen and the concentration of that antigen. However, in chronic HIV-1 infection, antibody is normally present in vast molar excess over viral antigen (Klasse and Moore, 2004), therefore, the proportion of viral epitopes bound as equilibrium is approached, approximately depends on the avidity of the interaction and the concentration of the antibodies.

The relationship between intrinsic affinity and avidity is non-additive because of co-operative effects involving distinct binding sites. The degree of co-operativity that produces this synergy depends upon the relative spatial distributions of the epitopes and paratopes, and also the entropic penalty incurred by stabilizing Fab domains and envelope conformations that are otherwise free to move (reviewed in

(Greenspan, 2001)). A case in point: Torsional flexibility afforded by the IgG3 hinge region results in higher levels of HIV-1 neutralization than IgG1 molecules bearing the same Fab portions. This was originally attributed to increased steric hindrance afforded by the larger Fc portion of IgG3 (Cavacini *et al*., 1995). However, Scharff *et al.* demonstrated that hinge flexibility was more important. In these experiments, polyclonal IgG1 and IgG3 antibodies were digested with papain to produce monovalent Fab fragments and with pepsin to generate divalent $F(ab')_2$ fragments (covalently linked by a disulphide bond, but lacking the heavy chain Fc portion). The $F(ab')_2$ fragments of IgG3 neutralized more efficiently than those of IgG1, while Fab fragments derived from both isotypes neutralized similar amounts (Scharf *et al*., 2001).

1.10 Structural features of Env that limit binding to antibodies and BCRs

The human immunodeficiency virus has evolved several mechanisms that allow functional Env trimers to avoid high affinity interactions with immunologlobulins. Structurally-critical sites in HIV-1 envelope are conserved amongst successive generations of the virus quasispecies. However, other sites in Env exhibit structural plasticity and accommodate mutations without affecting Env functionality. Genetic diversity of HIV-1 is greatest in the envelope gene, which can differ by 20% between viruses from the same clade and by up to 35% between viruses from separate clades (Los Alamos HIV-1 sequence database). Mutations commonly arise because mechanisms that replicate HIV-1 genetic material are highly prone to error (Preston *et al*., 1988). Additionally, HIV-1 RT can "jump" between strands of the dimeric RNA genome, resulting in high rates of recombination (Jetzt *et al*., 2000). Mutations in Env accumulate over the course of infection, particularly in the variable loops. Consequently, antibodies that neutralize virus by binding to non-conserved sites rapidly select escape variants (Richman *et al*., 2003, Wei *et al*., 2003).

Several structural features of HIV-1 envelope protect the conserved sites from binding to antibodies.

I. The gp120 core is shielded by N-linked glycans (Wei *et al*., 2003).

II. Structurally conserved sites are sterically hindered within the gp120 core, while other sites are occluded within the Env trimer. (Labrijn *et al*., 2003)

III. Conformational epitopes, such as those induced by interactions with CD4, are only transiently exposed, which provides a short-kinetic window for antibody binding.

IV. Antibodies that bind to conformational epitopes incur an entropic penalty which limits the strength of antibody binding by conformational masking (Kwong *et al*., 2002).

The latter mechanism of antibody escape is determined by the thermodynamics of antibody binding to HIV-1 Env. The free energy that corresponds to the binding affinity of an epitope-paratope interaction has two components. The first component is enthalpy, which corresponds to the internal energy of covalent and non-covalent bonds. The second component is entropy, which acts to disrupt the order imposed by these bonds. Antibodies that bind to the receptor binding sites of gp120 must stabilize the highly flexible structure and induce unfavourable changes in entropy and compensatory changes in enthalpy. Consequently, affinity-guided selection of antibodies favours epitope-paratope interactions that do not incur entropic penalties. This includes epitopes on monomeric gp120 that are not present within native envelope trimers and are therefore non-neutralizing (Kwong *et al*., 2002).

1.11 Antibodies that circumvent the structural defenses of Env

In spite of the evolving structural defenses of HIV-1 envelope glycoproteins, most chronically infected patients produce antibodies that neutralize virus, *in vitro*, to some extent (Deeks *et al*., 2006b). There is considerable variation in the neutralizing efficacy of antibody responses between patients, and a minority develop antibodies capable of inhibiting a diverse range of virus isolates. Investigations of these patients have occasionally led to the discovery of monoclonal antibodies with potent neutralizing activity. Most of these NAbs have unusual structural features that circumvent the structural defences of HIV-1 Env. These antibodies can be divided into categories defined by the following epitopes:

I. Epitopes overlapping the CD4 binding site (CD4bs).

II. Conserved motifs within the variable loops.

III. High-mannose moieties of N-linked carbohydrates.

IV. CD4 induced (CD4i) epitopes (ie. the co-receptor binding site).

V. Epitopes in gp41.

VI. Epitopes that are only exposed on Env trimers.

Antibodies b12 (Burton *et al*., 1994), m14 (Zhang *et al.*, 2004b) and VRC01 (Zhou *et al.*, 2010) all target the CD4bs. Atomic level structures have revealed that b12 and m14 have unusually long heavy-chain CDR3 loops (HCDR3) that are the product of atypical V(D)J recombination events (Saphire *et al*., 2001). It was thought that these protruding loops were required to access a recessed cavity in the CD4bs; however, crystal structures of b12 in complex with gp120 core demonstrated that this was not the case. Interestingly, only the heavy chain of b12 makes contact with gp120 and the long HCDR3 loop separates the envelope from the light chain CDRs (Zhou *et al.,*2007). Thus, the b12 epitope is restricted to conserved residues in and around the CD4bs. It remains to be seen whether this is true for the other CD4bs antibodies.

The co-receptor binding site is highly conserved and is the target of neutralizing antibodies 17b, X5 and 48d. The binding affinities and the neutralizing activities of these antibodies increase in the presence of soluble CD4 (Moulard *et al*., 2002). Antibodies 17b and X5 also have long HCDR3 loops that include acidic residues to mimic the N-terminal gp120-binding domain of CCR5. Additionally, sulphated tyrosines in the CDR3 region mimic post-translational modifications of the CCR5 receptor (Huang *et al*., 2004). Fab domains of 17b, X5 and 48d bind and neutralize virus better than whole IgG, suggesting that the Fc domains pose steric constraints that limit access to the coreceptor binding site of CD4-bound Env (Labrijn *et al*., 2003).

Steric constraints may also limit antibody access to the gp41 domain. Neutralizing antibodies 2F5 and 4E10 have been shown to bind to the membrane proximal external region (MPER) of gp41 and have long hydrophobic HCDR3 domains that bind to lipid moieties in the cell membrane. This autoreactivity is essential for neutralizing activity, but non-essential for gp41 binding. Ontogenic analyses of murine B cells have revealed that autoreactivity precedes Env-specificity in the development of MPER-specific antibodies (Barton Hayes; presented at Keystone 2010, abstract #X5006), suggesting that self-reactivity of immunoglobublin BRCs may be important in the development of this type of antibody response. Another example of partial autoreactivity has recently been demonstrated for the CD4i antibody 21c. Crystal structures demonstrated that this antibody contacts both the CD4 antigen and the CCR5 coreceptor binding site of gp120 (Diskin *et al*., 2010).

High mannose moieties within carbohydrates are the targets of antibody 2G12 (Scanlan *et al*., 2002). Carbohydrates are attached to the envelope glycoprotein by host cellular machinery and are generally not immunogenic. However, 2G12 has a unique structure whereby the two VH domains are interlocked producing a single paratope consisting of four variable domains (Calarese *et al*., 2003). The neutralizing activity of this antibody is highly potent, yet attempts to elicit 2G12-like antibodies by vaccination have so far proved unsuccessful.

As mentioned, the majority of antibodies targeting the variable loops rapidly select escape mutants at minimal expense to viral fitness. Consequently, the neutralizing activity of these antibodies is generally restricted to the autologous virus that primed the original response. However, V3 contains a conserved motif at its crown (GPG(R/Q)) which is the target of NAb, 447-52D. Additionally, 447-52D has been shown to interact with atoms on the amino acid main-chain of V3, which facilitates binding to diverse strains (Stanfield *et al*., 2004). The majority of clade B isolates have GPGR sequences. By contrast, the

majority of clade C isolates have GPGQ motifs at the same position and are generally resistant to neutralization by this antibody.

Two recently discovered antibodies, PG9 and PG16, have been shown to bind preferentially to Env trimers and potently neutralize approximately 80% of HIV-1 isolates from all clades (Walker *et al*., 2009). Crystal structures of these antibodies have revealed long CDR3 loops with sulphated tyrosine residues (Pancera *et al*., 2010). Mutagenesis analyses suggest that PG9 and PG16 bind to epitopes on gp120 formed from conserved parts of V2, V3, the V1/V2 stem and part of the co-receptor binding site. Inducing antibodies that target trimeric envelope is a desirable outcome of HIV-1 vaccination because antibodies that bind to monomeric gp120, without binding to oligomeric envelope, are non-neutralizing (Moore *et al*., 1995).

Passive infusions of neutralizing antibodies have been shown to protect macaques against chimeric SIV viruses that express the HIV-1 envelope (SHIV) (Baba *et al*., 2000, Emini *et al*., 1992, Mascola *et al*., 1999, Mascola *et al*., 2003, Mascola *et al*., 2000, Putkonen *et al*., 1991, Zhang *et al*., 2004a). This has placed a considerable emphasis on the immunogenic potential of the HIV-1 envelope glycoprotein and its capacity to elicit cross-reactive NAbs. It is not the NAbs *per se* that the field aims to identify, rather the cognate epitopes to which they bind. However, the unusual antibody structures and post-translational modifications of these antibodies are rarely found *in vivo,* and attempts to elicit them have so far failed. For this reason, the CD4bs specific antibody, VCR01, holds considerable promise because its structure is the product of normal V(D)J gene arrangements. Notably, VRC01 has an affinity and neutralizing potency that rivals all other HIV-1 specific antibodies, suggesting that induction of potent NAbs by vaccination is a realistic possibility. Work is currently underway to use antibodies, such as VCR01, as structural-scaffolds and selective-agents for the design of relevant immunogens by techniques collectively termed reverse-engineering (Kwong *et al*: presented at HIV Vaccines, Keystone, 2009: X5011)

In spite of occasional discoveries of unsually potent NAbs, the majority of HIV-1 infected patients do not posses single NAb clones with high levels of neutralizing activity. However, broad and potent neutralizing activity can be achieved from many partially-effective antibodies (Scheid *et al*., 2009). Since part of this thesis investigates the role of HIV-1 specific antibody responses that arise under ordinary circumstances, the mechanisms that contribute to neutralization in the majority of cases needs further discussion.

1.12 Mechanisms of virus neutralization

Dimmock makes the distinction between neutralization and virus inactivation (Dimmock, 1984). The former involves virus-antibody interactions that lead directly to reductions in infectivity, while the latter involves secondary factors such as complement or cells that act in concert with antibodies to eliminate virus. Sattentau and Klasse define neutralization as all virus-antibody interactions that result in losses of infectivity, but they excluded inhibition by antibodies that bind to receptors on the cell-surface (Sattentau and Klasse, 2001). However, this definition is perhaps no longer appropriate since NAb 21c has been shown to neutralize by binding gp120 and CD4 simultaneously (Diskin *et al*. 2010). For the purpose of this thesis, neutralization is defined as all antibody-virus interactions that lead to virus inhibition. Particular mechanisms cannot be precluded unless they can be empirically confirmed not to participate.

Neutralizing activity has been detected with antibodies that bind to MHC and ICAM-1 receptors incorporated within virus particles upon budding from the cell membrane (Arthur *et al*., 1995, Losier *et al*., 2003). Although ICAM-1 has been implicated in virus attachment, there is no evidence that MHC augments virus entry, so why should MHC-specific antibodies neutralize? It is suggested that immunoglobulins, which are large molecules approximately 12.5 nm in length, inhibit virus attachment through steric hindrance. In a study by Parren *et al*., half-maximal neutralizing titres of antibodies were

shown to match half-maximal binding titres to HIV-1 Env, confirming that functional affinity and antibody concentration were critical determinants of neutralization (Parren *et al*., 1998). This was true for all antibodies tested, irrespective of the whether the cognate epitope was a conserved region involved in virus entry, such as the receptor binding sites, or a carbohydrate motif. In light of these data it has been suggested that sufficient levels of antibody binding to Env is all that is required to inhibit infection (Burton *et al*., 2001). Why then, are some HIV-1 Env-binding antibodies incapable of neutralizing?

An antibody will fail to neutralize if it cannot occupy enough sites on the surface of functional virus envelope trimers to prevent virus entry. Thus, neutralization follows a "multi-hit" model, which dictates that more than one antibody is required to inhibit entry of a single virion (Della-Porta and Westaway, 1978). By measuring antibody neutralization of viruses with mixtures of neutralization-sensitive and neutralization-resistant envelope glycoproteins, Yang *et* demonstrated that all trimers need to be bound in order to neutralize the virus and that each trimer is inactivated when bound to a single antibody (Yang *et al*., 2005). This was true for nine antibodies with different specificities to epitopes in Env.

The relationship between epitope occupancy and neutralization is further corroborated by the observation that non-neutralizing antibodies that bind to epitopes overlapping the b12 binding site, do not interfere with the neutralizing activity of b12 (Herrera *et al*., 2003). However, the same non-neutralizing antibodies were shown to have higher binding affinities than b12 for envelope proteins on the surface of infected cells, so why do these non-neutralizing antibodies fail to reach the occupancy threshold required to neutralize the virus, and why do they not compete with b12 for binding to Env? The answer may be that these non-neutralizing antibodies bind to epitopes that are not present on functional envelope trimers, but are present on uncleaved gp160 trimers and monomeric gp41/gp120 envelope proteins. Monomeric, non-functional envelope glycoproteins have been detected on the surface of virus particles and infected cells, and it has been suggested that these proteins stimulate the production of antibodies that are non-neutralizing (Moore *et al*., 2006) (Figure 1.6).

Figure 1.6 Models of neutralizing and non-neutralizing antibodies

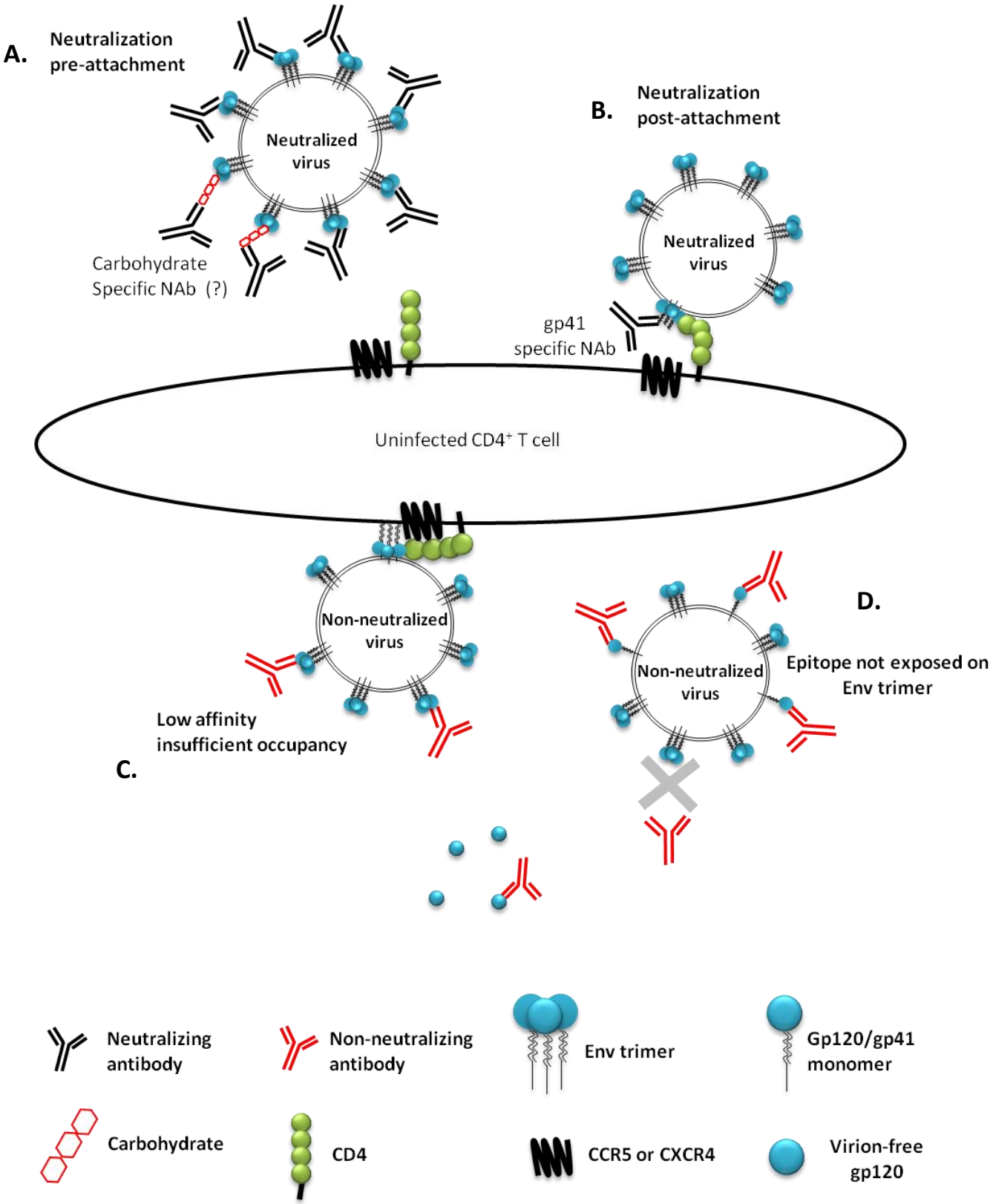


Figure 1.6 Models of neutralizing and non-neutralizing antibodies

A. Antibodies neutralize HIV-1 by binding to all envelope trimers on the surface of the virus, thus blocking attachment to the host-cell receptors. Antibody 2G12 has been shown to bind to high mannose carbohydrates. Carbohydrate-specific antibodies are rarely found *in vivo.*
B. Antibodies can neutralize virus by binding to epitopes exposed on Env at a post-attachment stage of virus entry.
C. Low affinity antibodies that do not exceed the occupancy threshold required for neutralization will not block virus entry.
D. Antibodies that bind to soluble gp120 or gp41/gp120 monomers on the surface of the virion, but not to functional Env trimers, will not neutralize the virus.

Antibodies that block the initial adsorption of virus to cells will neutralize. However, this is not the only mechanism of neutralization. For instance, antibodies 2F5 and 4E10 do not block HIV-1 attachment, and neutralize by blocking later stages of virus fusion (Binley *et al*., 2003). Additionally, antibodies have been shown to alter Env conformation on binding, which can lead to dissociation of gp120 from gp41 (Poignard *et al*., 1996), thus lowering the occupancy threshold required for neutralization. There is some controversy as to whether an antibody can bind to fusion-competent envelope trimers without inhibiting the function of these trimers (Herrera *et al*., 2003, York *et al*., 2001). York *et al.* detected binding of non-neutralizing antibodies to envelope glycoproteins from neutralization-resistant primary isolates suggesting that different neutralization sensitivities do not relate to levels of antibody binding (York *et al*., 2001). However, this study did not distinguish between antibody interactions with functional and non-functional envelopes. The carbohydrate specificity of antibody 2G12 provides additional evidence that the precise epitope location may be important in determining levels of neutralization. Multiple N-linked glycans contribute to the 2G12 epitope and mutating each of these individually has been shown to variably affect levels of neutralization, suggesting that the position of these glycans is important in determining whether they mediate neutralization or not (Scanlan *et al*., 2002). Nevertheless, studies have demonstrated that binding-affinity and epitope occupancy, are strong determinants of neutralization, *in vitro* (Yang *et al*., 2006, Parren *et al*., 1998). The situation *in vivo* is complicated by the fact that polyclonal responses consist of NAbs with diverse specificities that, together, may exceed the occupancy threshold required for neutralization, even if individual low-affinity antibody clones cannot, by themselves, neutralize.

In summary, antibodies will neutralize if they block virus attachment to host cells. Additionally, antibodies that bind to Env at post-attachment stages of virus entry can also block virus entry. It is clear that antibody affinity and antibody concentration are critical determinants of epitope occupancy, but it

is less clear whether these are the only factors that contribute to mechanisms of virus neutralization, *in vivo*.

1.13 Non-neutralizing roles of antibody in HIV-1 infection

The constant Fc part of the antibody molecule binds to the Fcγ family of receptors expressed on the surface of phagocytes, monocytes, neutrophils, B lymphocytes, natural killer cells (NK), follicular dendritic cells (FDCs), and myeloid and plasmacytoid dendritic cells. Antibodies that cross-link virus form immune complexes which bind to Fcγ receptors on FDCs. These FDC-bound immune-complexes maintain virion infectivity for long periods *in vivo* and *in vitro*. Thus, FDCs may cooperate with non-neutralizing antibodies to enhance virus infection (Smith-Franklin *et al*., 2002).

Several classes of Fcγ receptors have been defined. All but one of these have cytoplasmic tails with immuno-receptor tyrosine-based activation motifs (ITAM) (Takai, 2002). Interactions between the Fc part of neutralizing antibodies and Fcγ receptors has been shown to augment virus-neutralization by 100 -1000 fold in cultures of monocytes or dendritic cells, possibly by promoting endocytosis and degradation of virus in acidic lysosomes (Holl *et al*., 2006) (Figure 1.7). This mechanism of Fc-dependant virus-neutralizing could be important in the acute stages of infection because dendritic cells and macrophages are some of the first cells to contact HIV-1 following transmission. Virus particles that are endocytosed by antigen-presenting cells (APCs) are processed into peptides then presented to $CD4^+$ T cells in complex with MHC class II receptors. This process serves as an important link between humoral and cellular immune responses, because $CD4^+$ T cells are required for the development of HIV-1 specific NAb responses and CTL responses. Interestingly, antibodies that bind to the CD4bs of gp120 have been shown to inhibit MHC class II restricted antigen presentation, possibly by stabilizing gp120 conformations and inhibiting proteolysis (Tuen *et al*., 2005).

Figure 1.7 Effector functions of antibodies that involve Fcγ receptors and cellular immune responses

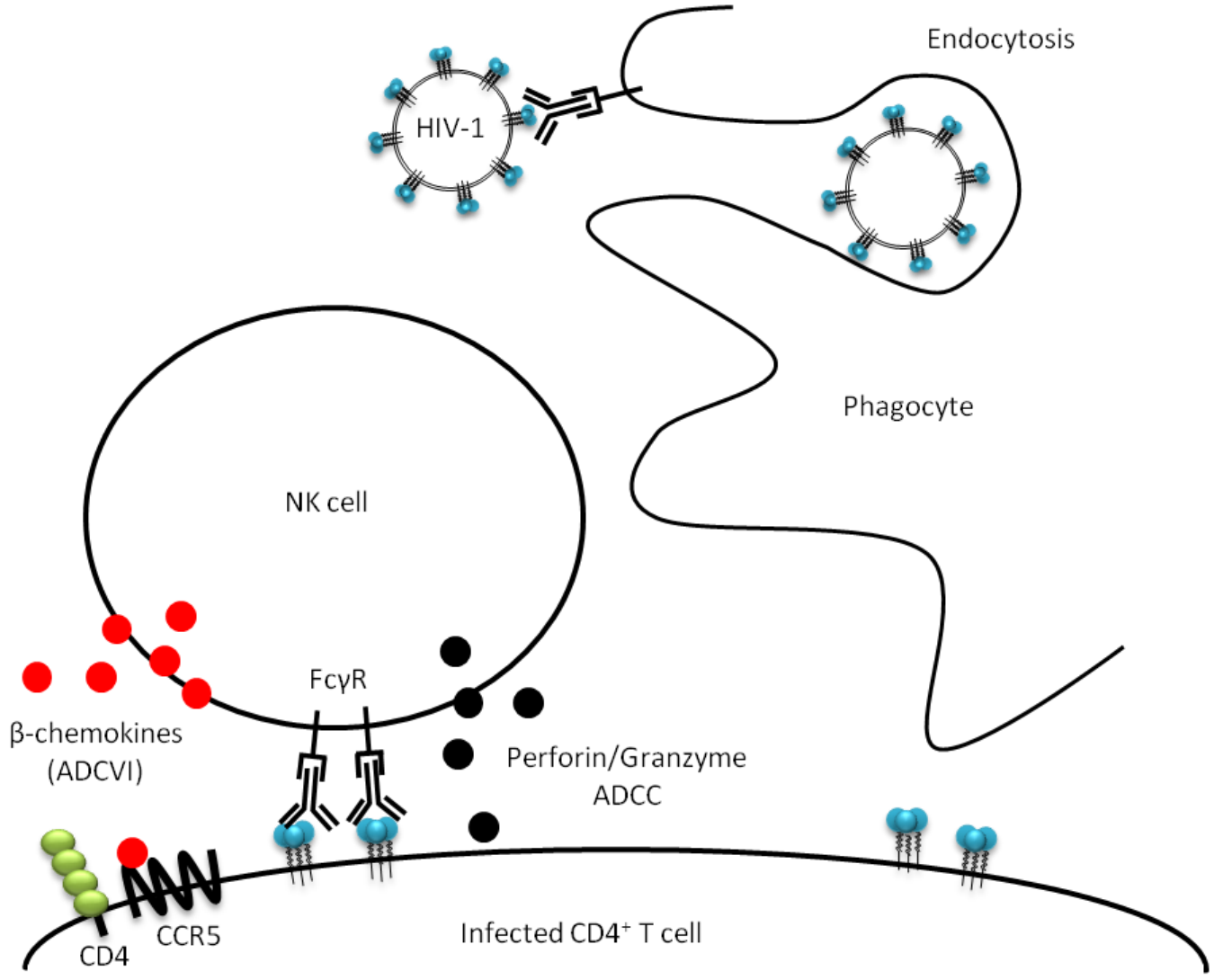


Figure 1.7: The Fcγ receptors bind to the Fc portion of antibodies. Fc:Fcγ receptor interactions have been shown to enhance neutralization of virus infection of phagocytes such as monocytes and dendritic cells, *in vitro*. HIV-1 Infected $CD4^+$ T cells express viral-envelope glycoproteins. Antibodies that bind to Env cross-link Fcγ receptors expressed on NK cells, which stimulates the release of cytoplasmic granule toxins (perforin and granzyme) and β-chemokines, leading to mechanism of ADCC and ADCVI, respectively.

Antibodies that bind to Env expressed on the surface of infected cells cross-link FcγRs expressed on NK cells, macrophages, neutrophils and γδ T cells, which leads to targeted cell killing, *in vitro*. Antibody-dependant cell-mediated cytoxicity (ADCC) has been shown to correlate with NK cell degranulation measured by expression of the CD107a antigen (Chung *et al*., 2009). Additionally, NK cells may also contribute to mechanisms of antibody-dependant cell-mediated virus inhibition (ADCVI), whereby Fcγ receptor cross-linking leads to the production of β-chemokines the inhibit HIV-1 replication without killing the infected cell (Forthal *et al*., 2005) (Figure 1.7)

1.14 Assays of HIV-1 neutralization

This thesis focuses on neutralizing antibody responses that develop in HIV-1 infected patients. Therefore, a suitable neutralization assay was required to measure the neutralizing activity of antibodies present in plasma samples derived from patients. Assays that measure neutralization *in vitro* are tissue culture systems consisting of the following components: antibody, target cell, and virus. Additionally, each assay requires a suitable end-point measure of virus infection. The choice of neutralizing agent is straightforward and depends on the scientific objective. Monoclonal antibodies that bind to known epitopes in Env are typically used to characterize neutralization phenotypes of virus isolates. Conversely, neutralization assays can be used to characterize the breadth and potency of polyclonal antibodies in plasma or sera derived from HIV-infected or vaccinated individuals.

Differences in target cell phenotype can affect levels of neutralization detected *in vitro*, as can properties of the virus that are unrelated to Env structure. Given the importance of neutralization assays to the development of HIV-1 vaccines, standardization and validation is critical if they are to provide biologically relevant data. To this end, an international collaboration, named NeutNet, was setup in 2004 to evaluate different neutralization assays by means of inter-laboratory comparisons using standardized reference reagents (Fenyo *et al*., 2009). The authors concluded the following:

"no single assay can be recommended for the measurement of HIV-1 neutralization because the assay results vary significantly depending on both the virus and the reagent used"

Clearly, the choice of neutralization assay is not trivial. The following sections (1.15 and 1.16) discuss how the phenotype of the virus and the target cell can influence levels of neutralization detected *in vitro.*

1.15 Virological factors that affect neutralization *in vitro*

Early neutralization assays used viruses that were adapted to grow in immortalized T cell lines (Robert-Guroff *et al*., 1985). Most of these T cell line adapted (TCLA) viruses use the CXCR4 co-receptor. Extensive passage of HIV-1 in the absence of NAbs has been shown to select variants that are highly sensitive to neutralization. This has been attributed to "open" envelope conformations that expose epitopes, particularly in V3, that are usually not exposed on functional-trimeric envelopes of primary isolates (Beddows *et al*., 1998, Moore *et al*., 1995, Malenbaum *et al*., 2000). Additionally, TCLA viruses are more likely to shed gp120 from functional trimers, thus lowering the site occupancy threshold required for neutralization (Poignard *et al*., 1996). For these reasons, TCLA viruses are poorly representative of the majority of field isolates, yet are still used to screen patient sera for low levels of neutralizing activity (Seaman *et al*., 2010).

In order to study patient viruses, assays were developed to detect virus neutralization in peripheral blood mononuclear cell (PBMC) cultures (Mascola, 1999). By this method, infectious virus is isolated from plasma or infected cells by co-culture with mitogen-stimulated PBMCs derived from healthy donors. Infection is usually measured from levels of p24 by enzyme-linked immunosorbant assays (ELISA). However, levels of p24 in tissue-culture supernatant may not reflect quantities of virus particles, because p24-antigen is shed from infected cells. Alternatively, RT activity can be quantified from viral

lysates derived from culture supernatants. Unlike p24 antigen, HIV-1 RT activity has been shown to be associated with whole-virion production (Fernie *et al*., 1991).

Primary isolates are generally less sensitive to neutralization than TCLA strains and are considered to be more biologically relevant. However, there are several disadvantages associated with using wild-type PBMC-cultured virus. Firstly, the act of culturing virus rapidly selects variants with differing neutralization sensitivities (Spira and Ho, 1995, Voronin *et al*., 2007). Secondly, it is difficult to identify genetic correlates of neutralization from diverse molecular quasispecies. Finally, the phenotype of PBMCs used to culture the virus may vary between donors and is subject to the conditions of cell culture. Since virus phenotype reflects that of the producer-cell membrane, differences in the incorporation of host proteins can lead to inconsistencies in virus titre and neutralization sensitivity (Hioe *et al*., 1998, Bounou *et al*., 2004). These factors limit the reproducibility of neutralization assays that use primary HIV-1 isolates, which has led to the development of alternative systems that use molecularly cloned viruses expressed in mammalian cell lines.

Mammalian cell lines transfected with cloned envelope genes, *cis*-linked to downstream transcription promoters, express functional envelope proteins. These proteins are incorporated within virus-like particles by co-transfecting a second plasmid, encoding the remaining HIV-1 genes. Transfected envelope genes lack LTRs that are required to bind viral integrase (Balakrishnan and Jonsson, 1997). Consequently, the envelope gene does not integrate and Env-pseudotyped viruses (pseudoviruses) are capable of only a single infectious cycle (Wei *et al*., 2003). In contrast to the evolving quasispecies of primary HIV-1 isolates, clonal envelope plasmids used to construct pseudoviruses are relatively stable. For this reason, pseudoviruses constructed with sequenced envelope clones are useful tools for mapping epitopes targeted by NAbs (Seaman *et al*., 2010).

Although pseudoviruses are useful models of wild-type HIV-1, they are structurally distinct in ways that can influence virus infectivity and neutralization-susceptibility. Louder *et al.* demonstrated that a single passage of molecularly cloned virus through mitogen-stimulated PBMCs led to a significant reduction in sensitivity to NAbs. Interestingly, viruses isolated directly from 293T cells were shown to incorporate significantly fewer envelope trimers than PBMC-passaged viruses, which may explain the differences observed (Louder *et al*., 2005). In contrast to these findings, Provine *et al.* demonstrated that levels of Env-incorporation in molecularly cloned virions had minimal impact on the sensitivity to neutralizing antibodies (Provine *et al*., 2009).

Comparative studies have suggested that pseudovirus assays are generally more sensitive at detecting neutralization than assays using replication competent virus, although each type of assay uses different cells to measure infection, making it difficult to delineate the true cause for these discrepancies (Fenyo *et al*., 2009, Polonis *et al*., 2008). To address this problem, Heyndrikx *et al.* compared the neutralizing effects of virus entry inhibitors with Env-pseudotyped viruses and replication competent HIV-1 stocks in PBMCs and reported that pseudoviruses were, on the whole, more readily neutralized than wild type viruses (Heyndrickx *et al*., 2008).

1.16 Target cell factors that affect neutralization *in vitro*

Most of the immortalized T cells do not express CCR5 and are limited to investigations of X4-tropic variants. In contrast, a wider range of clinical isolates can be assessed using mitogen-stimulated PBMCs that more closely resemble the natural targets of HIV-1. The physiological relevance of the PBMC assay is demonstrated by its capacity to predict quantities of NAbs that protect macaques from subsequent challenge with SHIV (Mascola *et al*., 2000). Nevertheless, PBMC-based assays are labor intensive and require a constant supply of cells from healthy donors. Therefore, reporter-cell lines are required for

many applications that require high-throughput neutralization screening or in situations where primary HIV-1 isolates are not available.

The TZM-bl reporter cell line is widely used to assess neutralization of Env-pseudotyped viruses. This cell line, also known as JC53BL-13, was derived from a sub-clone of JC-53, which is a $CD4^+$ Hela cell line (HI-J) transduced with a retroviral vector encoding CCR5. HeLa cells endogenously express CXCR4, in fact a cDNA library derived from HeLa cells was used in the discovery of CXCR4 as a co-factor for HIV-1 entry (Feng *et al*., 1996). Two reporter genes encoding β-galactosidase and luciferase were introduced into JC-53 cells separately, each under transcriptional control of an HIV-1 LTR (Wei *et al*., 2002). The LTR promoter is transactivated by viral Tat protein, which results in the transcription of both reporter genes, thus allowing quantification of virus infection using X-gal or D-luciferin substrates.

Parent cell lines of TZM-bl were used to determine the contribution of CCR5 cell-surface concentrations on rates of HIV-1 entry and neutralization sensitivity. Platt *et al*. used sub-clones of JC53 that expressed different levels of CCR5 to show that co-receptor expression levels are limiting for virus infection (Platt *et al*., 1998a). Subsequently, Reeves *et al.* showed that high cell-surface concentrations of CCR5 resulted in rapid rates of fusion and resistance to the gp41 antagonist, T20 (Reeves *et al*., 2002). Because T20 binds to the C-terminal HR domain of gp41 at an intermediary stage of virus entry, it was suggested that the surface concentration of CCR5 controlled the time during which the virus was sensitive to neutralization (Reeves *et al*., 2002). In support of this finding, a small molecule antagonist of CCR5, SCH-351125, has been shown to act synergistically with T-20 by decreasing the availability of the virus co-receptor, thus slowing rates of fusion and increasing the period that HIV-1 is susceptible to gp41 antagonism (Tremblay *et al*., 2002). Chodhury *et al.* showed that levels of CCR5 expression correlated with resistance to monoclonal antibodies that bind to CD4 inducible epitopes (Choudhry *et al*., 2006). Conversely, sensitivity to b12 is not significantly affected by CCR5 surface concentrations. This is

unsurprising because b12 blocks attachment to CD4, which occurs prior to CCR5 engagement. From these data it is clear that the cell-surface concentration of the co-receptor is a critical determinant of virus neutralization for some, but not all, NAbs.

Expression of CCR5 is approximately 100-fold higher in TZM-bl cells than PBMCs, which may partly explain why NAbs such as X5 are more effective in PBMC assays (Choudhry *et al*., 2006). However, disparities in neutralization data obtained with each system are dependent on NAb specificity. For example, Binley *et al.* compared the neutralization phenotypes of 125 primary isolates assayed in PBMCs to the corresponding Env-pseudotypes assayed in U87 reporter cells. Overall, discordant neutralization sensitivities were observed in 24% of all cases. More neutralizing activity was detected with X5 in the PBMC assay, while the opposite was true for antibody 4E10. On the other hand, b12 neutralized similar proportions of virus in both systems (Binley *et al*., 2004). Differences in target cell phenotype may be responsible for these inconsistencies, but the authors could not rule out virus-dependant factors because different types of virus were used in each assay. Additionally, it is unlikely that high CCR5 expression in PBMCs were responsible for the higher levels 4E10 activity because Chodury *et al.* reported that CCR5 expression negatively correlates with 4E10 neutralization (Choudhry *et al*., 2006). Consequently, there are likely to be unknown cellular and viral factors that effect levels of neutralization detected *in vitro* and the results reported by any neutralization assay should be interpreted with caution.

1.17 The natural course of early HIV-1 infection

The majority of HIV-1 infections are acquired sexually by transmission through the genital tract or rectal mucosa. Homogeneity amongst HIV-1 genomes sampled early in infection indicates that most infections arise from a single founder virus, while approximately 10-20% of individuals are infected with two to five antigenically-distinct virions (Keele *et al*., 2008). Studies of rhesus macaques intra-vaginally challenged

with SIV suggest that productive infection initiates in $CD4^+$ T cells expressing the CCR5 chemokine receptor (Li *et al*., 2009a, Miller *et al*., 2005). Intraepithelial dendritic cells (DC) and Langerhan cells in the lamina propria facilitate dissemination of the transmitted virus to $CD4^+$ T cells by a process known as *trans*-infection (Geijtenbeek *et al*., 2000). Dendritic cells capture HIV-1 with C-type lectins, such as DC-SIGN, and deliver virus to $CD4^+$ T cells across a virological synapse (Hubner *et al*., 2009). It has been suggested that direct cell-to-cell transmission of virus may limit the effectiveness NAbs *in vivo*, however, inhibition of *trans*-infection by NAbs has recently been reported (Martin *et al*., 2010).

Replication of HIV-1 remains localized to the mucosa and draining lymph nodes for approximately 10 days, a period known as the eclipse phase because viral RNA is not detectable by conventional clinical assays (Busch and Satten, 1997, Keele *et al*., 2008). Limiting numbers of CD4+ T lymphocytes initially restricts viral replication, but these foci of infection are subsequently expanded, in part, by chemokine-secreting plasmacytoid dendritic cells that recruit additional $CD4^+$ T cells to the mucosa. Li *et al.* demonstrate that SIV infection can be prevented by blocking recruitment of CD4+ T lymphocytes to the endocervical mucosa with anti-inflammatory agents that inhibits the production of chemokines, such as MIP-3α (Li *et al*., 2009a). These encouraging findings suggest that HIV-1 is vulnerable to elimination during the early stages of infection. The challenge to vaccine research is to prime immune responses capable of developing into secondary immune responses within the first few weeks of HIV-1 infection. Therefore, understanding the factors that control early antibody responses to HIV-1 is of central importance to vaccine research and will be the subject of chapter 5.

At the end the eclipse phase the virus disseminates through the lymphatic system. Dendritic cells and macrophages facilitate this process by transporting the virus between the mucosa and lymphoid tissue, particularly gut-associated lymphoid tissue (GALT), which is a major source of $CD4^+CCR5^+$ T cells and bears the brunt of immune destruction during the early stages of infection (Brenchley *et al*., 2004).

Studies of SIV-infected macaques demonstrate that as VL reaches peak levels 30%-60% of all memory $CD4^+$ T cells become infected and die by immune-mediated cell killing or viral cytolysis (Mattapallil *et al*., 2005). Concomitant with increasing viraemia, a systemic immune response ensues, partly due to translocation of commensal bacteria and LPS through compromised GALT tissue in the gut lumen. Leukocytes of myeloid and lymphoid lineage respond to high levels of viraemia by producing type I interferons (IFN), tumour necrosis factor alpha (TNF-α) and interleukins (IL)-1, IL-15, IL-18 and IL-22 (Stacey *et al*., 2009). Although several of these soluble factors have antiviral activity (IFN-α and IFN-β for example), this "cytokine storm" enhances viral replication and contributes to CD4+ T cell apoptosis (Brule *et al*., 2007, Lapenta *et al*., 1999).

During PHI there is a 50% loss of B cell germinal-centers from the GALT (Levesque *et al*., 2009). Additionally, HIV-1 infected patients have unusually high numbers of B-cell subsets characterized as immature cells, exhausted cells and antibody-producing plasmablasts. Most of these features are attributed to the high levels of viraemia, either directly through virus-antibody interactions with the CD21 complement receptor, or through indirect bystander effects mediated by cytokines and cellular interactions. High-level viraemia leads to B cell hyperactivity, hypergammaglobulinaemia, B cell proliferation, expression of apoptosis-signaling molecules, and high incidences of B cell malignancies (reviewed in (Moir and Fauci, 2009b)) (Titanji *et al*., 2005, Ho *et al*., 2006), additionally, low levels of memory B cells have been reported at all stages of infection and this is not associated with levels of vireamia.

Peak levels of viraemia, frequently exceeding 10^6 RNA copies per ml, coincide with the detection of HIV-1 specific antibodies and an associated seroconversion illness (Fiebig *et al*., 2003, Little *et al*., 1999). The most common symptoms are fever, myalgia, arthralgia, rash and night sweats (Daar *et al*., 2001). The severity of seroconversion-illness and the extent and duration of vireamia are associated with rates of

disease progression (Mellors *et al*., 1995). In a study of 2176 acutely infected individuals, a small proportion (7%) spontaneously controlled VL below 400-500 RNA copies per ml and exhibited slower CD4 declines (Madec *et al*., 2005b).

In the absence of ART, VL declines to a stable set-point by 12-20 weeks (Rodriguez *et al*., 2006). Immune hyperactivation persists into the chronic phase of disease and this continues to contribute to T cell loss. Viral load set-point is minimally predictive of progression to AIDS in chronic infection, whereas markers of T cell activation, including CD38 and HLA-DR, have been shown to be strong positive correlates of HIV-1 disease progression (Rodriguez *et al*., 2006, Deeks *et al*., 2004, Giorgi *et al*., 1999) .

Mathematical models based on rates of VL decrease following intervention with ART indicate the average half life of an infected $CD4^+$ T cell is approximately 0.7 days (Markowitz *et al*., 2003). Despite this, relatively steady CD4 counts and VLs are maintained by rates of cell proliferation that exceed 10^9 cells per day and daily viral turnovers exceeded 10^{10} virions (Ho *et al*., 1995, Perelson *et al*., 1996). However, continuous high-level replication of HIV-1 leads to a progressive CD4 T cell loss at a rate of 30-90 cells /mm^3 per year (Stein *et al*., 1992). Eventually, this leads to severe immunosuppression and patients become susceptible to AIDS-defining illnesses. The median CD4 count associated with the development of an AIDS-defining illness was shown to be 67 cells/mm^3, with 10% of patients developing an illness with CD4 counts <200 cells/mm^3 (Taylor *et al*., 1995).

1.18 The role of cellular immune responses in the control of HIV-1

There is substantial evidence to suggest that $CD8^+$ cytotoxic T cell (CTL) responses contribute to the initial decline of VL and to durable control of VL set-points. The initial decline in VL coincides with the appearance of HIV-1 specific CTLs (Borrow *et al*., 1994). Additionally, macaques depleted of $CD8^+$ CTLs prior to challenge with SIV sustain high VLs, strongly inferring an important role for this subset in the early control of viraemia (Schmitz *et al*., 1999). Additionally, a subset of HIV-1 infected patients who

control viraemia in the absence of ART have been variably shown to exhibit strong T cell responses. Patients with VLs below 2000 copies/ml are termed viraemic controllers (VC) and tend to progress more slowly to AIDS. Approximately 1 in 300 patients maintain levels of viraemia below detectable limits of ultrasensitive assays and are known as elite controllers (EC) (Deeks and Walker, 2007). Pereya *et al.* detected higher levels of $CD8^+$ CTLs and $CD4^+$ T helper cells in 124 ECs and VCs compared to 30 subjects with progressive disease. Factors associated with T cell mediated viral control included high levels of expression of IL-2 and IFN-α, and specificity to MHC-restricted epitopes in Gag (Pereyra *et al*., 2008a). The mechanism by which CTLs control HIV-1 replication was thought to be through direct-cytolysis of infected T cell, but this mechanism has recently been questioned by macaque studies that failed to identify changes in rates of $CD4^+$ T cell killing following $CD8^+$ cell depletion. Therefore, other mechanisms, such as the antiviral effects of cytokines, may be more important (Klatt *et al*., Wong *et al*.).

Genetic-linkage studies have shown that HLA-B57, HLA-B27 and HLA-B51 alleles are associated with better prognoses (Carrington and O'Brien, 2003). These genes encode MHC class I molecules involved in antigen-presentation to $CD8^+$ CTLs. Individuals that carry these alleles have been shown to develop potent $CD8^+$ T cell responses directed at epitopes in HIV Gag, which concurs with the bias for Gag-specific CTL responses in ECs (Crawford *et al*., 2007). Population wide analyses of these genetic polymorphisms provide convincing evidence for a protective role of $CD8^+$ T cell responses (Fellay *et al*., 2007), but on an individual basis they are not always predictive of better clinical outcomes. For example, in a HIV transmission pair (ie two patients infected with an antigenically similar virus), rapid disease progression was observed in the transmitter, while the recipient controlled VL to undetectable levels, despite both patients carrying the HLA-B*57 allele (Bailey *et al*., 2008). Overall, these findings support a protective role for $CD8^+$ T cell reponses *in vivo*, but suggest that other factors may also be important.

1.19 The role of neutralizing antibodies in the control of viral load.

The role of neutralizing antibodies in the control of VL is unclear. Anti-HIV-1 IgM has been detected within 3 days after the onset of symptoms (Cooper *et al*., 1987). However, standard clinical assays generally detect antibodies targeting p24 core antigen within 4 to 10 weeks after transmission. The first antibodies targeting Env may be gp41-specific. Tomaras *et al.* detected gp41-specific IgM within virion-antibody immune complexes 8 days after VL was first detected. Antibody-dependent complement-mediated HIV-1 inactivation is observed *ex vivo* with plasma from acutely infected individuals (Aasa-Chapman *et al.,* 2005), and there are conflicting reports as to whether this contributes to early viraemia control (Huber *et al*., 2006, Tomaras *et al*., 2008).

Mature IgG responses capable of neutralizing autologous virus have been detected within 4 weeks after the onset of symptoms. However, most NAb responses are first detected after 12 weeks or more following transmission, after the initial decline in VL (Gray *et al*., 2007, Wei *et al*., 2003 ,Aasa-Chapman *et al.,* 2004). Therefore, it is unlikely that NAbs control viraemia during the early stage of PHI. However, it is less clear whether NAbs contribute to the durable control VL set-point at later stages of infection.

Passive infusions of b12 exerted minimal control on established HIV-1 infection in a SCID-humanized mouse model of HIV-1 infection, although transient suppression of VL was observed in mice administered cocktails of b12, 2G12 and 2F5 (Poignard *et al*., 1999). Neutralization sensitive viruses were isolated from b12 treated mice, indicating that neutralizing titres of antibody were ineffective at inhibiting the replication of HIV-1 *in vivo*. However, in these experiments proviruses were isolated from cells of spleen and lymph node biopsies, which may not reflect actively replicating virus (Nickle *et al*., 2003, Ruff *et al*., 2002). In fact, the majority of virus isolates were neutralization resistant and escape mutants were detected 7 days after b12 transfusion, suggesting that escape occurred rapidly. Rapid

selection of NAb-escape mutants does not imply ineffective neutralization; it indicates that neutralization-sensitive viruses can be eliminated by neutralizing antibodies.

In humans, antibody escape mutants have been detected as early as 12 weeks post infection (Goonetilleke *et al*., 2009). Goonetillike *et al.* identified replacement of wild-type founder sequences with viruses carrying envelope mutations at known neutralizing epitopes. Complete loss of founder virus sequences implies that NAbs effectively eliminated the quasi-species majority, which confirms that NAbs exherts some control on viral replication. However, the authors did not confirm the neutralization-sensitivities of the wild-type and mutant viruses. Although these mutations were previously shown to confer neutralization resistance in other studies, there is no guarantee that these mutations transfer similar phenotypes to antigenically-distinct viruses. Nevertheless, if these findings can be confirmed, it seems likely that NAbs may inhibit viral replication early in infection.

Transient selection of neutralization escape mutants does not imply durable control of VL. However, several studies conducted in the late 1980's and 1990's claimed that NAb responses correlated with slower rates of disease progression. Cross-sectional and longitudinal studies showed higher levels of neutralization in long-term non-progressors (LTNPs) compared with rapid progressors (Karpas *et al*., 1988, Cao *et al*., 1995, Pilgrim *et al*., 1997, Scarlatti *et al*., 1996, Zhang *et al*., 1997). However, in none of the studies was it possible to decipher the clinical impact of NAbs from other confounding factors. Cecilia *et al.* attempted to resolve this issue by studying NAb responses in pairs of LTNPs and rapid progressors matched according to age, sex, race, and number of circulating CD4+ lymphocytes (Cecilia *et al*., 1999). Neutralizing responses were shown to be significantly lower in the rapid progressors when they had developed AIDS, but prior levels of neutralization were not predictive of these differing rates of disease progression. Thus, it was not clear whether low-level neutralizing activity was cause or effect of AIDS pathogenesis. Notably, a case study of heterozygotic perinatally-infected twins reported lower

levels of NAbs and antibody-dependent cellular cytotoxicity in the child that rapidly progressed to AIDS (Hutto *et al*., 1996). Lambotte *et al.* also observed higher levels of antibody-dependant cell mediated cytotoxicity in ECs compared with normal chronic progressors (Lambotte *et al*., 2009). Therefore, it is possible that non-neutralizing effector functions of antibodies may be important correlates of disease control.

Studies conducted more recently suggest that NAb responses are not associated with better clinical outcomes and may positively correlate with VL. In a study by Li *et al,* fewer elite controllers had broad neutralizing activity than viraemic patients (Li *et al*., 2007). Furthermore, Doria-Rose *et al.* investigated 24 ECs, 37 patients with low viraemia and 52 chronic progressors and demonstrated that only 25% of the ECs had broad NAb activity compared to 42% in the other two groups (Doria-Rose *et al*., 2009). Mahalanabis *et al.* reported variable levels of neutralization against autologous viruses derived from viraemic controllers, although neutralizing-serum titres varied according to the autologous HIV clone used in the neutralization assay. Interestingly, NAb-sensitivity did not vary amongst HIV-clones derived from one of two patients with elite control of viraemia, which may indicate that NAb responses effectively limited viral diversity in this individual (Mahalanabis *et al*., 2009b). Bailey *et al.* also demonstrated low levels of Env diversity in ECs and equivalent levels of neutralizing titres to chronic disease progressors (Bailey *et al*., 2006).

A possible reason for the discrepant results reported by investigation of NAb responses *in vivo*, relates to differences in study design. The early studies grouped patients according to CD4 count, while more recent studies have tended to group patients according to VL (Table 1.2A vs. Table 1.2B). Additionally, the early studies compared LTNPs, who had been infected for several years, with rapid progressors, who had been infected for shorter periods. This is problematic because broad and potent neutralizing

Table 1.2A Studies that suggest a positive correlation or no correlation between NAb potency and viral load

Study	Year	Group*	General NAb trend	n	VL RNA copies/ml	CD4 count cells/mm^3	Notable exceptions	Neutralization Assay	Virus
Harrer et al	1996	LTNP CP	Similar	10 7	<50- 302,000 -	>500 for >10 years na		PBMC	Het
Bailey et al	2006	ES CP	Similar	9 7	<50 >10,000	- -		Pseudovirus & TCLA	Aut & Het
Pereya et al	2008	EC VC CP		17 17 20	<50 50-2,000 >10,000	- - -	ECs had Variable NAb response	Pseudovirus	Aut & Het
Doria-Rose et al	2009	LTNP SP CP		24 37 52	mean <50 mean 1,665 mean 1,8531	- - -	25% ECs had broad NAb response	Pseudovirus	Het
Li et al	2007	LTNP SP CP		18 8 6	<1,000 1,000-12,000 2,500 -250,000	>500 - <500		Pseudovirus	Het
Lambotte et al	2009	VC CP		13 75	<400 4,000-2,7127	- -	ECs had higher levels of ADCC	Pseudovirus	Het
Deeks et al	2006	VC CP		8 19	<2,000 500-1,000	- -		Pseudovirus	Aut & Het
Mahalanabis et al	2009	EC CP		2 11	<75 <2,000	- -	Variable NAb responses	Pseudovirus	Aut

Table 1.2B: Studies that suggest NAb responses are associated with slower rates of disease progression

Study	Year	Group*	General NAb trend	n	VL	CD4 count	Notable exceptions	Neutralization Assay	Virus
Pantaleo et al	1995	LTNP CP		15 18	70,000 >1,000,000	>600 for >7 yrs 200-600		TCLA	Het
Cao et al	1995	LTNP CP		10 4	- -	>500 -		PBMC	Het
Harrer et al	1996	LTNP STNP CP		6 6 5	- - -	>600 for >10 yrs >600 for 2-7 yrs 10-371		PBMC & TCLA	Aut & Het
Montefiori et al	1996	LTNP CP		12 13	- -	>600 for >7 yrs <20-800		PBMC & TCLA	Aut & Het
Cecilia et al	1998	LTNP RP		14 14	- -	>316 for 7 yrs decline >53 cells per qtr		GHOST (GFP)	Het

Table 1.2A: Studies that suggest a positive correlation or no correlation between NAb potency and VL

Two studies reporting similar levels of neutralizing activity between patients grouped according to VL are shown along with eight studies reporting lower levels of neutralizing activity in patients with low VLs compared to patients with high VLs. The patient groups (Long-term non-progressors (LTNP), elite controllers (EC), chronic progressors (CP) and viraemic controllers (VC)) are shown in the third column and correspond to the definitions given in each study. For these studies, VLs were used to assign patients to each group. Note that the criteria for each group differ between the studies (column 6). The assays used by each study are shown in the far right columns. Three studies assayed neutralization with autologous (Aut) and heterologous (Het) viruses, while five studies assayed responses with heterologous viruses only.

Table 1.2B: Studies that suggest NAb responses are associated with slower rates of disease progression

Five studies are shown that report higher levels of neutralizing activity in LTNPs compared to CPs, short term non-progressors (STNPs), and rapid progressors (RPs). These studies grouped patients according to their $CD4^+$ T cell counts and durations of infections. GHOST cells are human osteogenic sarcoma (HOS) cells that stably express the virus entry receptors along with a green fluorescence protein (GFP) reporter gene which is used to detect HIV-1 infection.

responses develop in response to sustained levels of viraemia (Sather *et al*., 2009). This supports the view that sustained levels of antigen are required to stimulate B cell responses, as demonstrated by observations that antibodies to HIV-1 occasionally become undetectable in patients receiving ART (Hare *et al*., 2006). Therefore, NAbs may accumulate and mature in viraemic LTNPs, while elite controllers may lack sufficient levels of viraemia to stimulate antibody production.

1.20 The impact of ART on the control of HIV-1 infection

Since HIV-1 was first discovered as the causative agent of AIDS, there has been considerable progress in the development of ART. The first drug to be licensed was Zidovudine in 1987, which was shown to decrease mortality and the risk of opportunistic infections in a randomized placebo-controlled trial of patients with AIDS defining illnesses (Fischl *et al*., 1987). This drug falls into the class of nucleoside reverse transcriptase inhibitors (NRTIs) which are metabolized by cellular kinases to form nucleotide analogues that lack 3' hydroxyl groups required during RT-dependent cDNA synthesis (Horwitz J.P., 1964). Four additional mechanistic classes of ART have since been licensed for the treatment of HIV-1, namely, non-nucleoside RT inhibitors (NNRTIs), protease inhibitors (PIs), integrase inhibitors and viral-entry inhibitors. Current British guidelines for the treatment of HIV-1 recommend initiation of combination ART consisting of dual NRTI with either a PI or NNRTI (Gazzard *et al*., 2008).

An editorial published in the New England Journal of Medicine in 1996, entitled "Time to hit HIV, early and hard" advocated the early initiation of combination therapy and it was common practice to initiate therapy in patients with CD4 counts less than 500 cells/mm^3 (Ho, 1995). However, an international collaborative study of 62,760 participants demonstrated that although ART reduced the overall risk of death by approximately 50%, the survival benefit was only 1% for patients with CD4 counts more than 500 cells/mm^3 (Hogg *et al*., 2001). Observations of virologic failure and drug resistance are major arguments against early therapy, because treatment efficacy needs to be sustained throughout the course of the disease. Drug toxicities and complicated dosing regimens lead to poor drug adherence

rates, which in turn leads to the development of drug resistant virus (reviewed in (Rowland-Jones and de Silva, 2008)). For this reason current UK, US, and WHO guidelines recommend commencing treatment when $CD4^+$ counts reach 350 cells/mm^3 (Office of AIDS Research Advisory Council (OARAC), December 2009) (Gazzard *et al*., 2008).

There is some evidence supporting the use of ART-initiation at thresholds greater than 350 cell/mm^3. Notably the NA-ACCORD and UK CHIC studies reported lower rates of mortality and morbidity in patients who initiated therapy with CD4 counts greater than 350 cell/mm^3 (Kitahata *et al*., 2009, Phillips *et al*., 2007). However, NA-ACCORD was not randomized and was limited by large numbers of patient exclusions. Although UK-CHIC analysed larger numbers of patients (17,609), insufficient data was collected on causes of morbidity and mortality to ascertain net-benefit to risk ratios associated with commencing ART in the presence of high CD4 counts. Randomized trials are therefore needed to definitively address the optimal timing for initiating ART with respect to CD4 count.

1.21 Rationale for administering ART in early infection

There is now a strong case for early treatment regimes aimed at limiting immune destruction in PHI. Firstly, lower levels of VL are associated with less viral diversity, which may limit escape from adaptive immunological responses (Altfeld *et al*., 2001). Secondly, early treatment has been associated with restoration of B and T lymphocyte number and function, which has been associated with improved antiviral responses (Hoen *et al*., 2007, Titanji *et al*., 2005). Thirdly, some preliminary reports show long-lasting virus suppression and sustained levels of $CD4^+$ T cell counts after termination of early therapy; ultimately, this may prolong the duration of symptom-free disease and reduce the demand for ART in the long-term (Steingrover *et al*., Hecht *et al*., 2006). Finally, lower VLs in primary infection are associated with reduced rates of transmission (Wawer *et al*., 2005, Attia *et al*., 2009)

Early initiation of ART has been shown to lead to a more robust immunological recovery following PHI. A study by Streeck *et al.* monitored HIV-1 specific $CD8^+$ T cell responses in 20 acutely infected individuals by IFN-γ enzyme-linked immunospot assay (ELISpot) and flow cytometry. The 12 patients who opted to initiate early ART for 24 weeks had HIV-specific $CD8^+$ T cells that showed enhanced differentiation from an effector memory to an IFN-γ^+ phenotype. Six months after treatment ended, patients had higher levels of $CD8^+$ T cell activation and preserved $CD4^+$ T cell numbers compared to untreated patients, despite similar levels of VL to treatment naïve patients (Streeck *et al.*, 2008). This suggests that short courses of ART in PHI may have long-term benefits. Early initiation of ART may also result in the restoration of HIV-specific $CD4^+$ T helper cell responses, which has been associated with transient control of viraemia following treatment interruption (Malhotra *et al*., 2000, Ferrantelli *et al*., 2004).

Studies have shown that ART administered in acute infection can preserve B cell function. Morris *et al.* demonstrated that B cell hyperactivity and hypergammaglobulinaemia resolve in response to ART administered during acute and chronic stages of infection (Morris *et al*., 1998). Additionally, early initiation of ART has been associated with reduced rates of B cell apoptosis, and partial restoration of memory B cell pools (Titanji *et al*., 2005). Preservation of B cell responses was recently reported following early initiation of ART in HIV-1 infected infants (Pensieroso *et al*., 2009). However, B cell memory cells were not restored by ART in chronic infection, suggesting that early intervention may be required to prevent permanent B cell depletion (Hart *et al*., 2007). Limiting B cell and $CD4^+$ T cell dysfunction with short courses of ART in PHI could potentiate NAb responses, which may contribute to the control of viraemia after treatment cessation.

Although several studies have demonstrated clinical benefits following early-ART intervention, it is unclear whether these protective effects are limited to the duration of therapy. Currently, decisions regarding early treatment are not evidence based and are left to the discretions of the clinician and patient. In order to determine the long-term impact of early treatment more data are needed from

suitably-powered randomized-controlled trials, such as the Short Pulse Antiretroviral Therapy at seroConversion (SPARTAC) study. This trial is ongoing and has recruited 366 eligible participants from genitourinary medicine clinics in the UK, Australia, Italy, Uganda, South Africa, Spain and Brazil. Upon confirmation of PHI, each patient is randomized to receive either 12 weeks or 48 weeks ART, or no therapy. The primary outcome measure is the time taken for CD4 counts to decrease below 350 cells per/mm^3 on two consecutive occasions, assessed one month apart. All patients are to be followed until 130 primary end-point events are detected. The primary objective of SPARTAC is to determine whether administering ART for a limited period during PHI can slow rates of $CD4^+$ T cell loss after treatment ends (Babiker and Gibb, 2006). The decision to treat patients for a minimum period of three months was informed by a pilot study of 90 patients (Fidler *et al*., 2002) that showed this intervention was well tolerated and did not induce ART resistance. The 48 week treatment arm was included to assess whether longer treatment regimes improved the clinical outcome further, although SPARTAC is not specifically-powered to detect a difference between the 12 and 48 week trial arms.

Clinical specimens are collected from patients enrolled into SPARTAC at 4 to 12 week intervals and used to assess the impact of early ART on humoral and cellular immune responses. Work in our own lab has focused on neutralizing responses that develop after patients discontinue therapy. Because investigators are blinded to the treatment arm of the patient, it is currently not possible to compare patients who received early ART with those who did not. However, neutralizing responses can be assessed in individuals randomized into the two ART treatment arms.

1.22 Outline of this thesis

The SPARTAC study provided a useful platform with which to study changes in neutralizing antibody activity that develop after patients discontinue ART. We hypothesized that rebounding VLs stimulate the production of neutralizing antibodies after ART cessation, resulting in an association between quantities of circulating virus and subsequent levels of neutralizing activity. Furthermore, NAb reponses were

predicted to inhibit the replication of neutralization-sensitive quasispecies and select NAb-resistant virus. In order to determine whether antibody selection contributed to the control of viral load, sequencing analysis of HIV-1 *env* was undertaken in one patient with a clinical history that was suggestive of antibody-mediated control of VL. The patient, who was enrolled into the SPARTAC pilot study, was diagnosed with a lymphoplasmacytic B cell lymphoma. He had also been diagnosed with an acute hepatitis B virus (HBV) infection two years prior to HIV-1 seroconversion. Following a three-month course of early ART the patient developed a VL set point of 10^5 RNA copies per ml. Three years later the patient became unwell and his lymphoma required treatment with a monoclonal antibody (rituximab) that targets and depletes $CD20^+$ B cells. Surprisingly, this led to a transient 1.7 $\log_{10}$ increase in HIV-1 VL. The patients HBV infection also reactivated following rituximab therapy. The clinical details of this case led us to hypothesize that NAbs were important in controlling the patient's HIV-1 VL. In order to investigate this possibility, several techniques were employed to characterize the patient's virus and NAb response before and after B cell depletion. The results of this unique case study will be presented in chapter 4.

This thesis examines three aspects of HIV-1 antibody research. Firstly, the development and validation of an HIV Env-pseudotype neutralization assay will be reported, along with novel techniques that improve the sensitivity and specificity of this type of assay. Secondly, we examine the role of NAbs in natural infection. We report the only documented case of B-cell depletion in an HIV-1 infected human and present compelling evidence that NAbs contributed to HIV-1 control in this individual. The relevance of this case to the wider field will be discussed. The final chapter examines how levels of viraemia during the early stages of HIV-1 infection control the development of neutralizing antibody responses. This investigation focuses on patients enrolled into the SPARTAC trial who received early, short-courses of ART. This allowed us to examine the temporal association between developing NAb responses and VL rebound after ART-cessation.

Chapter 2

Materials and Methods

2.1 Mammalian cell lines and tissue culture maintenance

The human epithelial kidney cell line 293T clone 17 (293T/17) is a derivative of the 293tsA1609neo cell, which constitutively expresses the simian virus 40 (SV40) large T-antigen (DuBridge *et al*., 1987). Clone 17 has been specifically selected for its high transfectability and its capacity to produce high titres of infectious retrovirus (American Type Culture Collection (ATCC), CRL-11286). The indicator cell line, TZM-bl was used to quantify infectious pseudovirus particles (described in section 1.16) (National institute for health (NIH) AIDS Research and Reference Reagent Program) (Wei *et al*., 2002). Both cell lines were cultured in complete Dulbecco's modified eagle's medium (complete DMEM), containing 4.5 g/l glucose, L-glutamine, 10 % (v/v) fetal-calf serum (FCS) (heat inactivated at 56°C for 1 hour), 100 U/ml penicillin G and 100 µg/ml streptomycin (Invitrogen Life Technologies, UK).

Cells were passaged when 80-90% confluent. Adherent-cell monolayers were washed once with Trypsin-ethylenediaminetetraacetic acid (Trypsin-EDTA) (Invitrogen) and incubated with Trypsin-EDTA at 37°C for 2-5 min. Cells were resuspended in 10 ml of complete-DMEM and centrifuged at 400 g for 5 min. Cell pellets was resuspended in complete-DMEM and one twentieth of the volume was transferred to a tissue culture flask in 5-6.25 ml of complete DMEM per cm^2 of the flasks surface area.

2.2 DNA vectors used for cloning, sequencing and pseudovirus construction

Plasmid pcDNA3.1(+) and phagemids KS Bluescript II and SK Bluescript II (Stratagene) were used to clone HIV-1 envelope genes (Figure 2.1). Expression vector pMD-G encodes vesicular stomatitis virus G-protein (VSV-G) from a CMV promoter (Naldini *et al*., 1996). Expression vector pHXB2-*env* contains the HIV-1 envelope gene expressed from an SV40 promoter. The HIV-1 backbone pNL4-3Δenv is derived from a full-length HIV-1 chimera (pNL4-3) consisting of the 3' half of HIV_{LAV} and the 5' half of HIV_{NY5}. The blunt-ended proviral DNA genome was cloned into the multiple cloning site (MCS) of pUC18 (Adachi *et al*., 1986). The LAV envelope gene was made defective by mutating at the start codon and at a unique KpnI restriction site (Dorfman *et al*., 2002) (Figure 2.2).

Figure 2.1 DNA vectors used for HIV-1 envelope cloning

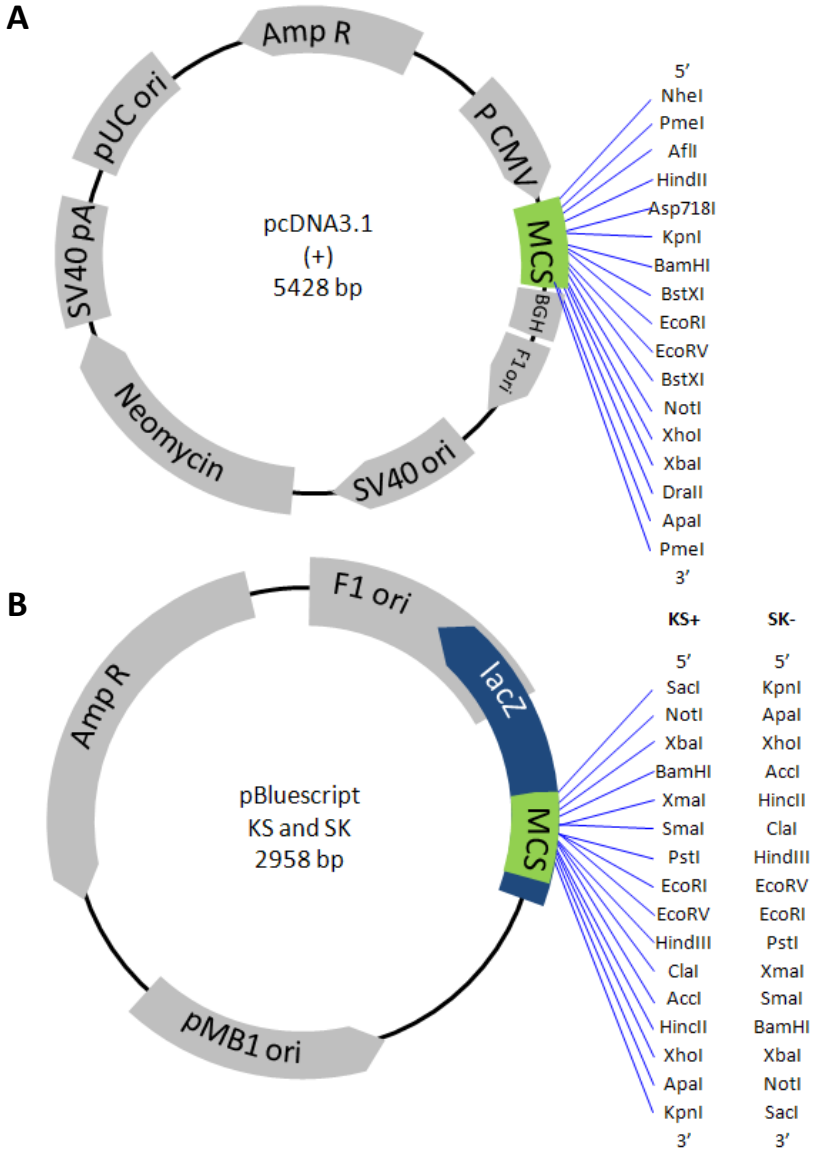


Figure 2.1 A: PCR amplified HIV-I *env* was cloned in plasmid pcDNA3.1 using 5'XhoI-3'ApaI or 5'NotI-3'ApaI restriction sites downstream of the CMV promoter (P CMV) and upstream of the bovine growth hormone polyadenylation sequence (BGH). The neomycin resistance gene (neomycin) is expressed with an SV40 early promoter and origin (SV40 ori) and SV40 polyadenylation sequence (SV40 pA) (neomycin selection was not used). The pUC origin of replication (pUC ori) initiates plasmid replication in *E.coli*. The F1 origin (F1 ori) initiates plasmid replication in phage and was not used. Figure 2.1B: Envelope genes from pcDNA.*env* were subcloned into phagemids KS pBluescript II and SK pBluescript II. Both phagemids are identical except for oppositely orientated MCS which intersperse a *lacZ* gene and *lac* promoter. The pMB1 origin of replication (pMB1ori) replicates plasmids in *E.coli.* The ampicillin resistance gene (Amp R) confers antibiotic resistance.

Figure 2.2 DNA vectors used for pseudovirus construction

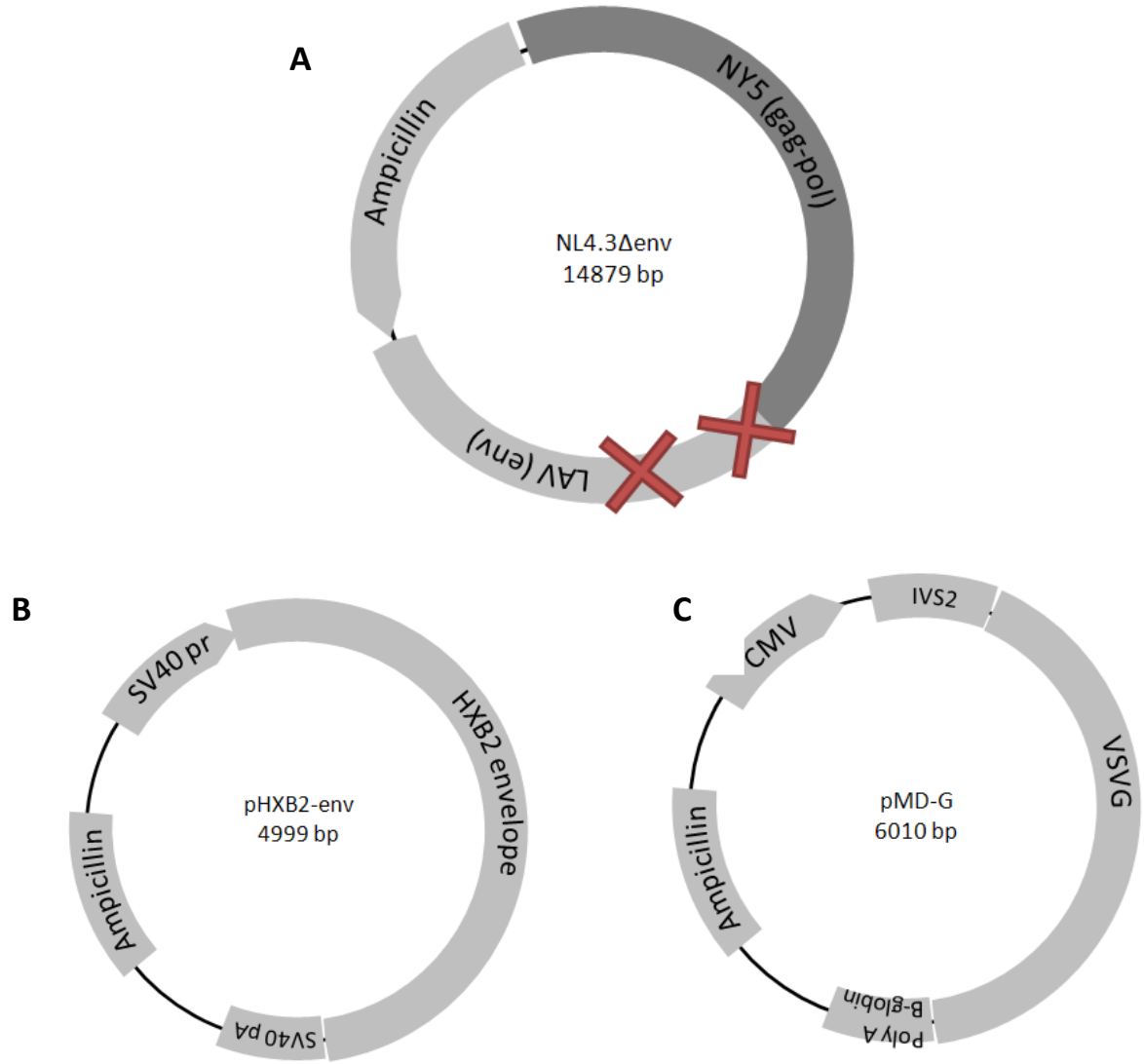


Figure 2.2 A: The full-length HIV-I backbone, NL4-3Δenv, is a chimera of the HIV-1 strains, HIV_{NY5} and HIV_{LAV}. The native 5' LTR of HIV_{NY5} serves as a promoter for transcription. The HIV_{LAV} *env* gene is non-functional owing to frame-shift mutations at the start codon and at a unique KpnI restriction site (red crosses).

Figure 2.2 B: pHXB2-env encodes full length HIV_{HXB2} envelope under transcriptional control of an SV40 promoter (SV40 pr).

Figure 2.2 C: Plasmid pMD-G consists of a *vsv-g* gene flanked by a 5' intervening sequence 2 (IVS2) and polyadenylation sequence from a human β-globin gene. The *vsv-g* gene is transcribed from a CMV-immediate-early promoter (CMV). Plasmids pNL4-3Δenv, pHXB2-env and pMD-G encode an ampicillin resistance gene for antibiotic selection in *E.coli*.

Dr Massimo Pizzato kindly provided pHXB2-env, pMDG and pNL4-3Δenv. Plasmids encoding HIV-1 clade B and clade C reference envelopes were obtained from the NIH AIDS Research and Reference Reagent Program (Li *et al*., 2005, Bailey *et al*., 2006).

2.3 Antibodies, plasma and recombinant proteins.

Pooled plasma derived from HIV-uninfected donors was obtained from Autogen Bioclear. Neutralizing monoclonal antibodies 447-52D and 2G12 were obtained from the National Institute for Biological Standards and Control (NIBSC, Potters Bar, UK). Antibodies b12 and 4.8d were gifts from Professor Dennis Burton (Scripps Research Institute, La Jolla, US). The CD4 peptide mimic, M33, is a 27 amino-acid peptide mimicking the gp120 binding site of CD4 and was provided by Professor Quentin Sattentau (William Dunn School of Pathology, Oxford University, UK) (Martin *et al*., 2003). Recombinant gp120 derived from clade B HIV-I strain BaL, expressed in Chinese hamster ovary (CHO-K1) cells, was provided by Dr Simon Jeffs (Jefferiss Trust Laboratories, Imperial College, UK).

2.4 Clinical assays of HIV-1 viral load

The PCR-based Amplicor HIV-1 Monitor v1.5 Assay (Roche) quantifies HIV-I RNA from plasma samples mixed with known concentrations of a synthetic protein-coated RNA construct which serves as an internal quantitation standard (QS). The RNA is RT-PCR amplified using *gag* specific primers and *Thermus thermophilus* DNA polymerase (*rTth pol*), which has RT and DNA polymerase activity. Biotin labeled oligonucleotide probes are hybridized to amplified DNA products to allow quantification of the QS and viral RNA with avidin-horseradish peroxidase (HRP) conjugates. The amount of bound amplicon is determined using an ELISA plate reader after the addition of an HRP-specific colorimetric substrate.

The Chiron v3.0 or Versant branched DNA (bDNA) HIV-RNA v3.0 assay (Bayer, NY, US) uses bDNA nucleic acid hydribization to quantify VL without amplifying the RNA target. Oligonucleotides are used

to capture viral RNA to the base of a microtitre well, while a second set of oligonucleotides amplifies a chemiluminescent signal.

2.5 Clinical assays for the quantification of antibodies.

Quantification of total IgG, IgM and IgA was performed using an automated immunonephelometric Beckman Immage system (Beckman-Coulter Diagnostics, USA). The technique measures the light-scattering properties of antibody/latex-particle immune complexes (Denham *et al*., 2007). Anti-hepatitis B surface antigen (HBsAb) was quantified by ELISA using the Axsym Abbott system (Abbott Diagnostics, Wiesbaden, Germany). Both assays are validated for diagnostic purposes and were performed at the Clinical Biochemistry Laboratory at St Mary's Hospital, Paddington.

2.6 Extraction of viral RNA from human plasma for RT-PCR amplification *env*

Viral RNA was extracted from cryo-preserved, EDTA or acid-citrate-dextrose (ACD) plasma, for RT-PCR amplification of HIV-1 *env.* Where stated, virus was concentrated from 3 ml of plasma mixed with 9 ml of phosphate buffer saline (PBS) (Sigma Aldrich), by ultracentrifugation at 60,000 g for 2 hr at 4°C (Sorvall Combi AH-629 rotor). Supernatants were decanted and viral pellets were resuspended in 140 µl of PBS. Concentrated virus, or 140 µl of unconcentrated plasma were processed using a QIAamp viral RNA extraction kit (QIAGEN, UK). Virus was lysed with 540 µl of buffer AVL (supplied) containing 10 ng/µl poly-A carrier RNA. After 10 min incubation at room temperature (18-22°C), samples were diluted twofold with ethanol, vortexed for 15 sec and passed through a silca-resin centrifuge column at 16,000 g for 1 min. Adsorbed RNA was washed with 500 µl each of buffers AW1 and AW2 (supplied) by successive centrifugations at 16,000 g for 1 min. The column was dried by a further 2 min centrifugation at 16,000 g and viral RNA was eluted with 30-60 µl of buffer AVE (supplied).

2.7 Reverse transcription of viral RNA

Viral RNA was reverse transcribed to cDNA using the *nef*-specific primer, EnvN (Table 2.1). First, 10-30 µl of viral RNA was annealed to 2 pmol of EnvN and 10 nmol of each of the deoxyribonucleotide triphosphates (dNTPs) (deoxyribo-adenosine triphosphate (dATP), deoxyribo-thymidine triphosphate (dTTP), deoxyribo-cytidine triphosphate (dCTP), and deoxyribo-guanosine triphosphate (dGTP)), by heating to 65°C for 5 min in a GeneAmp PCR System 9700 thermocycler, then incubating on ice for 1 min. Two-hundred units (U) of recombinant Moloney murine leukemia virus RT (Superscript III, Invitrogen) was added to each reaction in the manufacturers supplied buffer to yield final concentrations of 5 mM 1,4-dithiothreitol, 50 mM Tris-HCl (pH 8.3), 75 mM potassium chloride (KCL), 3 mM magnesium chloride ($MgCl_2$), 500 µM dNTP and 100 nM EnvN. Reverse transcription was performed at 25°C for 15 min, then at 55°C for 2 hr. The reaction was terminated by denaturing Superscript III RT at 70°C for 15 mins.

2.8 PCR amplification of full-length HIV-1 envelope for construction of expression plasmids.

Full length HIV-I *env* was amplified from cDNA by nested-PCR with Easy-A high fidelity PCR cloning enzyme (Stratagene, UK). This enzyme is a fusion of 5 U/µl Thermus aquaticus (Taq) DNA polymerase (5 U/µl), 4 U/µl recombinant Pyrococcus furiousus (Pfu) DNA polymerase, and 40 ng/µl recombinant Pfu polymerase enhancing factor (P45). Viral cDNA was added to the supplied enzyme-reaction buffer supplemented with 200 µM dNTPs, 100 nM outer-sense primer EnvA, and 100 nM outer-antisense primer, EnvN, made-up to a final volume of 50 µl with nuclease-free water (Sigma). First-round products were amplified using a thermo-cycler programmed as follows: 2 min denaturation at 95°C followed by 10 cycles consisting of denaturation (95°C for 40 s), annealing (50°C for 30 s) and extension (72°C for 3 min 30 s) followed by a further 25 cycles of denaturation (95°C for 40 s), annealing (55°C for 30 s) and extension (72°C for 3 min 30 s). Thermo-cycling was followed by a final incubation at 72°C for 5 min. One microlitre of each reaction was used as the template for second-round amplifications with 100 nM inner

Table 2.1 Primers used for PCR amplification, sequencing, mutagenesis and quantitative-RT PCR

Application	Primer	Orientation	Sequence (5'→3')	HXB2 numbering	Restriction site	Ref
Reverse transcription HIV-1 *env*	EnvN	anti-sense	CTG TCA ATC AGG GAA GTA GCC TTG TGT	5954←5982		1
PCR amplification HIV-1 *env*	EnvA	outer sense	GGC TTA GGC ATC TCC TAT GGC AGG AAG AA	9145→9171		1
	EnvN	outer anti-sense	CTG TCA ATC AGG GAA GTA GCC TTG TGT	5954←5982		1
	EnvF2	inner sense*	GGG CTC GAG GCG GCC GCG AGC AGA AGA CAG TGG CAA TG	6207→6227	*XhoI-NotI*	this study
	EnvF3	inner sense*	GGG CTC GAG GCG GCC GCG AGC AGA AGA CAG TGG CAA TGA	6207→6228	*XhoI-NotI*	this study
	EnvR2	inner anti-sense*	AAA TCT AGA GGG CCC CCA CTT GCC ACC CAT RTT A	8793←8811	*XbaI-ApaI*	this study
	EnvR3	inner anti-sense*	AAA TCT AGA GGG CCC CCA CTT GCC ACC CAT RTT ATA GC	8789←8811	*XbaI-ApaI*	this study
	Env10F	outer sense	CTA TGG CAG GAA GAA GCG GAG AC	5968→5990		2
	Env13R	outer anti-sense	CTA TCT GTC CCC TCA GCT ACT GC	8707←8685		2
	Env11F	inner sense	GCA TGA GGA TAT AAT CAG TTT ATG GG	6536→6561		2
	Env12R	inner anti-sense	CAA ATG AG TTT TCC AGA GCA ACC C	8035←8012		2
	JAE1	sense	CACAGTACAATGTACACATG	6953→6972		3
	JAE4	anti-sense	ACAATTTCTGGGTCCCCTCC	7320←7339		3
Mutagenesis HIV-1 *env*	R339E/F	sense	ATT GTA ACA TTT CTA GAG TAG AAT GGG AAG ACA CCT TAA	7213→7251	*XbaI*	this study
	R339E/R	anti-sense	TTA AGG TGT CTT CCC ATT CTA CTC TAG AAA TGT TAC AAT	7213←7251	*XbaI*	this study
	R339N/F	sense	ATT GTA ACA TTT CTC GAG TAG AAT GGA ATG ACA CCT TAA	7213→7251	*XhoI*	this study
	R339N/R	anti-sense	TTA AGG TGT CAT TCC ATT CTA CTC GAG AAA TGT TAC AAT	7213←7251	*XhoI*	this study
	Q363R/F	sense	TAA AAC AAT AAT CTT TAA TCG ATC CTC AGG A	7292→7322	*ClaI*	this study
	Q363R/R	anti-sense	TCC TGA GGA TCG ATT AAA GAT TAT TGT TTT A	7292←7322	*ClaI*	this study
Sequencing HIV-1 *env*	ENV12F	sense	AGG AGG GGA CCC AGA AAT TG	7319→7338		1
	ENV11R	anti-sense	TGG GAG GGG CAT ACA TTG C	7521←7539		1
	Env11F	sense	GCA TGA GGA TAT AAT CAG TTT ATG GG	6536→6561		1
	Env12R	anti-sense	CAA ATG AGT TTT CCA GAG CAA CCC	8035←8012		1
SG-PERT BMV	BMV129	sense	GGT CTC TTT TAG AGA TTT ACA GTG			4
	BMV131	anti-sense	CGT GGT TGA CAC GCA GAC CTC TTA C			4
	BMVF1	sense	TTG TCG GCT TTA CCT GCT TT			this study
	BMVR1	anti-sense	TAG TTG TTG GGC TTC GCT TT			this study

Table 2.1 The oligonucleotides shown in this table were used for RT-PCR amplification of HIV-1 *env* (section 2.7-2.8), mutagenesis of Rit.336d.c3 *env* (section 2.24), sequencing (section 2.27), and the SYBR-Green II product enhanced reverse transcriptase assay (SG-PERT) described in section 2.25. Primers designed by the candidate are indicated. Equal amounts of primers EnvF2 and EnvF3 were mixed prior to use in PCR amplifications of full length HIV-1 *env*, as were primers EnvR2 and EnvR3 (*). Restriction sites used for cloning and mutagenesis are underlined. Primers indicated by the following references have been described in previous studies: 1 (Derdeyn *et al*., 2004), 2 (Oelrichs *et al*., 2000), 3 (Voulgaropoulou *et al*., 1999) and 4 (Silver *et al*., 1993). All primers were synthesized by Eurogentec, UK.

sense primer, EnvF2/F3, and 100 nM inner-antisense primer, EnvR2/R3 (Table 2.1), using the same buffer conditions as the first-round reaction. The inner primers contained degenerate nucleotide bases to account for common variations in the primer binding sites identified in the Los Alamos sequence database. Thermo-cycling conditions were the same as for the first-round amplification, except for a shorter extension time of 2 min 45 sec. Five microlitres of each second-round PCR product were mixed with 1 µl of DNA loading dye (Promega) and analysed by electrophoresis through 1% agarose gel (1% (w/v) agarose, Tris-acetate-EDTA (TAE) electrophoresis buffer (40mM Tris acetate, 1 mM EDTA) and 0.5 µg/ml ethidium bromide). After 40 min electrophoresis at 120 Volts, separated DNA was visualized under ultraviolet (UV) light with a transilluminator (Gel-Doc).

2.9 Purification of PCR amplified DNA

Amplified envelope genes were purified using Genejet spin columns (Fermentas) using the buffers supplied by the manufacturer. Each PCR product was mixed with 2 volumes of binding buffer, which contains the chaotropic salt, guanidine thiocyante, to precipitate proteins and to provide the high-salt conditions necessary to adsorb DNA to the silica-resin of the Genejet spin column. The DNA solution was passed through the column by centrifugation and the absorbed DNA was washed twice with an ethanol-based wash solution and dried by centrifugation at 16,000 g for 1 min. Purified DNA was eluted under low salt conditions with 2 x 40 µl volumes of Tris EDTA (TE) buffer (10 mM Tris, pH 8.0, 1 mM EDTA).

2.10 DNA digestion

2.10.1 DNA digestion for plasmid construction

Purified *env* PCR product or 5 µg of plasmid DNA was digested with 40-80 U of restriction enzyme in the supplied reaction buffer made up to a 100 µl with MilliQ purified water. Typically, PCR amplified *env* DNA was digested with 40 U each of *ApaI* and *XhoI* restriction enzymes at 37°C for 6 hr.

2.10.2 Analytical restriction digest

For restriction analysis of plasmid DNA, 500 ng of plasmid was incubated with 20 U of restriction enzyme in the supplied reaction buffer, made up to 20 µl with Milli-Q purified water. Reactions were incubated at 37°C for 1 h. Digested DNA products (10 µl) were analysed by electrophoresis through 1% (w/v) agarose gel.

2.11 Gel Extraction

Products of DNA digestion intended for cloning were separated by electrophoresis through 0.8% (w/v) agarose gel. A GeneJet gel extraction kit (Fermentas) was used to purify separated DNA from agarose-gel slices. Each gel piece was mixed with equal weights of binding buffer and incubated at 50 °C until the agarose had dissolved. Solubilised agarose solution was passed through a GeneJet purification column by centrifugation at 16,000 g for 1 min. The absorbed DNA was washed once with binding buffer and twice with an ethanol-based wash solution. Columns were dried by centrifugation and DNA was eluted with 2 x 50 µl volumes of TE buffer.

Eluted DNA was concentrated by ethanol precipitation prior to ligation or nucleotide sequencing. DNA samples destined for ligation were mixed with 2.5 M ammonium acetate, while samples prepared for sequencing were mixed with 300 mM sodium acetate. Salt-adjusted DNA samples were mixed with two volumes of ice-cold ethanol and incubated on ice for 1 hr. Precipitated DNA was centrifuged at 16,000 g for 1 hr at 4 °C. Supernatants were discarded and DNA pellets were washed with 70% ethanol by centrifugation at 16,000 g for a further 20 min. Decanted supernatants were discarded and the DNA pellets were left to dry before each was dissolved in 15 µl of nuclease-free water (Sigma Aldrich). A microvolume spectrophotometer (NanoDrop ND-1000, Thermofisher scientific) was used to assess nucleotide purity and measure DNA concentration.

2.12 DNA ligation

Restriction-digested *env* amplicons and pcDNA3.1 were ligated with T4 ligase (NEB), which catalyses the formation of phosphodiester bonds between juxtaposed 5' and 3' hydroxyl termini of cohesive or blunt ended DNA. Purified, restriction-digested insert and vector were combined at a molar ratio of 1:6, yielding a final molar concentration of 100 nM in a reaction buffer composed of 50 mM Tris-HCl (pH7.5), 10 mM $MgCl_2$, 1mM ATP, 10 mM dithiothreitol (DTT), and 2,000 units of T4 ligase. The final reaction volume was made up to 15 µl with nuclease-free water. Ligation reactions were incubated overnight at 16°C.

2.13 Production of competent bacteria

Strains of *Escherichia coli* (*E.coli*) DH5-α, XL1-blue and MACH1 (Stratagene) were made chemically-competent for transformation with plasmid DNA using the Inoue method (Inoue *et al*., 1990). Briefly, non-competent bacteria were streaked onto Petri dishes containing LB-agar (1.5% (w/v) agar dissolved in lysogeny broth (LB) (10 g/l Bacto-tryptone, 5 g/l yeast extract, 171 mM sodium chloride (NaCl), pH 7.4)). Plates were inverted and left to grow overnight at 37°C. A single colony was used to inoculate 25 ml of super-optimal broth (SOB) (2% Bacto-tryptone, 0.5% yeast extract, 10 mM NaCl, 2.5 mM KCL, 10 mM $MgCl_2$ and 10 mM magnesium sulphate ($MgSO_4$)), which was incubated at 37°C in an orbital shaker. After 6 hours, 4 ml of cultured bacteria was transferred to an Erlenmeyer flask containing 250 ml of super-optimal broth (SOB) and this was incubated for a further 8-16 hr in an orbital shaker at 18°C. Bacterial growth was monitored by spectrophotometry and when light absorbance at wavelength of λ=600nm (A_{600}) reached 0.5 – 0.8, the flask was transferred to an ice-water bath. Chilled bacteria were harvested by centrifugation at 2500 g and resuspended in ice-cold transformation buffer (TB) (10mM piperazine-N,N′-bis (2-ethanesulfonic acid) (PIPES), pH 6.5, 55 mM manganese chloride ($MnCl_2$), 15 mM

calcium chloride ($CaCl_2$), 250 mM KCL). Bacteria were centrifuged again and resuspended in 20 ml of TB supplemented with 7% (v/v) dimethyl-sulfoxide (DMSO). After 10 min incubation on ice, 100 µl aliquots of competent bacteria were snap-frozen in liquid nitrogen and stored at -80°C. The OneShot TOP10 strain of *E.coli* was purchased from Invitrogen in a transformation-competent state.

2.14 Transformation of competent *E.coli*

For bacteria transformation, 4 µl of DNA-ligation reaction or 100 ng of purified-plasmid DNA were added to a partially-thawed aliquot of competent E.coli and incubated on ice for 30 min. Transformation reactions were "heat-shocked" for 1 minute in a water bath set to 42°C, then incubated with 500 µl of super-optimal broth with catabolite repression (SOC) (SOB with 20 mM Glucose) in an orbital shaker at 37°C. After 1 hr incubation, 100 µl of the transformed bacteria were spread onto LB-agar containing 120 µg/ml ampicillin. Plates were inverted and incubated at 37°C overnight.

2.15 Screening bacterial clones for the intended plasmid construct

Ampicillin-resistant bacteria colonies were screened for the presence of correctly-sized expression vectors by electrophoresis of bacteria-colony lysates. This method was developed for high-throughput screening of 96 colonies per run (Figure 2.3). Colonies were harvested with sterile 20 µl pipette tips, which were transferred to a 96-well pipette-tip holder. Once filled with bacteria-coated pipette tips, the pipette tip holder was used to inoculate all wells of a 96-well plate containing 100 µl of LB with 120 µg/ml ampicillin. Pipette tips were removed and the inoculated cultures incubated at 37°C for 4 hrs. Residual bacteria, still attached to the 96 pipette tips, were transferred to microtitre wells containing 15 µl of lysis buffer (50 mM Tris HCl, pH 8.0, 10 mM EDTA, 10 µg/ml RNAase A, 50 µg/ml chicken-egg-white lysozyme, 0.05% (w/v) 3,3',5,5'-tetrabromophenolsulfonphthalein (Bromophenol Blue), 10% glycerol). After 5 min incubation at room temperature, the pipette tip holder was removed and 2 µl of

Figure 2.3 High throughput colony screening method for the identification of pcDNA.*env* constructs.

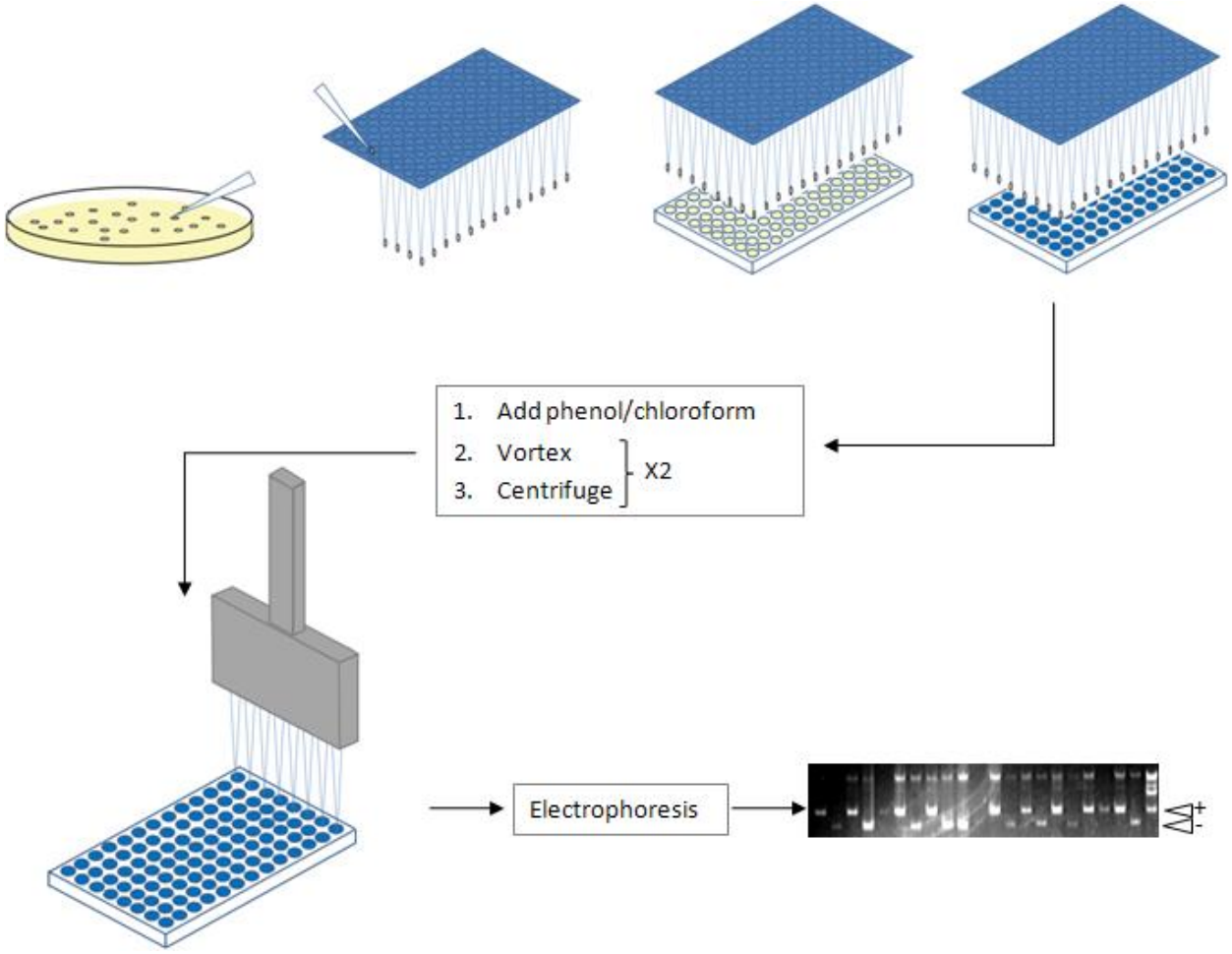


Figure 2.3 shows the high throughput screening method used to identify correctly sized HIV-1 envelope constructs by colony lysis. Colonies were selected with sterile pipette tips and transferred to a 96-well pipette-tip holder. The pipette tips were transferred to a microtitre plate containing LB/ampicillin, then to a second plate containing bacteria lysis buffer. Samples were processed in bulk as described in section 2.15, then analyzed by electrophoresis through 1 % agarose. Positive colonies were identified from the migration rates of super-coiled DNA plasmids and the corresponding wells of the LB/ampicillin plate were used to set-up small scale bacteria cultures for alkaline lysis minipreperation.

phenol:choloform:isoamyl alcohol (25:24:1) were added to each well. Microtitre plates were sealed with adhesive plastic covers and vortexed to emulsify the contents. Plates were centrifuged at 2,000 g for 2 min then vortexed and centrifuged once more at 2,000 g for 5 min. Supercoiled-plasmid DNA contained within the aqueous phase of each well was separated by electrophoresis through 1% agarose. Separate bacteria lysates containing pcDNA3.1 or pcDNA.*env* (previously confirmed to be correct by nucleotide sequencing) were added to the agarose gel as negative and positive controls, respectively. Correctly sized DNA plasmids were identified as those that migrated through agarose at the same rate as the pcDNA.*env* control. Positive transformants from the bacteria-culture plate were used to inoculate 5 ml of LB/ampicillin (100 µg/ml) which was incubated at 37°C in an orbital shaker for 12-16 hr. Bacteria were harvested by centrifugation at 4,000 g for 10 mins and the bacteria pellets were processed by alkaline-lysis mini-preparation or stored at -80°C until needed.

2.16 Monitoring growth of pcDNA.*env* transformed *E.coli*

Growth of bacteria, transformed with pcDNA.*env* plasmids, was monitored by spectrophotometry at hourly intervals. Once light absorption values (A_{600}) reached 0.4, an aliquot of each culture was diluted $1:10^6$ in LB and 100 µl was spread onto LB agar plates with or without ampicillin. After 12 hr incubation at 37°C, colonies were counted on each plate and used to determine the relative proportion of transformed and non-transformed *E.coli.*

2.17 Alkaline-lysis mini-preparation of plasmid DNA.

DNA plasmids were purified from bacteria by alkaline-lysis using a GeneJet miniprep kit (Fermentas). Bacteria were resuspended in 250 µl of resuspension buffer (containing RNAase A) and lysed with 250 µl of lysis solution containing sodium dodecyl-sulphate (SDS) and sodium hydroxide, which denatures bacterial protein and DNA, respectively. After 5 min, lysis reactions were terminated with 350 µl of neutralization buffer containing potassium acetate. Precipitated bacterial proteins and chromosomal

DNA were pelleted by centrifugation at 16,000 g for 5 min. Supernatants, containing the plasmid DNA, were passed through a silica-membrane spin column by centrifugation (16,000 g for 1 min) and the flow-through was discarded. Columns were washed twice with an ethanol-based wash solution (16,000 g for 1 min) and residual wash buffer was removed by centrifuging the empty column (16,000 g for 2 min). DNA was eluted into 50 µl of elution buffer (10 mM *Tris*-HCl, pH 8.5) that was passed through the column by centrifugation at 16,000 g for 1 min.

2.18 Large-scale alkaline-lysis maxi-preparation of DNA plasmids with high copy number.

One-hundred ml of LB containing 120 µg/ml ampicillin were inoculated with single colonies of MACH1 *E.coli,* transformed with high-copy number plasmids, pHXB2-env or plasmids from the clade B or clade C HIV-1 envelope reference panels. Bacteria were incubated at 37 °C for 16-18 hr in an orbital shaker before harvesting by centrifugation at 4,000 g for 15 min. In order to grow MACH1 *E.coli,* transformed with the low-copy number plasmids, pNL4-3Δ*env* or pMD-G, 20 ml of LB containing 120 µg/ml ampicillin, was inoculated with a single transformed colony and incubated at 37°C in an orbital shaker for 8 hours. Four milliliters of this culture were added to 200 ml of LB with ampicillin and incubated at 37 °C. After 5 hours, light absorbance was monitored at hourly intervals by spectrophotometry. When A_{600} reached 0.8 the bacteriostatic antibiotic, chloramphenicol, was added to a final concentration of 170 µg/ml and bacteria were incubated for a further 12 hr before harvesting by centrifugation at 4,000 g for 15 min.

A QiaFilter maxi-preparation kit (Qiagen) was used to purify DNA plasmids from bacterial pellets. Bacteria were resuspended in 10 ml of resuspension buffer (Buffer P1) (50 mM Tris HCl, pH 8.0, 10 mM EDTA, 10 µg/ml RNASE A), then mixed with 10 ml lysis buffer (P2) (200 mM sodium hydroxide, 1% (w/v) SDS). After 5 min, lysis reactions were stopped with 10 ml of chilled neutralization buffer P3 (3.0 M potassium acetate, pH5.5). The resulting solution was decanted into the barrel of a QIAfilter cartridge

and incubated at room temperature for 10 min to allow a precipitate to float to the surface. Bacterial lysates was passed through the QIAfilter into a QIAGEN-tip 500 column, pre-equilibrated with 10 ml of buffer QBT (750 mM NaCl, 50 mM MOPS, pH 7.0, 15% (v/v) isopropanol; 0.15% (v/v) Triton® X-100). Once all the sample had passed through the anion-exchange resin, the column was washed twice with 30 ml of buffer QC (1 M NaCl, 50 mM MOPS, pH 7.0, 15% (v/v) isopropanol), and DNA was eluted with 15 ml of buffer QF (1.25 M NaCl, 50 mM Tris-Cl, pH 8.5, 15% (v/v) isopropanol). The eluent was mixed with 0.7 volumes of room-temperature isopropanol to precipitate DNA, which was harvested by centrifugation at 4,000 g for 1 hr at 4°C. The supernatant was discarded and the DNA pellet was washed with 5 ml of 70 % ethanol (v/v). After a further 30 min centrifugation at 4,000 g the DNA pellet was air-dried then re-dissolved in 500 µl of TE buffer. The DNA concentration was measured using a NanoDrop ND-1000 and the sample was stored at -20°C.

2.19 Construction of HIV-1 Env-pseudotyped viruses

2.19.1 Transfection of 293T/17 cells with linear polyethyleneimine

Envelope-pseudotyped viruses were constructed by co-transfection of 293T/17 cells with pcDNA.*env* and pNL4-3△*env* using linear polyethyleneimine (PEI; 25 kDa) (Polysciences Inc, Warrington, PA, US) (Kirschner *et al*., 2006). Stocks of PEI were prepared in nuclease-free water to a concentration of 1 mg/ml and adjusted to pH 7 with 5M HCl. Solutions were filter-sterilized and stored at -80°C. The following method was used to transfect cells in polylysin-coated 24-well plates. Quantities of PEI and DNA used to transfect 293T/17 cells in larger receptacles (T25 tissue culture flasks and 10 cm diameter Petri dishes) were scaled-up according to the surface area of the cell monolayer.

One day prior to transfection, 293T/17 cells were seeded at a density of $2x10^5$ cells per well. When cells reached 80-90% confluence, tissue culture medium was replaced with 500 µl of DMEM containing 10% (v/v) FCS without antibiotics. Transfection mixtures were prepared by mixing 533 µg of pNL4-3△*env*

with 267 µg of pcDNA.*env* in 250 µl of serum-free Optimem medium. Solutions of DNA were mixed with 250 µl of Optimem containing 2.4 µg of PEI and incubated at room temperature for 30 min to allow DNA-PEI complexes to form. Transfecting-DNA mixtures were mixed with the 293T cell supernatants and the 24-well plate was incubated at 37°C in a humidified, 5% CO_2-gassed incubator. After 4 hours, tissue-culture medium was replaced with complete DMEM (with antibiotics). Supernatants, which contained pseudovirus particles, were harvested 48 hr and 72 hr post-transfection and clarified by centrifugation at 800 g for 30 min. Transfected-cell supernatants harvested from larger tissue-culture receptacles were passed through a 45 µm Luer-lock syringe filters and stored at -80°C prior to virus titration and neutralization experiments.

Virus pseudotyped with VSV-G, and non-enveloped virus-like particles, were constructed for use as experimental controls in virus titration and neutralization assays. Both types of control virus were produced in 293T/17 cells, pre-seeded in T25 tissue culture flasks. Envelope-deficient virus was constructed by transfecting 9.6 µg pNL4-3△*env* with 22.5 µg of PEI, while VSV-G pseudotyped virus was constructed by transfecting 9.6 µg of pNL4-3△*env* and 3.2 µg pMD-G plasmid DNA with 22.5 µg of PEI.

2.19.2 Transfections with lipofectamine 2000

Where stated, 2 µl of the cationic-lipid, Lipofectamine 2000 (Invitrogen Life Science, UK), were used in place of 2.4 µg of PEI for the construction of Env-pseudotyped viruses by transfections in 24-well tissue-culture plates. The methods for transfection were the same as for PEI transfections (section 2.19.1).

2.20 Infectivity screening of HIV-1 Env-pseudotyped virus.

The TZM-bl reporter cell line (section 2.1) was used to detect infectious pseudoviruses in supernatants harvested from small scale (24-well plate) 293T/17 cell transfections. Ninety-six well white-opaque microtitre plates (Costar, product code: 3917) were pre-seeded with $1.5x10^4$ TZM-bl cells in 100 µl of

complete-DMEM. Plates were left at room temperature for 2 hr to allow cells to distribute evenly before transferring to a 37°C incubator containing 5% CO_2. After 24 hours, cell supernatants were aspirated and replaced with 200 µl of pseudovirus supplemented with 10 µg/ml diethylaminoethyl-dextran (DEAE-Dextran). Each pseudovirus was added to quadruplicate wells.

After 48 hr incubation, infected-cell monolayers were fixed with 0.2% gluteraldehyde and histochemically stained with bromo-chloro-indolyl-galactopyranoside (X-gal) staining solution (2 mM MgCl2, 5mM potassium ferrocyanide ($K_4Fe(CN)_6$), 5mM potassium ferricyanide ($K_3Fe(CN)_6$), 137 mM NaCl, 2.7 mM KCl, 10 mM disodium phosphate (Na_2HPO_4), 1.76 mM monopotassium phosphate (KH_2PO_4), pH 7.4 and 1 mg/ml of X-gal stock solution dissolved in N,N-dimethylformamide). Infected cells, expressing β-galactosidase, produced "blue" focus forming units (FFU) after 6 hr incubation at 37°C. Cell monolayers were washed twice with tap water and then left to air dry.

An ELISPOT reader (AID, model no. ELR06) was calibrated to count the number of FFU in each well. The AID EliSpot software (v3.0) collected images in each well, across a surface area of 24 mm^2, which is 75% of the total surface area. Image correction parameters were optimized to achieve a high-contrast between FFU and background artifact produced from dense clusters of uninfected cells. The camera shutter speed was set to 1/2046 sec and the video processing amplification parameters were set to the following values: Brightness 122, gain 0, hue 158, colour saturation 1, sharpness 255 (max), gamma 129, white balance (red) 138, white balance (blue) 160. All FFU that produced an image-intensity greater than 12 were counted. Pseudoviruses producing more than 200 FFU per well were scaled-up by large-scale transfections in T25 tissue cultures flasks or 10cm diameter Petri dishes for virus titrations and neutralization experiments.

2.21 Titration of HIV-1 Env and VSV-G-pseudotyped virus.

White-opaque microtitre plates were seeded with $1.5x10^4$ TZM-bl cells in 100 µl of complete-DMEM, 24 hr prior to pseudovirus titrations (section 2.20). Frozen aliquots of supernatant, containing filter-purified pseudovirus, were thawed at room temperature and serially diluted fivefold in complete DMEM (six dilutions ranging from 1:1 to 1:3125). Each dilution was mixed with equal volumes of complete-DMEM supplemented with 20 µg/ml DEAE-dextran (10 µg/ml final concentration). Supernatants from the pre-seeded microtitre plate were removed and 200 µl of each pseudovirus dilution were added to triplicate wells. Plates were incubated for 48 hr at 37 °C, fixed with 0.2% gluteraldehyde and stained with X-gal (section 2.20). Focus forming units were counted using an ELISpot plate reader (AID) and infectious titres were calculated from virus dilutions that produced FFU within a linear range of 10 – 800 FFU per image. Pseudovirus titres are given as infectious units (IU) per ml, however, these titres are only applicable to microtitre wells (0.32 cm^2) containing 200 µl of supernatant.

2.22 Assessing antibody-mediated neutralization of HIV-1 Env-pseudotyped virus

Neutralization of Env-pseudotyped viruses was assessed with patient-derived plasma and NAbs using a modified version of the standardized luciferase assay (Montefiori, 2009). This assay was adapted to incorporate automated cell counting of β-galactosidase expressing TZM-bl cells. Plasma was heat-inactivated at 56°C for 1 hour, then serially diluted 3-fold from 1:10 to 1:2430. Each plasma dilution was mixed with an equal volume of pseudovirus, supplemented with DEAE-dextran (20 µg/ml), yielding 6000 IU/ml of pseudovirus, 10 µg/ml DEAE-dextran and dilutions of plasma ranging from 1:20 to 1:4860. Where stated, plasma was substituted for NAbs, b12 or 2G12, at final concentrations ranging from 0.0781 µg/ml to 20 µg/ml. Pseudovirus was incubated with plasma or NAb for exactly 1 hr at room temperature, then 200 µl of each mixture was added to triplicate microtitre wells containing TZM-bl cell monolayers, pre-seeded 24 hr previously (see section 2.20). Virus-only controls consisted of well

containing 200 µl of supernatant containing 6000 IU/ml of pseudovirus and 10 µg/ml of DEAE-dextran. In order to confirm that heat-inactivated virus did not contain infectious virus particles, plasma diluted 1:20 in complete-DMEM was added to microtitre wells in the absence of virus. Plates were incubated at 37°C in a humidified, 5% CO_2-gassed incubator. After 48 hours, cell monolayers were washed twice with PBS, fixed with 0.2% gluteraldehyde, and stained with X-gal. After two more washes with water, plates were dried at room temperature and FFU were counted using an ELISpot plate reader (AID) (see section 2.20). Neutralization was calculated as the percentage reduction of FFU mediated by each plasma dilution relative to the virus-only controls. Percentage neutralization was plotted against log plasma dilutions (or log NAb concentration) and curves were fitted to the data points using XLfit curve fitting software (IDBS, UK). Half-maximal neutralizing titres (IC_{50}) were interpolated from neutralization curves and are presented as reciprocal dilutions of plasma or concentrations of NAb.

2.23 Quantification of pseudovirus infection by luciferase detection

Where stated, pseudovirus infected TZM-bl cells were quantified by luminometry using D-luciferin (BriteLite Plus, PerkinElmer), which is metabolized by luciferase to produce oxyluciferin in a chemiluminescent reaction. Forty-eight hours post-infection, supernatant fluids were aspirated from each well and replaced with 100 µl of D-luciferin and 100 µl of fresh DMEM without phenol red (Sigma-Aldrich). Cells were lysed by vigorous pipetting and after 10 min incubation at room temperature relative light units (RLU) were quantified using a luminometer (XS, Harta, UK). Background levels of luminescence were recorded from wells that received TZM-bl cells without virus.

2.24 Site directed mutagenesis

Plasmids pcDNA.*env*(E339/R363), pcDNA.*env*(N339/R363) and pcDNA.*env*(N339/Q363) were obtained by site-directed mutagenesis of pcDNA.*env*(Rit336d) using the quick-change method (Papworth 1996). The R339E and R339R mutations were introduced to pcDNA.*env*(Rit.336d.c3) prior to the Q363R mutations .

Mutagenesis primers were designed to incorporate restriction sites that encoded synonymous-mutation, so that successfully mutated clones could be identified by restriction analysis (Table 2.1). Primers R339E/F and R339E/R introduced and R to E mutation at site 399 and an *XbaI* restriction site, while primers R339N/F and R339N/R introduced an R to N mutation at site 339 and an *XhoI* restriction site (Table 2.1). Plasmid pcDNA.*env*(RitD336) was used as the template for PCR amplification using *Pfu*UltraII Fusion HS (Stratagene) in buffer supplied by the manufacturer supplemented with 200 µM dNTPs, 3% DMSO and 10 nM of each primer. Each reaction was subjected to the following thermo-cycling conditions: Five min denaturation at 95°C followed by 18 amplification-cycles consisting of denaturation (95°C for 50 sec), annealing (60°C for 50 sec), and extension (68°C for 9 min). Thermo-cycling ended with a final incubation at 68°C for 12 min. The reactions were digested with 10 units of *Dpn*I restriction enzyme to remove *dam*-methylated PCR template, and the products of digestion were used to transform competent MACH1 *E.coli*. Plasmid envelopes, purified from bacteria by alkaline lysis mini-preparation, were screened for the intended mutations by analytical restriction digests with *XbaI* (R339E mutants) and *XhoI* (R339N mutants). Mutant envelope plasmids were mutagenised further using primers Q363R/F and Q363R/R, which introduced a Q to R mutation at site 363 and a *ClaI* restriction site. Double-mutant clones were identified by restriction-digestion with *ClaI* and the final mutants clones were verified by sequencing of mini-scale plasmid DNA preparations.

2.25 Quantification of HIV-1 reverse transcriptase activity.

Relative concentrations of pseudovirus particles in supernatant fluids were assessed using a product-enhanced reverse transcriptase (PERT) assay that quantifies cDNA reverse transcribed from an RNA template by HIV-1 RT. Quantities of the cDNA product are measured by real time PCR using the asymmetric cyanine nucleic acid stain, SYBR Green I (SG), which absorbs blue light (λmax = 488 nm) and emits green light (λmax = 522 nm) when bound to double stranded DNA. Purified plant-viral RNA

derived from Brome Mosaic virus (BMV) is used as the template because of a lack of sequence homology with retroviral and mammalian genomes. Additionally, this virus lacks a DNA phase to its life cycle, thus reducing the potential for false-positive results from DNA contaminants. This assay was developed in house (Pizzato *et al*., 2009). The sensitivity of the assay was subsequently improved by redesigning the PCR primers to prevent the formation of primers-dimers and eliminate RNA-dependant *Taq* polymerase activity (Table 2.1).

The modified SG-PERT assay was executed as follows. Supernatants were mixed with equal volumes of viral lysis buffer (100 mM Tris-HCl (pH7.5), 50 mM KCl, 0.2 mM DTT, 0.25 % (v/v) Triton X-100, 50 % (v/v) glycerol and 0.4 U/µl RNase inhibitor (Fermentas)) and incubated at room temperature for 5 min. Viral lysates were diluted ten-fold in dilution buffer (20 mM Tris-HCl, 20 mM KCl and 5 mM ammonium sulphate $(NH_4)_2SO_4$, pH8.3), then 10 µl of each sample was added to a LightCycler capillary (Roche) with 10 µl of reaction buffer (20 mM Tris-HCl, 20 mM KCl, 5 mM $(NH_4)_2SO_4$, 200 µM dNTPs, 0.5 µM sense primer BMVF1, 0.5 µM antisense primer BMVF2, BSA 0.1 µg/ml, 1/20000 SYBR green I, 12 ng BMV template RNA and 0.2 U Hotstart Taq (MBI Fermentas)). Capillaries were placed in a LightCycler 2.0 (Roche) instrument and incubated at 37°C for 30 min. The reverse transcribed BMV cDNA product was amplified using the following program: 5 min *Taq* polymerase activation at 95°C followed by 45 amplification cycles of denaturation (5 sec at 95°C), annealing (5 sec at 55°C), extension (15 sec at 72°C) and data acquisition (7 sec at 83°C). Amplification curves were generated by the LightCycler software (v4) from log fluorescence (λ = 530mn) measured during the acquisition step. For each amplification curve the software calculated a crossing point, defined as the cycle number at which the real-time fluorescence rises above background fluorescence recorded prior to PCR amplification. After the final amplification cycle, melting temperatures of the DNA products were determined by cooling the samples to 55 °C then heating to 95°C at a rate of 0.1°C per second, while constantly monitoring the decline in fluorescent signal.

2.26 Competitive binding assays

Antibody specificity was mapped using a competitive-binding enzyme-linked immunosorbent assay (ELISA). High-binding ELISA plates (Greiner) were coated with 1 mg/ml of recombinant BaL-strain gp120 and incubated at 4°C overnight. Plates were washed three times with wash buffer (PBS, pH 7.4, 0.05% Tween-20) using an automated microtitre-plate washer (M96, MTX LabSystems), and blocked with 200 µl of blocking buffer (PBS, pH 7.4, 0.05% tween-20, 2% milk powder) to limit non-specific antibody binding. After 1 hr incubation at room temperature, plates were washed three times and each well received either 50 µl of sample buffer (PBS 0.05% Tween-20, 1% BSA), or 50 µl of sample buffer containing 5 µg/ml of M33. Plates were incubated for a further hour, during which time plasma samples were diluted three-fold in sample buffer, yielding dilutions ranging from 1:10 to 1:2190. Without washing the plate, 50 µl of each plasma dilution were added to duplicate wells and after 1 hr incubation, plasma dilutions were mixed with 100 µl of biotinylated-NAb to yield 50% saturating titres (4.6 µg/ml b12, 0.36 µg/ml 2G12 or 0.8 µg/ml 447-D). Biotinylated NAb 4.8d (2.4 µg/ml) was added to wells that previously received M33 peptide. After one hr incubation, plates were washed three times and bound NAb was detected with 1.25 µg/ml of streptavidin-HRP conjugate and 3,3',5,5'-tetramethylbenzidine (TMB) colorimetric substrate (Thermofisher). After 20 min incubation the reaction was stopped with 0.08 M sulfuric acid and light absorbance at λ=450nm (A_{450}) was measured with a spectrophotometer plate reader (BioRad, model 3550). Plasma-mediated inhibition of NAb-binding was determined as the percentage reduction in A_{450} relative to wells that received sample buffer instead of plasma.

2.27 Evolutionary analyses of HIV-1 envelope genes

2.27.1 PCR amplification of HIV-1 envelope for sequencing reactions.

For clonal sequencing analysis of the C1-C3 region of HIV-1 envelope (bases 6536-9797, HXB2 referencing), reverse-transcribed viral RNA (cDNA) was amplified by nested PCR using outer primers

Env10F/Env13R and inner primers Env11F/Env12R. Reaction mixtures contained 2 µl cDNA (or 1 µl of first round product), 200nM dNTP, 1 U platinum *Taq* polymerase (Invitrogen Life Sciences, UK), 2mM $MgCl_2$, 200 nM of each primer, made up to 50 µl in the 1X reaction buffer supplied by the manufacturer. Thermo-cycling parameters were as follows: 2 min denaturation at 94°C, followed by 35 cycles consisting of denaturation (95°C for 30 sec), annealing (55 °C for 30 sec) and extension (72 °C for 3 min 30 sec). Thermo-cycling was followed by a final incubation at 72°C for 5 min.

2.27.2 TOPO TA cloning of HIV-1 envelope genes for sequencing analyses

Amplification products were cloned using a TOPO TA Cloning Kit according to the manufacturer's instructions (Invitrogen Life Sciences). Briefly, 4 µl of agarose-gel purified PCR product were mixed with 1 µl of reaction mix containing *Vaccinia* virus Topoisomerase I which ligates overhanging 3' desoxyadenosines (added by *Taq* polymerase) to the recessed 5' terminus of the linearized pCR2.1 vector. After 30 min incubation at room temperature, 1 µl of ligated DNA was used to transform TOP10 *E.coli.* Bacteria colonies were grown on LB-agar with 120 µg/ml ampicillin and individual clones were expanded for DNA purification by alkaline-lysis mini-preparation (section 2.17). Sequencing reactions were prepared in Big Dye Terminator v3 reaction mixtures (Applied Biosystems, UK) containing of 3.7µL H_20, 1.5µL BigDye buffer, 625 nM of primers ENV11F/ENV11R or ENV12F/ENV11R, 0.8µL BigDye Terminator v3 reaction buffer and 2µL of TOPO TA cloned envelope plasmid. Alternatively, the C2-V3 region was amplified from pcDNA.*env* clones using outer primers CV1/CV4 and inner primers JAE1/JAE4. The PCR reaction was performed on a Peltier Thermal-cycler (PTC-200, MJ Research, UK) using the following conditions: 30 cycles of denaturation (96° for 10 sec), annealing (50° for 5 sec) and elongation (60° for 2 min). Amplified products were purified by ethanol precipitation with 300 mM sodium acetate (section 2.11), then sequenced using an ABI 3700 DNA analyzer (Applied Biosystems, UK).

2.27.3 Phylogenetic analyses

Evolutionary studies of HIV-1 envelopes genes were conducted by Dr Gary Huang and colleagues at the Peter Medawar Institute (University of Oxford, UK). Sequences were aligned manually using X11, Sequencher (version 4.8, Gene Codes Corporation) and Se-Al (v2.0a11) software. Alignments were used to construct rooted phylogenetic trees using a Markov chain Monte Carlo (MCMC) algorithm that estimates sequence diversity and evolutionary divergence time. The MCMC algorithm was implemented using BEAST software which uses a relaxed molecular clock to estimate rates of evolution. BEAST software was also used to calculate effective population sizes for Bayesian skyline plots. For all analyses a general time-reversible model of nucleotide substitution was used, which has the following assumptions i) for any given site the rate of change from one base to another is independent of the base that occupied it previously (Markov property) ii) nucleotide substitution rates are constant iii) the relative frequencies of each base are at equilibrium. The GTR model used a specific nucleotide substitution matrix (Q) derived from priors calculated using BEAST software. In order to identify sites under positive selection, maximum likelihood (ML) phylogenetic trees were converted to parenthetical notation and used as input files for the CODEML algorithm implemented by PAML software. The CODEML algorithm applies models of non-synonymous (N) and synonymous (S) substitution rates (dN/dS; the ω parameter) and tests the likelihood that the observed data fits each model using empirical Bayes and X^2 tests.

2.28 HLA typing

Where stated the patients HLA type was determined to the oligo-allelic level using Dynal RELITM reverse sequence-specific oligonucleotide kits for the HLA-A and HLA-B, loci (Dynal Biotech). To obtain four-digit typing, Dynal Biotech sequence-specific priming kits were used, in conjunction with the Sequence-Specific Oligonucleotide type (Duda *et al*., 2009).

2.29 IFN-γ ELISPOT assays.

Cytotoxic T cell function was assessed by IFN-γ ELISPOT by Dr John Frater and colleagues (Oxford University). Polyvinylidene microtitre plates (Millipore) were pre-coated with 0.5 µg/ml anti–human IFN-γ monoclonal antibody (Mabtech). A total of 10^5 freshly isolated PBMCs were added per well in a volume of 100 µL of R10 medium (RPMI 1640 supplemented with 10% FCS , 10 mM 4-(2-hydroxyethyl)-1-piperazineethanesulfonic acid (HEPES), 2 mM L-glutamine, and 50 U/ml penicillin-streptomycin). Peptides were added at a final concentration of 2 µg/ml. Negative controls consisted of wells containing PBMCs incubated with medium alone. Positive controls consisted of wells containing PBMCs and 12.5 µg/ml of the mitogen, phytohaemagglutinin (PHA) (Murex Biotech). Plates were incubated overnight at 37°C in a 5% CO_2 incubator and washed the next day. To each well, 0.5 µg/ml biotinylated anti–IFN-γ antibody (7-B6-1; Mabtech) was added and incubated for 1.5 hr, then the plates were washed and incubated with streptavidin-alkaline phosphatase (ALP) conjugate (Mabtech) for 45 min. Plates were developed with the ALP-substrate, 5-bromo-4-chloro-3-indolyl phosphate and nitro-blue tetrazolium chloride in Tris buffer (pH 9.5). The reaction was terminated by washing with water after the appearance of blue spots in the positive control wells. Spots were counted on an ELISpot plate reader (AID), and responses were considered to be positive if the number of spots per well minus the background value was three standard deviation greater than the responses in the negative control wells.

Chapter 3

A high through-put neutralization assay for HIV-1 Env-pseudotyped viruses.

3.1 Introduction

Microtitration of envelope-pseudotyped HIV-1 is widely used to study infectivity (Pastore *et al*., 2006), drug susceptibility (Petropoulos *et al*., 2000, Zennou *et al*., 1998, Ogert *et al*., 2009) and virus tropism (Pastore *et al*., 2004), and has been standardized for quantitative and qualitative assessments of NAb responses (Wei *et al*., 2003). Pseudovirus infectivity assays allow for high through-put assessment of NAb responses and this has facilitated the discovery of novel antigenic targets for HIV-1 vaccine research. For example, the discovery of the first gp120 trimer-specific NAbs, PG9 and PG16, required prior screening of approximately 1800 HIV-1 infected donors and 30,000 B cell clones (Scheid *et al*., 2009, Simek *et al*., 2009). This level of through-put was achieved using standardized panels of heterologous Env-pseudotypes which represented a genetically-diverse array of recently transmitted viruses with various neutralization epitope specificities. However, when assessing the role of NAbs *in vivo,* it follows that it is necessary to assay the patient's plasma for antibodies against their autologous virus.

Envelope cloning is a significant rate-limiting step in neutralization assays that use autologous Env-pseudoviruses. It is often necessary to screen tens of cloned envelopes in order to identify those that are both representative of the quasispecies majority and capable of producing high enough titres to assay antibody-mediated inhibition of infection. Alternative methods have been described that circumvent envelope cloning, by splicing mammalian transcription promoters onto amplified envelope genes using PCR (Beels *et al*., 2008, Kirchherr *et al*., 2007). However, amplification of plasmid DNA in bacteria is still widely used in the construction of Env-pseudotypes, because it is more straight-forward and less error-prone than amplifying large amounts of DNA by PCR.

Envelope cloning is complicated by HIV-1 envelope cytotoxicity in *E.Coli*, which has been attributed to cell membrane permeabilisation, mediated by the carboxy and transmembrane regions of the gp41

fusion peptide (Chernomordik *et al*., 1994, Arroyo *et al*., 1995, McDonald and Burnett, 2005). Herein, we report marked variation in the cytotoxicity of different envelope variants, and provide a solution for cloning toxic envelope genes. These findings have implications for phenotypic assays of HIV-1 Env pseudoviruses, where it is important to avoid selection-bias when sampling viral quasispecies.

Pseudovirus infectivity can be quantified using HIV-1 permissible reporter cell lines that stably express reporter genes under regulatory control of HIV-1 or SIV LTR sequences (Montefiori, 2005). One such cell line, TZM-bl, expresses β-galactosidase (β –Gal) and luciferase in response to the viral Tat protein (Platt *et al*., 1998b, Wei *et al*., 2002). Luciferase activity is quantified from D-luciferin-treated cell lysates by luminometry. Alternatively, β–Gal-expressing cells can be stained with X-gal substrate and quantified by spectrophotometry of cell lysates, or manually counted on fixed-cell monolayers (Figure 3.1). Automated counting procedures for high-throughput quantification of histochemically-stained cell monolayers have been reported (Morcock *et al*., 2008, Patiris and Hanson, 2005). Here, we report the validation of this technique for assaying neutralization of HIV-1, and demonstrate sensitivity and reproducibility equivalent to those of standardized luciferase-based neutralization assays.

Figure 3.1: Schematic representation of the HIV-I Env-pseudotype neutralization assay

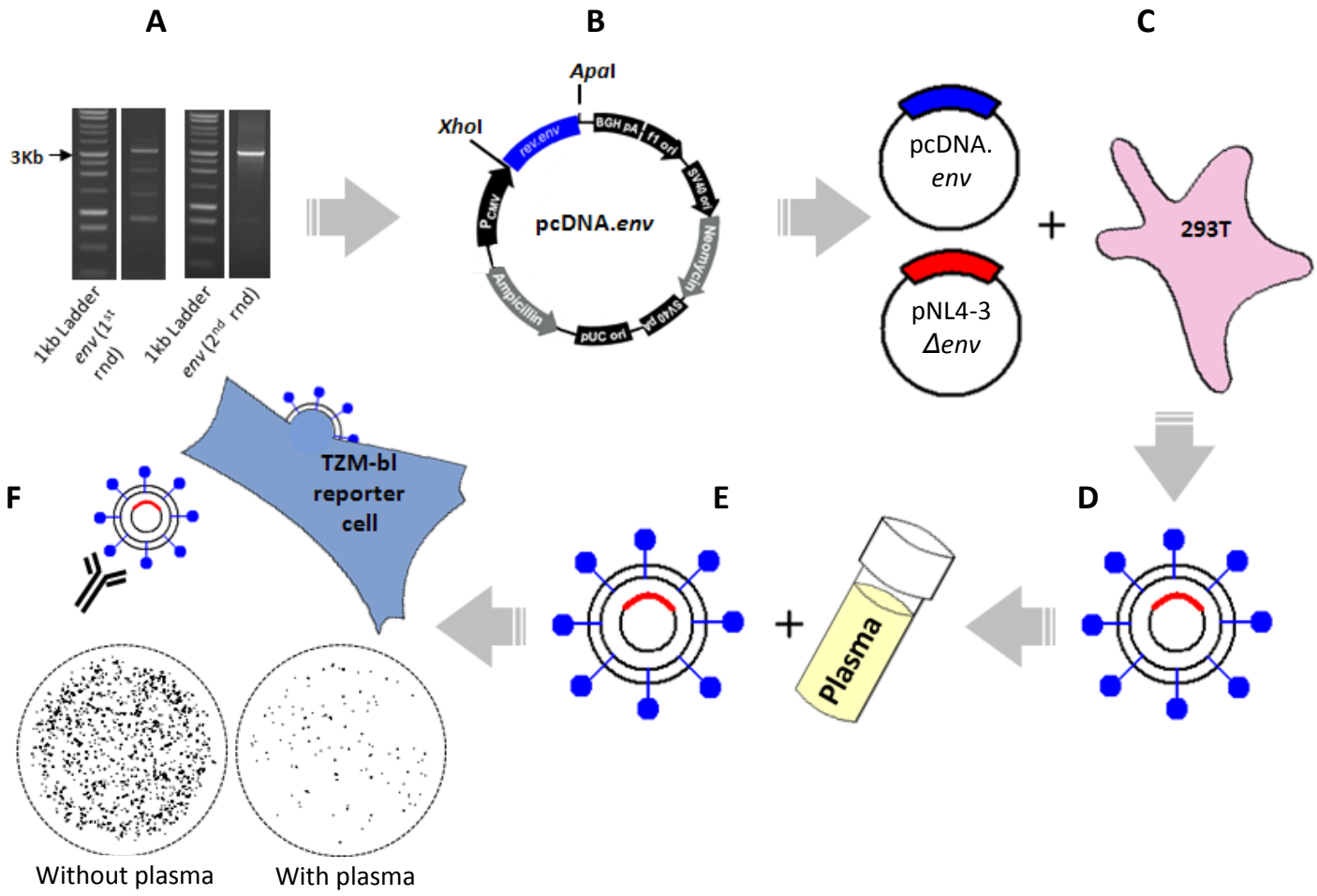


Figure 3.1 demonstrates the key steps of the HIV-1 pseudovirus neutralization assay:

A. Full length HIV-1 *env* is amplified by nested RT-PCR from viral RNA extracted from plasma.

B. Amplified Env amplicons are restriction-cloned in the eukaryotic expression vector pcDNA3.1.

C. Cloned envelope expression plasmids (pcDNA.*env*) are mixed with the HIV-I backbone, pNL4-3Δ*env*, and transfected into 293T cells.

D. Transfected 293T cells produce virus particles pseudotyped with Env-glycoprotein expressed from pcDNA.*env*. Virions incorporate NL4-3Δ*env* genomic RNA but lack function envelope genes.

E. Env-pseudotyped virus is titrated, and known quantities of virus are neutralized with plasma (or NAbs) and added to TZM-bl reporter cells.

F. Infected cells express β-Galactosidase in response to the viral Tat protein. Cells are fixed and stained with X-gal substrate and infected cells are counted. Neutralization is calculated as the percentage reduction in infected cells, relative to wells that receive virus without plasma.

3.2 Results

3.2.1 Optimization of molecular cloning to construct HIV-1 Env-expression cassettes.

Envelope expression cassettes (pcDNA.*env*) were cloned from viral RNA extracted from plasma of 22 HIV-1 infected patients enrolled into the SPARTAC clinical trial. These envelopes were used to construct Env-pseudotyped viruses for neutralization experiments that will be described in Chapter 5. Full-length *env* genes were PCR-amplified from reverse transcribed viral-RNA derived from 14 patients. Initial attempts failed for eight patients with low viral loads ranging from 120 to 1,490 RNA copies per ml of plasma (Figure 3.2A). Hence, viral RNA isolations were repeated using 3 ml of plasma that were ultracentrifuged for 1 hr to pellet the virus prior to RNA extraction. Subsequently, the entire 30 µl of eluted viral RNA were used in the RT step. After 70 cycles of nested-PCR, amplified envelope genes were detected by agarose-gel electrophoresis (Figure 3.2B, amplified *env* from patient S37 is shown). In the case of patient S10, who had the lowest VL, envelope genes were successfully amplified from approximately 360 RNA copies (Table 3.1).

Initial attempts to clone full-length *env* amplicons into pcDNA3.1 (+) using *ApaI* and *XhoI* restriction sites resulted in digestion of the PCR product for patient S37 (Figure 3.2B). This was not surprising as 5% of all clade B and clade C HIV-1 envelope sequences in the Los Alamos database contain the CTCGAG *XhoI* restriction site. For this reason, each envelope primer had been designed to include two 5' restriction sites, which allowed us to repeat the restriction digest using *ApaI* and *NotI* without destroying the envelope open reading frame (ORF).

Cloned plasmids of the correct size were identified by agarose-gel electrophoresis of transformed-bacterial lysates. For the majority of patient-*env* libraries (18/22), the percentage of screened colonies containing the envelope insert ranged between 80%-100%. In contrast, repeated attempts to transform

Figure 3.2 Isolation of *env* by RT-PCR amplification of viral RNA was variably efficient

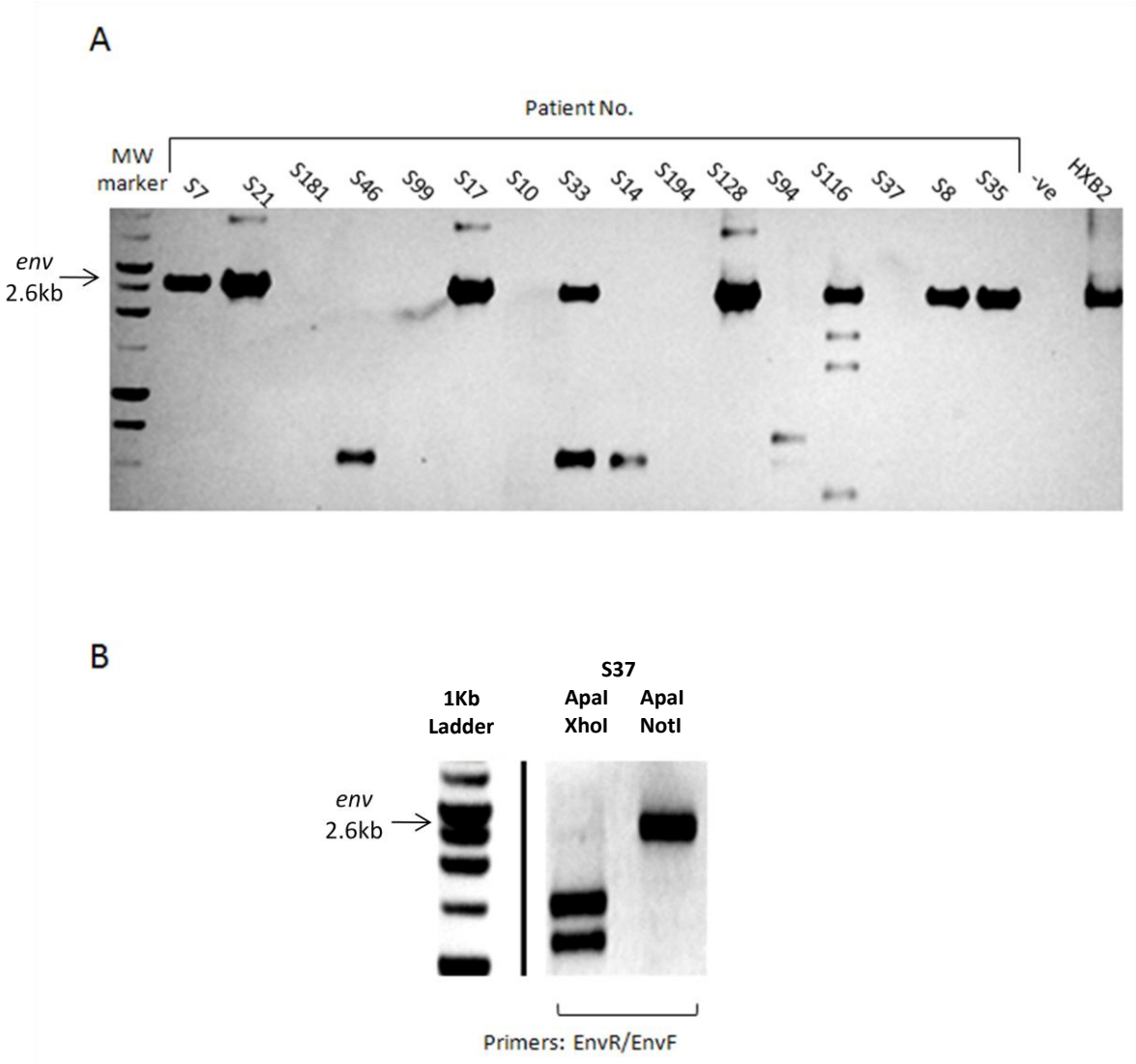


Figure 3.2 A: Amplification of viral *env* from plasma taken from 8/16 patients is shown (S7, S21, S17, S33, S128, S116, S8 and S35), demonstrating inconsistency of the reaction at low VL (see Table 3.1). Five microlitres of each second-round-PCR product were separated by agarose-gel electrophoresis and amplicons were visualized by UV-transillumination. Plasma collected from uninfected donors was processed using a Viral RNA Extraction Kit (Qiagen) and subjected to RT-PCR as a negative control. pHXB2-*env* (100ng) was subjected to nested PCR as a positive control. A molecular weight (MW) marker (1Kb, Promega), is shown in lane 1.

Figure 3.2 B: Ultracentrifugation of plasma derived from patient S37 yielded a DNA product after 2x35 cycles of nested RT-PCR. Restriction enzymes *ApaI* and *XhoI* digested the S37 PCR product at a restriction site within *env*. The 2.6Kb *env* gene was left intact following digestion with *ApaI* and *NotI*.

Table 3.1. Identification of samples with low VL that underwent ultracentrifugation prior to RT-PCR

Patient	VL	Weeks post ART	Plasma ultracentrifugation	Alternative restriction sites
S3	16311	12		
S7	17890	4		
S8	28253	4		
S10	120	4	Yes	
S14	187	4	Yes	
S17	62875	12		
S21	20200	4		
S33	361246	12		
S35	N/T	4		
S37	255	12	Yes	*ApaI/NotI*
S41	6289	4		
S46	400	12	Yes	
S94	292	12	Yes	
S99	1490	12	Yes	
S116	42604	12		
S128	74857	4		
S132	39354	4		
S171	1030	12		
S181	400	4	Yes	
S185	8060	4		
S194	851	12	Yes	
S199	5264	12		

Table 3.1. Ultracentrifugation was used to pellet virus from eight patients with VL <1500 RNA copies per/ml prior to RNA extraction and RT-PCR. To produce Env-expression plasmids, *env w*as cloned into pcDNA3.1 using *ApaI/XhoI* restriction sites for all samples except S37, which was cloned with *NotI* and *ApaI*.

E.coli with pcDNA.*env* derived from patient samples S3, S199, S8 and S17 yielded fewer colonies, none of which contained *env*. Restriction digested *env* DNA was gel-extracted then concentrated by ethanol precipitation and molarities of pcDNA.*env* were normalised to 83 nM (1.1 µg per reaction, 888.132 kDa) prior to DNA ligation. This suggested that the low cloning efficiencies were not due to insufficient quantities of *env*, particularly as 1.1 µg of *env* derived from patient S194 was used in a ligation reaction that efficiently transformed *E.coli* (40/40 positive colonies). Alternative reasons for the failure to clone HIV-1 envelopes from these patients included low efficiencies of restriction-digestion or T4-ligation steps that preceded transformation. However, transforming DNA samples for patients S3 and S194 both contained ligated pcDNA.*env* product that produced similar signal intensities when analyzed by agarose-gel electrophoresis, suggesting that the cause of these cloning failures lay down stream of *E.coli* transformation (Figure 3.3)

Previous reports of HIV-1 envelope-mediated cytopathology suggested the possibility that expression of *env* in *E.coli* may be inhibiting the growth of transformed bacteria (Miller *et al*., 1993, Comardelle *et al*., 1997, Chernomordik *et al*., 1994, Arroyo *et al*., 1995). This rationale was based on reports of transcription in *E.coli*, initiated from the eukaryotic CMV-promoter located upstream of the MCS of pcDNA3.1 (Lewin *et al*., 2005). To test the contribution of gene-promoter activity to the stability of pcDNA.*env*-transformed *E.Coli*, the problematic *env* genes were religated into Bluescript II vectors with MCS orientated in either direction. For KSbluescript II, this placed *env* in the opposite orientation to the prokaryotic *lac* promoter. Conversely, the same vector with the reverse MCS (SKbluescriptII) put *env* downstream of this promoter. Only transformation with KSBluescript.*env* produced stable colonies containing the *env* insert (Figure 3.4), inferring that transcription of HIV-*env* was inhibiting bacterial growth. Excising *env* from KSbluescript and re-ligating into pcDNA3.1 failed to yield stable colonies, even at a lower incubation temperature of 22°C, previously shown to stabilise HIV-envelope plasmids in replicating bacteria (McDonald and Burnett, 2005).

Figure 3.3: Efficiency of ligation reactions used to construct *env* expression plasmids

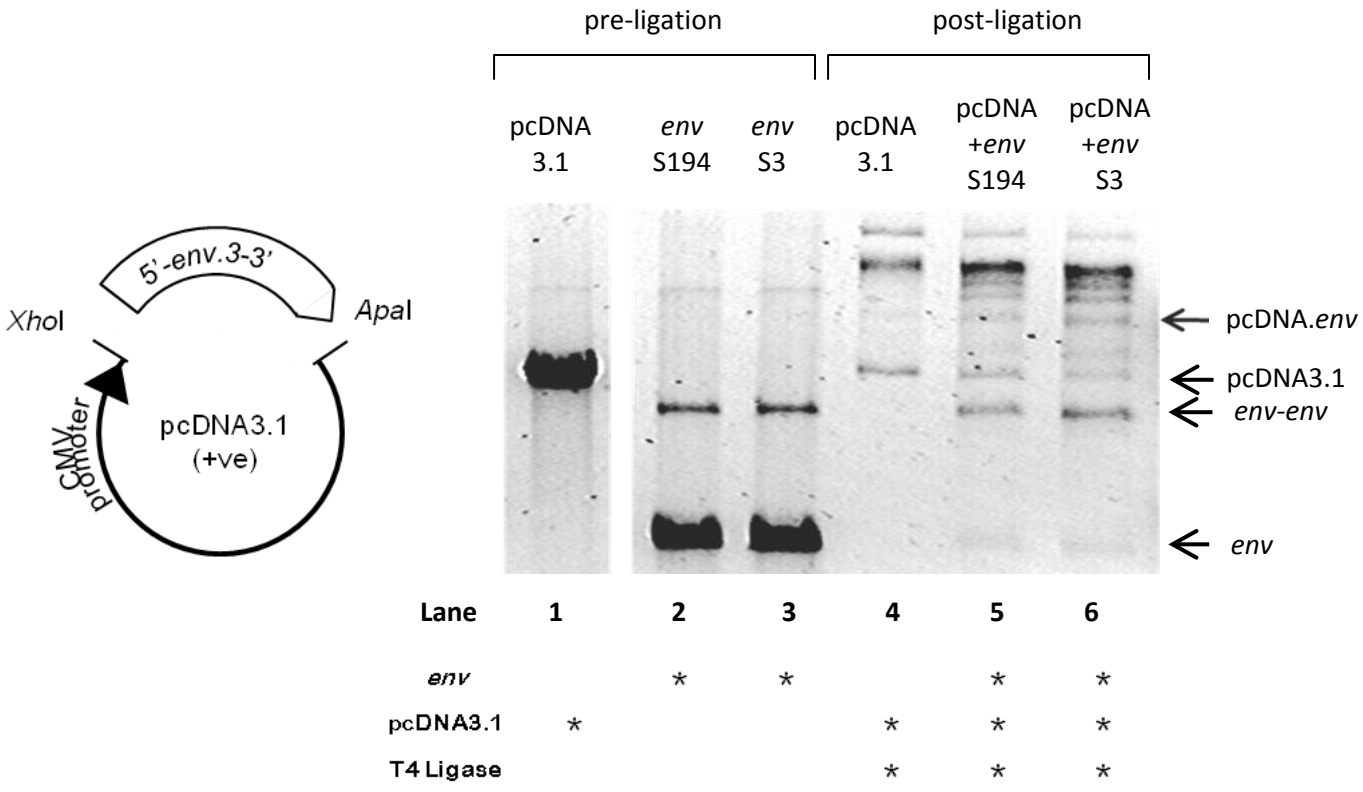


Figure 3.3: Agarose-gel electrophoresis was used to visualise *env* amplicons from patients S194 and S3 before and after ligation into pcDNA3.1 using *ApaI* and *XhoI* restriction sites (lane 1). Nucleotide concentrations of restriction-digested PCR-products were standardized after agarose gel-purification and ammonium-acetate ethanol precipitation (lanes 2 and 3). Lanes 5 and 6 show products of overnight ligation with T4 ligase. Final products composed of pcDNA3.1 and *env* (8kb) are visible in lanes 5 and 6, but not lane 4 (ligated vector without insert).

Figure 3.4: Toxicity of HIV-1 *env* variants in *E.coli* is associated with transcription-promoters orientated with the *env* ORF.

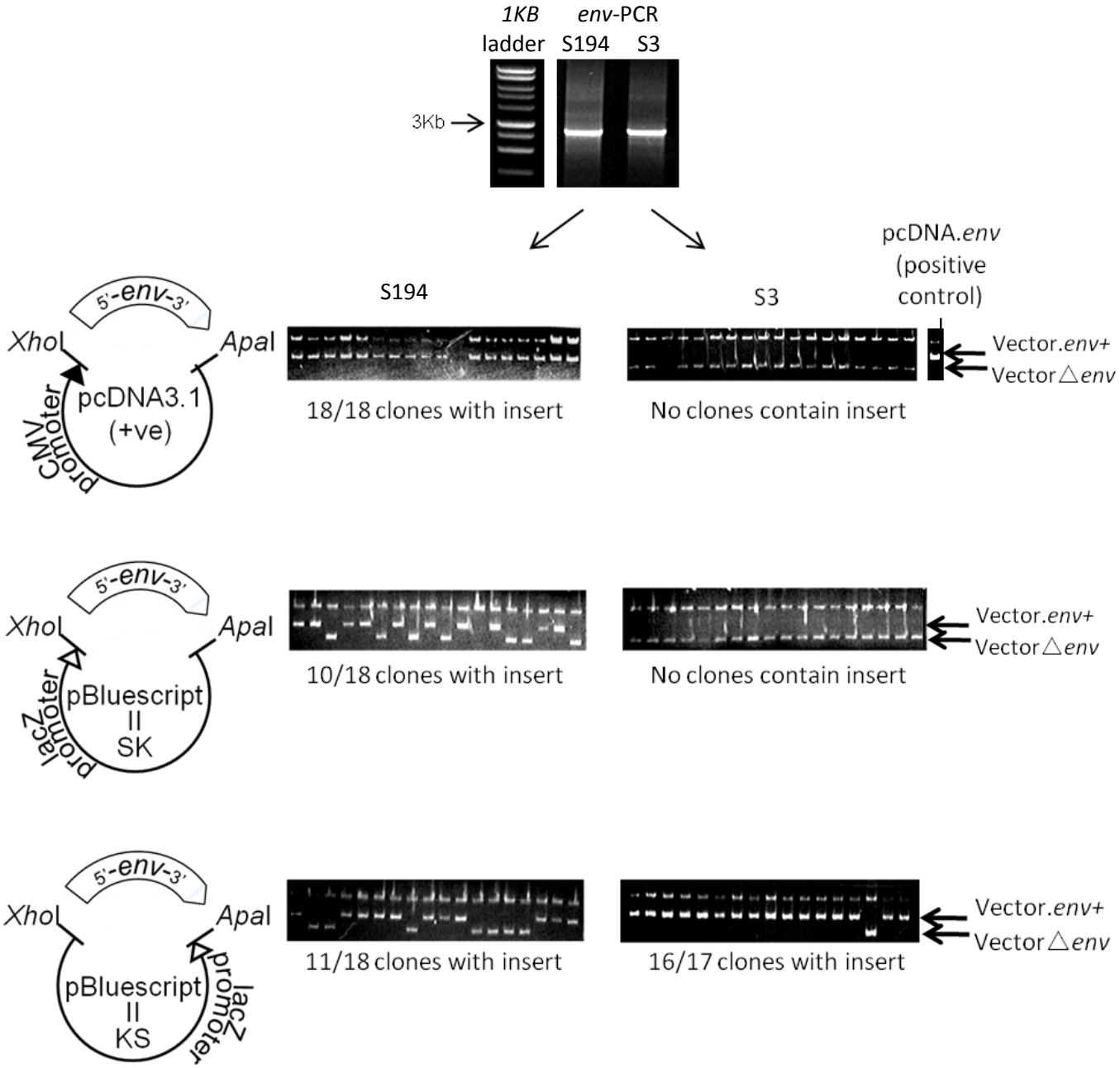


Figure 3.4 demonstrates variable cloning efficiencies for RT-PCR amplified envelope genes derived from two SPARTAC subjects. Transformed XL1-Blue strain *E.Coli* colonies were screened by agarose gel-electrophoresis of bacterial lysates. Migration of larger-supercoiled plasmids containing *env* was slower compared to those lacking the insert. All clones for patient S194 incorporated full-length *env* (confirmed by sequencing), while clones derived from patient S3 did not. Restriction-digested *env* from patients S3 was successfully cloned into KSBlueScript II but could not be cloned into the same vector with a reversed MCS (SKBluescript II), which placed the *env* open reading frame in the same orientation as the *LacZ* promoter (see Figure 2.1 for details of Bluescript vectors).

3.2.2 MACH-1 strain *E.Coli* are partially resistant to HIV-envelope toxicity.

These data provided an explanation for the failure to clone *env* from patients S199, S8, S17 and S3, but did not explain why these particular *env* variants were more problematic than the others, nor did it offer a solution for cloning these particular *env* genes into mammalian-expression vectors. The production of Env-pseudotyped viruses in 293T cells requires the expression of envelope glycoprotein, which in turn requires fusion of *env* to a promoter sequence that is functional in eukaryotic cells. The possibility of using plasmids encoding alternative viral promoters derived from SV40 or HIV-I was not pursued, because the early SV40 promoter and the 5' HIV-1 LTR have been shown to have structural features used by *E.coli* RNA pol to initiate transcription (Lewin *et al*., 2005).

Ignoring these patients would have introduced selection-bias into the study, so alternative strains of *E.coli* were tested for their capacity to host pcDNA.*env* libraries. Competent strains of K12 *E.coli* (TOP10, DH5α, and XL1-blue) all failed to host pcDNA.*env*, while transformation of W strain *E.coli,* MACH-1, produced stable colonies from the same DNA-ligations. In contrast to the K12 strains, MACH-1 transformations yielded a mixture of large and small colonies (approximate diameter, 1 mm *vs.* 2 mm after 16 hr incubation at 37 °C). Only smaller colonies contained *env*, while the larger colonies contained re-ligated pcDNA without full-length envelope, confirming that HIV-1 *env* was inhibiting bacterial growth (Figure 3.5 shows a representative example for S3). This assorted pattern of colony growth was not apparent for all patient-derived envelopes, suggesting that some inhibited bacterial growth more than others.

Previously, Monogram Biosciences (Trophile) had been unable to clone HIV-1 envelope from patient S17 as part of a separate collaborative study with our group. Although reasons for this cloning failure were not given, it is possible that envelope-mediated cytotoxicity was responsible, particularly as envelope expression cassettes used in the Trophile assay are produced in K12 strain *E.coli* (US Patent 7169551 B2).

Figure 3.5: Susceptibility to HIV-*env* toxicity is dependent on *E.coli* strain

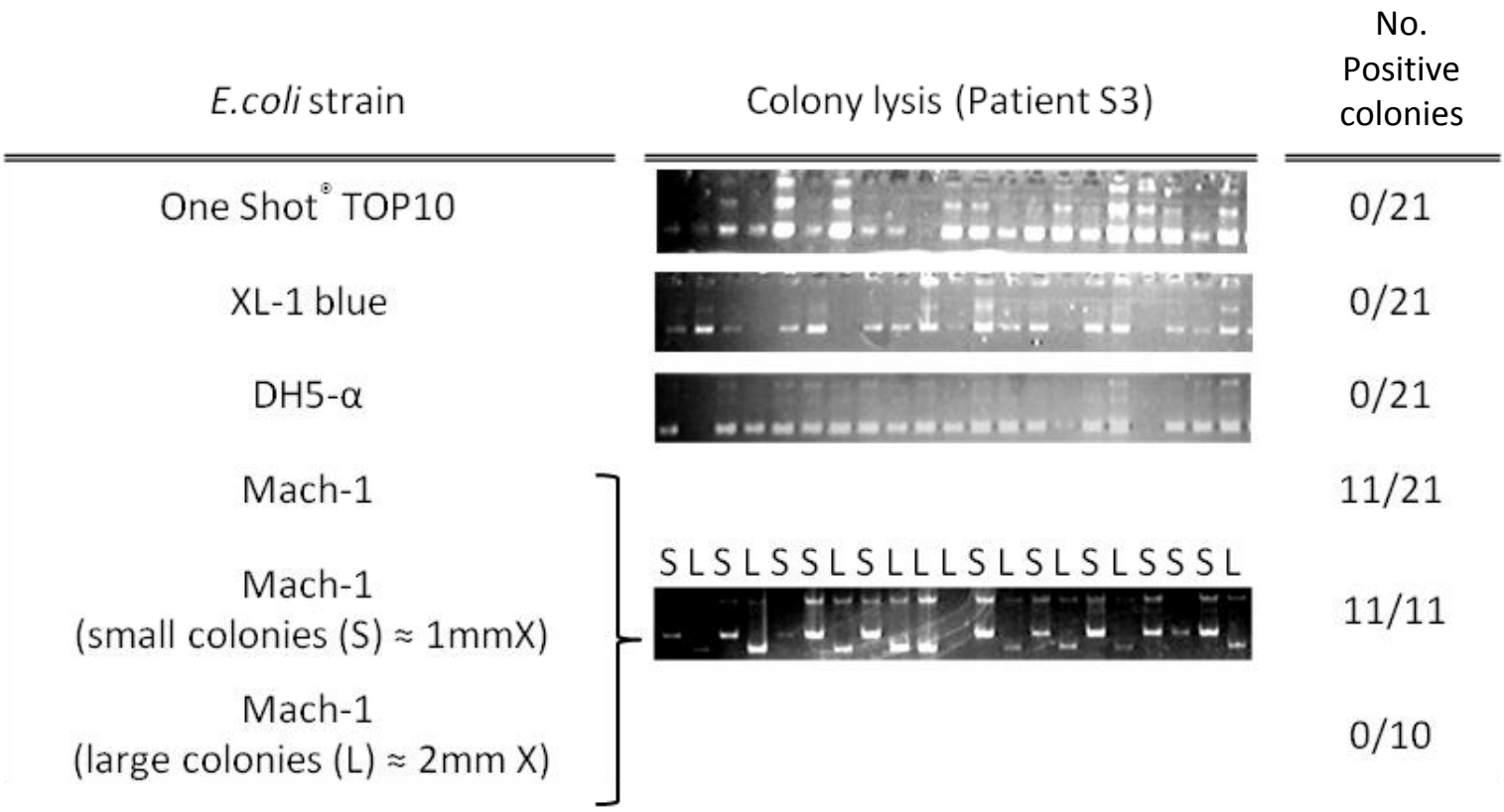


Figure 3.5: Competent *E.coli* strains were transformed with 300 ng of a pcDNA.*env* library derived by T4-ligation of *env* (Patient S3) with pcDNA3.1. Colony lysates were subjected to agarose-gel electrophoresis in order to identify plasmids containing the *env* insert. All colonies of DH5-alpha, XL1-blue, and commercial preparations of TOP10 (Invitrogen) contained ligated vector without *env,* while MACH-1 transformed colonies stably hosted pcDNA.*env* (confirmed by nucleotide sequencing). Small (S) and large (L) MACH-1 colonies were identified by visual inspection.

3.2.3 Envelopes derived from different HIV-I isolates exhibited variable levels of toxicity in *E.coli*

In order to confirm the apparent variation in cytopathic effect mediated by different *env*-variants, bacterial growth curves were plotted for *env*-transformed MACH-1 cultures. However, because β-lactamase is a secreted protein, outgrowth of bacteria lacking pcDNA.*env* was anticipated, which would have masked the inhibitory effect of Env on bacterial growth. To control for this, cultures were diluted and plated onto LB-Agar and the proportion of bacteria that had lost pcDNA.*env* was calculated by comparing the number of colonies grown on Amp^+ and Amp^- LB-agar. Cultures sampled at an A_{600} of 0.75-0.89 produced 1.5-2 fold more bacterial colonies on Amp^- LB-agar than on Amp^+ LB-agar, confirming that pcDNA.*env* had been lost from a proportion of cells when cultures reached high densities. However, there was no significant difference in the number of colonies at lower absorbances (A_{600}) of 0.31-0.6 in the absence of ampicillin, confirming that cultures at this stage of bacterial growth consisted of a homogenous suspension of stably transformed bacteria (Table 3.2). Differences in the rates of bacterial growth after short periods of culture were, therefore, not due to outgrowth of pcDNA.*env* $^-$ bacteria.

Comparison of bacterial-growth curves plotted for each MACH-1 transformation showed temporal variation in the lag-phases of growth between pcDNA.*env* variants, with those clones that failed to grow in K12 *E.coli* taking longer to reach the logarithmic phase of growth (Figure 3.6). All pcDNA.*env* clones showed some inhibition of bacterial growth relative to control cultures transformed with pcDNA3.1 without *env*, suggesting that all envelopes were partially toxic. By contrast, pcDNA3.1-transformed XL-1 blue *E.coli* took 5 hr longer to reach the log-phase, in accordance with the rapid doubling times of the MACH-1 strain. Bacterial-growth entered the log-phase at A_{600} values of approximately 0.4; above this value no difference was observed in the doubling times of clones. Cloned envelope derived from patient S3 exhibited the greatest cytopathic effect and produced a noticeably less turbid culture after 16 hr which yielded 3-fold less plasmid DNA than for the other patients. Overall, these data demonstrate that the rapid growth rate of MACH-1 *E.coli* is partially able to circumvent HIV-1 Env cytotoxicity that is fatal to slower-growing strains.

Table 3.2: Stability of pcDNA.*env* plasmids in transformed MACH-1 *E.coli*

pcDNA.*env* clone	*E.Coli* culture A_{600}	Colony forming units (10^7 per ml)	
		Amp +ve	Amp -ve
S46 c2	0.31	8.5	4.0
S194 c4	0.31	9.9	7.9
S181 c16	0.31	5.3	3.4
S99 c17	0.32	4.5	3.0
S21 c1	0.32	7.1	6.3
S185 c8	0.32	4.1	3.7
S171 c10	0.34	2.8	2.6
S35 c22	0.37	4.6	4.4
S132 c16	0.37	3.2	3.3
S128 c4	0.41	2.6	2.7
S41 c19b	0.46	2.3	2.5
S8 c4	0.48	3.4	3.6
S10 c4	0.51	2.6	3.0
S17 c13	0.55	1.8	2.5
S3 c4	0.60	3.1	5.1
S33 c12	0.60	3.2	5.8
S46 c2*	0.75	7.0	11.4*
S194 c4*	0.81	8.4	12.6*
S181 c16*	0.89	9.0	17.8*

Table 3.2: To assess the stability of patient-derived pcDNA.*env* transformed-*E.coli,* loss of ampicillin resistance was quantified from samples of bacterial cultures containing ampicillin (120 µg/ml). One envelope clone (c) was sampled from each patient. Cultures were sampled when light absorbance (A_{600}) reached values of 0.3-0.6. Bacteria were diluted $1:10^6$ and incubated overnight on Amp^+ and Amp^- LB-agar. Three cultures sampled at higher absorbance values (0.75 to 0.89) produced more bacteria on plates without ampicillin (*).

Figure 3.6: Envelope clones exhibit variable levels of toxicity in *E.coli*.

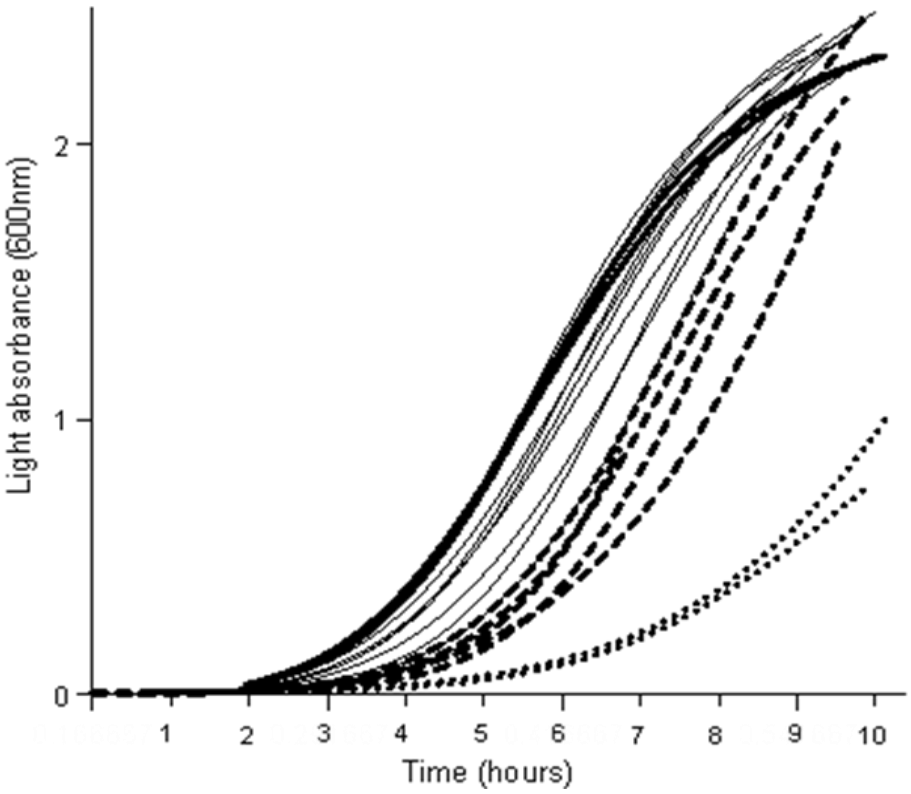


Figure 3.6. Competent MACH-1 strain *E.coli* were transformed with 100 ng of patient-derived pcDNA.*env* plasmids derived by standard alkaline-lysis and silica-resin based purification techniques (Fermentas, Genejet). Bacterial growth was assessed at 40 minute intervals by spectrophotometry at λ=600nm. took longer to reach the logarithmic phase of bacterial growth. All pcDNA.*env*-transformed MACH-1 cultures grew slower than bacteria transformed with pcDNA3.1, while pcDNA3.1-transformed XL-1 blue *E.coli* took approximately 5 hr longer to reach the logarithmic phase of growth.

Legend

	E.Coli Strain	Plasmid	Visible toxicity (small colonies)
———	MACH-1	pcDNA.*env*	No
- - - - -	MACH-1	pcDNA.*env*	Yes
———	MACH-1	pcDNAΔ*env*	No
.....	XL1	pcDNAΔ*env*	No

3.2.4 Optimization of 293T/17 cell transfections for the construction of Env-pseudotyped viruses

Pseudovirus particles were produced by co-transfection of 293T/17 cells with cloned envelope genes and a full-length HIV-1 NL4-3△*env* plasmid. A modified version of the microtitration assay described by the Central-reference laboratory at Duke University medical centre (North Carolina, US) was used to quantify infectious titres of pseudovirus in 293T/17 cell supernatant fluids (Montefiori, 2009). In this modified assay, β-galactosidase activity was quantified in place of luciferase, both of which are expressed by infected TZM-bl reporter cells under regulatory control of a Tat-responsive LTR-promoter. Initially, fixed-cell monolayers were histochemically stained with X-gal substrate and "blue" foci were counted manually under light microscopy.

Pseudoviruses constructed with HIV-1 *env* sequences from five patients by transfection with Lipofectamine had an infectious titre below $2x10^3$ IU/ml, which was insufficient to assay neutralization. Therefore, non-branched PEI (25kDa) was investigated as an alternative transfection reagent. In order to optimize pseudovirus expression by PEI transfection, molecular weight ratios of DNA to PEI, ranging from 1:1 to 1:10, were tested using HXB2 pcDNA.*env* and the infectious titres of the pseudovirus were compared. Transfection with 800ng of DNA (533 µg of pNL4-3△*env* and 267 µg of HXB2 pcDNA.*env*) with 2.4 – 4.0 µg of PEI produced pseudovirus titres of approximately $1.5\ x10^5$ IU/ml, which were 1.5-fold higher than viruses produced with Lipofectamine using the same quantity of DNA (Figure 3.7A). Quantities of PEI greater than 4.0 µg per ml of DMEM caused 293T cell monolayers to detach following a 4 hr incubation period, indicating that PEI-mediated cytoxicity was responsible for the decreases in infectious titre observed with DNA:PEI ratios greater than 1:5 (Figure 3.7A). In contrast to Lipofectamine transfections, optimized PEI transfection conditions produced infectious Env-pseudotyped virions for all patients selected for study.

In order to rule out 'carry-over' of residual DNA:PEI complexes during pseudovirus titrations, NL4-3△*env* plasmid was transfected without *env* to produce non-infectious ΔEnv-virions. Harvested supernatants titrated onto TZM-bl cells did not produce foci of infection after 48 hrs, confirming that the reporter cells had not been transfected (Figure 3.7B). Nevertheless, 293T cells were washed after each transfection and supernatants were filtered prior to the virus-titration and neutralization experiments.

To test whether patient-derived HIV-1 envelopes were toxic to mammalian cells, TZM-bl monolayer confluency was visually inspected by light microscopy, and Trypan-Blue dye exclusion was quantified after 48 hrs infection with 200 IU per well of each pseudotype. The percentage viability of Trypan-Blue stained trypsinized-monolayers ranged between 82% - 100%, and monolayer confluence was estimated to be greater than 95% in all cases. Cell viability was not a specific property of individual Env-clones, because variations between different Env-pseudotypes were of similar magnitude to variation observed between triplicate wells receiving the same virus. Moreover, there was no correlation between Env toxicity in TZM-bl cells and *E.coli.* In fact, TZM-bl cell monolayers infected with S3 Env-pseudotyped virus reached 100% confluence, despite cytopathic effects of S3 pcDNA.*env* in *E.coli* (Figure 3.7B). Infectious titres greater than $5x10^3$ IU/ml resulted in monolayer confluence less than 50% for virus pseudotyped with HXB2. It was not possible to compare all viruses at this level of infectivity because the majority had titres below $5x10^4$ IU/ml. Eukaryotic cytotoxicity resulting from HIV-I *env* expression in 293T cells could not be ruled out because of the cytotoxic effects of the PEI transfection reagent.

Figure 3.7 Optimization of pseudovirus production by PEI transfection

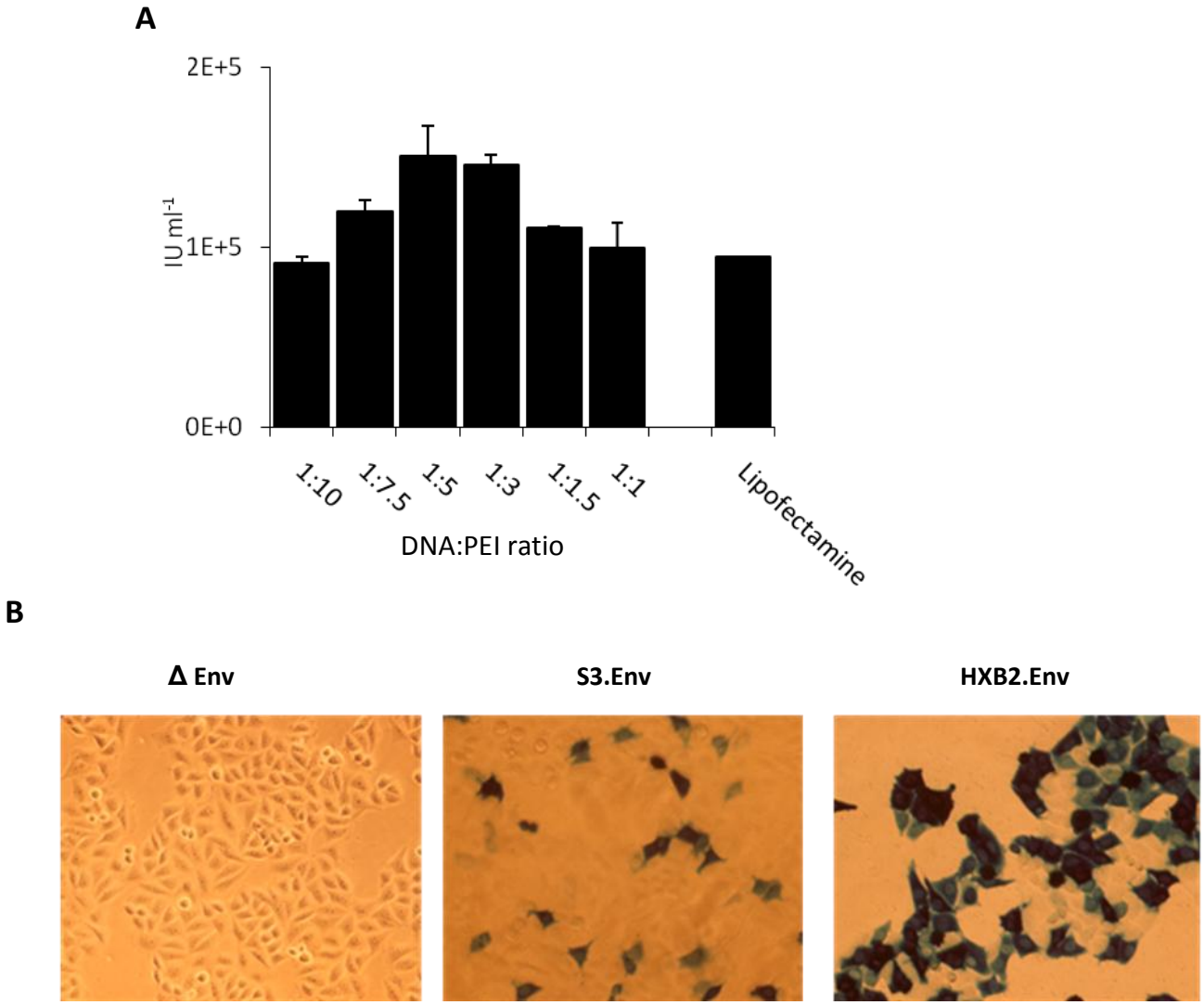


Figure 3.7A. Co-transfection procedures were optimized for pseudovirus production with plasmids NL4-3Δenv and HXB2.*env*, mixed in a ratio of 3:1. A total of 800 ng of DNA mixture was combined with relative quantities of PEI shown on the x axis. Pseudoviruses were harvested after 48 hr and titrated on TZM-bl cells, and infectious titres (IU/ml) were calculated from the number of infected cells in each well.

Figure 3.7B. Viruses pseudotyped with functional HIV-1 envelopes infect TZM-bl cells, leading to expression of β-Gal. Virus like particles that lack functional envelopes cannot infect the reporter cells (left panel). After 48 hr incubation with 200 IU of S3 pseudotype, TZM-bl cells remained 90-95% confluent (central panel). Conversely 50% of the TZM-bl cell monolayer detached following infection with $5x10^4$ IU/ml of HXB2-Env pseudotyped virus (right panel).

3.2.5 Optimization of a high-throughput pseudovirus-microtitration assay.

Manually counting pseudovirus-infected cells proved to be time-consuming, unreliable and subjective, as counts varied between different assay operators. Therefore, conditions were optimized for automated counts with an ELISpot plate reader (AID). An important step in the modification of this assay was achieving an evenly-distributed cell-monolayer that improved the reproducibility of the assay. For this, opaque 96-well microtitre plates were seeded with reporter cells 24 hr prior to the addition of virus-plasma combinations. This method was compared to the cell-seeding protocol described for the standardized luciferase-based assay in which pseudovirus is added simultaneously with freshly-trypsinized cells. The striking infection-enhancing effect of this minor amendment can be seen in Figure 3.8. In addition to a more even cell distribution, pre-seeded cell monolayers were more permissible to infection, producing 3-5 fold more infectious foci than in the original protocol.

Uninfected cells did not produce a background-noise with the image correction settings described in section 2.20. However, pipette scratches occasionally left distinctive lines on the base of microtitre wells, causing with the ELISpot-reader software to erroneously count high numbers of FFUs. Therefore, each image was manually inspected and automated-counting errors caused by these pipette scratches were corrected. With careful pipetting this affected less than 0.2% of microtitre wells.

The quantifiable limits associated with β-Gal or luciferase as the readouts for the pseudovirus-infectivity assay were compared. A five-fold serial dilution of HXB2 Env-pseudotyped virus was quantified by luminometry and by automated counts of infected-cell foci (Figures 3.9A and 3.9B, respectively). The quantifiable-linear ranges resulting from both readouts reached a plateau above 10^3 foci per well ($8.7x10^5$ relative light units; RLU). Above this limit, light detection approached saturating levels and it was not possible to differentiate between individual stained-foci and clusters of β-galactosidase expressing cells. Automated cell counting slightly increased the sensitivity of the assay to permit detection of single cell infections, in comparison to light detection from D-luciferin-treated cell lysates, which approached background levels below 10 infectious particles per well ($2.5x10^4$ RLU). Virus titres

Figure 3.8 Optimised cell-seeding protocol for HIV-1 pseudotype microneutralization assays.

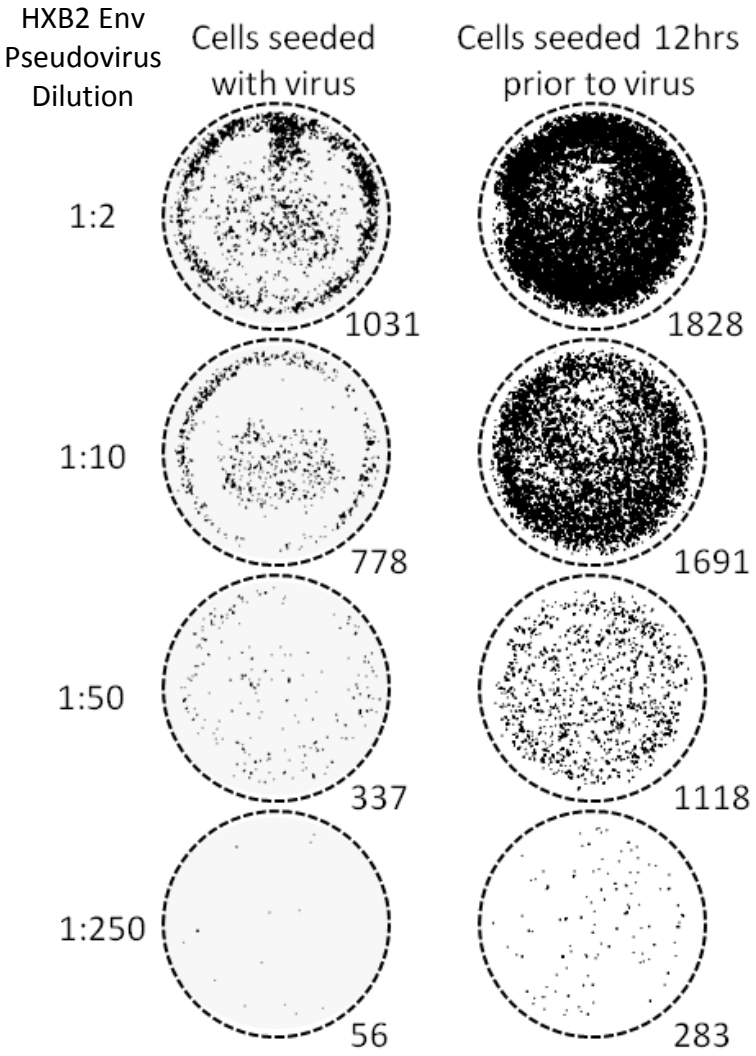


Figure 3.8: An even distribution of cells is a prerequisite for accurate counts of pseudovirus-infected TZM-bl reporter cells using ELISpot readers for automated read-outs. The cell-seeding protocol described by the Duke University Central Reference Laboratory (left panels) was compared to the modified protocol (right panels), in which cells were seeded 12 hr prior to titration of HXB2 pseudovirus. Cell distribution patterns resulting from each protocol are shown by images acquired with an AID ELISpot plate reader. A “halo” effect was observed when virus was mixed with freshly-trypsinized cells which substantially reduced counts of infected cells, given by the numbers to the right of each image

Figure 3.9 Comparison of luminometry with automated spot counting for TZM-bl based pseudovirus infectivity assays.

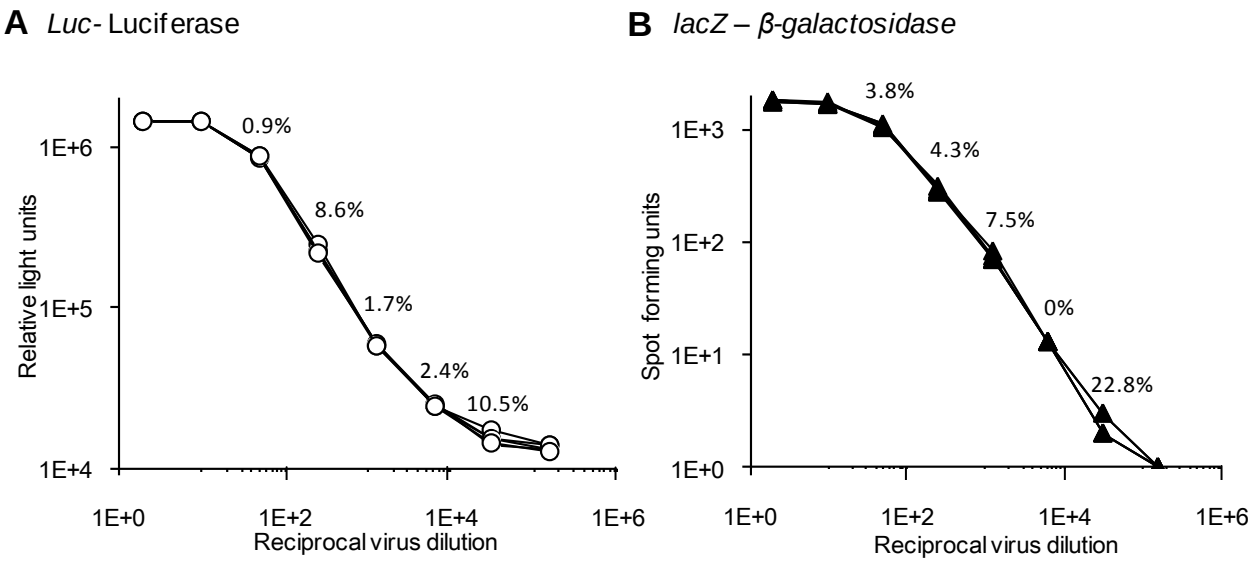


Figure 3.9. The quantifiable-linear range of pseudovirus infected TZM-bl cells was assessed by luminometry (Figure 3.9A) and automated spot counting (Figure 3.9B). Titrations of HXB2 Env-pseudotyped virus were prepared in parallel and assayed for luciferase expression using a luminometer (section 2.23) or β-Gal expression by automated spot-counting of X-gal stained cell monolayers using an ELISpot plate reader (section 2.21). Readouts for both techniques reached a plateau above 10^3 infected cells per well ($5x10^4$ IU/ml or $8.7x10^5$ RLU). Percentages give the intra-assay coefficient of variance for 10 replicates of virus dilutions assayed using each technique.

that fell within a linear range of 10-10^3 infectious particles per well produced standard deviation to mean ratios below 1:10 for both protocols, confirming equivalent levels of accurate reproducibility. Histochemically stained cells were dried prior to reading, so plates could be kept indefinitely at ambient temperatures and anomalous results could be reassessed. This offered a distinct advantage over the original luciferase assay.

3.2.6 Validation of the β-Gal neutralization assay.

The optimized β-galactosidase infectivity assay was validated as a means of measuring neutralization with patient plasma by direct comparison with the luciferase-based assay. The plasma-titres required to neutralize 50% of a HXB2-Env pseudotyped virus (IC_{50}) were calculated from neutralization curves derived from each assay. Using the β-gal system, mean IC_{50} plasma-titres calculated for patients S181 and S10 were 1:25 and 1:232, respectively (Figures 3.10A and 3.10B, respectively). These values fell within the 95% confidence intervals of titres detected by the luciferase-assay, confirming that the protocol modifications do not bias the neutralization recorded for patient plasma. Sub-neutralizing concentrations of both plasma enhanced virus infectivity by 10-30%. This level of enhancement corresponded to 15-45 infected cells, which was not detected by the luciferase assay. Optimising the cell distribution had the knock-on effect of reducing the variance of replicate tests, thus narrowing the confidence intervals of the β-gal assay (Figures 3.10C and 3.10D). Overall, automated counting of pseudovirus-infected cell monolayers provided a cost-effective alternative to luciferase-based luminometry with similarly high-levels of throughput, sensitivity and reproducibility.

Figure 3.10 Validation of the high-throughput microneutralization assay for HIV-Env pseudotypes.

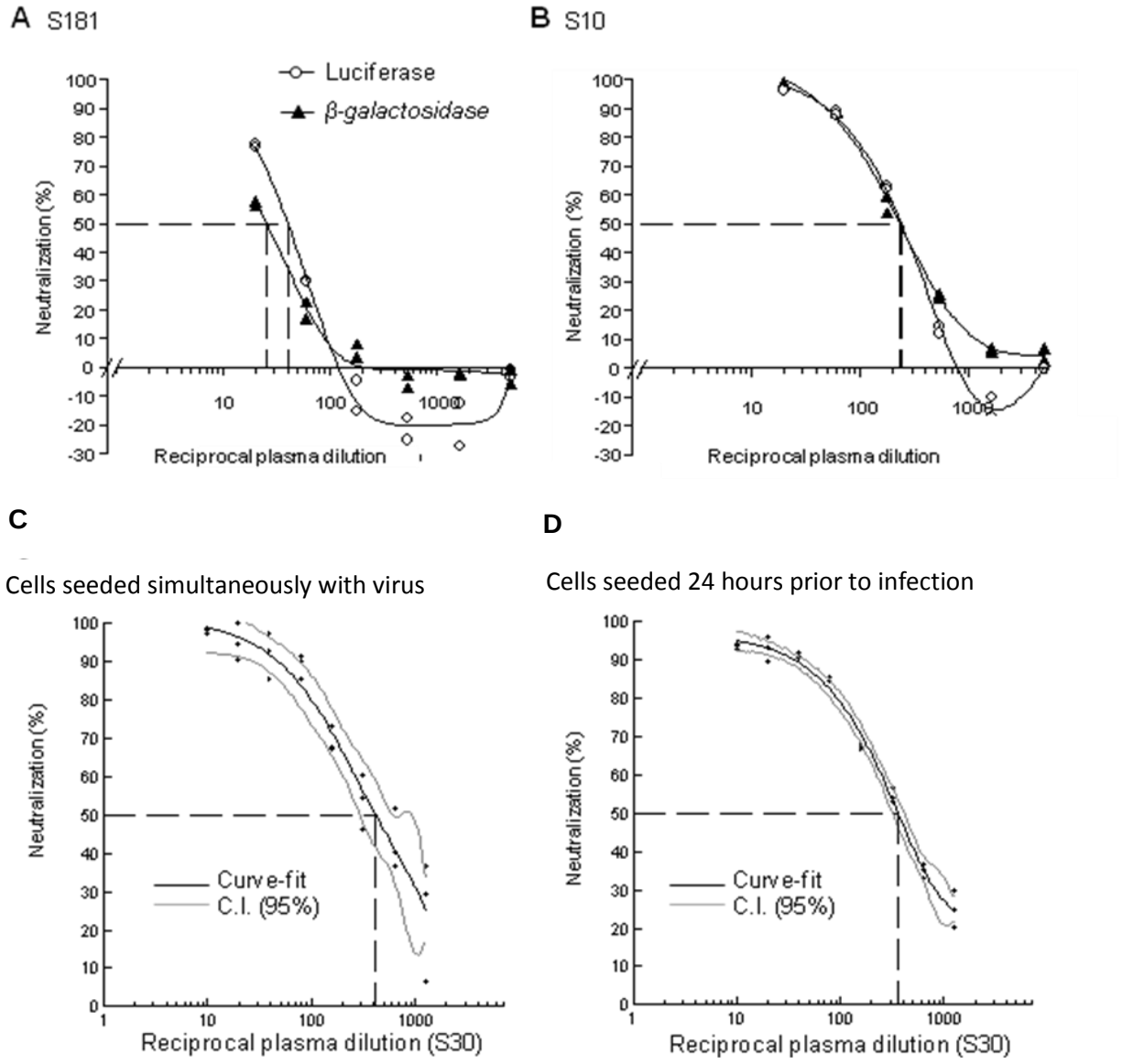


Figure 3.10. The β-gal microneutralization assay was compared to the standardized luciferase-based assay. Neutralization of a HXB2 *env*-pseudovirus is shown for plasma derived from representative patients exhibiting low neutralization (Figure 3.10A; patient S181) or high neutralization (Figure 3.10B; patient S10). Similar patterns of neutralization were detected by luminometry (open circles) and automated cell counting (black triangles). Neutralization curves (black lines) were plotted from the percentage-reductions in spot-forming units (y-axes) relative to no-plasma controls. Neutralizing plasma titres (IC_{50}) are shown by dashed-intercepting lines. Curve fits were plotted using XLfit software. Figure 3.10C gives an example of a HXB2-neutralization curve (β-Gal) acquired using the cell-seeding protocol described by the original assay. Virus was neutralizing with plasma derived fom patients S30, for whom pseudovirus was not cloned. For comparison Figure 3.10D shows the equivalent result generated using the modified protocol. The 95% confidence intervals (grey lines) were narrower when virus-plasma mixtures were added to pre-seeded plates.

3.3 Discussion

The Env-pseudotype HIV-1 neutralization assay has produced an invaluable tool with which to identify and characterise HIV-1 neutralizing antibodies. However, the assay was primarily developed for vaccine research, so its capacity to measure natural antibody responses *in vivo* requires appraisal. Adapting the endpoint measurement from luciferase detection to quantification of β-galactosidase did not affect the intra-assay variation and marginally improved sensitivity to allow detection of a single infected cell. This added sensitivity is unlikely to improve assessments of 50% or 90% neutralizing titres, but could offer a benefit to studies of the non-neutralized fractions of HIV-1 that are commonly detected at saturating concentrations of NAbs *in vitro* (Burton *et al*., 2001).

Seeding cells one day prior to incubation with virus/plasma enhanced susceptibility to pseudovirus infection four-fold, perhaps because trypsinisation removes virus-receptors required for entry into host cells. This protocol amendment should also be considered for the original luciferase system, to reduce the number of rejected *env*-pseudotypes with titres that are considered too low for viral-inhibition assays.

Arguably, PBMCs and wild-type viruses are more relevant to the NAb response, *in vivo,* than reporter cell systems engineered to be susceptible to molecularly cloned virus, although lectin-stimulated PBMCs are not representative of HIV-1 target cell populations *in vivo* (Jackson *et al*., 1988). However, levels of neutralization detected by PBMC-based assays are confounded by the effects of i) cytokines and chemokines that can inhibit or enhance virus replication (Kinter *et al*., 1996) ii) Fcγ-receptor-dependent cellular mechanisms involving non-neutralizing antibodies (Holl *et al*., 2004) iii) heterogeneity between PBMCs populations from different donors (Polonis *et al*., 2009) iv) variable replication kinetics of quasi-populations of cultured virus (Binley *et al*., 2004) and v) variable plasma concentrations of p24 antigen and anti-p24 antibodies that interfere with the end-point measurement of the assay (Mascola and

Burke, 1993). Consequently, an international collaborative study by NeutNet reported that pseudovirus assays generate results that are generally more reproducible than PBMC-based approaches (Fenyo *et al*., 2009).

This withstanding, the possibility of selecting minority *env*-clones that are unrepresentative of the major circulating quasispecies is a problem with assays using molecularly cloned virus. This problem is further exacerbated by the findings of this study, which demonstrates variable degrees of HIV-1 Env-mediated cytotoxicity in K12 *E.coli* strains that are widely used for virus cloning. Potentially, this could bias the selection of patient viruses in favour of those Env-variants that are non-cytotoxic. These findings are particularly relevant to HIV-1 pseudotype assays used in the clinical setting, including the Trofile assay currently licensed to predetermine susceptibility to CCR5-anatagonist, virus-entry-inhibitor, Maraviroc (Pfizer). The possibility of Maraviroc-treatment failure resulting in the selection of minority X4-tropic virus requires this assay to be highly sensitive (Archer *et al*., 2009, Fatkenheuer *et al*., 2008, Saag *et al*., 2009). Therefore, the possibility of Env-toxicity leading biased-sampling of virus quasispecies should be assessed, specifically in this clinical setting.

Previously described methods of culturing *env*-transformed bacteria at ambient temperature did not yield envelope clones from some patients (McDonald and Burnett, 2005), whereas competent MACH-1 cells derived from *E.coli* strain W, facilitated *env* cloning from all patients selected for study. On a per cell basis, it seems likely that MACH-1 cells are susceptible to *env* toxicity, but compensate with rapid rates of cell division. Correspondingly, those *env* genes that were toxic to K12 *E.coli* strains produced 'small' MACH-1 colonies that took longer to reach logarithmic phases of growth in suspension culture. Negative-selection mediated by toxic plasmids resulted in outgrowth of faster-growing *E.coli* that lacked pcDNA.*env* at A_{600} values greater than 0.8, which may partly explain why toxic and non-toxic envelopes exhibited similar kinetics of logarithmic-growth. However, this does not explain why cultures of *E.coli* transformed with the most toxic envelope clone, derived from patient S3, were considerably less turbid

after 16 hr of growth, and yielded significantly less plasmid DNA than the other cultures. This suggests that death rates were dissociated from higher rates of cell division during the initial part of the logarithmic phase, but subsequently caught-up, causing bacterial growth to plateau prematurely. This is to be expected, given a delay in *env* expression following mitosis, in keeping with the association of *env* toxicity with mammalian-transcriptional promoters that are not optimised for prokaryotic systems.

Occasionally, repeated attempts were required to grow MACH-1 cultures transformed with particularly problematic envelopes. Therefore, this cloning adaptation may still fail for certain *env* genes, if the toxicities are greater than those observed here. Nevertheless, MACH-1 cells provide a marked improvement over the more commonly used K12 strains, in terms of their potential to limit sampling bias of HIV-1 *env* genes. A previous study demonstrates that viral promoters derived from SV40, CMV and HIV-1 possess structural elements that initiate transcription in *E.coli*, whereas the viral promoter derived from the thymidine kinase gene of herpes simplex virus 1 (HSV1) does not lead to gene transcription in K12 *E.coli*. Therefore, expression plasmids that use this HSV1 promoter should be assessed as alternative vectors for eukaryotic expression of HIV-I Env (Lewin *et al*., 2005).

Previous studies have identified amphipathic α-helical structures within the gp41 fusion peptide, termed lentiviral-lytic peptides that permeabilise membranes of eukaryotes and prokaryotes (Chernomordik *et al*., 1994, Arroyo *et al*., 1995). This mechanism, along with transduction of signaling cascades through gp41-binding of calmodulin, has been implicated in human cytopathology (Tencza *et al*., 1997, Tencza *et al*., 1995). In this study, we did not detect Env-dependent cytotoxicity in the 293T or TZM-bl mammalian cell lines. However, pseudotyped viruses, that do not package HIV-1 *env* genes, are unsuitable for this investigation and observations in *E.coli* are of limited relevance to human infection. Further investigations into effects of more or less toxic envelope genes could indentify correlates of virus-mediated pathogenesis.

Chapter 4

B cell depletion in an HIV-1 infected human reveals a role for NAbs in the control of VL

4.1 Introduction

During the chronic stage of HIV-1 infection, VL is maintained at a set-point that reflects a balance between antiviral immune responses and continuous viral turnover from steadily declining numbers of $CD4^+$ T cells. Immunological control of viraemia varies considerably between individuals and a minority (less than 1%) maintains VLs below detectable levels (Lambotte *et al*., 2005, Madec *et al*., 2005a). Several studies have detected strong "polyfunctional" $CD8^+$ and $CD4^+$ T cell responses in some elite controllers (Betts *et al*., 2006, Emu *et al*., 2008, Migueles *et al*., 2002, Sarez-Cirion *et al*., 2007, Streeck *et al*., 2008, Pereyra *et al*., 2008b, Potter *et al*., 2007). Conversely, NAb responses against heterologous isolates are rare and responses against autologous viruses are frequently of lower potency in elite controllers than in chronic progressors (Bailey *et al*., 2006, Lambotte *et al*., 2009, Li *et al*., 2009b, Mahalanabis *et al*., 2009b, Pereyra *et al*., 2008a). In spite of low levels of circulating Env antigen, a minority of elite controllers have been shown to develop neutralizing responses (Doria-Rose *et al*., 2009, Scheid *et al*., 2009), but functional data linking such antibodies to the control of viraemia is lacking. Furthermore, the controlling effects of partially-neutralizing responses detected in the majority of chronically infected patients has been difficult to determine, due to other confounding factors that limit virus replication, such as T-cell responses, virus fitness and host genetics (Carrington and O'Brien, 2003).

Lymphocyte depletion experiments have yielded information about the functional importance of specific immunological compartments. For instance, depletion of $CD8^+$ T cells in SIV-infected macaques results in higher VLs and accelerated rates of $CD4^+$ T cell destruction (Jin *et al*., 1999, Lifson *et al*., 2001, Metzner *et al*., 2000). Similarly, macaques depleted of B cells prior to SIV infection develop high levels of viraemia that inversely correlate with levels of anti-SIV IgG (Miller *et al*., 2007, Schmitz *et al*., 1999). While such data are readily available from animal models, they are rarely available in man.

Rituximab is a mouse-human monoclonal antibody that targets and depletes CD20+ B cells by NK cell-mediated and complement-mediated cytotoxicity (Gong *et al*., 2005, Taylor and Lindorfer, 2008). It does

not deplete antibody-producing plasma cells, because expression of CD20 ceases when late B cells differentiate into plasma cells (Ahuja *et al*., 2008). The natural ligand of CD20 has not been defined, although it is thought to be involved in B cell activation and cell proliferation (Popoff *et al*., 1998). Rituximab therapy has been associated with declining antibody titres in the treatment of autoimmune disorders, such as systemic lupus erythmatous, pemphigus vulgaris and mixed cryglobulinaemia vulgaris (Eming *et al*., 2008, Saadoun *et al*., 2008, Stasi *et al*., 2007). Here, we report a unique case in which rituximab monotherapy was used in a patient with stable HIV-1 viraemia, in the absence of ART. This led to a reversible loss of HIV-1 control, associated with reciprocal changes in NAb titres. Sequence analysis revealed diversification of virus as antibody levels declined, with subsequent selection of NAb-resistant mutants at sites consistent with antibody selection. These data suggest that B cell function contributed to long-term control of VL in this individual, and that NAbs may be more important in controlling chronic HIV-1 infection than previously suspected.

The study described in this chapter was led by Professor Paul Klenerman (Nuffield Department of Clinical Medicine, Oxford University, Oxford). All neutralization assays, envelope mutagenesis, reverse transcriptase quantification and protein-binding experiments were carried out by the candidate. The phylogenetic analyses (shown in Figures 4.5-4.7) were carried out by Dr Gary Huang and Dr Aris Katzourakis at Oxford University. The $CD8^+$ T cell functional analysis and the HLA typing was conducted by Dr John Frater at Oxford University. All clinical data ($CD4^+$ T cell counts, HIV-1 VL, Hepatitis B VL, immunoglobulin quantification, and liver function testing) were acquired at clinical laboratories as part of the care the patient received at St Mary's Hospital, London.

4.2 Clinical History

The patient, a Caucasian male, was diagnosed with an asymptomatic lymphoplasmacytic lymphoma (LCL) in 1972. He did not receive treatment at the time. In 1999, he was diagnosed with acute Hepatitis B virus (HBV) infection. In 2002, aged 58, he was diagnosed with HIV-1 seroconversion illness (clade B). The date at which HIV-1 seroconversion was confirmed is designated as d0 throughout this case study. Following seroconversion, the patient was noted to have elevated numbers of $CD138^+$ pre-B cells in the bone marrow and raised IgM (κ-light chain) paraprotein levels, attributed to progression of his LCL.

On diagnosis of HIV-1 infection the patient was recruited into a prospective, non-randomised observational study of early treatment and received three months of combination ART (the pilot study to SPARTAC, Fidler *et al*., 2002). Thirty months later he received thalidomide treatment for a rising paraproteinaemia without clinical effect. Rituximab therapy was initiated the following month, 1075 days after HIV-1 seroconversion. Four months after the final dose of rituximab the patient became unwell with malaise, fever and unexplained pulmonary infiltrates. This coincided with a 1.7 $\log_{10}$ rise in HIV-1 VL, peaking at 737,400 copies/ml. In addition to rising HIV-1 VL, the patient's HBV VL, previously undetectable, reached peak levels greater than $6x10^6$ copies/ml and he developed a biochemical hepatitis (peak alanine transaminanse (ALT) 851 international units (IU) per L). In the absence of ART, HIV-1 VL declined over 3 months, reaching a nadir of 175 RNA copies per ml. Subsequently, long-term combination ART was initiated, 1392 days after seroconversion (emtricitabine, tenofovir disoproxil fumarate and lopinavir/ritonavir). His $CD4^+$ count remained above 350 cells/mm^3 throughout the follow-up period, and the patient recovered with supportive treatment (Figure 4.1).

Figure 4.1 Clinical course of HIV-1 in relation to rituximab therapy

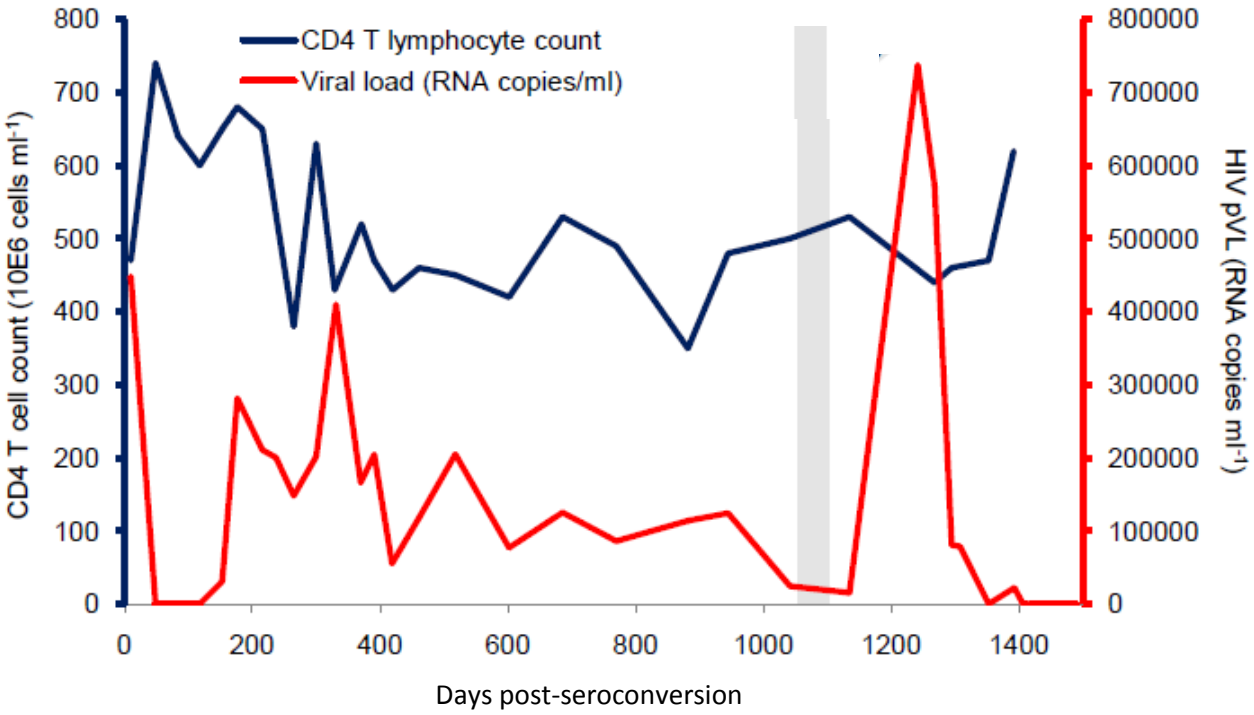


Figure 4.1: The plasma VL (red; right y-axis) and CD4 count (blue; left y-axis) of the individual studied are displayed over time (days since seroconversion). The brief dip in VL over the first 100 days corresponds to course of ART administered as part of the short-course ART trial (d 0 - d 164). Subsequently, VL was maintained at approximately 10^5 copies per ml over approximately 1000 days without ART. The four week course of rituximab therapy is indicated by the grey shaded area.

4.3 Results

4.3.1 Impact of B cell depletion on plasma antibody concentration

Before the first dose of rituximab, total IgG plasma concentrations were 16.1 g/l, which is within the normal range for a healthy adult (0.8 - 18 g/l, American Society for Clinical Laboratory Science). Fifteen days after the peak VL measurement, total IgG decreased to 10.8 g/l then subsequently increased to 17.3 g/l as VL dropped. Reductions in IgG concentration coincided with reductions in total IgA and IgM κ-light chain paraprotein concentrations. Subsequently, IgA levels returned to pre-rituximab levels, whereas IgM-paraprotein concentrations did not increase. These clinical data suggested that rituximab therapy resulted in modest decreases in total concentrations of different antibody isotypes, which is in keeping with a non-specific depletion of $CD20^+$ B cells (Eming *et al*., 2008, Saadoun *et al*., 2008, Stasi *et al*., 2007). However, despite only modest changes to total antibody concentrations, antibody levels to the HBV surface antigen (HBsAb) declined from 7.8 IU/ml to undetectable levels (<1IU/ml) by the peak of HIV-1 VL (Table 4.1). This discrepancy implied that the effects of rituximab on different antibody idiotypes were variable.

4.3.2 Neutralizing plasma titres against HIV-I temporarily decreased following rituximab therapy.

The reciprocal association between antibody concentration and HIV-1 VL prompted the hypothesis that rituximab therapy caused a transient decrease in HIV-1 NAb titre and a transient loss of viraemia control. To evaluate NAb activity throughout this period, pseudoviruses were constructed from autologous *env* sequences derived from d 366 and d 1042 plasma. Despite sequence variation within the C2V3 *env* region involving less than 2% of the 770 sequenced nucleotides, there was no significant difference in neutralization sensitivity between three heterogenous clones assessed for each time point. Neutralizing plasma titres of three clones derived from each time point are shown in Table 4.2. Serum obtained prior to the first dose of rituximab (d 1042) potently neutralized pseudovirus constructed with

Table 4.1 Impact of rituximab on plasma immunoglobulin concentrations

Days post-seroconversion	IgG (g/l)	IgA (g/l)	IgM-κ paraprotein (g/l)	HBsAb (IU/ml)	Clinical details
883				12.43	
1028	16.1	0.7	38		
1094	16	0.8	37		Pre rituximab
1144	15.6	0.7	29		Post rituximab
1204	12	0.5	24		
1239				7.8	During acute illness
1254	10.8	0.6	25		
1295				<1	
1298	11.6	0.7	26		
1308				2.86	
1449	17.3	0.8	23		On ART post-convalescence
1700				100.76	

Table 4.1 Total immunoglobulin concentrations were assessed at the Diagnostic-Immunology Laboratory at St Mary's hospital as part of follow-up investigations of the patient's LCL. Total IgG and IgA concentrations were assessed by immune-nephelometry (Beckman-Coulter) and concentrations of HBsAb were assessed by ELISA. Both assays are validated for clinical diagnositic purposes (section 2.5).

Table 4.2: Impact of rituximab on neutralizing plasma titres (IC_{50}).

Days post-seroconversion	d 336 pseudovirus	d 1042 pseudovirus	Mutant 339E/363R	HXB2	VSV-G	Clinical details
1042	>775	150	n/t	850	<20	Pre-Rituximab
1135	>775	225	300	1000	n/t	Post-Rituximab
1239	220	<120*	n/t	875	20	Peak viraemia
1295	250	150	n/t	325	20	
1308	360	375	n/t	1000	<20	
1353	600	425	600	3950	n/t	Post-convalescence
negative serum	<20	<20	n/t	<20	n/t	

Table 4.2. Half-maximal inhibitory concentrations of sera (IC_{50}, reciprocal dilutions) are shown for virus pseudotyped with Env-clones derived from d 336 and d 1042 plasma. Neutralization of a HXB2 Env-pseudotyped virus is also shown. Serum concentrations below 1:20 did not inhibit VSV-G pseudotyped virus indicating that neutralizing responses were HIV-Env specific. (*)1:120 was the highest concentration of d 1239 serum that could be tested against d 1042 virus due to limited availability. Mutant 339E/363R was constructed to represent envelope changes identified following rituximab therapy. "*n/t"* denotes virus-serum combinations that were not tested because of limited availability.
autologous envelopes derived 2 years previously (d336, $IC_{50}<775^{-1}$).

autologous envelopes derived 2 years previously (d336, IC_{50}<775^{-1}). The same serum neutralized contemporaneous Env-pseudotypes (d 1042), albeit to a lesser extent, with an IC_{50} of 1:150. This concurs with typical patterns of viral escape from NAbs previously reported (Mahalanabis *et al*., 2009b, Parren *et al*., 1999, Richman *et al*., 2003, Wei *et al*., 2003); it also confirmed this patient was able to mount a neutralizing response in spite of his LCL.

Following rituximab therapy, IC_{50} serum titres against d 336 and d 1042 Env-pseudotypes decreased by 2 to 3-fold and the neutralizing effects of 1:180 dilutions of sera reached nadir values concomitant with peak VL (Figure 4.2). Subsequently, neutralizing activity rebounded as viraemia was brought under control. Remarkably, as neutralizing plasma titres returned, VL decreased from 737,400 to 175 copies/ml in the absence of ART, despite a pre-rituximab VL set-point of 1.7×10^5 RNA copies/ml (± 8.3×10^4, d 153 to d 938,). Sera collected after VL had decreased neutralized d 1042 virus more effectively than sera collected before peak viraemia (Figure 4.2). Decreases in neutralizing activity against a HXB2 Env-pseudotyped virus were also observed, and the changes in IC_{50} titre were greater than that observed for autologous virus strains. The potent levels of neutralization observed against HXB2 were not surprising, as diverse virus strains stimulate antibodies that neutralize HXB2 (Binley *et al*., 2008).

To determine the breadth of this patients NAb response, heterologous NAb activity was tested against a standardized panel of clade-B reference strains. Eight of the twelve isolates were neutralized with titres ranging from 1:90 to 1:300 (Table 4.3). Virus pseudotyped with Env clones SC422661, RHPA4259, THRO4156, WITO4160, CAAN5342, were not neutralized by the patient's sera (IC_{50} > 20^{-1}). Six isolates were more neutralized by serum collected post-rituximab than serum collected pre-rituximab, in agreement with the increases in neutralization observed with autologous virus. In comparison to other studies, this patient's neutralizing response exhibited moderate breadth and potency with IC_{50} titres that fell within the inter-quartile ranges reported for chronically infected patients (Binley *et al*., 2008, Sather *et al*., 2009, Mahalanabis *et al*., 2009a). However, there was insufficient serum to assay heterologous

Figure 4.2: Autologous neutralizing antibody titres assayed over time.

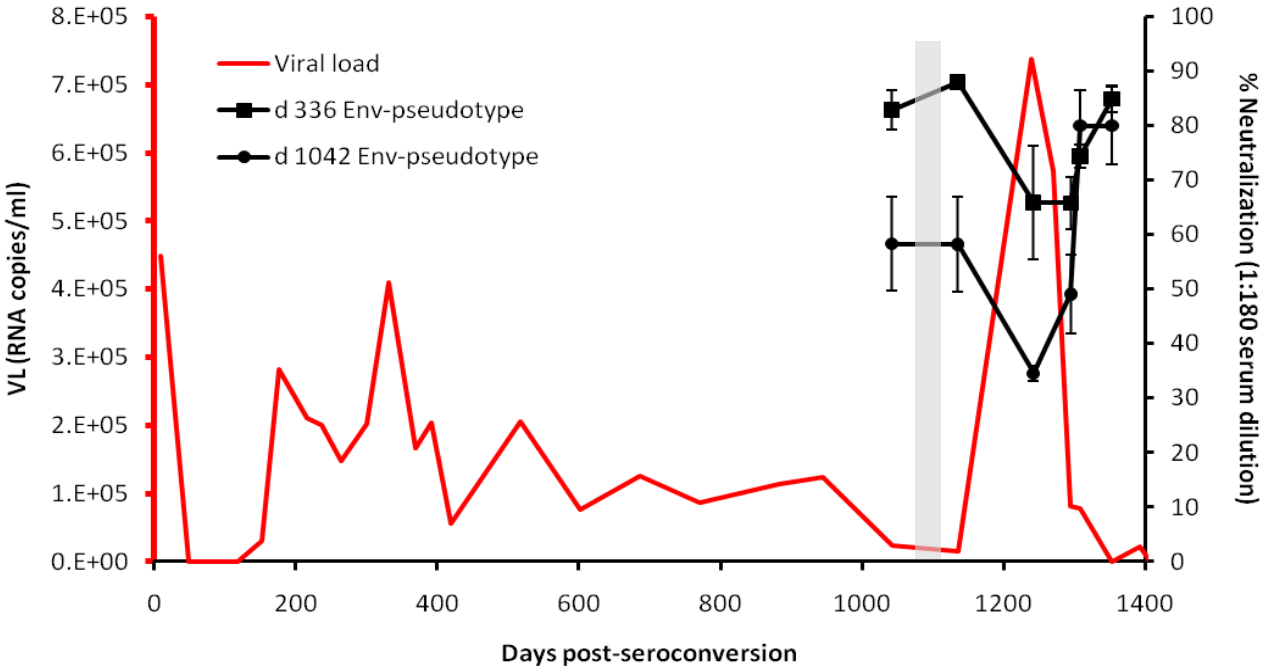


Figure 4.2: Autologous viruses, constructed with cloned *env* genes derived from d 336 (■) and d 1042 (●) post seroconversion, were neutralized with patient sera taken before and after rituximab therapy. Percentage reductions of infected cells mediated by serum diluted 1:180 in complete DMEM are shown (black lines: right y-axis). One representative clone from each time points is shown (Rit.336d. c3 and Rit.1042.c6). Plasma VL (red line; left y-axis) is shown over time (days post sero-conversion; x-axis). Grey shaded area indicates the four week course of rituximab therapy. Error bars show the standard deviations of triplicate tests for each clone.

Table 4.3 Neutralizing plasma titres against heterologous virus

Serum	Pseudovirus							
	6535	QH0692	PVO	TRO	AC10.0	pREJO 4541	pTRJO 4551	pRHPA 4259
d 1042 (pre rituximab)	220	220	90	120	90	140	50	50
d 1353 (post rituximab)	300	170	90	130	160	220	140	120
Negative	20**	<20	<20	<20	<20	20**	20**	<20

Table 4.3 A: Patient sera exhibited moderate neutralizing potency and breadth against heterologous pseudoviruses constructed from a standardized reference panel of heterogeneous envelopes (NIAID, NIH). (**) Reductions in FFU were detected with pooled HIV-1 negative sera, which were attributed to cellular toxicity that was not observed at concentrations below 1:20.

neutralizing activity at the peak of viraemia (d 1239), so we were unable to assess whether decreases in autologous-neutralization correlated with changes in neutralizing breadth.

These data suggest that, following B cell depletion, HIV-1 NAbs were transiently and partially-depleted, but returned with stronger neutralizing efficacy than pre-rituximab levels. Furthermore, the temporal relationship between VL and neutralizing plasma titre was in keeping with the hypothesis that NAbs contributed to the control of viraemia in this patient. However, it was important to characterize further the changes in NAb activity that followed rituximab therapy.

4.3.3 Antibody characterization

Neutralization was not detected against a VSV-G pseudotype. Because VSV-G envelope interacts directly with the lipid bilayer of the cytoplasmic membrane, VSV-G pseudotyped HIV-1 bypasses the requirement of the interaction between HIV-1 envelope and its receptor and coreceptor to enter cells and is therefore not susceptible to inhibition by HIV-1 neutralizing antibodies. Therefore, neutralizing activity detected against the HIV-1 Env-pseudotyped virus was assumed to be HIV-1 Env specific and antibody mediated. Additionally, HIV-1 negative serum did not neutralize the patient's Env-pseudotyped virus. However, B cell depletion has been shown to affect cytokine responses (Agarwal *et al*., 2004), which could potentially affect rates of viral replication *in vitro* and be mistaken for neutralization. Therefore, it was important to confirm that the changing neutralizing activity was HIV-1 envelope specific.

To define the specificity of the patient's NAbs, we measured binding competition with envelope-specific monoclonal antibodies using soluble-HIV envelope as the antigenic target (Figure 4.3). Viruses pseudotyped with BaL envelope are highly susceptible to neutralization by heterologous sera (Li *et al*., 2006b). Therefore, recombinant BaL gp120, purified from transfected CHO-K1 cell supernatants, was expected to bind antibodies in the patient's plasma that did not neutralize the patient's own virus.

However, by measuring competition between the patient's antibodies and biotinylated NAbs that are known to neutralize diverse HIV-1 isolates, it was possible to assess relative titres of antibodies that bind conserved epitopes. This experiment showed competition between patient sera and antibodies b12 and 447-52D (which targets a conformational epitope that includes a conserved GPXR motif in V3). Additionally, the patient's antibodies competed with 48d in the presence of the CD4 peptide mimic M33, confirming that this patient had antibodies overlapping with a CD4 inducible epitope. There was no competition observed with 2G12, which was not surprising because carbohydrate-specific antibody responses to HIV-1 are rarely detected *in vivo* (reviewed in (Haynes and Montefiori, 2006)) (Figure 4.3). Conversely, antibodies targeting the CD4bs, and V3 loop are commonly detected in patients with cross-neutralizing antibody responses (Binley *et al*., 2008).

The concentration of patient serum at which NAb binding was blocked by 50% were calculated for serum samples collected before and after the peak in VL. This revealed a transient decline in binding-competition with b12, 447-52D and 48d during the peak of viraemia, in accordance with decreasing neutralization titres detected with autologous virus and HXB2-env pseudotype (Figure 4.4). This confirmed that the individual had antibodies that bound to epitopes within gp120 and that HIV-1 specific antibodies were partially depleted following rituximab therapy. In order to establish a causal relationship between the dynamics of the NAb response and the observed changes in VL, phylogenetic analyses were carried out on virus envelope sequences derived at multiple time points before and after rituximab therapy. The aim of these experiments was to see if transient losses of antibody-selection pressure affected viral evolution.

Figure 4.3 Antibody binding to HIV-1 envelope decreased following rituximab therapy

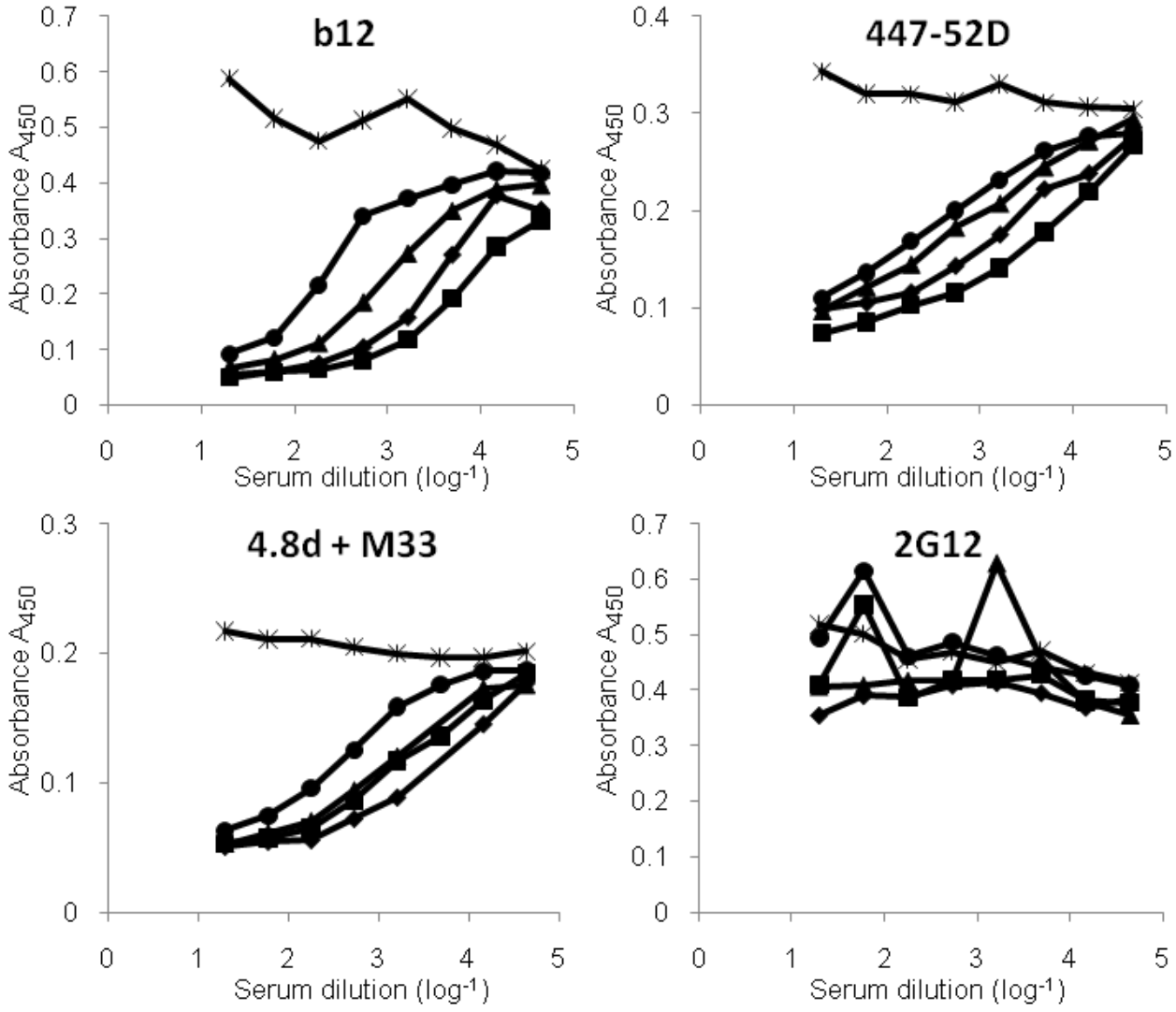


Figure 4.3: The Env-epitope specificities of the patient's antibodies were characterized by competitive-binding ELISA using a panel of biotinylated NAbs: b12, 447-52D, 2G12 and 4.8d. Serial dilutions of patient serum (x-axes) collected on 1042 d (◆), 1270 d (●), 1295 d (▲) and 1353 d (■) post-seroconversion were bound to gp120 and incubated with non-saturating concentrations of each NAb. Binding-competition corresponds to the reduction in light absorption (A_{450nm}, y-axes) after addition of a streptavidin-HRP conjugate and TMB substrate. To assay binding competition with NAb 447-52D, which binds to a CD4i epitope, patient sera was mixed with the CD4-peptide mimic, M33.

Figure legend

Figure 4.4 Antibody binding to HIV-1 envelope decreased following rituximab therapy

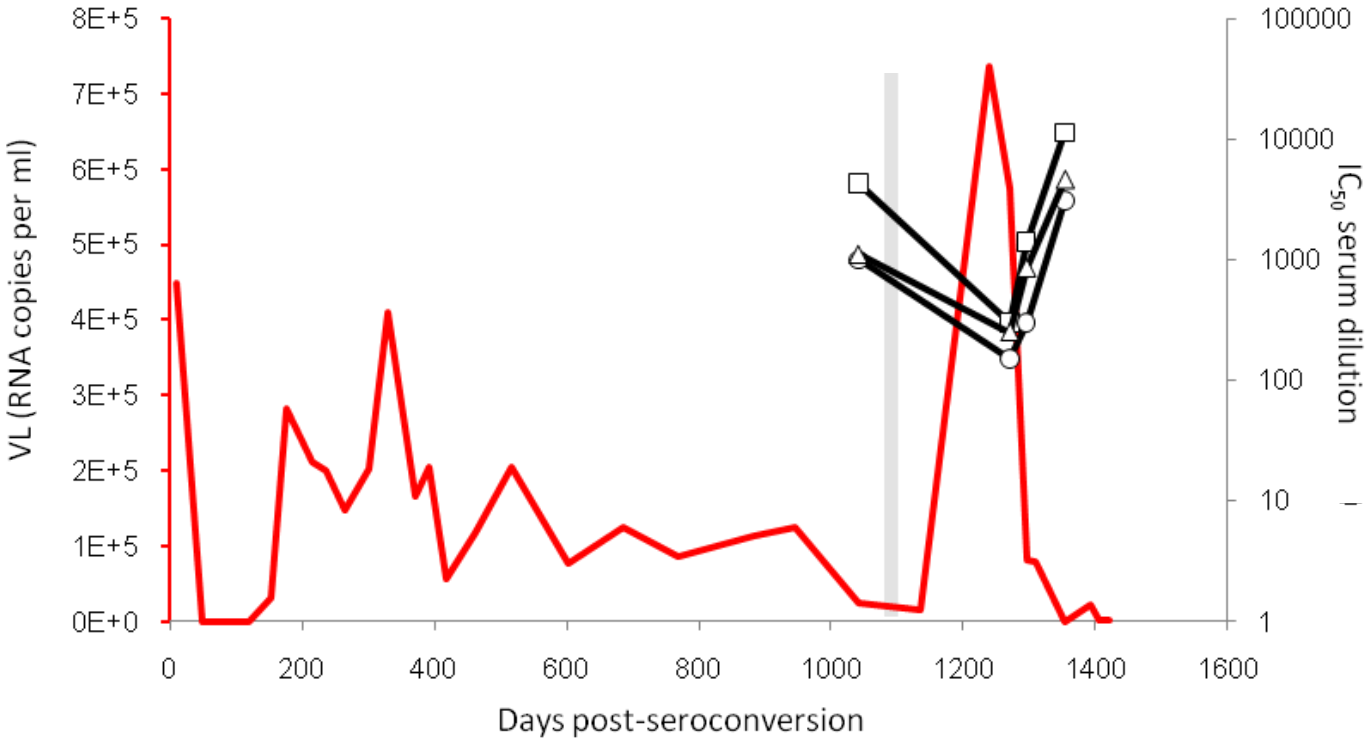


Figure 4.4 shows the reciprocal dilutions of sera collected from the patient before and after rituximab therapy (grey shaded area), that reduce gp120-NAb binding by 50% (IC50, right y-axis). Titres were calculated from interpolations plotted against the curves shown in Figure 4.3. One hundred percent binding was taken as that detected in wells containing either IgGb12 (□), 4.8d (△) or 447D (○) in the absence of patient sera. Corresponding VLs are shown by the red line (left y-axis).

4.3.4 Analysis of sequence evolution in HIV-1 envelope over time

The patient's virus was subtype B, confirmed using the REGA subtyping tool (100% bootstrap) (de Oliveira *et al*., 2005). To evaluate sequence evolution over time, partial *env* genes were cloned from amplified viral RNA derived prior to, and following, rituximab therapy (Figure 4.5A). This uncovered clear sequence diversification as the VL peaked after rituximab treatment. Prior to rituximab therapy the mean pair-wise genetic distance, calculated using the Juke-Cantor method (Section 2.27.3), was 0.004 base substitutions per sites, which increased to 0.02 at the peak of VL ($p<0.0001$) (Jukes, 1969). In order to determine the likely genealogy of the cloned envelope sequences, a time-structured phylogenetic tree was constructed using a Bayesian relaxed molecular clock, and a general time-reversible model of nucleotide substitution (Drummond *et al*., 2006, Drummond and Rambaut, 2007). This showed that the increase in genetic distance manifested as a 5-fold increase in effective population size (N_e), as shown by the skyline plot in Figure 4.5B. In other words, the number of genetically distinct viruses that contributed to successive generations increased at a time when NAb titres were decreasing, suggesting that selection pressures acting on the virus were temporarily relaxed following rituximab therapy.

An alternative explanation for the diversification of *env* following rituximab therapy was considered. Latent HIV-I is known to persist in resting CD4 T cells for several years and rates of viral evolution within these reservoirs are slow (Siliciano *et al*., 2003). However, sequences from latent reservoirs have increased intra-patient diversity because virus is archived at different times during infection (Nickle *et al*., 2003, Ruff *et al*., 2002). In this patient, high levels of HIV-1 or HBV viraemia could have resulted in reactivation of latently infected $CD4^+$ T cells, which would lead to increases in viral RNA sequence diversity. To assess whether diverse strains represented re-emergence of archived virus we analyzed proviral DNA from PBMC samples available from the time of seroconversion up to day 1042 and placed these sequences on a time-structured tree (Figure 4.6). Viruses found post-rituximab did not represent re-emergence of early archived strains; those strains present as VL peaked were most-closely related to strains present in plasma at day 1042, with a subset related to provirus DNA detected at day 1042. Seemingly, quasispecies had diversified from multiple lineages that were replicating before VL increased.

Figure 4.5 Diversification of HIV-1 *env* sequences after rituximab therapy

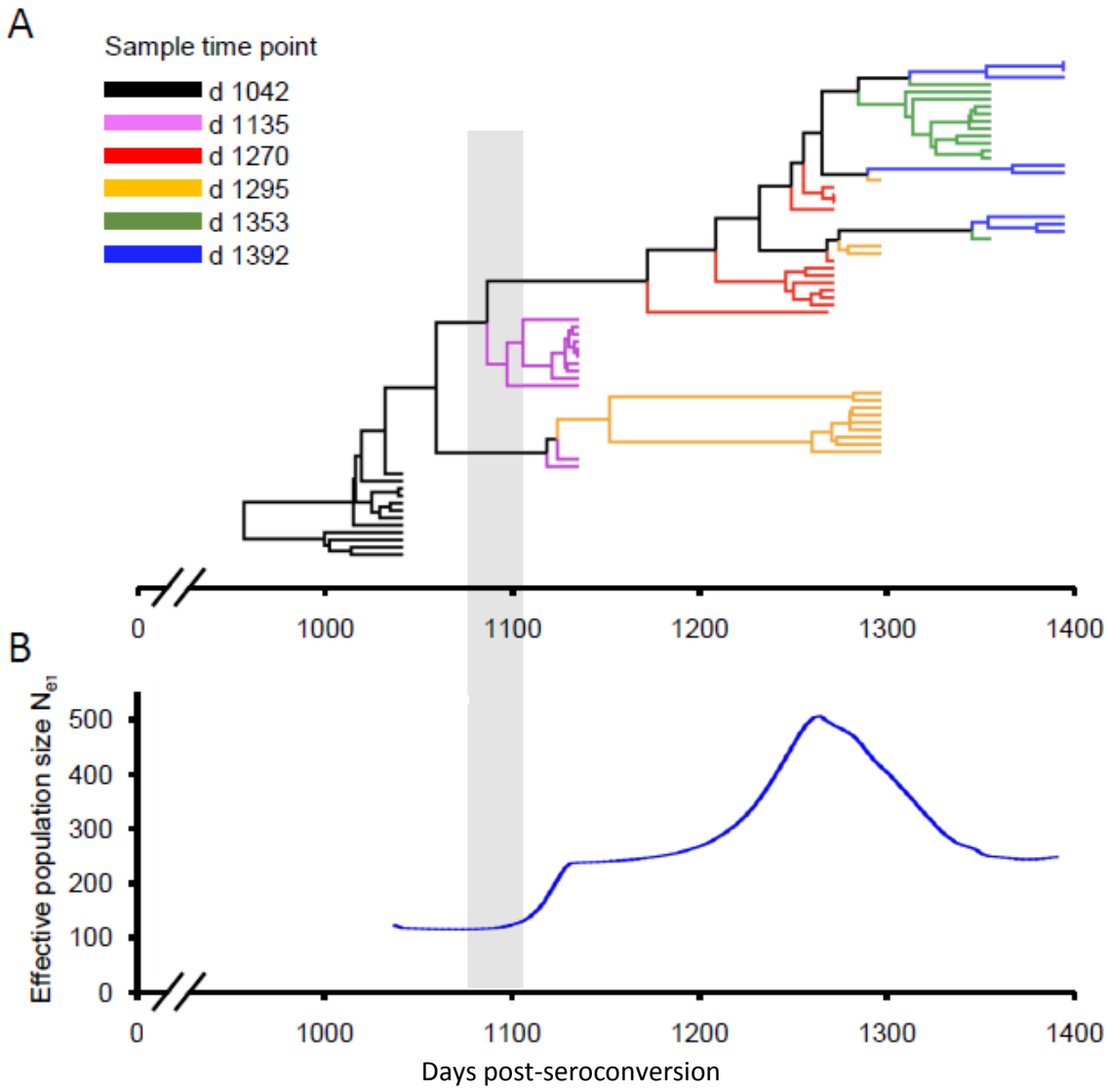
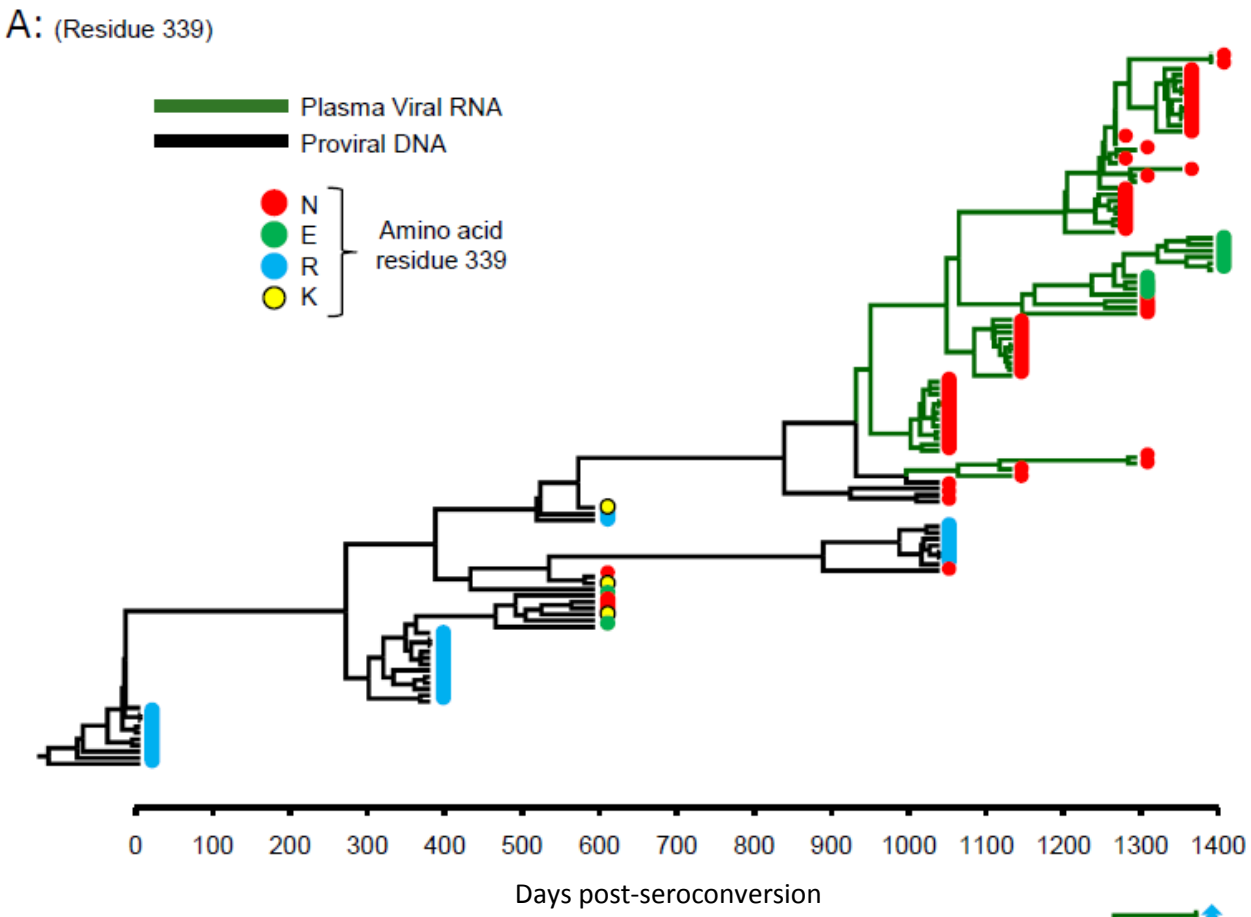


Figure 4.5A: A time-structured tree, showing divergence time estimates among intra-host plasma HIV-1 clonal sequences before and after rituximab therapy (shaded grey), based on a Bayesian relaxed molecular clock applied to 969 nucleotides (Drummond *et al*., 2006). The external nodes represent sequences taken from time-points indicated by the colours given in the Figure key (inset). The topology is a maximal-clade credibility tree calculated using BEAST, with branch lengths proportional to time estimates for the subtending nodes (summarising 60 million Markov chain Monte Carlo (MCMC) simulations, generated after discarding 6 million as burn-in). All the parameters in the MCMC started from random values, except for substitution rates and population size, where priors were imported from the combined proviral and plasma viral sequence data of the same host calculated by BEAST software. Figure 4.5B. The effective population sizes (N_e) were calculated using BEAST. The x-axis (days post-seroconversion) is the same as for Figure 4.5A (Drummond *et al*., 2005).

Figure 4.6 Ancestral analyses of emerging strains



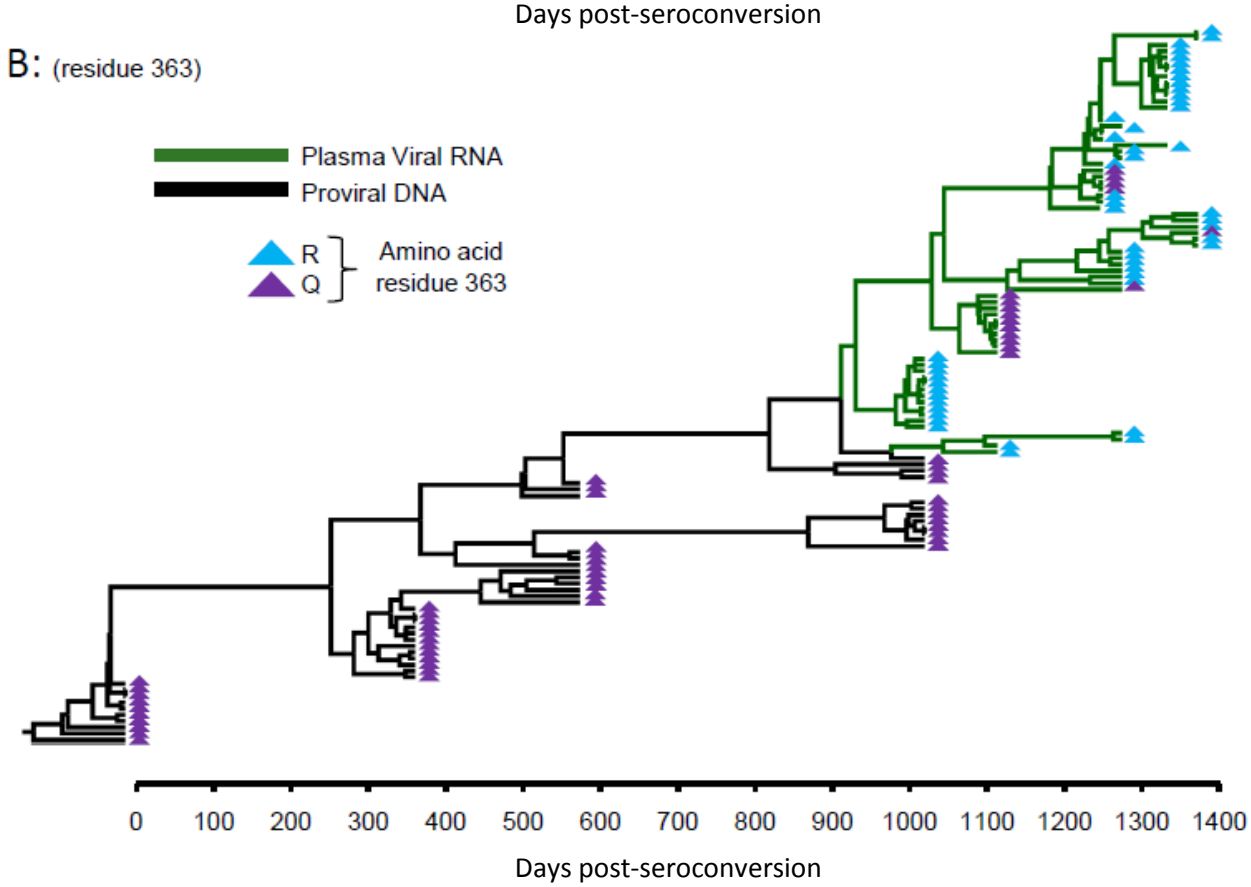


Figure 4.6 Ancestral analyses of emerging strains

Figure 4.6A: The amino acid status change in viral Env protein at site 339, which was under positive selection following rituximab therapy. A time-structured maximum clade-credibility tree, showing reconstruction of the probable ancestral amino acid changes at Env position 339 of the plasma viral samples and proviral samples over time. The maximum clade-credibility tree was constructed using methods described in Figure 4.5A.

Figure 4.6B: shows amino acid changes in viral Env proteins at position 363 over time (also under positive selection). Data are presented as described in the legend for Fig 4.6A.

This added credence to the argument that virus diversification had resulted from a transient loss of selection pressure.

Loss of immune selection may have resulted from the observed declines in NAb titres, or decreased B cell support of antiviral $CD4^+$ and $CD8^+$ T cell responses (reviewed in (Moir and Fauci, 2009a)). It was not possible to delineate either of these causes from a non-specific increase in viral diversity. However, as VL declined and neutralizing activity rebounded, envelope sequences became less diverse and the effective population size decreased. If sequence changes corresponded to reapplication of antiviral immunity, the emerging population would be expected to bear the hallmarks of selection at epitopes involved in antibody or T cell recognition. This prompted a search for epitopes in Env under positive selection.

Maximum likelihood phylogenetic trees were analysed using the CODEML algorithm, in order to identify sites under selection from rates of non-synonymous to synonymous mutations (dN/dS= ω) (Yang *et al*., 2000). By this method, the goodness-of-fit of two codon substitution models were compared using a χ^2-test. The first model (M7) assumes a beta distribution of ω without positive selection, whereas the second model (M8) assumes a beta distribution of ω with positive selection at individual sites (ie. ω>1). Two sites in Env were shown to be under positive selection: Position 339 (dN/dS=7.6; p<0.0001) and position 363 (dN/dS=6.977, p=0.03) (Figure 4.6 & 4.7). Interestingly, glycosylation at site 339 has previously been shown to affect neutralization by the carbohydrate specific antibody 2G12, while mutations at sites 339 and 363 have been shown to affect neutralization by the CD4bs antibody, b12 (Duenas-Decamp *et al*., 2008, Duenas-Decamp *et al*., 2009, Scanlan *et al*., 2002)

Residue 363 intersperses the β14 and β15 anti-parallel strands of gp120 and is exposed on the surface of the outer-domain in close proximity to the CD4 binding loop (Figure 4.8A) (Kwong *et al*., 1998). Computational modeling of atomic-level envelope structures has demonstrated that mutations proximal to the CD4-binding loop are critical in conferring resistance to CDbs antibodies (Wu *et al*., 2009). Furthermore, site-directed mutagenesis of site 363 has previously been shown to affect neutralization of the CD4bs antibody, M-14 (Zhang *et al*., 2004b). Prior to the first dose of rituximab (d 1042 post-

Figure 4.7 Tracking of selected envelope mutants

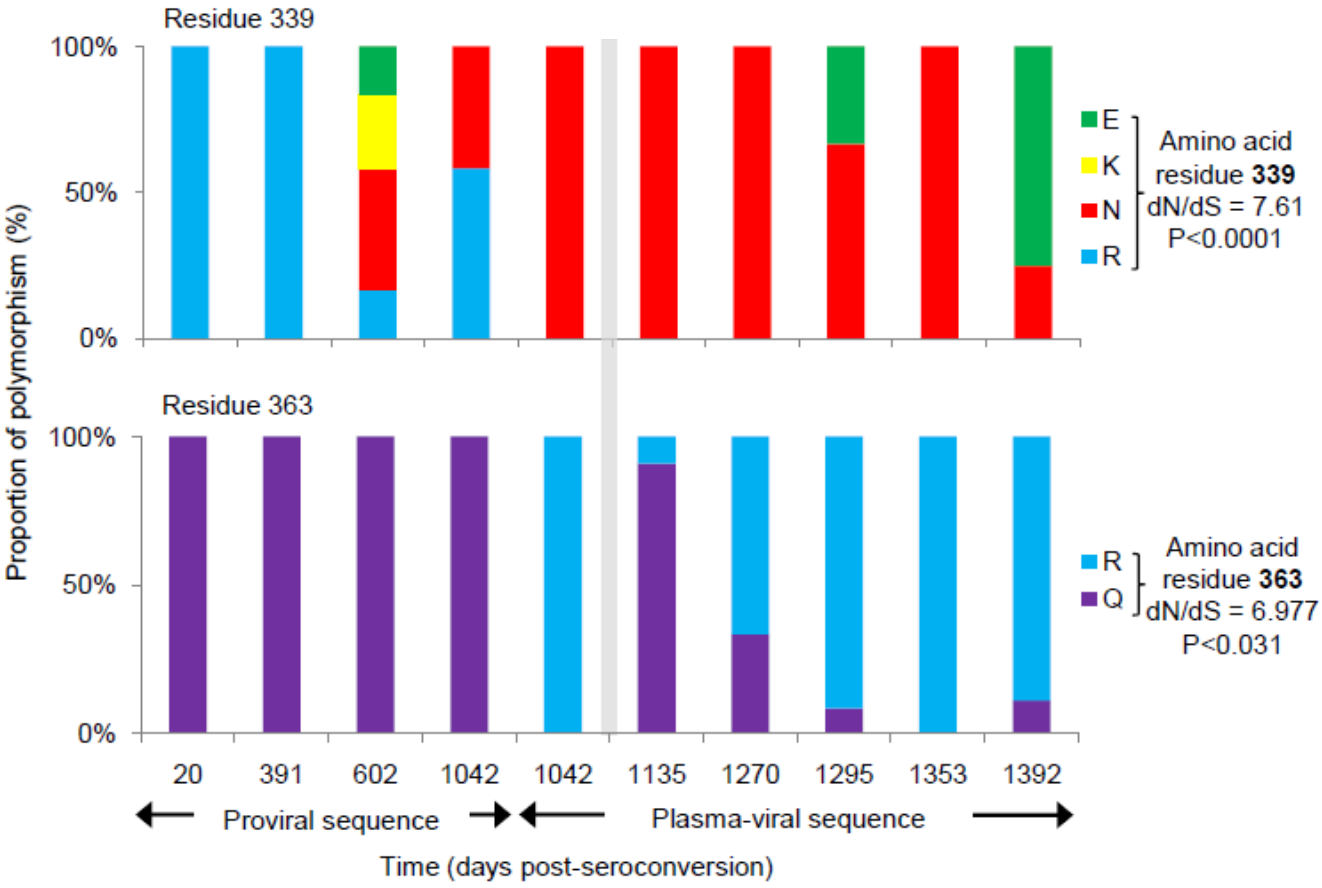


Figure 4.7. Stacked percentage histograms display the relative frequencies of polymorphisms at sites 339 (top panel) and 363 (bottom panel) from historical samples and plasma samples obtained at the time of rituximab therapy. Each bar shows the frequency of residues at these positions.

Figure 4.8 Locations of selected mutations within HIV-1 envelope.

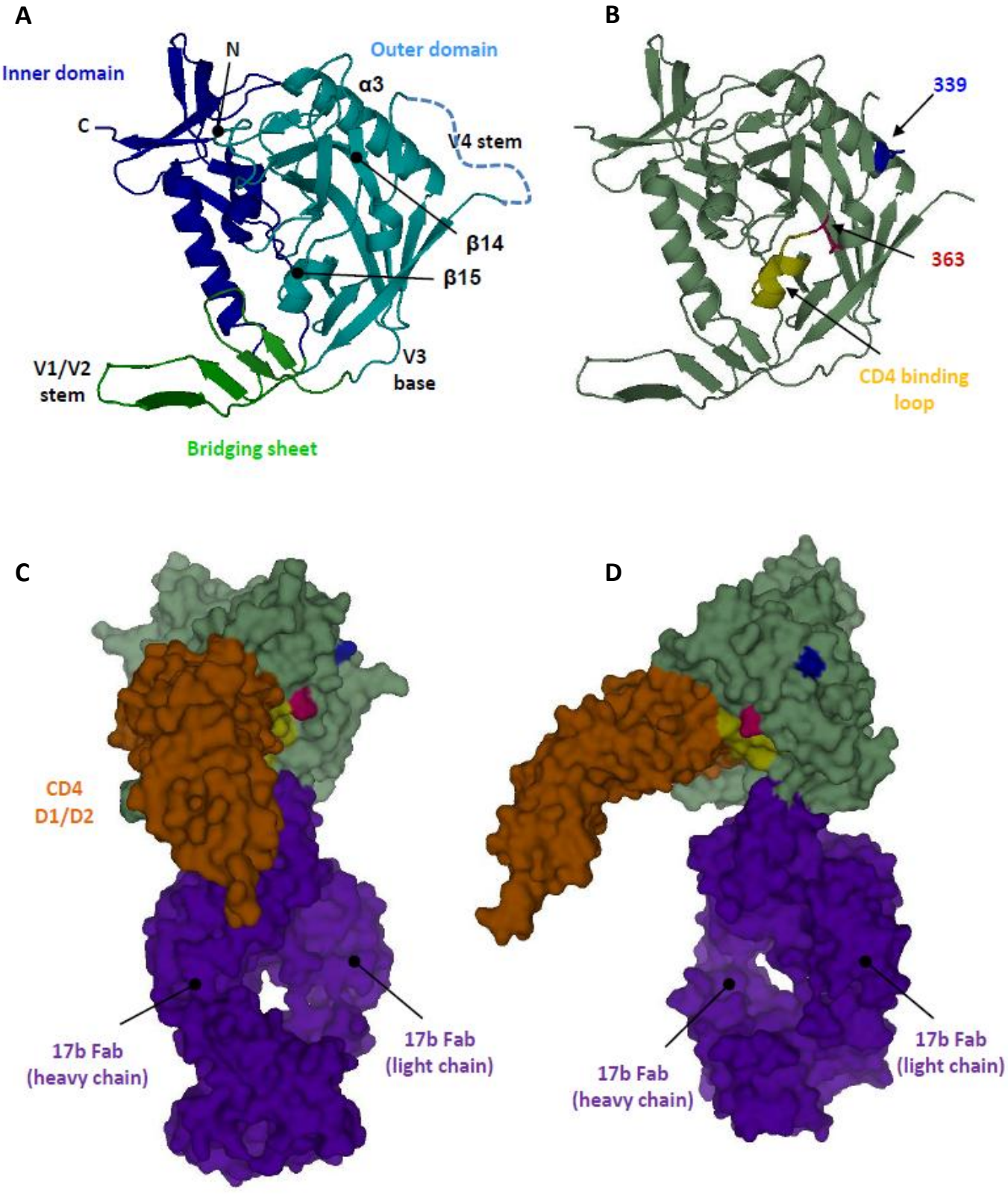


Figure 4.8 Locations of selected mutations within HIV-1 envelope.

Figure 4.8A. The ribbon diagram of the gp120 core structure (Kwong *et al,* 1998) shows the inner, outer and bridging domains. The structure is in a CD4-bound and 17b-bound state. Structural data were obtained from the RCSB protein data bank and imported into PyMol software to generate three-dimensional images. The α3 helix is highlighted, as are the β14 and β15 domains.

Figure 4.8B. Site 339 (blue), is located in the α3-helix, while site 363 (pink) is located proximal to the CD4 binding-loop (yellow).

Figure 4.8C shows the surface composition of gp120 (light blue) in the same rotational plane as Figure A and B. Sites 339 and 363 are exposed on the surface of the gp120 core. Site 363 is shown in close proximity to the bound CD4 molecule (D1-D2; orange), while the Fab domain of 17b (purple) indicates the approximate location of the co-receptor binding site.

Figure 4.8D is the same as Figure 4.8C, but rotated 80° to show the distance between residue 339 and the CD4bs.

seroconversion) position 363 was occupied by an arginine in all viral RNA sequences, while all proviral DNA clones sampled up-to, and including, d 1042 had a glutamine at the same position. Following rituximab therapy, R363 variants were temporarily replaced with Q363 variants, which reverted back to arginine residues as NAb titres rebounded and viraemia was controlled (Figure 4.7). Prior to rituximab therapy, an asparagine at site 339 formed part of a possible NDT glycosylation sequon. This residue is located within the α3 helix, which is exposed on the surface of the protein according to atomic level structures (Figure 4.8B). A previous study demonstrated site 339 is involved in 2G12-binding, and also affects b12 binding, despite being some distance away from the CD4bs (Figure 4.8C and 4.8D) (Scanlan *et al*., 2002). No other sites in envelope were found to be under positive selection, suggesting that sites 339 and 363, alone, conferred a selective advantage to the virus, thus leading to the founder effects observed in Figures 4.5 and 4.6.

4.3.5 Neutralization susceptibility of mutated Env-pseudotypes to NAbs and patient plasma

Although previous studies demonstrate that sites 363 and 369 are involved in NAb escape, it could not be assumed that different mutations at the same sites would affect neutralization of this patient's virus in a similar manner. Therefore, pseudoviruses mimicking N/E339 and R363 variants were constructed by site-directed mutagenesis and used in neutralization assays with the patient's serum and NAbs b12 and 2G12. The template used for site-directed mutagenesis was envelope clone 3 derived 336 days post-seroconversion (Rit.336d.c3), which had residues R339 and Q363 (the same clone shown in Table 4.1). This clone was shown to be partially susceptible to 2G12 and b12 neutralization with IC_{50} titres of 3μg/ml and 5μg/ml, respectively (Figure 4.9A and 4.9B). Concentrations of 20 μg/ml of either antibody neutralized less than 90% of the wild type virus (IC90>20 μg/ml). Mutant N339/R363, which corresponded to viral RNA sequences detected immediately prior to rituximab therapy, was more susceptible to 2G12 (IC_{90} 3μg/ml), indicating that this mutation introduced an N-linked glycan. The same mutant was less susceptible to b12 (IC_{50}<10μg/ml) and infectivity was enhanced by 10-20% in the presence of sub-neutralizing concentrations of antibody (1.25 – 0.08 μg/ml) (Figure 4.9B). Mutant virus mimicking the majority phenotype at peak viraemia, N339/Q363, was the most susceptible to 2G12

Figure 4.9 Impact of selected mutations on susceptibility of the virus to neutralizing antibodies

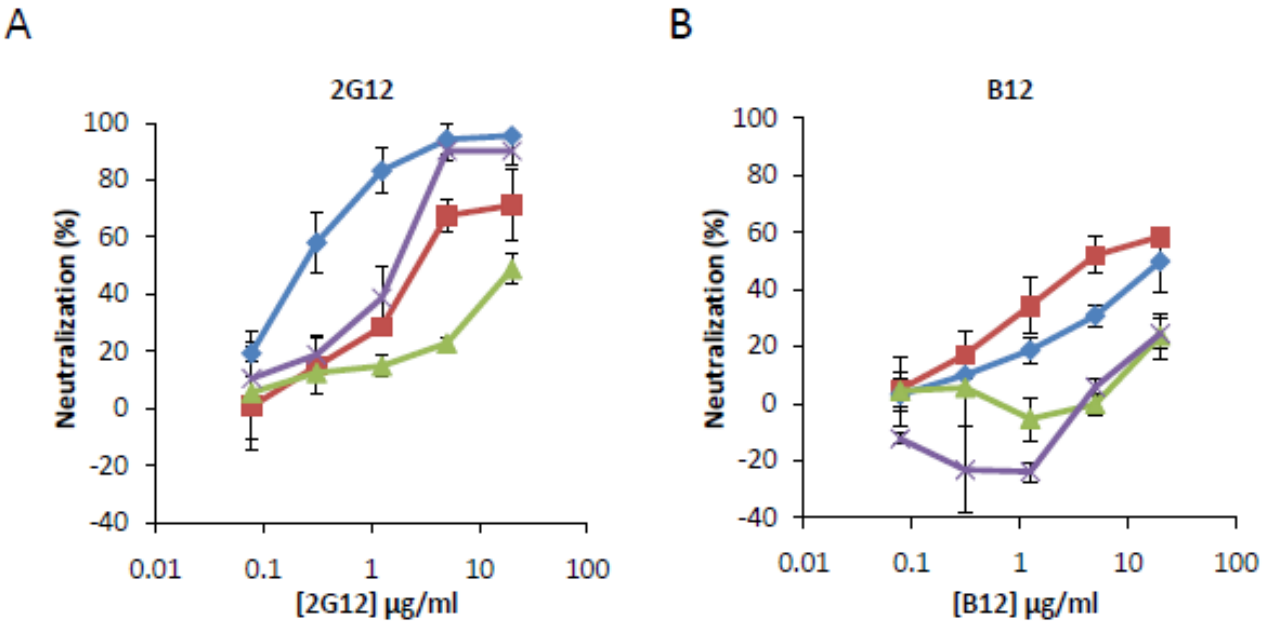
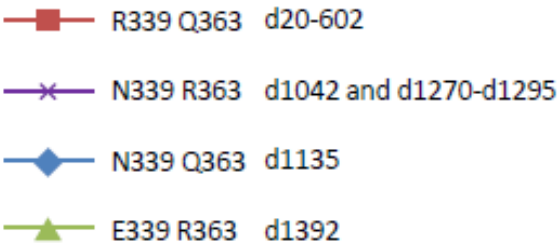


Figure 4.9A. Cloned HIV-1 envelope derived from the patient at d 336 (pre-rituximab) was mutated at sites 339 and 363, which introduced the specific sequence changes observed following rituximab therapy (see section 2.24 for methods). Each mutant virus, along with the d336 R339/Q363 wild-type variant, was used in the β-Gal neutralization assay to assess the impact of the selected mutations on neutralization sensitivity to antibody 2G12. Pseudotyped viruses are listed below in the order that each mutation occurred *in vivo*. The percentage neutralization of each mutant is given by the y-axis. The asparagines at site 339 formed part of an NDT glycosylation sequon.

Figure 4.9B Pseudoviruses mimicking the predominant variant immediately before peak viraemia (blue line; N339/Q363) were transiently more susceptible to b12 than variants present before rituximab therapy (purple line; N339 R363).

Figure Key



neutralization (IC_{50} 0.2 μg/ml). As VL declined the majority of virus clones acquired E339 and R363 mutations, which further reduced susceptibility to both NAbs. Twice the concentration of d1042 serum was required to neutralize 50% of the E363/R363 mutant in comparison to wild-type d 336 Env-pseudotype (IC_{50} 1:600 vs. 1:300) (Table 4.1). Thus, *env* mutations were selected over time that modified sensitivity to neutralizing antibodies, and to the patient's own plasma. Importantly, these mutations were temporally associated with a transient loss of viral control and reciprocal changes in antibody titres, indicating that NAbs contributed to the control of VL in this patient.

4.3.6 Mutant Env-pseudoviruses exhibited similar levels of infectivity after correction for RT activity

Intra-host diversity of HIV-1 envelope can affect virus infectivity (Nora *et al*., 2008), which could lead to selection by antibody-independent mechanisms. Therefore, the infectious titres of the mutant pseudoviruses were compared using the β-Gal infectivity assay. Initial titrations of mutant N339/R363 revealed an infectious titre that was 1.8-fold higher than wild-type virus (R339/Q363). However, it was not clear whether this resulted from the mutations in envelope or from higher concentrations of virions harvested from transfected 293T supernatants.

In order to standardize the concentration of pseudovirus particles prior to titration, RT activity was measured using the SG-PERT assay that was developed as part of a separate study, led by Dr Masssimo Pizzato in collaboration with the candidate (Pizzato *et al*., 2009) (see section 2.25). Retrovirus particles are quantified from levels of reverse transcribed BMV RNA (cDNA) using SYBR Green II-quantitative PCR. The quantitation standard (QS) for the assay consisted of an HIV-1 nl4-3 virus, previously shown to contain 355 ng/ml p24, 136 ng/ml RT and 11.6×10^9 HIV-1 RNA copies/ml (see (Pizzato *et al*., 2009) for details). Ten-fold dilutions of the standard revealed that levels of fluorescence tended to plateau prematurely after approximately 25 PCR amplification cycles (Figure 4.10A and 4.10B). This resulted in an amplification efficiency of 1.585 as determined from the slope of the standard curve (optimal efficiency = 2) (Figure 4.10C). Because differences in the infectious titres of the mutant pseudoviruses were subtle, the SG-PERT assay was first optimized before it was used to quantify RT activity in virus-containing supernatants.

Figure 4.10 Optimization of the SG-PERT assay for the quantification of pseudovirus particles

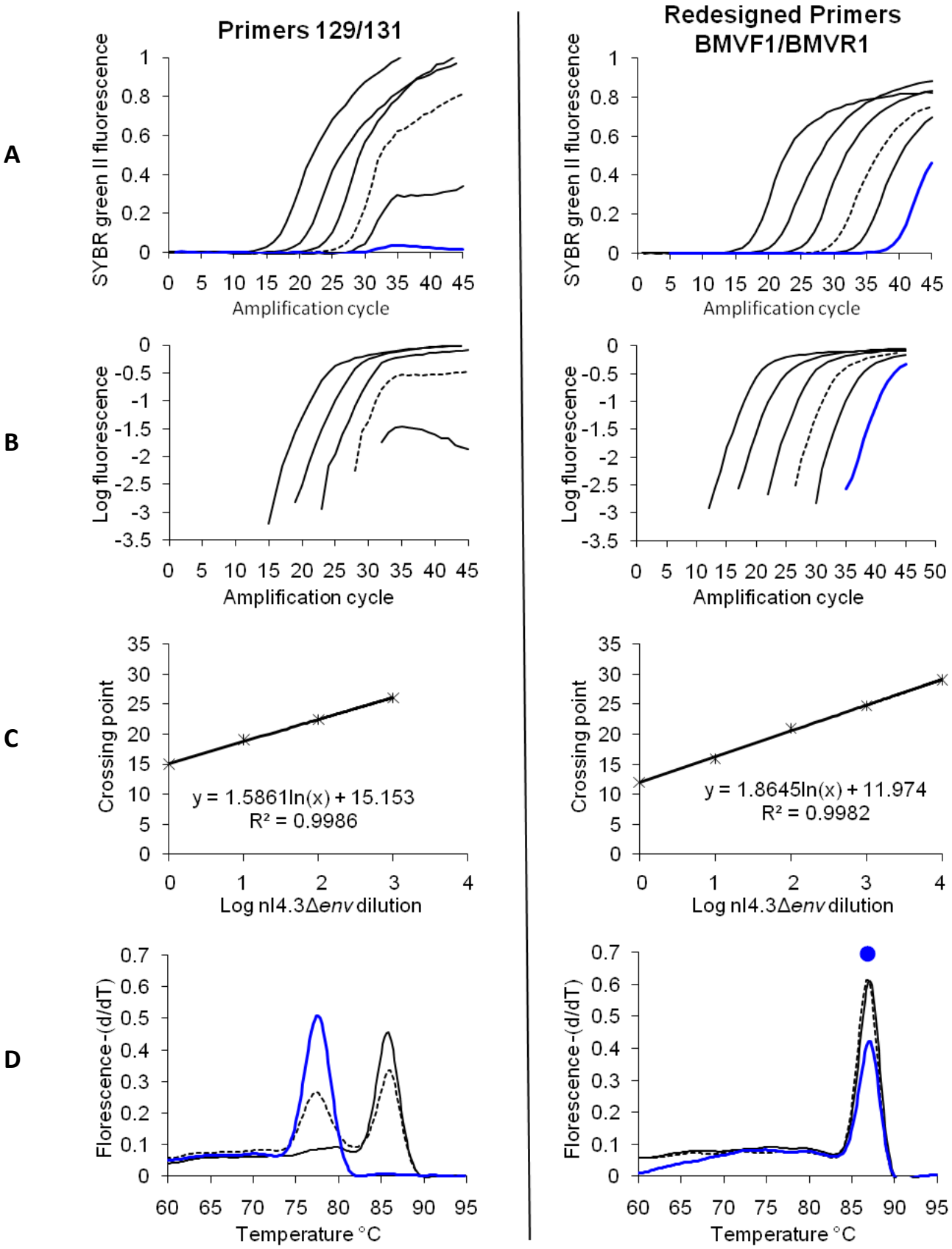


Figure 4.10 Optimization of the SG-PERT assay for the quantification of pseudovirus particles

The SG-PERT assay was used to compare efficiencies of RT-PCR amplification of BMV RNA using primers BMV131/BMV129 (left panels) and BMVF1/BMVR1 (right panels) with virion derived HIV-1 RT.Tenfold dilutions of nl4.3 virus were lysed then incubated with reaction mixes containing *Taq* polymerase and BMV RNA for 30 min to allow HIV-1 RT to reverse transcribe a BMV RNA template. The cDNA product was the quantified by SG-quantitative PCR. For primer sequences see Table 2.1 (Materials and Methods).

Figure 4.10A: Primers 129/131 produced amplification curves that plateaued prematurely in reactions containing low concentrations of virus ($1:10^4$, dashed line). Blue lines show amplification of DNA product in the absence of HIV-1 RT (negative control)

Figure 4.10B: The amplification cycle at which fluorescence exceed background levels recorded prior to PCR amplification (crossing points) was calculated by the LightCycler software from log fluorescence recorded for each reaction.

Figure 4.10C: Crossing-points were used to construct standard curves. The co-efficients of the logarithmic regression lines represent the amplification efficiencies of each primer set (BMV129/BMV131=1.5861, BMVF1/BMVR1 = 1.8645)

Figure 4.10D: Melting peaks of the final amplified products reveal two products in the reactions with primers BMV129/BMV131 and only one product in reactions with primers BMVF1/BMVR1.

Poor amplification efficiency could have been due to waning activity of *Taq* polymerase, degradation of other heat labile components within the reaction mixture, or sequestrations of reaction components within non-BMV specific amplifications. Non-specific products of amplification were identified by analyzing melting curves of the final PCR product. Negative-first-differential fluorescence, plotted against temperature, revealed two distinct melting peaks (Figure 4.10 D), which was consistent with the formation of primer-dimers.

Secondary structure predictions using the NetPrimer online tool (http://www.premierbiosoft.com/) identified five self-dimerising structures for forward primer BMV131 and three cross-dimers with primer BMV129. Three of these structure predictions had 3' recesses that would facilitate polymerase extensions and cause destruction of BMV-primer specificity. Primers were redesigned with the intention of eliminating all possible secondary structure formations. Primer-dimers were not detected using the modified primers (BMVF1/BMVR1), and the amplification curves did not plateau at low concentrations of virus. Additionally, the amplification efficiency increased from 1.585 to 1.86 (Figure 4.10 A-D). This suggested that eliminating the formation of primer dimers had the effect of reducing competition for PCR reagents within each reaction, thus allowing reliable detection of low levels of HIV-1 RT. However, the extra sensitivity afforded by the optimized primer set increased background detection of BMV amplified product in the absence of HIV-1 RT. This has previously been attributed to RNA-dependent DNA polymerase activity of the *Taq* enzyme which reverse transcribes BMV-RNA during PCR amplification cycles (Maudru and Peden, 1997). This was not considered to be a confounding factor because DNA product amplified in the absence of HIV-1 RT was not detected until after the 33rd amplification-cycle.

The modified SG-PERT assay was used to compare RT activity in mutants R339/Q363, N339/Q363 and E339/R363. Mutant N339/Q363, was constructed at a later time point and was not assessed in this

experiment. The amplification cycles at which amplified BMV DNA products were detected (crossing points) were 15.0, 15.3 and 16.4 for mutants N339/R363, E339/R363 and R339/Q363, respectively (Figure 4.11A). These crossing-points corresponded to the following concentrations of RT, determined from the standard curve shown in Figure 4.10 C (BMVR1/BMVF1 primers): 26.8 ng/ml (N339/R363), 22.85 ng/ml (N339/R363), 12.7 ng/ml (R339/W363). Therefore, the concentrations of reverse transcriptase detected in virus N339/R363 were 2.1-fold higher than that of the wild-type virus R339/Q363. After normalizing the concentrations of RT for each mutant and the wild type virus the resulting infectious titres, as assessed in the TZM-bl infectivity assay, ranged from $3.3x10^3$ – $3.7\ x10^3$ IU/ml (Figure 4.11B). Subsequently, supernatant fluid containing mutant N339/Q363 was shown to have an RT concentration of 17.3 ng/ml and produced an infectious titre of $3.0x10^3$. The difference between the highest and lowest infectious titre (N339/R363 and R339/Q363) was not significant because the coefficient of variation of the SG-PERT assay was previously calculated at 4.1-7.6%. These data suggest that the envelope mutations observed following rituximab therapy did not affect virus infectivity.

Figure 4.11 Impact of selected mutations on pseudovirus infectivity.

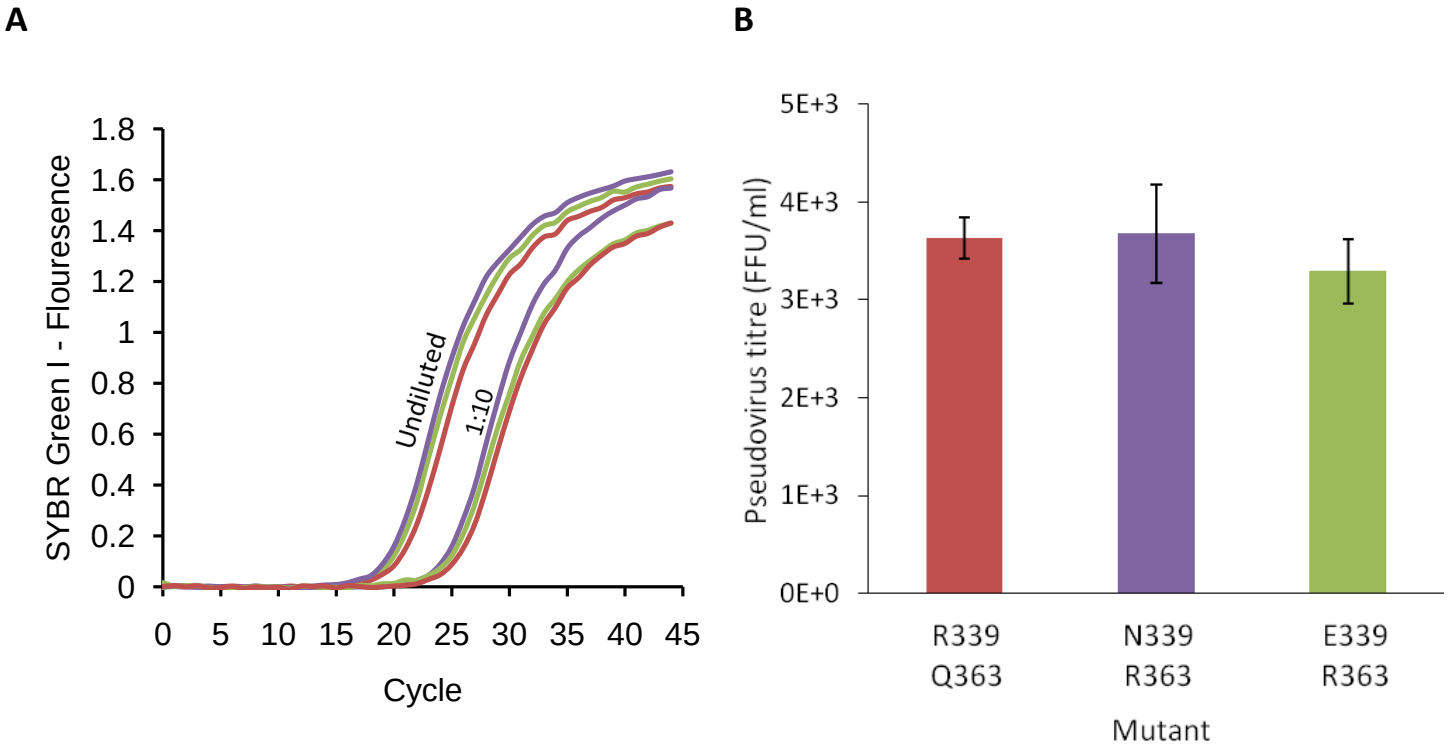


Figure 4.11A Supernatant harvests were assayed for reverse transcriptase activity by SG-PERT. The fluorescent signals (y-axis) correspond to quantities of reverse-transcribed, PCR-amplified BMV RNA template, which are proportional to concentrations of RT from lysed pseudovirus particles. Supernatants were assayed undiluted and diluted 1:10 in tissue culture medium. Mutants R339/Q363, N339/Q363 and E339/R363 are show with the same colour scheme used in Figure 4.11B.

Figure 4.11B. Concentrations of RT detected in each supernatant were normalized prior to titration onto TZM-bl cells. Titres of each mutant virus are shown by the y-axis.

4.3.7 Analysis of CTL responses prior to Rituximab therapy

Other possible causes for the clinical findings of this case were considered, particularly the possibility of an indirect impact on cellular immunity. The patient was found to be homozygous for HLA Class IB allele B0801 and heterozygous for Class IA alleles A0101 and A1101. Four A1101-restricted, optimal epitopes and six B0801-restricted optimal epitopes were identified from HIV-1 sequences published in the Los Alamos Database (www.hiv.lanl.gov). Six of these were in Gag, one was in Pol and three were in Nef. Peptides corresponding to these epitopes were designed to match the consensus sequence of the patient's virus, assessed 20 days after diagnosis of HIV-1 seroconversion. Each peptide was used in an IFNγ-ELISpot assay to assess CTL responses using PBMCs collected from the patient 1 year post-seroconversion and immediately prior to rituximab. Responses directed at three epitopes in Gag and one in Pol were detected 1 year post-seroconversion; only two of these (both in Gag) were detected prior to the first dose of rituximab, three years after seroconversion (Table 4.4).

Viral *gag pol* and *nef* genes were sequenced at d 20, d 1042 and d 1353 post-seroconversion. At day 1042 post-seroconversion, this patient had an N242T mutation in Gag that was not detected at d 20. This mutation is known to confer susceptibility to CTL responses in patients with HLA B57 alleles. It is possible that this mutation represents reversion to a fitter virus phenotype following virus transmission from an HLA B57 positive donor (Navis *et al.*, 2008). Mutations were detected in five epitopes that were relevant to the patients HLA class I phenotype. Two of these mutations corresponded to epitopes that elicited autologous CTL responses one year post seroconversion, but not immediately prior to rituximab therapy. Importantly, none of the observed mutations were temporally associated with the VL changes observed following rituximab therapy. From these data we concluded that CTL escape was not responsible for the sequence changes observed following B cell depletion. However, PBMCs were not available to assess T cell function at the peak of VL. Although loss of T cell function secondary to B cell depletion, may have contributed to increases in VL, this would not result in the envelope-sequence changes observed at this time (Table 4.4).

Table 4.4 Analysis of CD8+ T cell responses and epitope evolution over time

Patient HLA	Epitope		Mutation		IFN-γ response (SFU/10^6 PBMC)	
	Gene	Autologous Sequence	Pre-Rituximab	Post-Rituximab	Pre-Rituximab Year 1	Pre-Rituximab Year 3
A1101	*gag*	TLYCVHQK	K8N	Q7A	1200	-
A1101	*pol*	ACQGVGGPGHK	-	G9A	300	-
A1101	*nef*	QVPLRPMTYK	-	-	-	-
A1101	*pol*	AIFQCSMTK	-	-	-	-
B0801	*gag*	GGSKKYQLK	K3R/K7Q	K3R/K7Q	-	-
B0801	*gag*	ELKSLYNTV	-	-	160	200
B0801	*gag*	DIYKRWII	-	-	640	600
B0801	*gag*	DCKTILKAL	-	-	-	-
B0801	*nef*	WPKVRERM	K3G/E6D	K3R	-	-
B0801	*nef*	FLKEKGGL	K5Q	K5Q	-	-

Table 4.4 $CD8^+$ T cell responses were analysed by IFN-γ -ELISpot analysis against a panel of HLA-restricted autologous peptides (spot forming units/million PBMCs are shown). The patient's HLA Class IA and Class IB genotypes were shown to be A0101, A1101 and B0801 homozygous (Section 2.28). Sequencing of the corresponding peptides was carried out at the time-points shown, and mutating residues have been underlined. The results reveal that pre-rituximab there were two main T cell responses detectable, neither of which showed evidence of immune-escape throughout the rituximab-induced viral flare and recovery period.

4.3.8 Impact of rituximab monotherapy on HBV co-infection

Immune activation through recrudescence of other infectious agents may play a role in this case. Concurrent with the VL rise, the patient developed elevated levels of ALT which is released from damaged hepatocytes. This was associated with reactivation of the patient's HBV infection, which was confirmed by detection of HBV surface antigen (HBsAg) and HBV nucleocapsid (HBeAg) proteins that were previously undetectable. This is consistent with a previous report of reactivating HBV infections following rituximab therapy (Garcia-Rodriguez *et al*., 2008). Prior to rituximab, HBV DNA was not detectable, but following the final dose of rituximab, HBV VL increased to $6x10^6$ copies per ml (Figure 4.12). As shown in Table 4.1, changes in HBV viraemia were associated with reciprocal changes in antibody titres to HBsAg which declined to undetectable levels (<1 IU/ml) at the peak of viraemia. Importantly, HBV VL remained high as control of HIV-1 VL was regained. This dissociation between HIV-1 VL and HBV VL suggests that HBV replication was not responsible for the decrease in HIV-1 VL, or the sequence changes observed in Env. However, it is possible that reactivation of HBV infection observed following rituximab therapy contributed to the initial flare in HIV-1 VL.

Figure 4.12 Clinical course of HIV-1, HBV and ALT in relation to Rituximab therapy

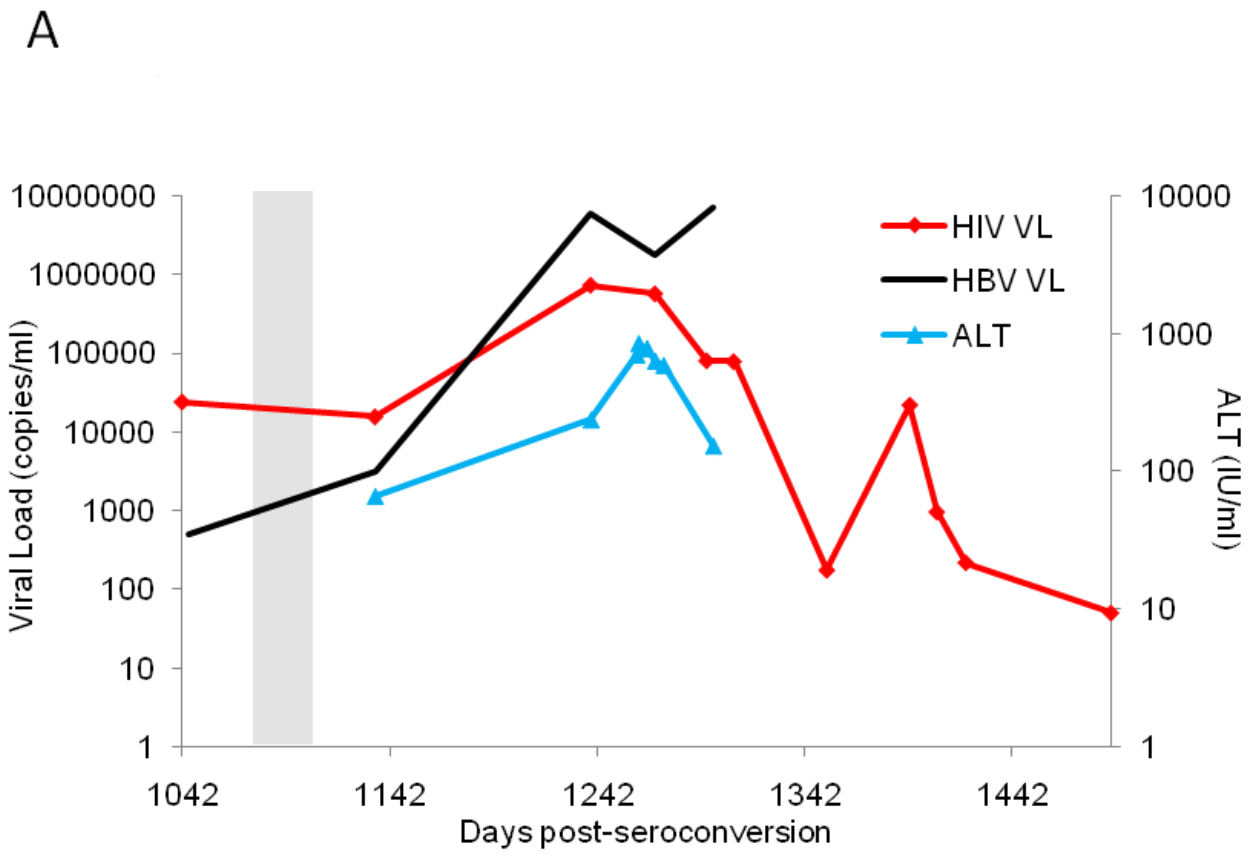


Figure 4.12 Plasma VL of HIV-1 and HBV, and the liver function marker, ALT, were quantified in clinical laboratories at St Mary's Hospital. Values are displayed over time (days post-seroconversion) and the time of rituximab therapy is indicated by the grey shaded area. The left y-axis corresponds to HBV VL (DNA copies /ml) and HIV-I VL (RNA copies /ml). The right y-axis shows quantities of ALT, which is an indicator hepatocyte damage.

4.4 Discussion

Rituximab therapy was used to treat a rising IgM-κ light chain paraproteinaemia in a patient who was also co-infected with HIV-1 and HBV. Following B cell depletion, the patient's VL increased concurrent with decreases in total IgG levels and HIV-1 neutralizing activity. Recovery of NAb titres coincided with control over viraemia. Multiple analytical techniques were employed to characterize the virus population that was selected as NAbs re-emerged. Emerging virus was defined by polymorphisms at two residues exposed on the virus envelope, both of which showed evidence of positive selection. These data led a strategy of mutagenesis which confirmed that the sequence changes detected affected susceptibility to neutralizing antibodies targeting the CD4bs. In short, all avenues of this investigation contributed to a coherent picture consistent with the hypothesis that NAbs played a major role in containing HIV-1 in this individual.

It was not surprising that this patient had antibodies targeting the CD4bs and V3 loop as these are frequently detected in chronically infected individuals (Binley *et al*., 2008, Scheid *et al*., 2009). Competitive-binding experiments were conducted with heterologous BaL envelope glycoprotein, so the titres reported may not reflect levels of antibody binding to autologous virus. This patient's virus was generally resistant to b12 neutralization as demonstrated by the fact that microgram quantities of antibody failed to neutralize more than 60% of wild type or mutant viruses and lower concentrations of antibody actually enhanced infectivity of the N339/R363 mutant. Antibody mediated enhancement of infectivity has been reported and is associated with sub-neutralizing concentrations of antibody (reviewed in (Burton *et al*., 2001)). Approximately 25% of clade B field isolates are resistant b12 (Binley *et al*., 2004, Li *et al*., 2005, Moore *et al*., 1995). However, mutations detected at site 363 resulted in

modest changes to b12 neutralization sensitivity, suggesting that antibodies targeting the CD4bs were partly responsible for driving viral evolution in this case.

Residue 363 is adjacent to the CD4 binding loop and a recent structural study demonstrates that residues proximal to the CD4 binding loop are important in conferring resistance to b12 and b12-like antibodies (Kwong *et al*., 1998, Wu *et al*., 2009). Sites surrounding the CD4bs are more amenable to sequence variation because they have greater structural plasticity than conserved sites directly involved with CD4 binding (D'Costa *et al*., 2001). Mutations at site 363 have been shown to confer resistance to the CD4bs antibody M-14 (Zhang *et al*., 2004a), so it is likely that this patient had antibodies targeting epitopes that included this residue. However, it is unclear how this residue affects neutralization by b12, because site 363 resides outside the b12 binding site (Zhou *et al*., 2007). Previous studies have also implicated this residue in resistance to b12. Duenas-Decamp *et al.* showed that P363Q mutations cooperate with S364P mutations to confer partial resistance to b12, yet P363Q alone had minimal effect on neutralization sensitivity (Duenas-Decamp *et al*., 2008, Duenas-Decamp *et al*., 2009). In this study we observed a transient arginine to glutamine mutation at residue 363 that effectively removed a positive charge at this site. This may have affected neutralization through interactions with other charged residues residing within the b12-binding site, or alternatively, these mutations may have altered local conformation at the antibody binding site and changed the shape-complementarity of the epitope/paratope interface (Lawrence and Colman, 1993) and reviewed in (Epa V.C. and Colman P.M., 2001).

Immediately prior to the first dose of rituximab there was an absolute discrepancy between proviral DNA and contemporaneous viral RNA sequences: All of the proviral DNA sequences had a glutamine at position 363 (n=12), while all of the viral RNA sequences had an arginine at the same position (n=12). Compartmentalization of distinct virus populations has been suggested as a possible explanation for

similar discrepancies between proviral DNA and viral RNA (Simmonds *et al*., 1991). However, this is unlikely as there was some overlap in the phylogeny of variants R363 and Q363 (Figure 4.6). An alternative explanation is that virions may have been sampled immediately after selection of R363 variants, before Q363 HIV-1 infected cells had died off. Therefore, it is possible that this patient had recently mounted an effective neutralizing response prior to rituximab-therapy and this may have contributed to the near log-fold decline in VL between d 995 and d 1042. However, this cannot be confirmed because serum was not available to assess neutralization prior to d 1042.

Relaxation of antibody selection pressure is likely to have decreased levels of purifying selection, thus increasing the effect of random genetic drift leading to diversification of the virus and increased N_e population size (Shriner *et al*., 2004). Alternatively, previously acquired antibody-escape mutations that incurred fitness costs to the virus may have reverted in the absence of antibody selection pressure leading to increased replication rates of individual variants. When antibodies returned, mutants carrying reversion type mutations conferring neutralization susceptibility would have been lost, which could explain why VL subsequently decreased to such low levels (175 RNA copies per ml). Previous studies have suggested that antibody escape does not impact on replicative fitness detected *in vitro* (Bunnik *et al*., 2010), and the mutations observed in this study did not significantly impact on TZM-bl infectivity. However, pseudovirus infectivity assays are not entirely suitable for investigating viral fitness because the envelope composition of pseudotyped virions differs from that of wild type virus (Louder *et al*., 2005). It is, therefore, not clear whether the transient reversion of R363Q detected at peak viraemia affected viral fitness.

Pseudotyped viruses with N339 mutations were more susceptible to 2G12 neutralization indicating that this site was glycosylated. It is not surprising that mutants lacking this NDT sequon remained partially susceptible to 2G12 because other N-linked glycosylation sites were present elsewhere in Env.

Mutations at residues 339 was not related to the transient loss of viraemia control because the R339N mutation occurred prior to rituximab therapy and the N339E mutation was not detected until peak VL had fallen. Nevertheless, glycosylation at this site may have contributed to neutralizing antibody resistance by shielding the conserved receptor binding sites (Koch *et al*., 2003, Li *et al*., 2008). Previous studies have demonstrated that site 339 can impact on b12 neutralization, despite being distal to the CD4bs (Scanlan *et al*., 2002).

Rituximab is commonly given to HIV-1 infected humans to treat lymphoma arising as a complication of late-stage HIV infection, whereas in this case, lymphoma preceded acquisition of HIV. Under normal circumstances antiretrovirals are routinely given, which would confound attempts to assess the impact of rituximab on HIV-1 VL. For this reason there are no published studies on the impact of rituximab in HIV-1 infection. Studies of acute SIV infection in macaques treated with rituximab indicate a role for NAb responses in containing post-acute VL (Miller *et al*., 2007, Schmitz *et al*., 1999). In contrast, a recent study of African Green monkeys did not reveal any impact from rituximab treatment during acute SIV infection (Gaufin *et al*., 2009). Moreover, the aforementioned animal studies initiated rituximab treatment before or immediately following virus inoculation. Future primate studies might investigate the effects of administering rituximab after NAb responses are detected.

The individual in this study received three months of ART started during his seroconversion illness. There is an association between rebounding NAb responses and viraemia control after ART-cessation (Montefiori *et al*., 2001, Montefiori *et al*., 2003). Early therapy may preserve numbers of B cells that are critical for NAb development, yet irreversibly depleted during untreated PHI (Titanji *et al*., 2005, Hart *et al*., 2007). Further investigations of NAb responses following early short-course therapy are warranted and will be discussed in chapter 5.

Given the unusual clinical nature of this case, is it likely that the effects of rituximab would be similar in the majority of HIV-1 infected patients? Prior to rituximab therapy, evolution of Nab responses and virus envelope sequences followed a typical pattern, resulting in modest neutralizing serum titres against autologous-contemporaneous virus, yet stronger responses against earlier strains (d1135 *vs.* d336; Table 4.2). Further analysis of the ability of this patient's serum to neutralize a panel of diverse strains revealed that the Nab activity was broadly directed (Table 4.3), although with average titres compared to other studies (Mahalanabis *et al*., 2009a, Sather *et al*., 2009, Binley *et al*., 2008). Thus, antiviral activity mediated by such a response may not be untypical.

It is possible that depletion of B cells had an indirect impact on VL through modulation of $CD4^+$ or $CD8^+$ T cell subsets. While we cannot exclude this, the mechanism for such an indirect effect is not clear and no impact on $CD8^+$ T cell responses has been observed in the SIV models quoted above (Miller *et al*., 2007). The delay of several weeks that is seen between rituximab treatment and the change in VL is consistent with the observed decline in antibodies, which have a half life of approximately 21 days (Morell *et al*., 1970). Conversely, disrupting direct B cell/T cell interactions would be expected to take effect immediately. Additionally, changes in the prevailing sequences (ie. reversion and subsequent re-selection of a mutated NAb epitope) are consistent with relaxation and reapplication of NAb-mediated selection pressure.

Declining antibody responses have not been reported by all human and animal studies of rituximab-mediated B cell depletion (reviewed in (Lund and Randall)), which does not deplete $CD20^-$ long-lived plasma cells (Ahuja *et al*., 2008). However, rituximab therapy will prevent *de novo* production of antibodies, which probably led to declining antibody titres in this case, particularly as B cells of HIV-1 infected individuals have relatively short half lives (Moir *et al*., 2004). In order to match rapid rates of virus evolution, the antibody response must evolve in parallel (Richman *et al*., 2003). Therefore, B cell

depletion may have preferentially depleted (or prevented) HIV-1 specific antibody responses that were most relevant to virus circulating at the time of rituximab therapy.

The impact of T cell responses on the control of VL is highly variable, with possession of the most favourable HLA allele (B57) delivering a mean affect on VL to the order of one log (Kiepiela *et al*., 2004). Additionally, subsets of elite controllers have been shown to have strong functional CTL responses directed at sites in HIV-1 Gag (Betts *et al*., 2006, Emu *et al*., 2008, Migueles *et al*., 2002, Sarez-Cirion *et al*., 2007, Streeck *et al*., 2008, Pereyra *et al*., 2008b, Potter *et al*., 2007). Although NAbs are low or absent in some elite controllers with detectable CTL responses, there is no evidence to suggest that T cell responses control VL independently of humoral immune system in the majority of cases. Likewise, it is not suggested that T cell responses were absent in this patient, particularly as sequence changes were detected at known HLA restricted epitopes prior to rituximab therapy. However, this individual did not have a B57 allele or any other HLA-type associated with HIV control, and it may be that the absence of an effective CD8+ T cell response allowed us to detect a NAb effects on VL.

The impact of other reactivating viruses on HIV-1 load is complex. Rituximab treatment has been shown to reactivate hepatitis B virus (HBV) (Aksoy *et al*., 2007) in patients with previously controlled infection (HBsAg-ve, HBcAb +ve). This implicates B cells in long-term control of HBV; a virus where CD8+ T cells also play an important role in acute disease. The relationship between HBV VL and HIV VL is not fully understood, but overall they appear to be independent (Rockstroh, 2006). In this case HBV and HIV VL rose within a similar timeframe. However, HIV-1 load was brought under control, while HBV load remained high, indicating that they were differentially regulated.

Overall, our findings support previous suggestions of paralleled evolution of virus and NAbs (Richman *et al*., 2003, Frost *et al*., 2005a). The speed and extent to which quantitative changes occurred following rituximab therapy, not only to the virus, but also to the evolving antibody response, are testament to the fragility of this balance. These findings appear at odds with previous studies that fail to confirm an

association between long-term virus control and Nab responses (Bailey *et al*., 2006, Bradney *et al*., 1999, Deeks *et al*., 2006c), but these studies have focused on patients with either strong or poor HIV-1 control, in whom other factors (such as T cell response) may be more important.

Cross-sectional studies of VL set-point and neutralizing activity are unlikely to confirm or refute the findings we report here because they overlook the dynamic complexity of the virus/host interaction. Modest NAb activity contributed to VL control in this patient, which implies that serum titres may be ineffective at gauging the clinical impact of NAbs. Furthermore, VL set-point may not be the most informative marker of viraemia control. Notably, VL remained above 10^5 copies per ml for more than two years prior to rituximab, despite strong evidence that antibodies subsequently controlled viral replication. Therefore, there is a need to assess both neutralizing titre and the continuously adapting virus in evaluating their overall relationship *in vivo*. Questions relating to the generaliseability of this case might be answered by longitudinal analyses of NAb response and virus evolution in subjects exhibiting significant changes in VL under other clinical circumstances.

This unique case study suggests that B cells, and their secreted NAbs, can impact upon HIV VL in chronic infection. This evidence, derived directly from observations in man, may inform the rational design of future immunotherapies and HIV-vaccines.

Chapter 5

The neutralizing response to HIV-1 following short course antiretroviral therapy in PHI

5.1 Introduction

Chapter 4 provided evidence for antibody-mediated control of HIV-1 VL in a single patient. However, there were several irregularities with this case, so it was necessary to investigate the importance of NAbs under more-typical circumstances.

Broadly-specific NAb activity has been detected in a minority of patients with suppressed viraemia and there is circumstantial evidence supporting a protective role for NAbs in control of VL set-point (Doria-Rose *et al*., 2009, Mahalanabis *et al*., 2009b, Deeks *et al*., 2006a, Richman *et al*., 2003, Rong *et al*., 2009, Wei *et al*., 2003). The most convincing of these demonstrate antibody-selection of neutralization-resistant viruses (Richman *et al*., 2003, Rong *et al*., 2009, Wei *et al*., 2003). Envelope mutations that confer antibody-resistance become fixed in HIV-1 quasispecies as early as 12 weeks after transmission, implying that humoral responses can eliminate neutralization-sensitive founder populations (Goonetilleke *et al*., 2009). Sequential rounds of selection could feasibly contribute to control of VL, yet several cross-sectional studies have failed to identify clinical correlates of NAb activity detected *in vitro* (Bailey *et al*., 2006, Euler *et al*.).

Passive transfusions of NAbs in macaques challenged with SHIV were shown to lower VL and delay early disease onset (Haigwood *et al*., 2004, Mascola *et al*., 2000). In humans, passive transfusion of NAbs and natural antibody responses may delay viral rebound after structured interruptions of ART (Montefiori *et al*., 2001, Trkola *et al*., 2004, Trkola *et al*., 2005). However, studies of treatment interruption in chronic infection are confounded by pre-existing antibody responses and immune-escape variants present pre-ART. Additionally, antiviral effects of NAbs are masked by the inter-dependence of Env-antigen load with antibody production. By contrast, studies of recently infected individuals undergoing treatment interruption are potentially more straightforward because the duration of antigen exposure is short and the clinical history is known.

The SPARTAC clinical trial considers the long-term impact of structured-intervention with short courses of ART administered during PHI. This international randomised-controlled trial compares the effect of ART taken for 48 weeks or 12 weeks with a no-intervention arm. Upon ceasing therapy, all patients continue to have regular blood samples taken with VL and immunology assessments. This trial provided a valuable platform for a longitudinal study of early antibody responses and the associated kinetics of VL, which rebound after discontinuing ART.

Following the termination of ART, autologous Env-pseudotyped viruses were used to assess neutralizing responses with the β-gal-based microneutralization assay described in chapter 4. The extent of neutralizing activity detected against autologous viruses positively correlated with VL, yet within the same system, delayed viral rebound was observed in those patients with detectable responses immediately post-ART. There was no evidence for NAb-mediated control after viral-rebound. However, the dynamic inter-dependency of neutralizing titre with viraemia helps to explain the limitations of cross-sectional analyses as a means of assessing the role of NAbs *in vivo.*

5.2 Results

5.2.1 Patient demographics

A total of 43 individuals were recruited from the SPARTAC cohort. All patients received either 12 weeks or 48 weeks ART following diagnosis of PHI and were selected for study on the basis of partial or complete VL suppression while on therapy. Those patients with CD4 counts that fell below 350 cell/mm^3 within 48 weeks of stopping primary ART were started on long-term ART and were excluded from this sub-study, so that neutralizing responses could be assessed from plasma samples that did not contain antiretroviral drugs. Most patients (32/43) presented with one or more symptoms characteristic of PHI. Seventeen patients had a non-specific, flu-like or glandular fever-like illness, with fever and rash being the commonest specific symptoms. The following criteria were used to confirm PHI: i) positive HIV-1 serology following a negative test within 6 months, ii) low level "incident" result (<0.6) using a detuned HIV-1 ELISA, iii) rising antibody levels detected by progression of protein bands on Western blot, or iv) positive HIV-1 proviral PCR or p24-antigen ELISA in the absence of HIV-1 specific antibodies (Fidler *et al*., 2002). The median duration of infection prior to the first dose of ART was 12 weeks (inter-quartile range (IQR): 8.8-14.3 weeks) (Table 5.1).

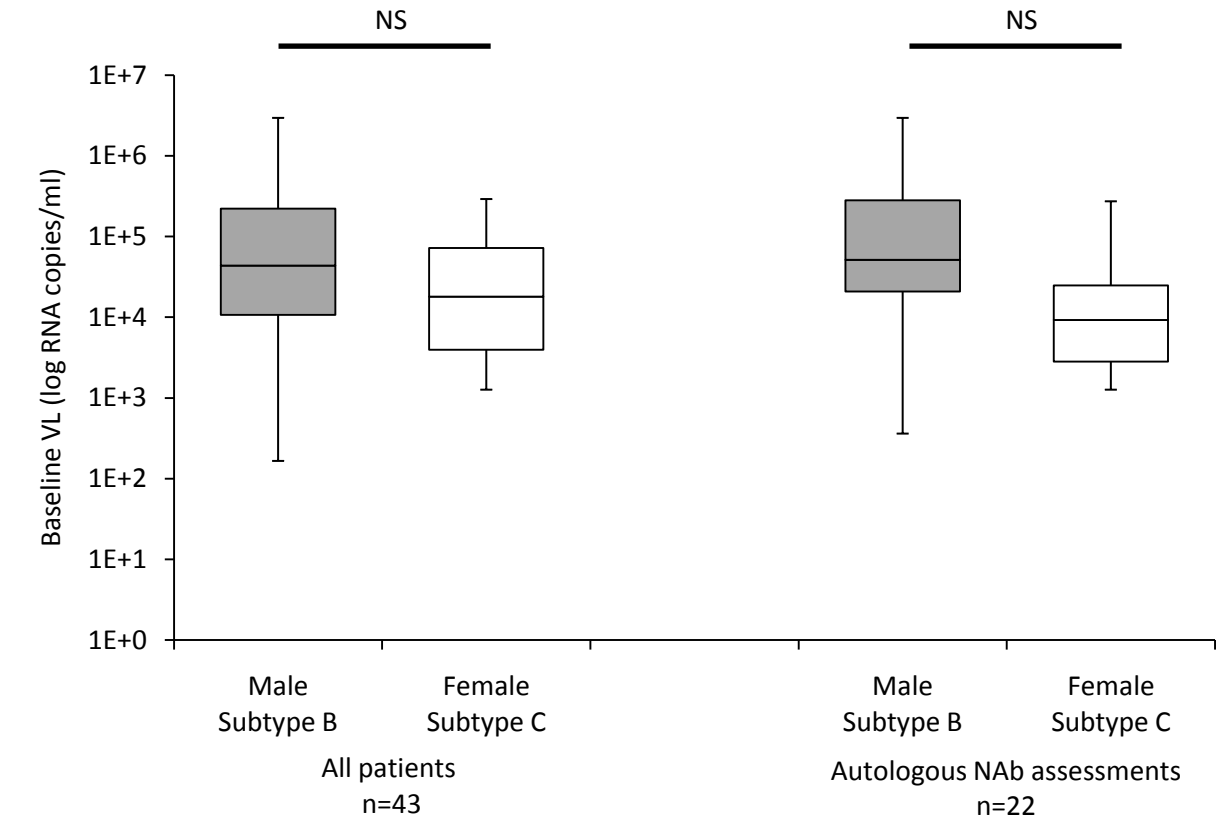
Most patients were European males of median age 35 (n=33, IQR: 32 – 40), while ten patients were South African females recruited at a median age of 28.5 (IQR: 21.75 – 38.5). All the men were infected with HIV-1 subtype B and the women with HIV-1 subtype C. This bias was unintentional and reflects the high rates of male to male transmission of HIV-1 subtype B in Europe and the high prevalence of subtype C infections in women living in Sub-Saharan Africa (UNAIDS, 2008 report) (Garcia-Calleja *et al*., 2006). There was no significant difference in baseline $\log_{10}$ VL between males and females (Mean ± SD, 4.6 ± 1.0 vs. 4.3 ± 0.8, P=0.3, student *t*-test) (Figure 5.1). Females infected with subtype C virus had significantly fewer CD4 T cells at enrolment into the trial compared with males infected with

Table 5.1 Patient demographics and clinical manifestations during PHI

Patient number	Gender	Age	PHI Pre-ART duration (days)	Symptoms during PHI	HIV-1 Clade	CD4 (cells per $mm^{3)}$	Baseline VL	Autologous neutralization assessed	Heterologous neutralization assessed
S1	F	47	125	Yes	C	384	291633		Yes
S3	M	36	73	Yes	B	486	60621	Yes	Yes
S7	M	24	129		B	400	41840	Yes	Yes
S8	M	43	46	Yes	B	670	736055	Yes	Yes
S9	M	40	41	Yes	B	380	186805		Yes
S10	M	29	68		B	680	29060	Yes	Yes
S11	M	55	93	Yes	B	550	36191		Yes
S14	M	31	44	Yes	B	550	2950628	Yes	Yes
S17	M	44	69	Yes	B	420	245502	Yes	
S19	F	37	86	Yes	C	472	5583		Yes
S21	F	24	93		C	575	15026	Yes	
S24	M	45	96	Yes	B	743	3099		Yes
S31	F	40	118	Yes	C	453	86620		Yes
S33	M	32	99	Yes	B	790	399142	Yes	Yes
S35	M	22	108	Yes	B	800	24580	Yes	
S37	M	32	18	Yes	B	660	362	Yes	Yes
S41	M	29	64	Yes	B	677	221523	Yes	
S46	F	20	123		C	599	3416	Yes	Yes
S51	M	31	72	Yes	B	930	16349		Yes
S61	M	39	81	Yes	B	550	476		Yes
S79	M	43	42		B	784	3055		Yes
S84	M	40	95	Yes	B	600	486534		Yes
S94	M	34	108	Yes	B	397	24293	Yes	Yes
S99	F	21	72		C	417	2614	Yes	Yes
S101	M	43	113		B	830	9010		Yes
S116	M	34	117	Yes	B	600	99410	Yes	Yes
S119	M	35	44	Yes	B	770	62948		Yes
S128	M	36	9	Yes	B	728	386758	Yes	
S130	M	35	88	Yes	B	1310	166		Yes
S132	M	40	71	Yes	B	400	9250	Yes	Yes
S147	M	35	77	Yes	B	870	129037		Yes
S150	M	57	86	Yes	B	530	130687		Yes
S152	M	35	40	Yes	B	720	43730		Yes
S162	M	34	18	Yes	B	660	500000		Yes
S165	M	38	84	Yes	B	410	313742		Yes
S171	F	39	137		C	482	1268	Yes	
S178	M	34	63		B	626	11143		Yes
S181	F	25	100	Yes	C	482	273423	Yes	Yes
S183	F	32	117		C	748	20894		Yes
S185	F	19	100		C	570	28160	Yes	Yes
S191	M	46	60	Yes	B	520	67580		Yes
S194	M	33	58	Yes	B	625	4503	Yes	Yes
S199	M	30	87	Yes	B	807	10667	Yes	Yes

Table 5.1. Details are shown for 43 patients undergoing assessment of neutralizing antibody activity against autologous and/or heterologous viruses. Clinical data were collected upon enrolment to the SPARTAC clinical trial prior to the first dose of ART.

Figure 5.1 Pre-ART CD4 counts and VLs were not significantly affected by gender or HIV-1 subtype



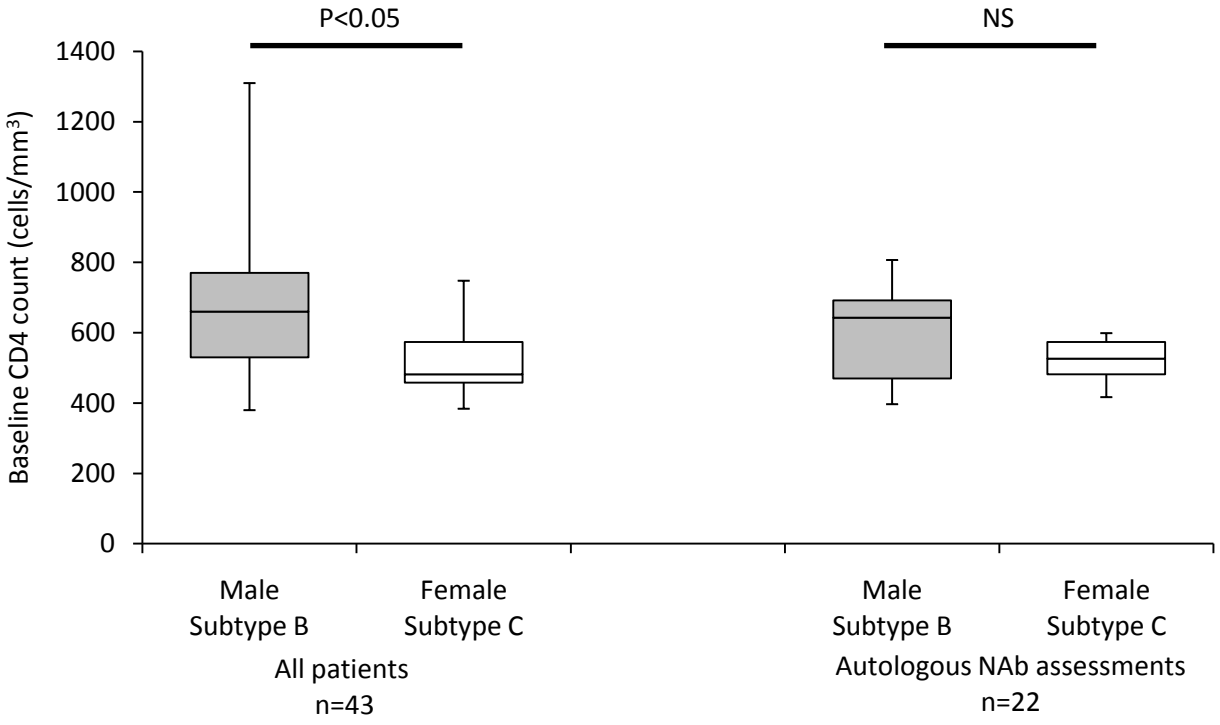


Figure 5.1 Viral load (top panel) and $CD4^+$ T cell counts (bottom panel) recorded at enrollment into the SPARTAC trial (baseline) are shown for European males infected with HIV-1 subtype B (grey boxes) and South African females infected with HIV-1 subtype C (white boxes). Boxes show the interquatile ranges and the verticle lines extend to the minimum and maximum values. Median values are shown as horizontal lines within each box. Data are shown for all 43 patients and the 22 patients for whom autologous neutralizing responses were assessed.

subtype B virus (Mean ± SD, 518 ± 106 vs. 651 ± 19, student *t*-test, P=0.04). From these forty-three patients, sixteen men and six women were selected for neutralization studies with autologous viruses (n=22). The women in this smaller subset of patients had lower baseline CD4 T cell counts (P=0.2) and Log_{10} VL (P =0.12) than the men although the differences were not statistically significant (Figure 5.1).

In accordance with previous studies, chronic VL set-points were calculated from geometric means of log_{10} VL measurements assessed longitudinally, starting 40 weeks after treatment cessation (the longest period observed before vireamia reached steady state levels) (Hollingsworth *et al.* 2010). The males had significantly higher VL set-points than the females (3.4 ± 0.6 vs. 4.5 ± 0.7, P=0.002) (Figure 5.2). Viral load set-points were used to assign patients to three groups: Low level viraemia (n=10 VL <3 log_{10} RNA copies per ml), intermediate viraemia (n=8 VL 4-5 log_{10} RNA copies per ml) and high level viraemia (n=4 ,VL >5 log_{10} RNA copies per ml). These groups were chosen to represent a diverse range of VL set-points and were used to compare the neutralizing activity of patient's plasma against autologous Env-pseudotyped viruses and against a panel of heterologous Env-pseudotyped reference strains.

Figure 5.2 Men infected with subtype B virus had higher VL set-points than women infected with subtype C virus

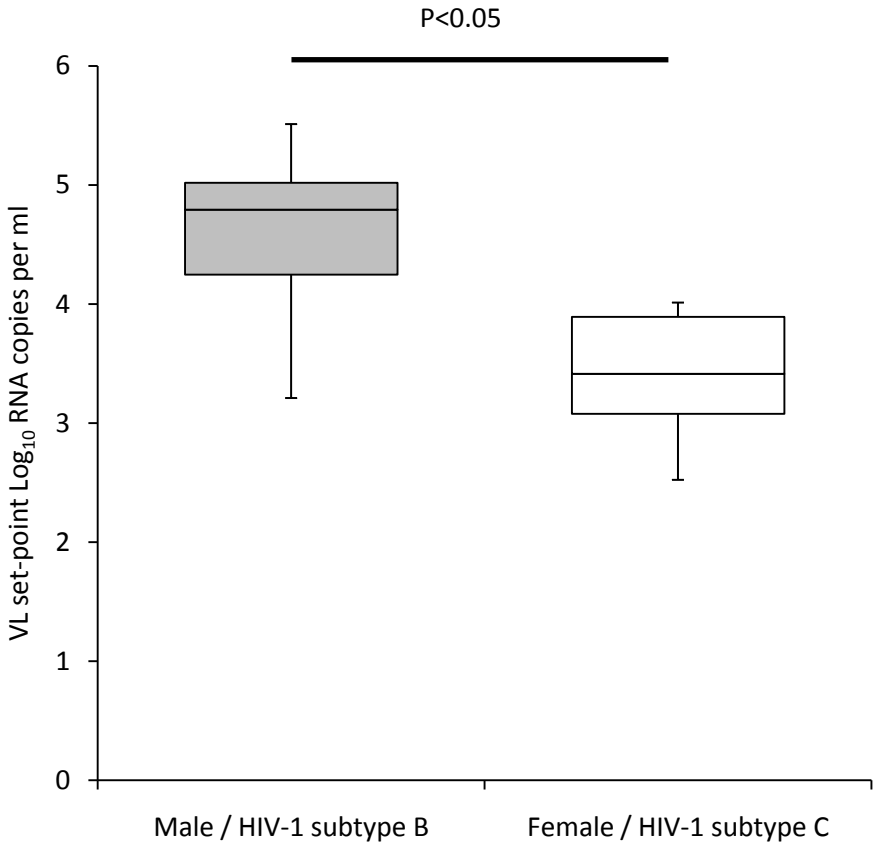


Figure 5.2 Viral load set-points were calculated from mean Log_{10} VL measurements assayed every 4-12 weeks from 40 weeks after ART cessation. Boxes show the IQ ranges and the vertical lines extend to the minimum and maximum values within each patient group. Data are shown for twenty-two patients who were assessed for levels of autologous neutralization. Grey boxes show VL set-points for men (n=16). White boxes show VL set points for women (n=-6).

5.2.2 Neutralizing responses were variably detected within 4-12 weeks of stopping ART.

In order to assess neutralization after the cessation of ART, virus pseudotyped with cloned envelopes were neutralized with contemporaneous-autologous plasma (n=22). Plasma collected from 11 patients after 4 weeks was used for HIV-1 envelope cloning, but due to difficulties in amplifying *env* from plasma containing low quantities of virus (≤ 50 RNA copies per ml in some cases), plasma collected after 12 weeks post-ART were used in the remaining 11 cases (see section 3.2.1). Importantly, contemporaneous-neutralizing plasma titres sampled at week 4 and week 12 were not statistically different (Mean IC_{50} ± SD; wk 4 31.0 ± 24.0 *vs.* wk 12 43.2 ± 49.4, p=0.52, unpaired student T test) (Table 5.2).

Plasma neutralized Env-pseudotyped viruses in a concentration-dependent manner and virus infectivity was not inhibited by pooled plasma collected from HIV-1 uninfected individuals. Furthermore, patient plasma did not inhibit a VSV-G pseudotyped NL4-3△*env* virus, ruling out neutralization by residual concentrations of ART (Figure 5.3). From these data it was deduced that neutralization was HIV-1 Env specific and, therefore, antibody-mediated.

Approximately half of the patients (12/22) had no detectable neutralizing activity against their contemporaneous virus (IC_{50}<20) and the majority of these patients (10/12) developed low VL set-points (group 1: VL <4 log). In contrast, eight of the remaining ten patients, who had detectable levels of neutralization immediately post-ART (IC_{50} 1:20 to 1:153), developed VL set-points greater that 10^4 RNA copies per ml (Figure 5.4A) (p=0.04, independent T-test). Prolonged exposure to high levels of Env-antigen are known to stimulate the production of NAbs, but it was not clear why high VL set-points were associated with preceding neutralizing responses.

It was hypothesized that antibody responses were primed prior to the initiation of ART. Hence, the extent of viraemia and the duration PHI prior to ART would be expected to influence post-ART NAb

Table 5.2 Half maximal neutralizing titres of patient sera tested with autologous Env-pseudotypes

Patient	HIV-1 clade	V3 crown sequence	Follow-up (weeks)	Log_{10} VL set-point	NS	Weeks post ART-cessation											
					4	12	24	36	40	48	60	72	84	96	108	120	132	144
46	C	I/GPGQ	96	2.6		<20*		<20		<20	<20	<20		<20				
194	B	I/GPGK	108	2.67		70*	111	375	342	187	127	158	245	266	323			
99	C	I/GPGR	84	2.87		<20*	<20	<20	<20	<20	<20	<20	<20					
181	C	I/GPGQ	84	2.92	<20*	<20	<20	<20		<20	<20	<20	<20					
37	B	I/GPGR	120	3.17		<20*				<20		<20	<20	<20	<20	<20		
199	B	I/GPGR	144	3.32		<20*	<20	<20		<20	<20	<20	<20	<20	<20		<20	<20
171	C	n/a	120	3.43		32*	78	134	137	138	212	805	480	518	437	516		
21	C	V/GPGQ	108	3.5	<20*	<20	<20	<20	<20	<20	<20	<20	<20	<20	<20			
94	B	I/GPGK	60	3.81		<20*	<20	42	65	74	102							
185	C	I/GPGR	108	3.94	<20*	<20	<20	<20	<20	<20		<20	<20	<20	<20			
132	B	I/GPGR	48	4.35	45*					431								
35	B	V/GPRR	48	4.37	51*					496								
10	B	I/GPGQ	84	4.57	<20*	<20	<20	<20	51	94	60	54	109					
128	B	I/GPGR	96	4.6	<20*	57				162	404	359		183				
8	B	I/GPGR	144	4.69	73*	55		127	173	250		335	363	1065	347	406	156	147
41	B	I/GAGR	108	4.72	<20*		415	183		465	1729	2946			539			
7	B	I/GPGR	48	4.83	58*					374								
17	B	I/GPGR	48	4.99		153*	370	332	759	650								
14	B	I/GPGR	48	5	54*					793								
3	B	I/GPGR	48	5.17		31*	33	57	113	230			403	369	1063			
116	B	I/APGR	144	5.2		118*	345		1284	1862	1220		1056	801	1379	1037	1742	1033
33	B	I/GPGR	48	5.42		<20*	32	34	40	95								

Table 5.2 Reciprocal plasma-titres that reduced autologous-Env pseudovirus infections by half (IC_{50}) are shown. Potent neutralizing responses are indicated by darker shades of grey. Patients are shown in ascending order of VL set-point calculated from 40 weeks post-cessation of ART. (*) denotes neutralizing response tested with virus and plasma from the same time points. All other plasma were tested against the same "earlier" pseudovirus. Patients S7, S14, S35, S132 were not tested regularly owing to limited availability of plasma. Titres reported as "<20" inhibited less than 50% of virus infections at the highest plasma concentration tested (1:20). The amino acid sequence of the conserved V3 crown motif is shown in column 3.

Figure 5.3: VSV-G pseudotyped virus was not neutralized by patient plasma

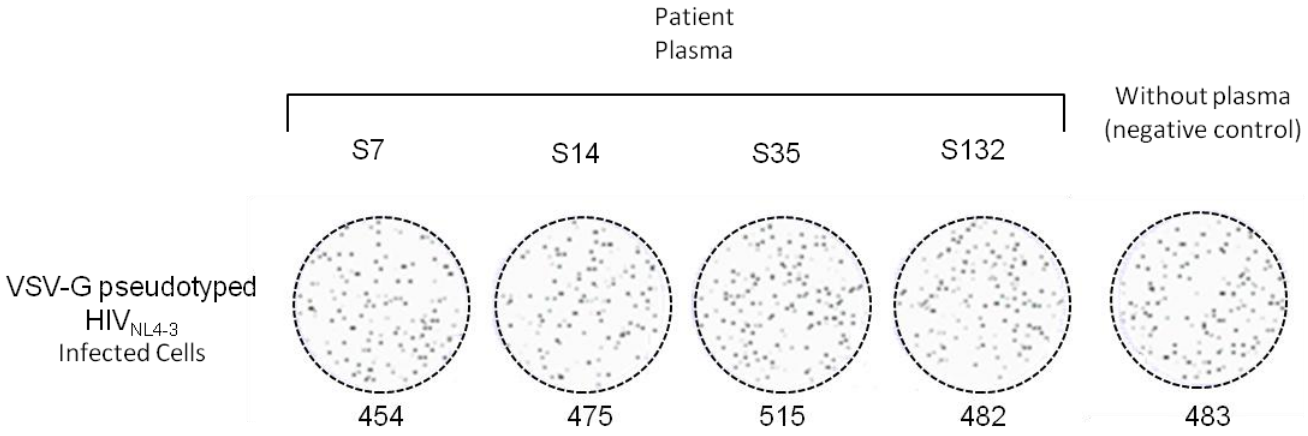


Figure 5.3: Virus pseudotyped with VSV-G was incubated with 1:20 dilutions of patient plasma for 1 hour before titrating onto TZM-bl reporter cells. Plasma derived from patients S7, S14, S35 and S132 was tested. Images show FFU detected by X-Gal staining and counted using an AID ELISpot reader. The number of infected cells counted by the ELISpot reader software is shown below each figure. The image on the far right shows FFU produced by VSV-G pseudotyped virus in the absence of plasma.

Figure 5.4: VL detected during PHI correlated with chronic VL set-points.

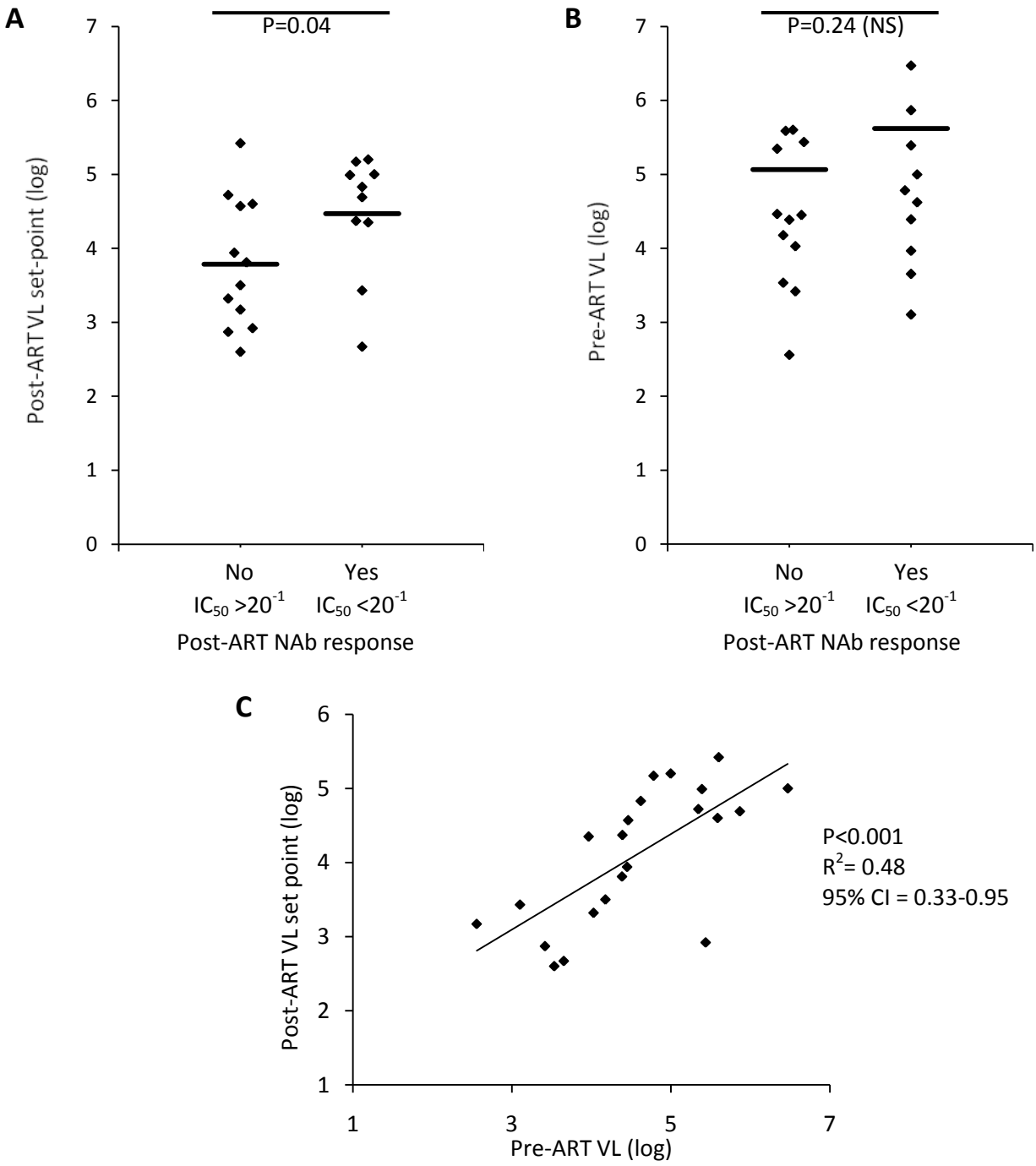


Figure 5.4A: Patients with detectable NAb responses after ART-cessation went on to develop significantly higher VL set-points compared to patients with undetectable NAb titres (reciprocal IC_{50}<20). Figure 5.4B: patients with detectable NAb response tended to have higher VL prior to the first dose of ART (Not statistically significant). Figure 5.4C: Post-ART VL set-points correlated with single VL measurements recorded pre-ART (linear regression with F-test).

levels. This could explain the association between NAb responses and subsequent VL set-points, because prolonged seroconversion illnesses, characterized by high levels of viraemia, have been associated with high VL set-points at later stages of infection (Madec *et al*., 2005b, Mellors *et al*., 1995). In fact, VLs assessed prior to the first dose of ART were approximately 0.5 log higher in patients with post-ART neutralizing activity than patients without detectable responses, although there was considerable variation in both groups and the difference was not statistically significant (mean ± standard deviations; 5.1 ± 5.2 vs. 5.6 ± 6.0, P=0.24) (Figure 5.4B). However, pre-ART VL measurements strongly correlated with VL set-points detected during the chronic stages of their infection (Figure 5.4C), suggesting that levels of vireamia in PHI were linked to subsequent neutralizing responses and high levels of VL detected post-ART.

The estimated duration of PHI prior to initiation of ART was not significantly different between patients with detectable neutralizing responses and patients without neutralizing responses (77 ± 36 vs. 86 ± 33 days, respectively). Furthermore, no correlation was observed between the duration of PHI and chronic VL set-points. However, clinical histories were not available for all patients so it was not possible to validate the estimated dates of infection. No correlation was detected between baseline $CD4^+$ counts and post-ART neutralizing responses, despite a two-fold discrepancy between the highest and lowest CD4 T cell count measurements (397 to 807 cells per mm^3). However, $CD4^+$ T cell counts are known to fluctuate during PHI and additional data were not available to validate these one-off measurements (Schacker *et al*., 1996).

High levels of VL were not always predictive of high levels of NAb response detected after ART was discontinued. For instance, patient S33 had a pre-ART VL of $4x10^5$ RNA copies per ml and went on to develop the highest VL set-point of all patients (5.42 log), yet NAb activity was not detected with week

12 plasma against his contemporaneous Env-pseudotyped virus. Additionally, patient S181 had a pre-ART VL of $2.73x10^5$ RNA copies per ml prior to ART, yet failed to develop a NAb response post-ART (Table 5.2).

In summary, the correlation between VL and neutralizing activity suggests that NAb responses were primed prior to the initiation of ART in patients with high levels of viraemia. However, the correlation between pre-ART VL and post-ART NAb responses was weak, thus implying that factors other than VL are also important in controlling the production of NAbs. However, from these single assessments it was unclear whether patients with undetectable levels of neutralization had low levels of NAbs, or neutralization resistant virus. Because previous studies have demonstrated that virus is less sensitive to neutralization by contemporaneous plasma than plasma derived later in infection, neutralizing responses were assessed longitudinally to determine whether all patients went on to develop detectable levels of neutralizing activity (Frost *et al*., 2005b, Richman *et al*., 2003, Wei *et al*., 2003).

5.2.3 Longitudinal assessment of NAb responses following discontinuation of early ART

Neutralizing responses were assayed longitudinally by testing sequential samples of autologous plasma against the same pseudovirus derived post-ART. Only plasma at week 4 and week 48 was available for patients S7, S14, S35 and S132. For the remaining patients, neutralization was assessed, on average, at 4-12 week intervals and the total follow-up period averaged 102 weeks (range: 60-144 weeks) (Figure 5.5A longitudinal assessments for patient S171 are shown). Throughout the follow-up period, 7/10 patients with VL set-points below 10^4 RNA copies per ml showed no improvement in IC_{50} plasma-titres, which were maintained below the 1:20 cut-off. A notable outlier was patient S194, who exhibited low-level neutralization 12 weeks after treatment cessation (IC_{50} 1:75) and subsequently developed an IC_{50} of 1:375 by week 48, despite maintaining a VL set-point below 10^3 copies per ml (Figure 5.5B).

All patients with intermediate and higher VL set-points (>4 logs) exhibited a significant increase in IC_{50} neutralizing-plasma titres by week 48, (paired sample T-test, $p<0.001$) (Figure 5.6A). Correspondingly, analysis of week-48 plasma responses stratified according to the three original sub-groups revealed a positive correlation with set-point vireamia (ANOVA, $p<0.01$; Figure 5.6B). In cases where neutralization was detected after ART-cessation, IC_{50} plasma titres reached peak levels after 36-108 weeks post-ART. Increases in neutralizing activity lagged behind rebounding-viraemia. Time taken to reach peak levels of neutralizing activity weakly correlated with time-to-peak viraemia, calculated from ART-cessation to the first VL not succeeded by a lower or similar measurement within 0.1 logs ($P<0.05$, $r^2=0.472$) (Figure 5.7). This lends further support to a causal link between antigen-load and NAb production.

Figure 5.5 Neutralizing responses rebounded after cessation of early ART

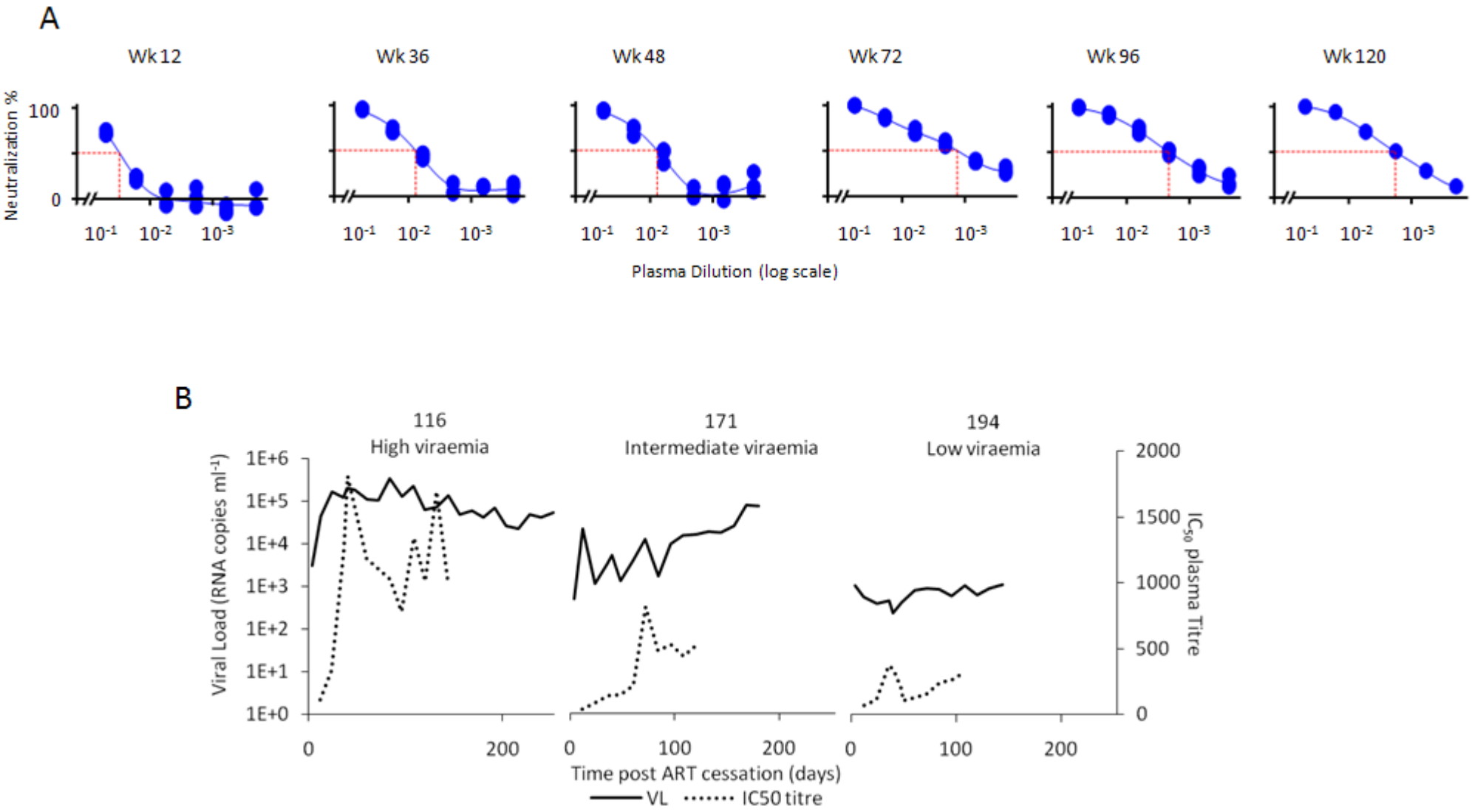


Figure 5.5 Neutralizing responses rebounded after cessation of early ART

Figure 5.5 A. Neutralizing plasma-responses against autologous Env-pseudotypes were assessed longitudinally from the point at which ART was stopped and at 4 to 12 week intervals (week 0; x-axes). Virus derived 12 weeks post-ART cessation was neutralized with sequential samples of plasma and inhibition of infection was assessed using the X-Gal neutralization assay. Six alternate assessments out of twelve are shown for patient S171. IC_{50} neutralizing titres were calculated from interpolations shown as red lines. The corresponding neutralizing titres are shown in Table 5.2.

Figure 5.5 B. Reciprocal IC_{50} titres (dashed lines; right y-axis) are shown with VLs (continuous lines; left y-axis) for three representative patients from each clinically defined subgroup: High VL (S116), intermediate VL (S171) and low VL (S194)



Figure 5.6 Rebounding neutralizing responses were associated with high VL set-point

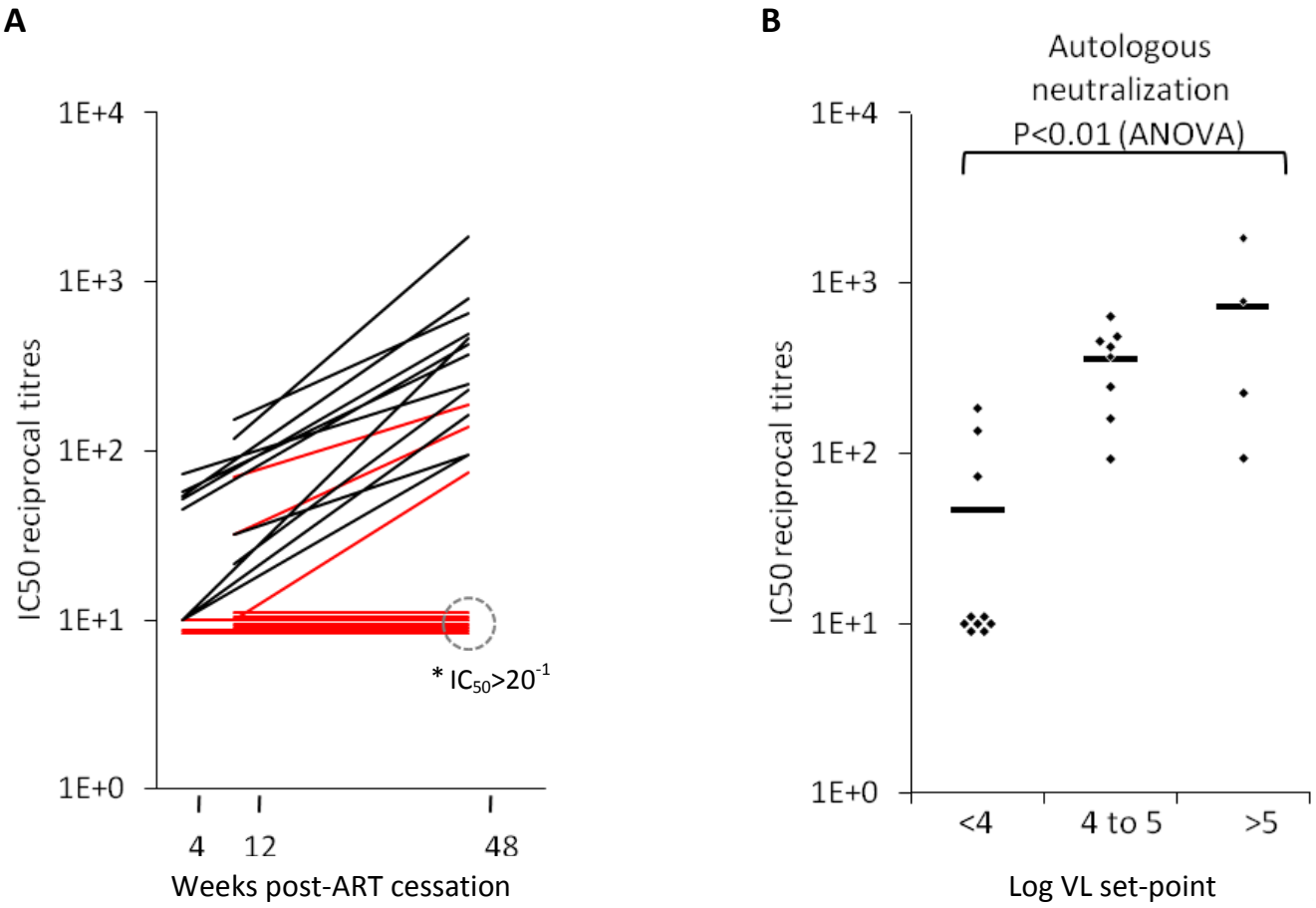


Figure 5.6A. Post-ART neutralizing plasma titres (IC_{50}) are compared with neutralizing responses assessed 36-48 weeks later. Patients with a mean VL greater than 10^4 RNA copies per ml (black lines) exhibited significantly higher neutralizing titres over the follow-up period (paired sample T-test, $p<0.001$). In comparison, titres of plasma from patients with a mean VL set-point below 10^4 RNA copies per ml (red lines) did not change significantly in 7/10 cases (Independent T-Test, low viraemics *vs.* intermediate and high viraemics, $P<0.001$).

Figure 5.6B. Neutralizing plasma responses detected 48 wk post-ART cessation (y-axis) show a positive association with patient sub-groups defined by VL set-point (x-axis) (ANOVA; $p<0.01$). Horizontal lines represent mean values for each group. Non-detectable neutralization titres are shown at half the detection limit of the neutralization assay (1:10) (*).

Figure 5.7 Neutralizing responses followed rebounding VLs

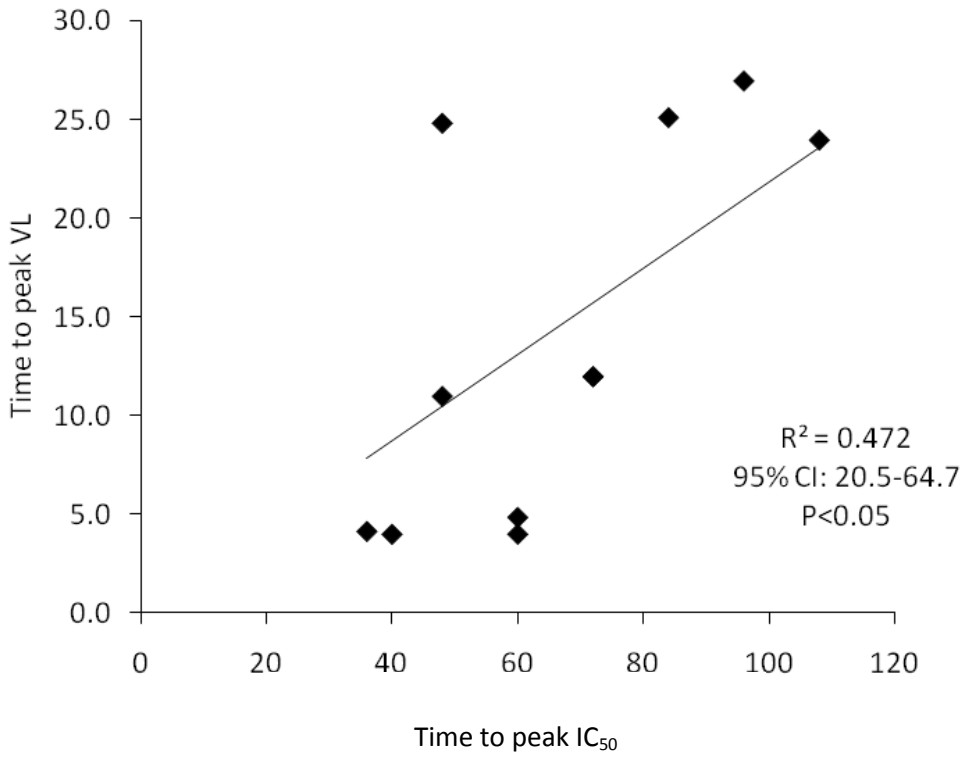


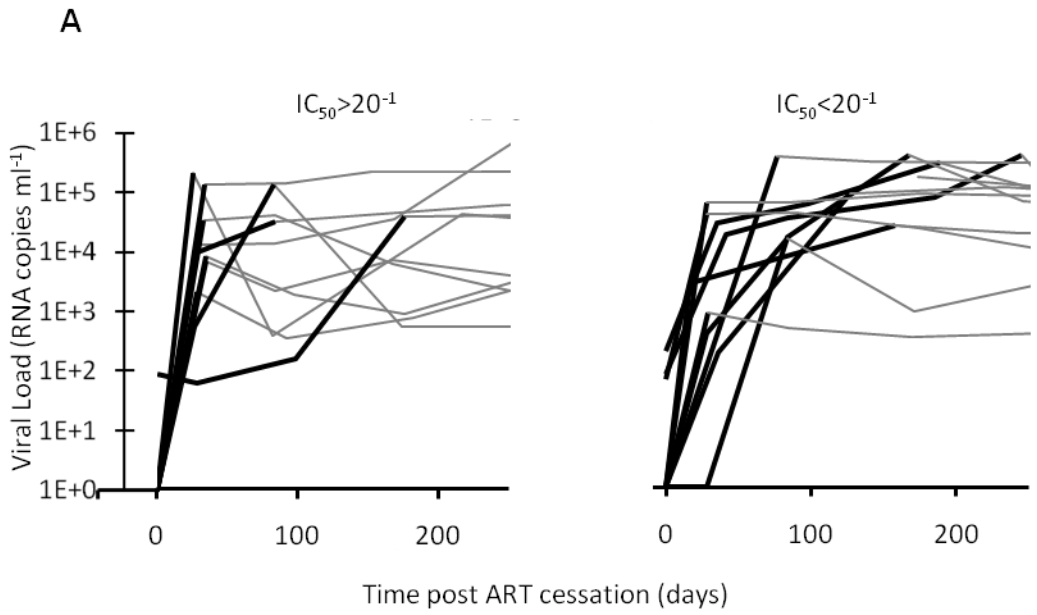
Figure 5.7 Univariate linear regression analysis showed a positive correlation of time-to-peak VL with time-to-peak IC_{50}. The number of weeks taken to reach peak-levels of VL and peak-levels of neutralizing activity are show for all patients with IC_{50} neutralizing plasma titres $<20^{-1}$.

5.2.4 NAb responses were associated with delayed viral rebound after cessation of early ART

To determine whether contemporaneous-autologous neutralizing responses affected the kinetics of VL-rebound when ART was terminated, the time taken for each patient to reach peak-viraemia was analysed. For this analysis, intervals were estimated from ART-cessation to the first VL that was not followed by a lower or similar measurement within 0.1 log (Figure 5.8A). Patients S46 and S116 were excluded from this analysis because neither patient suppressed VL $<10^3$ RNA copies/ml while on ART. Peak levels of viraemia were reached within one to four clinic visits (V1-V4) at average intervals of 5, 13, 26 and 37 weeks from ART cessation (standard deviations; V0-V1 ± 1.7, V1-V2 ± 3.1, V2-V3 ± 2.1, V3-V4 ± 3.3). An important caveat to this analysis is that actual peak VLs could have been reached before or after this measurement. Therefore, visit numbers rather than patient-specific time intervals were compared between patients. Patients with post-ART neutralizing responses detected with contemporaneous-autologous plasma took longer to reach peak viraemia than those patients with undetectable responses (p=0.03; Mann-Whitney U Test) (Figure 5.8B).

Neutralizing plasma titres were low immediately following-ART cessation (IC_{50} range 1:31 to 1:118) and may not have been sufficient to control viraemia. However, all but one patient developed IC_{90} titres at time points prior to peak VL. Furthermore, the actual levels of virus inhibition observed with the 1:20 dilution of the contemporaneous plasma ranged from 70% to 92%, while none of the other patient's plasma neutralized more than two standard deviations above background levels recorded with HIV-1 seronegative plasma. Potentially, neutralizing responses may have contributed to virus control and delayed viral rebound in these patients. However, as mentioned in the previous section, patients with detectable neutralizing responses at treatment-cessation tended to develop higher levels of viraemia. Therefore, the observed delay in viral rebound could simply represent the extra time required to reach VL set-points (Figure 5.8A). However, peak levels of viraemia between patients with neutralizing responses and those without neutralizing responses were not statistically significant (log_{10} RNA copies per ml, 4.3 ± 0.7 vs. 4.3 ± 0.8, p=0.3)

Figure 5.8 Neutralizing responses against autologous-contemperanous Env-pseudovirus were associated with delayed viral rebound.



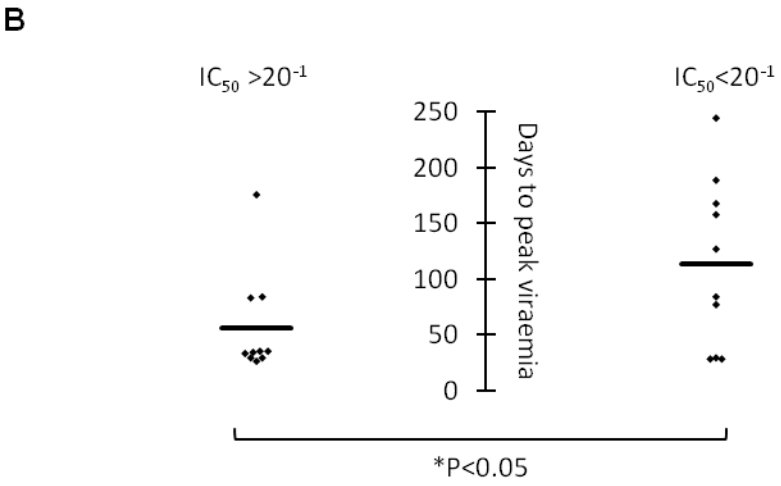


Figure 5.8A. Rebounding patterns of viraemia are shown for patients with contemporaneous–autologous neutralizing responses (left panel) and those without detectable responses (right panel) at ART cessation. Black lines give rebounding VLs prior to peak vireamia. Grey lines give VL data from peak viraemia up to 250 days after ART cessation.

Figure 5.8B compares the time-intervals from ART-cessation to peak viraemia for patients with neutralizing responses and those without (left and right panels, respectively). VLs for patients with no detectable neutralizing activity ($IC_{50}>20^{-1}$) decreased or plateaued to steady set-point levels sooner than those with detectable neutralizing responses.

5.2.5 Clade specific differences of VL and NAb response

The six females infected with subtype C virus fell within the low VL group and three of these had VL set-points below 10^3 RNA copies per ml. Only one of these patients exhibited any neutralizing activity against their autologous virus throughout the follow up period. Interestingly, two of the four clade C viruses that were not neutralized by the patient's own plasma had unusual V3 domains (Table 5.2). Typically, clade C viruses possess a conserved isoleucine at position 309 followed by a GPGQ motif at the crown of the V3 loop, whereas envelope consensus sequences for patients S21 and S99 revealed a V/GPGQ and I/GPGR motif, the latter of which is more commonly found in clade B viruses.

In contrast to the findings we report here, previous studies have shown strong autologous responses associated with recently transmitted clade C viruses that tend to have shorter, less glycosylated envelopes. We did not observe a difference in sequence length or glycosylation across C2V3 sequences of clade B and clade C clones. However, the sequenced regions only covered the C2V3 region and did not include the hypervariable V1/V2 regions that are more commonly associated with subtype C variation after transmission. Sequencing was not intended to identify genetic correlates of neutralization. Envelopes were sequenced to confirm that each patient clone closely resembled direct-consensus PCR sequences, to rule-out cross-contamination between patient samples.

5.2.6 Neutralization of heterologous HIV-1 Env-pseudotypes

The breadth and potency of neutralizing responses against diverse heterologous isolates were assessed for thirty-eight patients using plasma sampled two years after enrolment onto the clinical trial. Plasma from an additional twenty-one patients with clade B infection and five patients with clade C infection were included in this analysis, while patients S171, S35, S128, S41 and S17, could not be investigated because plasma samples were not available.

Plasma samples were tested against an HXB2 Env-pseudotype virus and a diverse panel of clade-matched reference isolates. These panels are widely used to identify broad antibody responses, and consist of envelope clones from diverse HIV-1 field isolates grouped according to neutralization sensitivity (Li *et al*., 2005, Bailey *et al*., 2006). Tier 1B isolates are generally more sensitive to neutralization by heterologous plasma than tier 2 isolates. Table 5.3A shows IC_{50} plasma titres for patients infected with subtype B virus, while Table 5.3B gives heterologous responses for those infected with subtype C virus. Plasma from patients infected with clade B virus exhibited detectable levels of neutralization against HXB2 with IC_{50} titres ranging from 1:20-1:2712. In general, HXB2-pseudovirus was more readily neutralized than the patient's own autologous virus (Mean IC_{50} with standard deviations; 278 ± 711 *vs.* 666 ± 278, P<0.001, paired sample T-test). Comparison of mean neutralizing titres stratified according to VL set-point revealed a similar pattern to that observed for the autologous virus (Figure 5.9 A). However, we observed dissociation between responses against autologous virus and HXB2, particularly for patients with low-level viraemia (Figure 5.9 B). Notably, four patients with undetectable titres against their own virus (IC_{50}<20) neutralized HXB2 (IC_{50} 58-477), suggesting that undetectable levels of autologous neutralizing activity did not reflect absent titres of HIV-1 Env-specific immunoglobulin. Clearly, these patients had antibodies that failed to neutralize their own virus.

Plasma derived from patients infected with subtype C virus exhibited significantly less HXB2-neutralization than plasma from subtype B HIV-1 infected patients (p<0.01, independent sample T-test), despite similar mean VLs in each group (average log VLs: 4.3±0.8 vs. 4.1±1, for clade B and C, respectively). Furthermore, neutralization of tier 1B viruses was not always predictive of neutralizing activity against tier 2 isolates. In particular, patient S1 poorly neutralized two Tier 1B isolates (reciprocal $IC_{50} \leq 30$, HXB2 and ZM109F), yet neutralized three tier 2 isolates with IC_{50} titres ranging from 1:130 to 1:556. Plasma from S84, infected with a clade B virus, neutralized the full panel of clade B reference isolates, including a tier 2 isolate (QH0692c3) with an IC_{50} titre of 1:1421.

Table 5.3A Breadth and potency of neutralizing responses assayed in chronic infection.

Clade B isolates.

Patient ID	Log VL set point	HXB2	6535, c3	QH0692	SC 422661.8	TRO, c11
		Tier 1B	Tier 1B	Tier 2	Tier 2	Tier 2
S3	5.3	1432*	75	<20	<20	<20
S8	4.9	541*	47	329	<20	<20
S10	4.9	236*	108	<20	25	<20
S33	5.5	462*	161	25	<20	<20
S37	3.6	58*	50	<20	<20	n/t
S7	4.9	457*	147	31	<20	<20
S14	5.0	2712*	942*	58	<20	168
S132	4.4	1194*	161	54	<20	<20
S94	4.0	957*	84	29	<20	<20
S116	5.0	1208*	111	217	<20	<20
S194	2.8	662*	<20	<20	<20	<20
S199	3.5	477*	78	23	<20	n/t
S119	3.6	928*	n/t	<20	<20	<20
S84	4.8	696*	141	1421*	20	136
S162	4.8	1256*	29	<20	<20	<20
S165	5.0	236*	190*	<20	20	<20
S79	5.1	294*	<20	<20	<20	<20
S9	5.2	823*	140	<20	<20	<20
S147	3.9	1987*	250	<20	<20	142
S11	4.1	336*	89	20	<20	<20
S191	4.3	358*	64	<20	<20	63
S152	4.4	521*	<20	20	<20	<20
S150	4.6	264*	180	<20	20	20
S130	2.6	143*	91	71	<20	n/t
S178	3.3	280*	<20	<20	<20	n/t
S101	3.5	357*	<20	<20	<20	n/t
S61	3.6	403*	112	<20	<20	n/t
S24	3.6	116*	<20	<20	<20	n/t
S51	3.7	186*	<20	63	<20	n/t

Table 5.3B Breadth and potency of neutralizing responses assayed in chronic infection.

Clade C isolates.

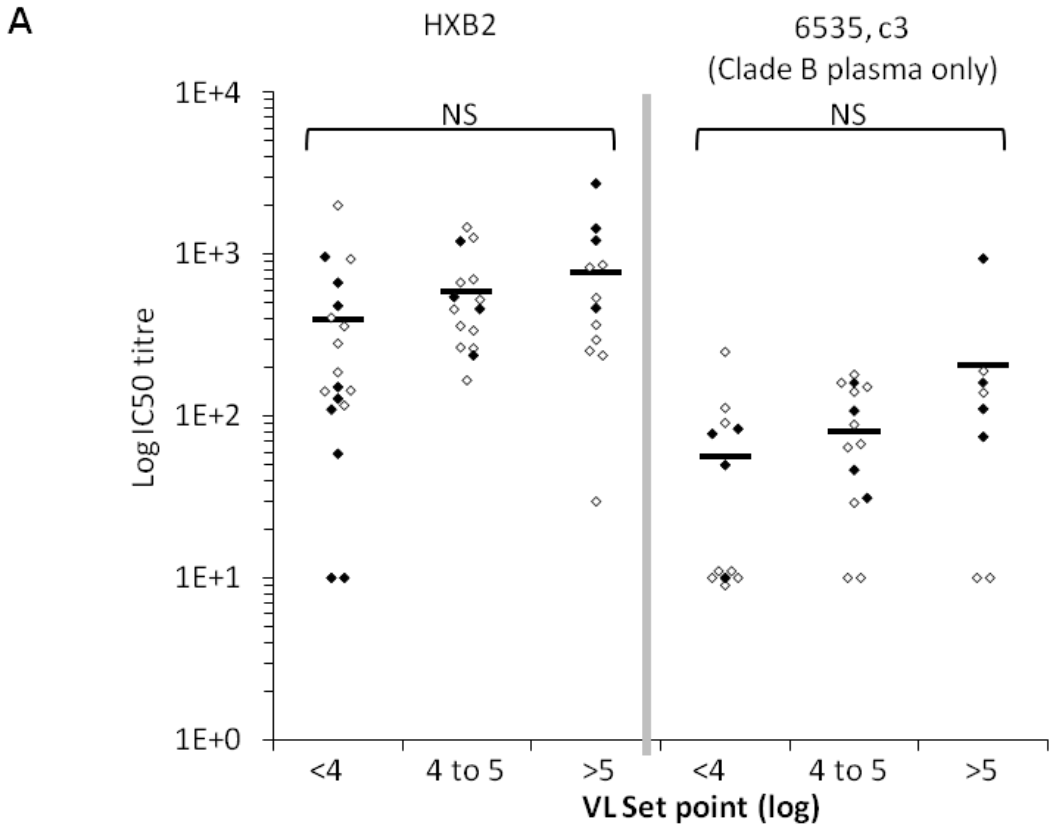
Patient ID	Log VL set point	HXB2 Tier 1B	ZM109F Tier 1B	ZM197M Tier 1B	ZM233M Tier 2	Du172.17 Tier 2
S46	2.6	<20	<20	<20	<20	<20
S181	3.0	<20	<20	<20	<20	70
S99	3.2	128*	<20	43	<20	<20
S185	4.0	109*	<20	<20	<20	40
S31	**4.8**	**261***	**<20**	**803***	**<20**	**26**
S19	5.0	364*	<20	557*	<20	<20
S1	**5.1**	**30**	**20**	**556***	**201***	**130***
S183	5.2	252*	24	<20	20	42

Table 5.3 Breadth and potency of neutralizing responses assayed in chronic infection.

Table 5.3A: Half maximal neutralizing titres of plasma (IC_{50}), collected after 108 weeks post-seroconversion are shown for subtype B standard-reference pseudoviruses (NIH, NAIDS) (Li *et al*., 2005). Patients infected with subtype B virus were identified by nucleotide sequencing of *env* and *pol* genes. Plasma was tested against an HXB2-Env pseudovirus along with two neutralization-sensitive (tier 1B) strains and two less-neutralization susceptible viruses (tier 2). Plasma responses that neutralized virus by 90% or more are marked with an asterisk (*).

Table 5.3B. Plasma collected from patients with subtype C virus were sampled 108 weeks post-seroconversion. Heterologous neutralizing activity was tested against HXB2 and an additional set of subtype-matched tier 1B and tier 2 pseudoviruses (Bailey *et al*., 2006). Serum responses that neutralized virus by 90% or more are marked with an asterisk (*).

Figure 5.9 Neutralization of Tier 1B heterologous strains weakly correlated with VL and autologous NAb titre.



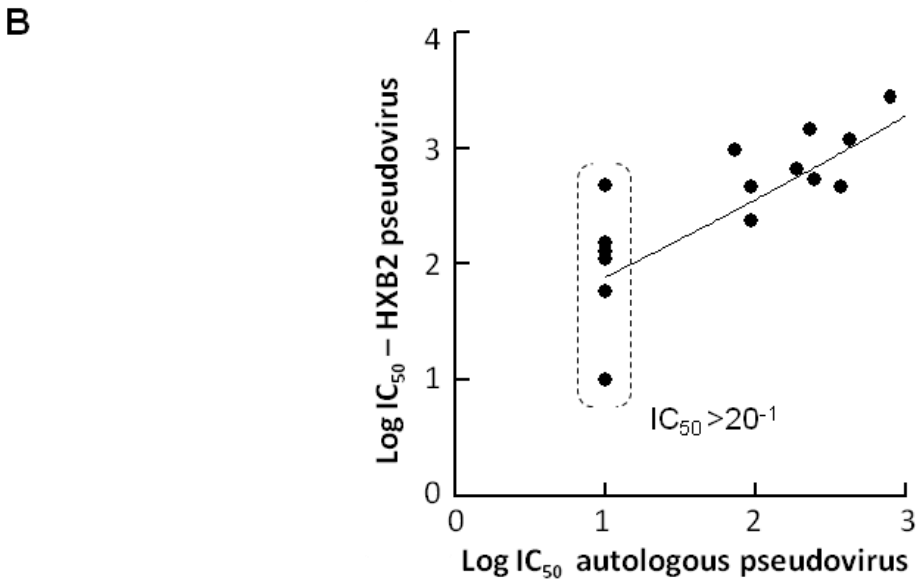


Figure 5.9 Neutralization of Tier 1B heterologous strains weakly correlated with VL and autologous NAb titre.

Figure 5.9 A: Neutralizing plasma responses against heterologous virus (y-axis) are shown for patients included in investigations of autologous neutralization (solid black squares) and additional patients not included in autologous neutralization studies (open squares). Neutralization is shown for two Tier 1B reference isolates, HXB2 and 6365. The observed trend was not statistically significant for either virus (NS, ANOVA).

Figure 5.9 B: Linear regression of autologous-neutralizing plasma titres revealed a significant positive correlation with neutralizing responses against heterologous HXB2-pseudotyped virus (R^2=0.64, P<0.001). The scatter plot highlights notable outliers with incalculable IC_{50} plasma titres against their own virus, despite having potent responses against a HXB2 pseudotype (dashed parentheses).

5.3 Discussion

For the majority of patients stopping ART, neutralizing responses exhibited progressively increasing titres that lagged behind rebounding VL. This is consistent with the theory that antibody production is a function of antigenic stimulation in early HIV-I infection (Piantadosi *et al*., 2009). In accordance with this, week 48 NAb responses strongly correlated with VL set-points and peaks of viraemia correlated temporally with peaks in neutralizing plasma titre. In contrast to these findings, Deeks *et al.* observed a weakly-negative correlation between VLs and autologous-NAb titres in individuals infected with HIV-1 for an average of 5.4 years (Deeks *et al*., 2006a). Additionally, Bailey *et al.* failed to detect an association between VLs and neutralizing responses in chronic progressors and elite controllers (Bailey *et al*., 2006). In these previous studies, there was substantial variation in duration of HIV-1 infection, which is an important determinant of NAb breadth and potency, even after several years of infection (Sather *et al*., 2009). Consequently, a major advantage of this study is that the time from transmission to the first dose of ART was similar for all patients. Knowing approximate exposure-times to viral antigen we could assess the relative importance of antigenic load on the development of NAb responses.

Approximately half the patients (10/22) had detectable neutralizing responses within 4/12 weeks of stopping ART. This was surprising as neutralizing responses were detected using Env-pseudotyped virus and plasma derived from the same time-point. In contrast, a previous study detected rebounding autologous responses within 2-4 weeks after structured ART interruptions in 4/9 subjects treated during chronic infection (Montefiori *et al*., 2001), but only one of these patients had detectable levels of neutralization against contemporaneous virus. Different assay sensitivities could explain this discrepancy; particularly as pseudoviruses are generally more sensitive to neutralization than wild-type primary isolates which were used in the aforementioned study (Fenyo *et al*., 2009). Alternatively, NAb responses may have been augmented by early interventions with ART. A possible mechanism for this

may be derived from studies that show preserved immune function and lower rates of viral evolution in response to ART-mediated VL suppression (Altfeld *et al*., 2001, Hecht *et al*., 2006, Malhotra *et al*., 2000). Specifically, B cell number and B cell phenotype have been shown to normalize in response to ART (Hart *et al*., 2007 , Moir *et al*., 2008b, D'Orsogna *et al*., 2007, Fondere *et al*., 2003). The effects of ART on NAb responses will be determined once the SPARTAC trial is unblinded, when patients who received early therapy can be compared with participants randomized to receive no therapy.

It is likely that NAb responses were primed during PHI because patients with detectable levels of neutralizing activity after short-course ART tended to have high levels of VL during PHI. Although the association was not statistically significant, a causal relationship was inferred by the fact that pre-ART VL and post-ART NAb responses both correlated with VL set-points reached later in infection. Moreover, the median duration of PHI prior to the first dose of ART was 3 months, which corresponds to the initial detection of NAb responses reported by others (Gray *et al*., 2007, Richman *et al*., 2003, Wei *et al*., 2003 , Aasa-Chapman *et al.,* 2004). However, it was not possible to confirm that neutralization pre-ART corresponded to the levels detected after treatment cessation, because baseline plasma was not available for this investigation.

Although we did not detect a direct correlation between NAb responses and baseline $CD4^+$ T cell counts, women with subtype C infections tended to have fewer $CD4^+$ T cells than the men infected with subtype B. The men tended to develop higher levels of neutralizing activity with higher VL set points, so it is possible that neutralization was affected by early changes to $CD4^+$ T cell number and/or function. The major antibody isotype of HIV-1 neutralizing responses is IgG, which is produced from B cells following $CD4^+$ T cell-dependant mechanisms of isotype switching and affinity maturation (Aruffo *et al*., 1993) (reviewed in (Parker, 1993)). Additionally, IgG antibody production requires the production of cytokines, such as IL-4, IFN-γ and TGF-β that are produced from activated $CD4^+$ Th1 and Th2 lymphocytes (reviewed

in (Stavnezer, 1996)). Wide-spread immune hyperactivation in PHI is associated with a "cytokine storm" that can lead to B cell hyperactivity, hypergammaglubulinaemia and depletion of B cell germinal centres (Hart *et al*., 2007, Moir *et al*., 2008a). Therefore, it is possible that high levels of VL could have augmented the production of NAbs indirectly, by stimulating cytokine production from $CD4^+$ T cells. Additional data on $CD4^+$ T cell number, phenotype and function will become available when the SPARTAC trial is unblinded. It will be interesting to see if changes in neutralizing activity correlate with rates of $CD4^+$ T cell decline.

Five patients exhibited up to 0.3-0.9 log decreases in neutralizing plasma titres. The reasons for this are unclear, particularly in the case of patient 116, who maintained a VL above $0.5x10^5$ copies per ml (Figure 5.5B). This patient failed to suppress VL while on ART, so it is possible that declining neutralizing titres were caused by B cell exhaustion and B cell germinal-centre depletion in response to sustained levels of viraemia (Carotenuto *et al*., 1998a). Alternatively, declines in neutralizing titre may have resulted from changes in antibody-affinity, leading to a loss of binding to the earlier Env-pseudovirus. In support of this, Richmann *et al*, also reported waning neutralizing titres against 'earlier' HIV-1 Env-pseudotypes, despite observing sustained levels of neutralization over time against contemporaneous virus (Richman *et al*., 2003). The observation that NAb activity declined in some patients highlights the importance of using a longitudinal models to compare neutralizing responses between patients.

High levels of VL were associated with the rapid development of autologous NAb responses in all patients with VL set-points greater than 10^4 RNA copies/ml. It is, therefore, unclear how patient S194 rapidly developed a neutralizing antibody response, despite maintaining a VL below 10^3 copies per ml. Doria-Rose *et al.* demonstrated broad and potent neutralizing responses in 25% of patients with elite control of viraemia (Doria-Rose *et al*., 2009). The longitudinal data for patient S194 adds to this finding by demonstrating the speed at which NAb responses can develop in the presence of low antigenaemia.

This is encouraging for HIV-1 vaccine research which aims to induce a strong antibody response in the absence of replicating virus. A second notable outlier was patient S33, who had a pre-ART VL of $4x10^5$ and a VL set-point of $5.42x10^5$ RNA copies per ml, yet failed to develop detectable levels of neutralizing activity until 6 months after the termination of ART. Patients S33 and S194 illustrate that factors other than VL are clearly important in controlling the production of NAbs. Possible explanations may relate to physiological variations in B cell sensitivity to Env-antigen, or variations in immune dysfunction during in PHI (Hart *et al*., 2007, Moir *et al*., 2008a). Alternatively, differences in the immunogenic potential of the Env-antigen could also result in variable levels of B cell stimulation and antibody production (reviewed in (Forsell *et al*., 2010)). More work is needed to understand why some patients respond well to low quantities of virus, while others fail to respond to high levels of virus replication.

Autologous neutralizing responses failed to supress viraemia, despite half-maximal neutralizing titres exceeding $1:10^3$. Why then did we fail to detect declines in VL following increases in NAb activity? Firstly, T cell responses and other host factors are known to be important in the control of viraemia and may well have been more important than NAb-responses in the cases examined here (Pereyra *et al*., 2008a, Pereyra *et al*., 2009). Secondly, small reductions of VL resulting from increases in neutralizing titre are likely to be overwhelmed by the reciprocal effect of antigen-stimulation, resulting in the production of more antibodies. Consequently, partially effective NAb responses in patients with higher VLs cannot be ruled out.

Patients with detectable NAb responses after ART-cessation took longer to reach peak levels of VL. The higher VL set-points observed in these patients may be the sole reason for this discrepancy. However, it is unclear why rates of VL increase tended to plateau in patients with detectable levels of neutralizing activity, while VL rebounded more abruptly in patients with undetectable responses. Additionally, peak VLs were not significantly different between these two groups. Previous studies of macaques and

humans have demonstrated that NAbs can delay viral rebound after treatment interruption in acute and chronic infections (Trkola *et al*., 2004, Trkola *et al*., 2005). Therefore, it is possible that neutralizing antibodies were responsible for delayed rebounds observed in this study. However, there is a caveat to our analysis: So long as the SPARTAC trial remains blinded to treatment arm, it is not possible to exclude the possibility that length of ART (either 12 weeks or 48 weeks) influenced the kinetics of rebound post-ART. Although patients who failed to suppress VL below 10^3 copies per ml were excluded from this analysis, patients S132 and S8 exhibited incomplete suppression of VL while on treatment (65 and 195 RNA copies per ml, respectively). Nevertheless, these patients took longer to reach peak viraemia than the majority, suggesting that incomplete suppression did not lead to rapid VL rebounds.

Five of the six patients infected with HIV-1 clade C virus failed to develop neutralizing responses against their autologous virus. This conflicts with previous reports showing rapid development of NAbs in clade C infections (Derdeyn *et al*., 2004, Blish *et al*., 2009, Li *et al*., 2006a). Li *et al.* reported a trend towards higher levels of neutralizing responses in patients infected with subtype C virus, compared with those infected with subtype B (Li *et al*., 2006a). However, in contrast to our findings, the majority of these patients developed VL set-points $>10^4$ copies per ml. Therefore, the low VL set-points of the subtype C infected patients is the most-likely reason for the discrepancy with previous reports and suggests that VL maybe more important than virus subtype in controlling the humoral response.

A major target of gp120-specific antibodies in subtype B infections is thought to be the V3 loop which is consequently, more variable than that of subtype C viruses (Gorny *et al*., 2004 , Wei *et al*., 2003, Zolla-Pazner *et al*., 2004). All patients infected with subtype B virus, including those without detectable responses against autologous virus, neutralized HXB2 pseudotyped virus by at least 50% and most had IC_{90} titres greater than 1:60. It is known that HXB2, and to a lesser extent 6535, are susceptible to NAbs targeting epitopes within the V3 loop. These antibodies are commonly found in HIV-1 infected patients,

but are thought to be ineffective against most primary viruses due to the cryptic nature of the V3 epitopes within trimeric conformations of Env (Moore *et al*., 1995, Sattentau *et al*., 1993, Sullivan *et al*., 1995, Xiang *et al*., 2002). Antibodies targeting the V3 loop are often dismissed as being clinically unimportant, since they fail to slow progression to AIDS (Hogervorst *et al*., 1995, Loomis-Price *et al*., 1998) and to protect against maternal-fetal transmission (Robertson *et al*., 1992). However, the impact of depleting these antibodies on virus infectivity has not been investigated. Maintaining resistance to V3-specific NAbs may incur a fitness cost to the virus in terms of replicative capacity and susceptibility to other neutralizing antibodies. Accordingly, studies of viral evolution in a laboratory worker accidently infected with a TCLA strain, Lai/IIIB, revealed an accumulation of mutations in V3 that induced resistance to broadly specific NAbs and soluble CD4 (Beaumont *et al*., 2004, Beaumont *et al*., 2001).

The clade C HIV-1 infected patient with the greatest neutralizing breadth and potency against a panel of clade C Tier II/III reference strains also had the lowest activity against the more sensitive Tier IB viruses. This finding highlights a caveat relevant to studies aiming to identify potential Env-antigen vaccine candidates by tiered assessment of neutralizing antibody responses (Mascola *et al*., 2005). Had we adhered to recommendations of limiting tier 2 tests to those plasma that neutralized tier 1 isolates, we would not have detected this neutralizing response. It will be interesting to see if this patient develops broader cross-clade neutralizing responses at a later stage of infection.

The strength of the association between VL and neutralization was greater for autologous assessments than heterologous assessments, and there was no correlation between VL and breadth of neutralizing response against diverse isolates. Using autologous viruses to assess the impact of neutralizing antibody responses in early infection is more informative than heterologous responses, which are a poor surrogate marker of neutralizing activity against the patient's own virus. Additionally, longitudinal assessments of VL and autologous antibody responses during early infection could be the only window

of opportunity for delineating cause from effect *in vivo*. This last point is illustrated by the fact that three patients with low VL set-points (<4 logs) showed increases in IC_{50} titre by the end of the follow-up period, suggesting that over time, NAb responses may begin to normalize across VL-stratified patient groups.

In conclusion, these data show that NAb reponses develop during the early stages of infection in response to high VL, in agreement with previous studies of chronic infection (Doria-Rose *et al*., 2009, Sather *et al*., 2009). However, the dynamics of the neutralizing response are highly variable between patients and other factors are also likely to be important. The weak association between baseline NAb responses and time-to-peak viraemia is interesting, but needs to be confirmed by larger studies with shorter intervals between VL and NAb measurements. Our data suggest that if neutralizing antibodies afford any degree of protection *in vivo,* they do so within a complex inter-dependent system that cannot be observed by means of cross-sectional analyses of viraemia and total NAb response alone.

Chapter 6

Conclusions

6.1 Conclusions

The antibody response to HIV-1 has been studied extensively to meet global demands for a protective vaccine. The modest success of the RV144 HIV-1 vaccine trial, which failed to elicit NAbs or CTL responses, has prompted speculation that non-neutralizing antibodies were responsible for the protective effects observed (Rerks-Ngarm *et al*., 2009). Although the antiviral effects of NAbs may be enhanced by Fc-dependent mechanisms of cell-mediated cytotoxicity, there is no direct evidence to suggest that ADCC alone protects against transmission of HIV-1, *in vivo* (Hessell *et al*., 2007). On the other hand, passive transfer studies in macaques have shown that infection with SHIV can be blocked with broadly-specific NAbs (Baba *et al*., 2000, Emini *et al*., 1992, Mascola *et al*., 1999, Mascola *et al*., 2003, Mascola *et al*., 2000, Putkonen *et al*., 1991, Zhang *et al*., 2004a). A fundamental hurdle to the development of a successful HIV-1 vaccine is the elicitation of antibodies capable of neutralizing diverse strains. A possible alternative may be the use of recombinant adeno-associated virus vectors to deliver genes encoding NAbs and NAb-like proteins to non-immune tissues (Johnson *et al*., 2009). This strategy has been shown to protect macaques against infection with SHIV, yet issues regarding the safety of gene therapy need to be resolved before studies can take place in humans. For now, eliciting immune responses by vaccination is the most-realistic approach towards curbing the HIV-1 pandemic.

The neutralizing activities of patient plasma and monoclonal NAbs were measured using a pseudovirus infectivity assay adapted to use automated-counting procedures to quantify infected TZM-bl reporter cells. In order to ensure that pseudoviruses could be constructed for all patients, envelope genes were cloned using MACH1 bacteria that were partially-resistant to the toxic effects of HIV-1 envelope. Unexpectedly, different envelope genes were shown to be variably toxic to transformed K12 strains of *E.coli* that are commonly used for HIV-1 envelope cloning. Only envelope genes *cis*-linked to transcriptional promoters inhibited bacterial growth, confirming the mechanism of cytotoxicity involved

envelope expression. It is possible that the discrepancies observed between different envelope isolates in this study relate to differential fusogenic potentials of gp41 (Chernomordik *et al*., 1994, Arroyo *et al*., 1995, McDonald and Burnett, 2005). Although this was not investigated, previous studies in *E.coli* suggest that gp41 can permeabilize cell membranes independently of virus receptors. Further investigations could determine whether particular HIV-1 envelopes mediate viral-cytolysis in mammalian cells independently of virus receptors, as this may uncover correlates of $CD4^+$ T cell depletion, *in vivo*. Use of MACH1 strains improved the success rate of envelope cloning. Additionally, the modifications described for the X-gal-based pseudovirus neutralization assay provided a high-throughput and cost-effective system to characterize NAb responses *in vitro.* The final optimized assay could be used in a variety of research and clinical settings, including phenotypic assays of virus infectivity, co-receptor typing and antiretroviral-resistance screening.

A primary aim of this study was to understand the factors that control the development of NAb responses in early infection. Autologous NAb activity was assessed in twenty-two patients who went on to develop VL set-points ranging from 3 to 5 $\log_{10}$ RNA copies per ml. As demonstrated, plasma derived from HIV-1 infected patients exhibited variable levels of neutralizing activity against autologous and heterologous viruses. All patients exhibited VL rebounds after ART-cessation. Seven patients who subsequently controlled their viraemia below 4 $\log_{10}$ RNA copies per ml failed to develop detectable levels of neutralizing activity, while patients with higher VL set-points developed peak-level neutralizing titres (IC_{50}) ranging from 95^{-1} to 2946^{-1}. The positive association between VL and NAb activity supports previous studies (Bailey *et al*., 2006, Piantadosi *et al*., 2009, Sather *et al*., 2009). However, low levels of VL were sufficient to stimulate the production of antibodies that neutralized an HXB2 Env-pseudotype. These data confirm that the production of HIV-1 specific antibodies is optimal in the presence of high concentrations of viral antigen. Furthermore, high levels of viraemia may need to be sustained in order to develop antibodies capable of neutralizing autologous viruses.

Two possible mechanisms could explain the concentration-dependant effect of VL on NAb production. Firstly, high levels of Env-antigen may be required to directly cross-link BCRs, leading to the differentiation and proliferation of antibody-producing plasma cells. Alternatively, high levels of viral replication could stimulate the production of NAbs indirectly, by activating $CD4^+$ T cell responses. The former mechanism is more likely to be dominant as $CD4^+$ T cell counts assessed prior to the initiation of ART did not correlate with levels of neutralizing activity. Additionally, wide-spread immune-activation in early infection leads to depletion and dysfunction of $CD4^+$ T cells and B cells, which would be expected to inhibit the development of neutralizing responses (Doria-Rose and Connors, 2009, Hart *et al*., 2007, Moir and Fauci, 2009b, Moir *et al*., 2004). Nevertheless, it will be interesting to see if NAb responses correlate with $CD4^+$ T cell number and function, assessed during the chronic stages of infection and this will be assessed when the SPARTAC trial has been unblinded. By extending this study to investigate those patients randomized to receive no therapy it will be possible to assess whether neutralizing antibody responses were augmented by short-course ART.

Variation in the rates at which antibody responses mounted in response to rebounding viraemia has implications for vaccine development because the window-of-opportunity to prevent chronic HIV-1 infection is limited to the first few days following transmission, before latent pools of HIV-1 become established (Haase, 2010, Virgin and Walker, 2010). Although neutralizing responses against autologous virus developed in most patients, the majority failed to develop antibodies capable of neutralizing Tier 2 heterologous Env-pseudotypes at 2 years post-infection. Clearly, high levels of VL were not sufficient to induce cross-reactive NAbs and longer durations of infection may be necessary to detect such responses (Sather *et al*., 2009, Piantadosi *et al*., 2009). This is not surprising as antibodies that contribute to broad neutralizing activity *in vivo* target conserved epitopes on functional Env trimers, particularly the CD4bs, although antibodies targeting the MPER region of gp41 may also be important in a minority of cases (Moore *et al*., 1994, Binley *et al*., 2008). The CD4bs-specific NAbs that have been isolated to date are

characterized by long CDR3 loops (Prabakaran *et al*., 2006, Saphire *et al*., 2001, Wilkinson *et al*., 2005, Zhang *et al*., 2004b) and high levels of affinity maturation (Zhou *et al*., 2010). The former requires an atypical V(D)J recombination event and the latter involves successive rounds of AID-dependant point mutations. A continual supply of envelope antigen is required for affinity-guided selection of B cells and the likelihood that these processes will give rise to CD4bs-specific antibodies increases with time. With this in mind, in order to elicit protective titres of NAbs by vaccination, it may be necessary to administer several doses of Env antigen over long periods of time.

A second objective of this study was to determine whether NAbs contribute to the control of HIV-1 VL in established HIV-1 infection. The answer to this question has implications for the development of vaccines which aim to limit disease progression in vaccinated individuals that become infected. Additionally, it is important to understand why some patients are able to control levels of viraemia, while others maintain high VL set-points and progress rapidly to AIDS. If the immunological correlates of long-term non-progression can be established, it may be possible to develop therapeutic vaccines and immunotherapies aimed at inducing clinically-beneficial responses in HIV-1 infected patients (reviewed in Cadogan and Dalgleish, 2008). Although several studies have shown that high levels of neutralizing activity are most-frequently detected in patients with high levels of viraemia, neutralizing activity has been detected in a minority of elite controllers and it is unclear if these responses contribute to the control of VL in these patients (Doria-Rose *et al*., 2009, Mahalanabis *et al*., 2009b). Additionally, it is not known if NAbs or non-neutralizing antibodies contribute to the control of VL at high set-point levels.

The interaction between the adapting NAb response and the counter-adapting virus has been likened to the Red Queen principle of evolutionary dynamics. The term is taken from Lewis Carroll's *Through the Looking-Glass and What Alice Found There*, in which the Red Queen tells Alice, *"It takes all the running you can do, to keep in the same place"* (van Valen, 1973). This analogy explicates how constant VL set-

points are maintained despite successive rounds of escape from co-evolving neutralizing responses (Frost *et al*., 2005a). However, until now, there was no direct evidence to suggest that low-levels of virus-neutralization detected with contemporaneous-plasma could contribute to the control of VL, *in vivo*. To take the analogy further, it was not clear what the consequences would be if Alice were to stop running.

In a unique case, rituximab-mediated B cell depletion led to a decline in antibody titre and increases in HIV-1 and Hepatitis B VL. Although the transient decline in NAb titre was not sufficient to attribute a causal link with the observed changes in VL, the impact of NAbs on viral replication was confirmed by evolutionary studies that showed site-specific selection of Env variants that were less susceptible to neutralization by autologous plasma and NAb, b12. These findings concur with previous studies that implicate the same sites in mechanisms of NAb escape (Duenas-Decamp *et al*., 2008, Duenas-Decamp *et al*., 2009, Scanlan *et al*., 2002). While HBV co-infection and B cell-associated changes in HIV-1 specific T cell activity may have contributed to the initial loss of viraemia control, there are no known mechanisms to link these factors to the sequence changes observed in Env.

In chapter 5, three patients (S194, S8, S41) were shown to exhibit fluctuations in IC_{50} titres of a similar magnitude to that observed following B cell depletion. Why then, did we not observe reciprocal associations between VLs and NAb titres in all patients? A possible explanation is that changes in neutralizing titre detected after ART-cessation reflects counter-adaption of the antibody response to mutating viral-envelopes and fluctuating VLs. On the other hand, decreased neutralizing activity detected after rituximab therapy occurred independently of changes in Env, which prevented the humoral response from counter-adapting to the evolving virus. By depleting $CD20^{+}$ B cells, *de novo* antibody responses to the evolving virus would have been inhibited, thus specifically affecting antibodies targeting the contemporaneous strain. At the same time, rituximab therapy does not deplete

archived $CD20^-$ plasma cells (Ahuja *et al*., 2008), which may continue to produce antibodies capable of neutralizing the "early" Env-pseudotypes but not the contemporaneous virus. In support of this suggestion, antibody-binding titres to HBsAb and the CD4bs of gp120 exhibited disproportionately greater decreases than total immunoglobulin concentrations.

In summary, longitudinal follow-up of HIV-1 infected patients in separate clinical settings revealed positive and negative correlations between levels of viraemia and levels neutralizing activity. As hypothesized, a positive correlation was detected between levels of viraemia and autologous NAb responses after the cessation of early ART, yet in a separate case study, decreases in NAb titre led to significant increases of HIV-1 VL. While these findings appear to conflict, they are not mutually exclusive, as distinct mechanisms are responsible for i) the affect of VL on the production of NAbs and ii) the affect of NAbs on the control of VL. Therefore, neutralizing titres are not predictive of antibody-mediated control of HIV-1 VL, because the relationship between VL and the neutralizing antibody response is interdependent.

The hypotheses of this thesis were constructed with the intention of resolving a question that is nearly as old as the discovery of HIV-1 itself: Are NAbs important in the control of HIV-1 VL? It is true that antibody responses must inhibit HIV-1 replication in cases where positive selection of NAb-resistant virus is detected. Chapter 4 is a case in point: the antibody resistant virus that emerged following B cell depletion did so only after neutralization-sensitive variants were eliminated. If antibodies eliminate neutralization-susceptible virus, then neutralizing responses must contribute, somewhat, to the immune control of HIV-1; to say this explicitly is almost a tautology. Despite this, many groups continue to suggest that neutralizing antibodies are not clinically important, or less important than other components of the immune response (Bunnik *et al.*, 2010, Bailey *et al.*, 2006, Euler *et al.*, 2010,

Piantadosi *et al*., 2009). A major conclusion of this thesis is that it is unscientific to speculate on the clinical importance of the antibody response.

Karl Popper, the father of critical rationalism, makes the following demarcation between scientific and non-scientific theory. *'Every "good" scientific theory is a prohibition: it forbids certain things to happen…the scientific status of a theory is its falsifiability, or refutability, or testability'*. (Popper, 1962) There is currently no consensus as to what constitutes a clinically important antibody response and there are no unifying measures that consolidate both sides of the dynamic relationship between antibody and virus. Therefore, it is currently not possible to falsify, refute or even test the theory that HIV-1 antibody responses are clinically important.

From a clinical perspective, defining the role of antibodies in HIV-1 pathology is less important than finding ways to enhance the protective effects of NAbs, *in vivo*. Perhaps the most interesting finding of this thesis was the observation that B cell depletion appeared to *enhance* control of VL set-point after an initial flare in viraemia. With this in mind, a working hypothesis is proposed to explain this finding: In subjects with evidence of antibody-mediated inhibition of viral replication, rituximab-mediated B cell depletion will cause transient losses of viral load control, sensitization of virus to NAb responses and enhanced control of viral load set-point when antibody responses rebound.

Theoretically, relaxing antibody-selective pressure will promote evolution of neutralization-susceptible virus that may be beneficial in the long-term. This hypothesis could be tested using SHIV-infected macaques and the ethical arguments against animal experimentation may be overcome using animals infected as part of vaccine trials. Not only would this corroborate or refute the hypothesis, B cell depletion may also help to determine if non-sterilizing immune responses, induced by vaccination, are clinically beneficial in controlling subsequent viral load set points.

In the proposed study, full-length envelope genes would be sequenced longitudinally subjected to time-structured Phylogenetic and CODEML analyses, as described in chapters 2 and 4, in order to detect antibody-mediated positive selection. B cell depletion would be targeted to cases where effective antibody response are evident. As an experimental control, B cell depletion could be conducted on infected animals without evidence of positive selection, but with evidence of genetic drift and diversification in *env*, indicative of an ineffective antibody response (see Footnote 1).

Knocking-out positive selective pressure should promote reversion to a neutralization-sensitive phenotype. Additionally, temporarily inhibiting B cell development should also relax antibody-mediated negative selection, leading to virus diversification and the acquisition of mutations that further sensitize the virus to the rebounding antibody response (see Footnote 2). If B cell depletion were to be sustained so that the least mutated genome carried at least one deleterious mutation, the decrease in viral fitness will become fixed in the viral population leading to enhanced control of viral load set-point; a mechanism known as Mullers Ratchet (Muller, 1964).

In conclusion, longitudinal follow-up of the neutralizing response in HIV-1 infected patients has revealed a dynamic, yet fragile, evolutionary balance between antibodies and virus. B cell depletion interferes with this relationship with surprising consequences and further work into this particular area could help elucidate the true potential of neutralizing antibodies in the control of HIV-1 viral load.

6.2 Footnotes

Footnote 1: It would be necessary to confirm that anti-CD20 therapy depleted those neutralizing antibodies responsible for the selection event. This would be done by isolating those B cell subclones that produce antibody capable of binding to autologous Env prior to, but not after, the selection event, using recently described techniques pioneered by Scheid *et al*, 2010. The antibody would subsequently be used in neutralization assays and competitive binding assays with serum collected prior to and after B cell depletion using autologous gp140 as the target protein. If rituximab effectively depletes the relevant antibody, binding competition would only be observed with serum derived prior to B cell depletion.

Footnote 2: It may also be possible to further promote evolution of a neutralization-susceptible virus while limiting the flare in viraemia expected from B cell depletion. Chloroquine has been shown to reduce viral load while inhibiting glycosylation of viral envelope leading to losses of N-link glycosylation sites and shortening of Env variable regions (Sperber *et al*., 1995 and 1997, Savarino *et al*., 2001 and 2004); a phenotype likely to be associated with increased susceptibility to NAbs.

References

(OARAC) (December 2009) Guideline for the use of antiretroviral agents in HIV-1-infected adults and adolescents.

AASA-CHAPMAN, M.M., HAYMAN, A., NEWTON, P., CORNFORTH, D., WILLIAMS, I., BORROW, P., BALFE, P., MCKNIGHT, A. (2004) Development of the antibody response in acute HIV-1 infection. *AIDS*, 18, 371-81.

AASA-CHAPMAN, M. M. I., HOLUIGUE, S., AUBIN, K., WONG, M., JONES, N. A., CORNFORTH, D., PELLEGRINO, P., NEWTON, P., WILLIAMS, I., BORROW, P. & MCKNIGHT, A. (2005) Detection of Antibody-Dependent Complement-Mediated Inactivation of both Autologous and Heterologous Virus in Primary Human Immunodeficiency Virus Type 1 Infection. *J. Virol.,* 79**,** 2823-2830.

ADACHI, A., GENDELMAN, H. E., KOENIG, S., FOLKS, T., WILLEY, R., RABSON, A. & MARTIN, M. A. (1986) Production of acquired immunodeficiency syndrome-associated retrovirus in human and nonhuman cells transfected with an infectious molecular clone. *J Virol,* 59**,** 284-91.

AGARWAL, A., VIEIRA, C. A., BOOK, B. K., SIDNER, R. A., FINEBERG, N. S. & PESCOVITZ, M. D. (2004) Rituximab, anti-CD20, induces in vivo cytokine release but does not impair ex vivo T-cell responses. *Am J Transplant,* 4**,** 1357-60.

AGRAWAL, A. & SCHATZ, D. G. (1997) RAG1 and RAG2 form a stable postcleavage synaptic complex with DNA containing signal ends in V(D)J recombination. *Cell,* 89**,** 43-53.

AHUJA, A., ANDERSON, S. M., KHALIL, A. & SHLOMCHIK, M. J. (2008) Maintenance of the plasma cell pool is independent of memory B cells. *Proc Natl Acad Sci U S A,* 105**,** 4802-7.

AKSOY, S., HARPUTLUOGLU, H., KILICKAP, S., DEDE, D. S., DIZDAR, O., ALTUNDAG, K. & BARISTA, I. (2007) Rituximab-related viral infections in lymphoma patients. *Leuk Lymphoma,* 48**,** 1307-12.

ALKHATIB, G., COMBADIERE, C., BRODER, C. C., FENG, Y., KENNEDY, P. E., MURPHY, P. M. & BERGER, E. A. (1996) CC CKR5: a RANTES, MIP-1alpha, MIP-1beta receptor as a fusion cofactor for macrophage-tropic HIV-1. *Science,* 272**,** 1955-8.

ALLAN, J. S., COLIGAN, J. E., BARIN, F., MCLANE, M. F., SODROSKI, J. G., ROSEN, C. A., HASELTINE, W. A., LEE, T. H. & ESSEX, M. (1985) Major glycoprotein antigens that induce antibodies in AIDS patients are encoded by HTLV-III. *Science,* 228**,** 1091-4.

ALTFELD, M., ROSENBERG, E. S., SHANKARAPPA, R., MUKHERJEE, J. S., HECHT, F. M., ELDRIDGE, R. L., ADDO, M. M., POON, S. H., PHILLIPS, M. N., ROBBINS, G. K., SAX, P. E., BOSWELL, S., KAHN, J. O., BRANDER, C., GOULDER, P. J. R., LEVY, J. A., MULLINS, J. I. & WALKER, B. D. (2001) Cellular Immune Responses and Viral Diversity in Individuals Treated during Acute and Early HIV-1 Infection. *The Journal of Experimental Medicine,* 193**,** 169-180.

ARCHER, J., BRAVERMAN, M. S., TAILLON, B. E., DESANY, B., JAMES, I., HARRIGAN, P. R., LEWIS, M. & ROBERTSON, D. L. (2009) Detection of low-frequency pretherapy chemokine (CXC motif) receptor 4 (CXCR4)-using HIV-1 with ultra-deep pyrosequencing. *Aids,* 23**,** 1209-18.

ARROYO, J., BOCETA, M., GONZALEZ, M. E., MICHEL, M. & CARRASCO, L. (1995) Membrane Permeabilization by Different Regions of the Human-Immunodeficiency-Virus Type-1 Transmembrane Glycoprotein gp41. *Journal of Virology,* 69**,** 4095-4102.

ARTHUR, L. O., BESS, J. W., JR., URBAN, R. G., STROMINGER, J. L., MORTON, W. R., MANN, D. L., HENDERSON, L. E. & BENVENISTE, R. E. (1995) Macaques immunized with HLA-DR are protected from challenge with simian immunodeficiency virus. *J Virol,* 69**,** 3117-24.

ARUFFO, A., FARRINGTON, M., HOLLENBAUGH, D., LI, X., MILATOVICH, A., NONOYAMA, S., BAJORATH, J., GROSMAIRE, L. S., STENKAMP, R., NEUBAUER, M. & ET AL. (1993) The CD40 ligand, gp39, is defective in activated T cells from patients with X-linked hyper-IgM syndrome. *Cell,* 72**,** 291-300.

ATTIA, S., EGGER, M., MULLER, M., ZWAHLEN, M. & LOW, N. (2009) Sexual transmission of HIV according to viral load and antiretroviral therapy: systematic review and meta-analysis. *AIDS,* 23**,** 1397-404.

BABA, T. W., LISKA, V., HOFMANN-LEHMANN, R., VLASAK, J., XU, W., AYEHUNIE, S., CAVACINI, L. A., POSNER, M. R., KATINGER, H., STIEGLER, G., BERNACKY, B. J., RIZVI, T. A., SCHMIDT, R., HILL, L. R., KEELING, M. E., LU, Y., WRIGHT, J. E., CHOU, T. C. & RUPRECHT, R. M. (2000) Human neutralizing monoclonal antibodies of the IgG1 subtype protect against mucosal simian-human immunodeficiency virus infection. *Nat Med,* 6**,** 200-6.

BABIKER, A. G. & GIBB, D. M. (2006) Considerations in the design of randomized controlled trials evaluating the optimal time to initiate antiretroviral therapy in previously untreated HIV-1-infected patients. *Current Opinion in HIV and AIDS,* 1**,** 488-494 10.1097/COH.0b013e328010f238.

BAILES, E., GAO, F., BIBOLLET-RUCHE, F., COURGNAUD, V., PEETERS, M., MARX, P. A., HAHN, B. H. & SHARP, P. M. (2003) Hybrid origin of SIV in chimpanzees. *Science,* 300**,** 1713.

BAILEY, J. R., LASSEN, K. G., YANG, H. C., QUINN, T. C., RAY, S. C., BLANKSON, J. N. & SILICIANO, R. F. (2006) Neutralizing antibodies do not mediate suppression of human immunodeficiency virus type 1 in elite suppressors or selection of plasma virus variants in patients on highly active antiretroviral therapy. *J Virol,* 80**,** 4758-70.

BAILEY, J. R., O'CONNELL, K., YANG, H. C., HAN, Y., XU, J., JILEK, B., WILLIAMS, T. M., RAY, S. C., SILICIANO, R. F. & BLANKSON, J. N. (2008) Transmission of human immunodeficiency virus type 1 from a patient who developed AIDS to an elite suppressor. *J Virol,* 82**,** 7395-410.

BALAKRISHNAN, M. & JONSSON, C. B. (1997) Functional identification of nucleotides conferring substrate specificity to retroviral integrase reactions. *J Virol,* 71**,** 1025-35.

BARRE-SINOUSSI, F., CHERMANN, J. C., REY, F., NUGEYRE, M. T., CHAMARET, S., GRUEST, J., DAUGUET, C., AXLER-BLIN, C., VEZINET-BRUN, F., ROUZIOUX, C., ROZENBAUM, W. & MONTAGNIER, L. (1983) Isolation of a T-lymphotropic retrovirus from a patient at risk for acquired immune deficiency syndrome (AIDS). *Science,* 220**,** 868-71.

BEAUMONT, T., QUAKKELAAR, E., VAN NUENEN, A., PANTOPHLET, R. & SCHUITEMAKER, H. (2004) Increased sensitivity to CD4 binding site-directed neutralization following in vitro propagation on primary lymphocytes of a neutralization-resistant human immunodeficiency virus IIIB strain isolated from an accidentally infected laboratory worker. *J Virol,* 78**,** 5651-7.

BEAUMONT, T., VAN NUENEN, A., BROERSEN, S., BLATTNER, W. A., LUKASHOV, V. V. & SCHUITEMAKER, H. (2001) Reversal of Human Immunodeficiency Virus Type 1 IIIB to a Neutralization-Resistant Phenotype in an Accidentally Infected Laboratory Worker with a Progressive Clinical Course. *Journal of Virology,* 75**,** 2246-2252.

BEDDOWS, S., LOUISIRIROTCHANAKUL, S., CHEINGSONG-POPOV, R., EASTERBROOK, P. J., SIMMONDS, P. & WEBER, J. (1998) Neutralization of primary and T-cell line adapted isolates of human immunodeficiency virus type 1: role of V3-specific antibodies. *J Gen Virol,* 79 (Pt 1)**,** 77-82.

BEELS, D., HEYNDRICKX, L., VEREECKEN, K., VERMOESEN, T., MICHIELS, L., VANHAM, G. & KESTENS, L. (2008) Production of human immunodeficiency virus type 1 (HIV-1) pseudoviruses using linear HIV-1 envelope expression cassettes. *J Virol Methods,* 147**,** 99-107.

BERMAN, H. M., WESTBROOK, J., FENG, Z., GILLILAND, G., BHAT, T. N., WEISSIG, H., SHINDYALOV, I. N. & BOURNE, P. E. (2000) The Protein Data Bank. *Nucleic Acids Res,* 28**,** 235-42.

BETTS, M. R., NASON, M. C., WEST, S. M., DE ROSA, S. C., MIGUELES, S. A., ABRAHAM, J., LEDERMAN, M. M., BENITO, J. M., GOEPFERT, P. A., CONNORS, M., ROEDERER, M. & KOUP, R. A. (2006) HIV

nonprogressors preferentially maintain highly functional HIV-specific CD8+ T cells. *Blood,* 107**,** 4781-4789.

BHASKARAN, K., HAMOUDA, O., SANNES, M., BOUFASSA, F., JOHNSON, A. M., LAMBERT, P. C. & PORTER, K. (2008) Changes in the risk of death after HIV seroconversion compared with mortality in the general population. *JAMA,* 300**,** 51-9.

BINLEY, J. M., CAYANAN, C. S., WILEY, C., SCHULKE, N., OLSON, W. C. & BURTON, D. R. (2003) Redox-Triggered Infection by Disulfide-Shackled Human Immunodeficiency Virus Type 1 Pseudovirions. *J. Virol.,* 77**,** 5678-5684.

BINLEY, J. M., LYBARGER, E. A., CROOKS, E. T., SEAMAN, M. S., GRAY, E., DAVIS, K. L., DECKER, J. M., WYCUFF, D., HARRIS, L., HAWKINS, N., WOOD, B., NATHE, C., RICHMAN, D., TOMARAS, G. D., BIBOLLET-RUCHE, F., ROBINSON, J. E., MORRIS, L., SHAW, G. M., MONTEFIORI, D. C. & MASCOLA, J. R. (2008) Profiling the specificity of neutralizing antibodies in a large panel of plasmas from patients chronically infected with human immunodeficiency virus type 1 subtypes B and C. *J Virol,* 82**,** 11651-68.

BINLEY, J. M., WRIN, T., KORBER, B., ZWICK, M. B., WANG, M., CHAPPEY, C., STIEGLER, G., KUNERT, R., ZOLLA-PAZNER, S., KATINGER, H., PETROPOULOS, C. J. & BURTON, D. R. (2004) Comprehensive Cross-Clade Neutralization Analysis of a Panel of Anti-Human Immunodeficiency Virus Type 1 Monoclonal Antibodies. *J. Virol.,* 78**,** 13232-13252.

BLISH, C. A., JALALIAN-LECHAK, Z., RAINWATER, S., NGUYEN, M.-A., DOGAN, O. C. & OVERBAUGH, J. (2009) Cross-Subtype Neutralization Sensitivity despite Monoclonal Antibody Resistance among Early Subtype A, C, and D Envelope Variants of Human Immunodeficiency Virus Type 1. *Journal of Virology,* 83**,** 7783-7788.

BORROW, P., LEWICKI, H., HAHN, B. H., SHAW, G. M. & OLDSTONE, M. B. (1994) Virus-specific CD8+ cytotoxic T-lymphocyte activity associated with control of viremia in primary human immunodeficiency virus type 1 infection. *J Virol,* 68**,** 6103-10.

BOUNOU, S., GIGUERE, J. F., CANTIN, R., GILBERT, C., IMBEAULT, M., MARTIN, G. & TREMBLAY, M. J. (2004) The importance of virus-associated host ICAM-1 in human immunodeficiency virus type 1 dissemination depends on the cellular context. *FASEB J,* 18**,** 1294-6.

BRADNEY, A. P., SCHEER, S., CRAWFORD, J. M., BUCHBINDER, S. P. & MONTEFIORI, D. C. (1999) Neutralization escape in human immunodeficiency virus type 1-infected long-term nonprogressors. *J Infect Dis,* 179**,** 1264-7.

BREITFELD, D., OHL, L., KREMMER, E., ELLWART, J., SALLUSTO, F., LIPP, M. & FÃ¶RSTER, R. (2000) Follicular B helper T cells express CXC chemokine receptor 5, localize to B cell follicles, and support immunoglobulin production. *J Exp Med,* 192**,** 1545-52.

BRENCHLEY, J. M., SCHACKER, T. W., RUFF, L. E., PRICE, D. A., TAYLOR, J. H., BEILMAN, G. J., NGUYEN, P. L., KHORUTS, A., LARSON, M., HAASE, A. T. & DOUEK, D. C. (2004) CD4+ T cell depletion during all stages of HIV disease occurs predominantly in the gastrointestinal tract. *J Exp Med,* 200**,** 749-59.

BRIGGS, J. A., SIMON, M. N., GROSS, I., KRAUSSLICH, H. G., FULLER, S. D., VOGT, V. M. & JOHNSON, M. C. (2004) The stoichiometry of Gag protein in HIV-1. *Nat Struct Mol Biol,* 11**,** 672-5.

BRULE, F., KHATISSIAN, E., BENANI, A., BODEUX, A., MONTAGNIER, L., PIETTE, J., LAURET, E. & RAVET, E. (2007) Inhibition of HIV replication: a powerful antiviral strategy by IFN-beta gene delivery in CD4+ cells. *Biochem Pharmacol,* 74**,** 898-910.

BUCHBINDER, S. P., MEHROTRA, D. V., DUERR, A., FITZGERALD, D. W., MOGG, R., LI, D., GILBERT, P. B., LAMA, J. R., MARMOR, M., DEL RIO, C., MCELRATH, M. J., CASIMIRO, D. R., GOTTESDIENER, K. M., CHODAKEWITZ, J. A., COREY, L. & ROBERTSON, M. N. (2008) Efficacy assessment of a cell-mediated immunity HIV-1 vaccine (the Step Study): a double-blind, randomised, placebo-controlled, test-of-concept trial. *Lancet,* 372**,** 1881-93.

BUNNIK, E. M., LOBBRECHT, M. S., VAN NUENEN, A. C. & SCHUITEMAKER, H. Escape from autologous humoral immunity of HIV-1 is not associated with a decrease in replicative capacity. *Virology, 2009,* 397**,** 224-30.

BURTON, D. R., PYATI, J., KODURI, R., SHARP, S. J., THORNTON, G. B., PARREN, P. W., SAWYER, L. S., HENDRY, R. M., DUNLOP, N., NARA, P. L. & ET AL. (1994) Efficient neutralization of primary isolates of HIV-1 by a recombinant human monoclonal antibody. *Science,* 266**,** 1024-7.

BURTON, D. R., SAPHIRE, E. O. & PARREN, P. W. (2001) A model for neutralization of viruses based on antibody coating of the virion surface. *in: Antibodies in viral infection ed: D.R Burton***,** 109-144.

BUSCH, M. P. & SATTEN, G. A. (1997) Time course of viremia and antibody seroconversion following human immunodeficiency virus exposure. *Am J Med,* 102**,** 117-24; discussion 125-6.

CADOGAN, M. & DALGLEISH, A. G. (2008) HIV immunopathogenesis and strategies for intervention. *The Lancet Infectious Diseases,* 8**,** 675-684.

CALARESE, D. A., SCANLAN, C. N., ZWICK, M. B., DEECHONGKIT, S., MIMURA, Y., KUNERT, R., ZHU, P., WORMALD, M. R., STANFIELD, R. L., ROUX, K. H., KELLY, J. W., RUDD, P. M., DWEK, R. A., KATINGER, H., BURTON, D. R. & WILSON, I. A. (2003) Antibody Domain Exchange Is an Immunological Solution to Carbohydrate Cluster Recognition. *Science,* 300**,** 2065-2071.

CAMUS, G., SEGURA-MORALES, C., MOLLE, D., LOPEZ-VERGES, S., BEGON-PESCIA, C., CAZEVIEILLE, C., SCHU, P., BERTRAND, E., BERLIOZ-TORRENT, C. & BASYUK, E. (2007) The Clathrin Adaptor Complex AP-1 Binds HIV-1 and MLV Gag and Facilitates Their Budding. *Mol. Biol. Cell,* 18**,** 3193-3203.

CAO, Y., QIN, L., ZHANG, L., SAFRIT, J. & HO, D. D. (1995) Virologic and immunologic characterization of long-term survivors of human immunodeficiency virus type 1 infection. *N Engl J Med,* 332**,** 201-8.

CAROTENUTO, P., LOOIJ, D., KELDERMANS, L., DE WOLF, F. & GOUDSMIT, J. (1998b) Neutralizing antibodies are positively associated with CD4+ T-cell counts and T-cell function in long-term AIDS-free infection. *AIDS,* 12**,** 1591-600.

CARR, J. K., FOLEY, B. T., LEITNER, T., SALMINEN, M., KORBER, B. & MCCUTCHAN, F. (Eds.) (1998) *Reference Sequences Representing the Principal Genetic Diversity of HIV-1 in the Pandemic*, Theoretical Biology and Biophysics Group, Los Alamos National Laboratory, Los Alamos, NM.

CARRINGTON, M. & O'BRIEN, S. J. (2003) The influence of HLA genotype on AIDS. *Annu Rev Med,* 54**,** 535-51.

CAVACINI, L. A., EMES, C. L., POWER, J., DESHARNAIS, F. D., DUVAL, M., MONTEFIORI, D. & POSNER, M. R. (1995) Influence of heavy chain constant regions on antigen binding and HIV-1 neutralization by a human monoclonal antibody. *J Immunol,* 155**,** 3638-44.

CECILIA, D., KLEEBERGER, C., MUNOZ, A., GIORGI, J. V. & ZOLLA-PAZNER, S. (1999) A longitudinal study of neutralizing antibodies and disease progression in HIV-1-infected subjects. *J Infect Dis,* 179**,** 1365-74.

CHAN, D. C., FASS, D., BERGER, J. M. & KIM, P. S. (1997) Core structure of gp41 from the HIV envelope glycoprotein. *Cell,* 89**,** 263-73.

CHEN, B., VOGAN, E. M., GONG, H., SKEHEL, J. J., WILEY, D. C. & HARRISON, S. C. (2005) Structure of an unliganded simian immunodeficiency virus gp120 core. *Nature,* 433**,** 834-41.

CHEREPANOV, P., MAERTENS, G., PROOST, P., DEVREESE, B., VAN BEEUMEN, J., ENGELBORGHS, Y., DE CLERCQ, E. & DEBYSER, Z. (2003) HIV-1 Integrase Forms Stable Tetramers and Associates with LEDGF/p75 Protein in Human Cells. *Journal of Biological Chemistry,* 278**,** 372-381.

CHERNOMORDIK, L., CHANTURIYA, A. N., SUSS-TOBY, E., NORA, E. & ZIMMERBERG, J. (1994) An amphipathic peptide from the C-terminal region of the human immunodeficiency virus envelope glycoprotein causes pore formation in membranes. *Journal of Virology,* 68**,** 7115-7123.

CHERTOVA, E., BESS JR, J. W., JR., CRISE, B. J., SOWDER, I. R., SCHADEN, T. M., HILBURN, J. M., HOXIE, J. A., BENVENISTE, R. E., LIFSON, J. D., HENDERSON, L. E. & ARTHUR, L. O. (2002) Envelope glycoprotein incorporation, not shedding of surface envelope glycoprotein (gp120/SU), Is the primary determinant of SU content of purified human immunodeficiency virus type 1 and simian immunodeficiency virus. *J Virol,* 76**,** 5315-25.

CHOUDHRY, V., ZHANG, M. Y., HARRIS, I., SIDOROV, I. A., VU, B., DIMITROV, A. S., FOUTS, T. & DIMITROV, D. S. (2006) Increased efficacy of HIV-1 neutralization by antibodies at low CCR5 surface concentration. *Biochem Biophys Res Commun,* 348**,** 1107-15.

CHUNG, A. W., ROLLMAN, E., CENTER, R. J., KENT, S. J. & STRATOV, I. (2009) Rapid Degranulation of NK Cells following Activation by HIV-Specific Antibodies. *J Immunol,* 182**,** 1202-1210.

CLAPHAM, P. R. & MCKNIGHT, A. (2001) HIV-1 receptors and cell tropism. *Br Med Bull,* 58**,** 43-59.

CLARKE, S. H., HUPPI, K., RUEZINSKY, D., STAUDT, L., GERHARD, W. & WEIGERT, M. (1985) Inter- and intraclonal diversity in the antibody response to influenza hemagglutinin. *J Exp Med,* 161**,** 687-704.

COMARDELLE, A. M., NORRIS, C. H., PLYMALE, D. R., GATTI, P. J., CHOI, B., FERMIN, C. D., HAISLIP, A. M., TENCZA, S. B., MIETZNER, T. A., MONTELARO, R. C. & GARRY, R. F. (1997) A synthetic peptide corresponding to the carboxy terminus of human immunodeficiency virus type 1 transmembrane glycoprotein induces alterations in the ionic permeability of Xenopus laevis oocytes. *AIDS Res Hum Retroviruses,* 13**,** 1525-32.

COOPER, D. A., IMRIE, A. A. & PENNY, R. (1987) Antibody response to human immunodeficiency virus after primary infection. *J Infect Dis,* 155**,** 1113-8.

CORNALL, R. J., CHENG, A. M., PAWSON, T. & GOODNOW, C. C. (2000) Role of Syk in B-cell development and antigen-receptor signaling. *Proc Natl Acad Sci U S A,* 97**,** 1713-8.

CRAWFORD, H., PRADO, J. G., LESLIE, A., HUE, S., HONEYBORNE, I., REDDY, S., VAN DER STOK, M., MNCUBE, Z., BRANDER, C., ROUSSEAU, C., MULLINS, J. I., KASLOW, R., GOEPFERT, P., ALLEN, S., HUNTER, E., MULENGA, J., KIEPIELA, P., WALKER, B. D. & GOULDER, P. J. (2007) Compensatory mutation partially restores fitness and delays reversion of escape mutation within the immunodominant HLA-B*5703-restricted Gag epitope in chronic human immunodeficiency virus type 1 infection. *J Virol,* 81**,** 8346-51.

D'COSTA, S., SLOBOD, K. S., WEBSTER, R. G., WHITE, S. W. & HURWITZ, J. L. (2001) Structural features of HIV envelope defined by antibody escape mutant analysis. *AIDS Res Hum Retroviruses,* 17**,** 1205-9.

D'ORSOGNA, L. J., KRUEGER, R. G., MCKINNON, E. J. & FRENCH, M. A. (2007) Circulating memory B-cell subpopulations are affected differently by HIV infection and antiretroviral therapy. *AIDS,* 21**,** 1747-52.

DAAR, E. S., LITTLE, S., PITT, J., SANTANGELO, J., HO, P., HARAWA, N., KERNDT, P., GLORGI, J. V., BAI, J., GAUT, P., RICHMAN, D. D., MANDEL, S. & NICHOLS, S. (2001) Diagnosis of primary HIV-1 infection. Los Angeles County Primary HIV Infection Recruitment Network. *Ann Intern Med,* 134**,** 25-9.

DE OLIVEIRA, T., DEFORCHE, K., CASSOL, S., SALMINEN, M., PARASKEVIS, D., SEEBREGTS, C., SNOECK, J., VAN RENSBURG, E. J., WENSING, A. M., VAN DE VIJVER, D. A., BOUCHER, C. A., CAMACHO, R. & VANDAMME, A. M. (2005) An automated genotyping system for analysis of HIV-1 and other microbial sequences. *Bioinformatics,* 21**,** 3797-800.

DEEKS, S. G., KITCHEN, C. M., LIU, L., GUO, H., GASCON, R., NARVAEZ, A. B., HUNT, P., MARTIN, J. N., KAHN, J. O., LEVY, J., MCGRATH, M. S. & HECHT, F. M. (2004) Immune activation set point during early HIV infection predicts subsequent CD4+ T-cell changes independent of viral load. *Blood,* 104**,** 942-7.

DEEKS, S. G., SCHWEIGHARDT, B., WRIN, T., GALOVICH, J., HOH, R., SINCLAIR, E., HUNT, P., MCCUNE, J. M., MARTIN, J. N., PETROPOULOS, C. J. & HECHT, F. M. (2006a) Neutralizing Antibody Responses against Autologous and Heterologous Viruses in Acute versus Chronic Human Immunodeficiency Virus (HIV) Infection: Evidence for a Constraint on the Ability of HIV To Completely Evade Neutralizing Antibody Responses. *Journal of Virology,* 80**,** 6155-6164.

DEEKS, S. G. & WALKER, B. D. (2007) Human Immunodeficiency Virus Controllers: Mechanisms of Durable Virus Control in the Absence of Antiretroviral Therapy. *Immunity,* 27**,** 406-416.

DELLA-PORTA, A. J. & WESTAWAY, E. G. (1978) A Multi-Hit Model for the Neutralization of Animal Viruses. *J Gen Virol,* 38**,** 1-19.

DENG, H., LIU, R., ELLMEIER, W., CHOE, S., UNUTMAZ, D., BURKHART, M., DI MARZIO, P., MARMON, S., SUTTON, R. E., HILL, C. M., DAVIS, C. B., PEIPER, S. C., SCHALL, T. J., LITTMAN, D. R. & LANDAU, N. R. (1996) Identification of a major co-receptor for primary isolates of HIV-1. *Nature,* 381**,** 661-6.

DENHAM, E., MOHN, B., TUCKER, L., LUN, A., CLEAVE, P. & BOSWELL, D. R. (2007) Evaluation of immunoturbidimetric specific protein methods using the Architect ci8200: comparison with immunonephelometry. *Ann Clin Biochem,* 44**,** 529-536.

DERDEYN, C. A., DECKER, J. M., BIBOLLET-RUCHE, F., MOKILI, J. L., MULDOON, M., DENHAM, S. A., HEIL, M. L., KASOLO, F., MUSONDA, R., HAHN, B. H., SHAW, G. M., KORBER, B. T., ALLEN, S. & HUNTER, E. (2004) Envelope-Constrained Neutralization-Sensitive HIV-1 After Heterosexual Transmission. *Science,* 303**,** 2019-2022.

DIMITROV, A. S., LOUIS, J. M., BEWLEY, C. A., CLORE, G. M. & BLUMENTHAL, R. (2005) Conformational changes in HIV-1 gp41 in the course of HIV-1 envelope glycoprotein-mediated fusion and inactivation. *Biochemistry,* 44**,** 12471-9.

DIMMOCK, N. J. (1984) Mechanisms of neutralization of animal viruses. *J Gen Virol,* 65 (Pt 6)**,** 1015-22.

DISKIN, R., MARCOVECCHIO, P. M. & BJORKMAN, P. J. Structure of a clade C HIV-1 gp120 bound to CD4 and CD4-induced antibody reveals anti-CD4 polyreactivity. *Nat Struct Mol Biol, 2010,* 17**,** 608-613.

DORFMAN, T., POPOVA, E., PIZZATO, M. & GOTTLINGER, H. G. (2002) Nef enhances human immunodeficiency virus type 1 infectivity in the absence of matrix. *J Virol,* 76**,** 6857-62.

DORIA-ROSE, N. A. & CONNORS, M. (2009) Antibody-secreting B cells in HIV infection. *Current Opinion in HIV & AIDS,* 4**,** 426-430.

DORIA-ROSE, N. A., KLEIN, R. M., MANION, M. M., O'DELL, S., PHOGAT, A., CHAKRABARTI, B., HALLAHAN, C. W., MIGUELES, S. A., WRAMMERT, J., AHMED, R., NASON, M., WYATT, R. T., MASCOLA, J. R. & CONNORS, M. (2009) Frequency and phenotype of human immunodeficiency virus envelope-specific B cells from patients with broadly cross-neutralizing antibodies. *J Virol,* 83**,** 188-99.

DRISCOLL, M. D. & HUGHES, S. H. (2000) Human immunodeficiency virus type 1 nucleocapsid protein can prevent self-priming of minus-strand strong stop DNA by promoting the annealing of short oligonucleotides to hairpin sequences. *J Virol,* 74**,** 8785-92.

DRUMMOND, A. J., HO, S. Y., PHILLIPS, M. J. & RAMBAUT, A. (2006) Relaxed phylogenetics and dating with confidence. *PLoS Biol,* 4**,** e88.

DRUMMOND, A. J. & RAMBAUT, A. (2007) BEAST: Bayesian evolutionary analysis by sampling trees. *BMC Evol Biol,* 7**,** 214.

DRUMMOND, A. J., RAMBAUT, A., SHAPIRO, B. & PYBUS, O. G. (2005) Bayesian coalescent inference of past population dynamics from molecular sequences. *Mol Biol Evol,* 22**,** 1185-92.

DUBRIDGE, R. B., TANG, P., HSIA, H. C., LEONG, P. M., MILLER, J. H. & CALOS, M. P. (1987) Analysis of mutation in human cells by using an Epstein-Barr virus shuttle system. *Mol Cell Biol,* 7**,** 379-87.

DUDA, A., LEE-TURNER, L., FOX, J., ROBINSON, N., DUSTAN, S., KAYE, S., FRYER, H., CARRINGTON, M., MCCLURE, M., MCLEAN, A. R., FIDLER, S., WEBER, J., PHILLIPS, R. E. & FRATER, A. J. (2009) HLA-

associated clinical progression correlates with epitope reversion rates in early human immunodeficiency virus infection. *J Virol,* 83**,** 1228-39.

DUENAS-DECAMP, M. J., PETERS, P., BURTON, D. & CLAPHAM, P. R. (2008) Natural Resistance of Human Immunodeficiency Virus Type 1 to the CD4bs Antibody b12 Conferred by a Glycan and an Arginine Residue Close to the CD4 Binding Loop. *J. Virol.,* 82**,** 5807-5814.

DUENAS-DECAMP, M. J., PETERS, P. J., BURTON, D. & CLAPHAM, P. R. (2009) Determinants Flanking the CD4 Binding Loop Modulate Macrophage Tropism of Human Immunodeficiency Virus Type 1 R5 Envelopes. *J. Virol.,* 83**,** 2575-2583.

EDELMAN, G. M. (1991) Antibody structure and molecular immunology. *Scand J Immunol,* 34**,** 1-22.

EMING, R., NAGEL, A., WOLFF-FRANKE, S., PODSTAWA, E., DEBUS, D. & HERTL, M. (2008) Rituximab exerts a dual effect in pemphigus vulgaris. *J Invest Dermatol,* 128**,** 2850-8.

EMINI, E. A., SCHLEIF, W. A., NUNBERG, J. H., CONLEY, A. J., EDA, Y., TOKIYOSHI, S., PUTNEY, S. D., MATSUSHITA, S., COBB, K. E., JETT, C. M. & ET AL. (1992) Prevention of HIV-1 infection in chimpanzees by gp120 V3 domain-specific monoclonal antibody. *Nature,* 355**,** 728-30.

EMU, B., SINCLAIR, E., HATANO, H., FERRE, A., SHACKLETT, B., MARTIN, J. N., MCCUNE, J. M. & DEEKS, S. G. (2008) HLA Class I-Restricted T-Cell Responses May Contribute to the Control of Human Immunodeficiency Virus Infection, but Such Responses Are Not Always Necessary for Long-Term Virus Control. *J. Virol.,* 82**,** 5398-5407.

EPA V.C. & COLMAN P.M. (Eds.) (2001) *Shape and Electrostatic Complementarity at Viral Antigen-Antibody Complexes. In: Antobodies in Viral Infection*.

EULER, Z., VAN GILS, M. J., BUNNIK, E. M., PHUNG, P., SCHWEIGHARDT, B., WRIN, T. & SCHUITEMAKER, H. Cross-reactive neutralizing humoral immunity does not protect from HIV type 1 disease progression. *J Infect Dis, 2010,* 201**,** 1045-53.

FARNET, C. M. & BUSHMAN, F. D. (1997) HIV-1 cDNA integration: requirement of HMG I(Y) protein for function of preintegration complexes in vitro. *Cell,* 88**,** 483-92.

FASSATI, A. & GOFF, S. P. (2001) Characterization of intracellular reverse transcription complexes of human immunodeficiency virus type 1. *J Virol,* 75**,** 3626-35.

FATKENHEUER, G., NELSON, M., LAZZARIN, A., KONOURINA, I., HOEPELMAN, A. I. M., LAMPIRIS, H., HIRSCHEL, B., TEBAS, P., RAFFI, F., TROTTIER, B., BELLOS, N., SAAG, M., COOPER, D. A., WESTBY, M., TAWADROUS, M., SULLIVAN, J. F., RIDGWAY, C., DUNNE, M. W., FELSTEAD, S., MAYER, H., VAN DER RYST, E., 1, T. M. & MOTIVATE 2 STUDY TEAMS (2008) Subgroup Analyses of Maraviroc in Previously Treated R5 HIV-1 Infection. *N Engl J Med,* 359**,** 1442-1455.

FELLAY, J., SHIANNA, K. V., GE, D., COLOMBO, S., LEDERGERBER, B., WEALE, M., ZHANG, K., GUMBS, C., CASTAGNA, A., COSSARIZZA, A., COZZI-LEPRI, A., DE LUCA, A., EASTERBROOK, P., FRANCIOLI, P., MALLAL, S., MARTINEZ-PICADO, J., MIRO, J. M., OBEL, N., SMITH, J. P., WYNIGER, J., DESCOMBES, P., ANTONARAKIS, S. E., LETVIN, N. L., MCMICHAEL, A. J., HAYNES, B. F., TELENTI, A. & GOLDSTEIN, D. B. (2007) A whole-genome association study of major determinants for host control of HIV-1. *Science,* 317**,** 944-7.

FENG, Y., BRODER, C. C., KENNEDY, P. E. & BERGER, E. A. (1996) HIV-1 entry cofactor: functional cDNA cloning of a seven-transmembrane, G protein-coupled receptor. *Science,* 272**,** 872-7.

FENYO, E. M., HEATH, A., DISPINSERI, S., HOLMES, H., LUSSO, P., ZOLLA-PAZNER, S., DONNERS, H., HEYNDRICKX, L., ALCAMI, J., BONGERTZ, V., JASSOY, C., MALNATI, M., MONTEFIORI, D., MOOG, C., MORRIS, L., OSMANOV, S., POLONIS, V., SATTENTAU, Q., SCHUITEMAKER, H., SUTTHENT, R., WRIN, T., SCARLATTI, G., MONTEFIORI, D. C., ZHOU, J. Y., MASCOLA, J. R., LOUDER, M. K., WINTER, C., PRABHAKARA, R., DE ROSA, S. C., DOUEK, D. C., HILL, B. J., GABUZDA, D., ROEDERER, M., POLONIS, V. R., BUNNIK, E. M., BROWN, B. K., WIECZOREK, L., SANDERS-BUELL, E., ROSA BORGES, A., ROBB, M. L., BIRX, D. L., MICHAEL, N. L., MCCUTCHAN, F. E., OCHSENBAUER, C. &

KAPPES, J. C. (2009) International network for comparison of HIV neutralization assays: the NeutNet report. *PLoS One,* 4**,** e4505.

FERNIE, B. F., POLI, G. & FAUCI, A. S. (1991) Alpha interferon suppresses virion but not soluble human immunodeficiency virus antigen production in chronically infected T-lymphocytic cells. *J. Virol.,* 65**,** 3968-3971.

FERRANTELLI, F., KITABWALLA, M., RASMUSSEN, R. A., CAO, C., CHOU, T. C., KATINGER, H., STIEGLER, G., CAVACINI, L. A., BAI, Y., COTROPIA, J., UGEN, K. E. & RUPRECHT, R. M. (2004) Potent cross-group neutralization of primary human immunodeficiency virus isolates with monoclonal antibodies--implications for acquired immunodeficiency syndrome vaccine. *J Infect Dis,* 189**,** 71-4.

FIDLER, S., OXENIUS, A., BRADY, M., CLARKE, J., CROPLEY, I., BABIKER, A., ZHANG, H. T., PRICE, D., PHILLIPS, R. & WEBER, J. (2002) Virological and immunological effects of short-course antiretroviral therapy in primary HIV infection. *AIDS,* 16**,** 2049-54.

FIEBIG, E. W., WRIGHT, D. J., RAWAL, B. D., GARRETT, P. E., SCHUMACHER, R. T., PEDDADA, L., HELDEBRANT, C., SMITH, R., CONRAD, A., KLEINMAN, S. H. & BUSCH, M. P. (2003) Dynamics of HIV viremia and antibody seroconversion in plasma donors: implications for diagnosis and staging of primary HIV infection. *AIDS,* 17**,** 1871-9.

FISCHL, M. A., RICHMAN, D. D., GRIECO, M. H., GOTTLIEB, M. S., VOLBERDING, P. A., LASKIN, O. L., LEEDOM, J. M., GROOPMAN, J. E., MILDVAN, D., SCHOOLEY, R. T. & ET AL. (1987) The efficacy of azidothymidine (AZT) in the treatment of patients with AIDS and AIDS-related complex. A double-blind, placebo-controlled trial. *N Engl J Med,* 317**,** 185-91.

FONDERE, J. M., HUGUET, M. F., YSSEL, H., BAILLAT, V., REYNES, J., VAN DE PERRE, P. & VENDRELL, J. P. (2003) Detection of peripheral HIV-1-specific memory B cells in patients untreated or receiving highly active antiretroviral therapy. *AIDS,* 17**,** 2323-30.

FORSELL, M. N. E. A., SCHIEF, W. R. B. & WYATT, R. T. A. Immunogenicity of HIV-1 envelope glycoprotein oligomers.

FORTHAL, D. N., LANDUCCI, G., PHAN, T. B. & BECERRA, J. (2005) Interactions between natural killer cells and antibody Fc result in enhanced antibody neutralization of human immunodeficiency virus type 1. *J Virol,* 79**,** 2042-9.

FREDERICKSEN, B. L., WEI, B. L., YAO, J., LUO, T. & GARCIA, J. V. (2002) Inhibition of endosomal/lysosomal degradation increases the infectivity of human immunodeficiency virus. *J Virol,* 76**,** 11440-6.

FROST, S. D., WRIN, T., SMITH, D. M., KOSAKOVSKY POND, S. L., LIU, Y., PAXINOS, E., CHAPPEY, C., GALOVICH, J., BEAUCHAINE, J., PETROPOULOS, C. J., LITTLE, S. J. & RICHMAN, D. D. (2005a) Neutralizing antibody responses drive the evolution of human immunodeficiency virus type 1 envelope during recent HIV infection. *Proc Natl Acad Sci U S A,* 102**,** 18514-9.

FROST, S. D. W., LIU, Y., POND, S. L. K., CHAPPEY, C., WRIN, T., PETROPOULOS, C. J., LITTLE, S. J. & RICHMAN, D. D. (2005b) Characterization of Human Immunodeficiency Virus Type 1 (HIV-1) Envelope Variation and Neutralizing Antibody Responses during Transmission of HIV-1 Subtype B. *Journal of Virology,* 79**,** 6523-6527.

GAO, F., BAILES, E., ROBERTSON, D. L., CHEN, Y., RODENBURG, C. M., MICHAEL, S. F., CUMMINS, L. B., ARTHUR, L. O., PEETERS, M., SHAW, G. M., SHARP, P. M. & HAHN, B. H. (1999) Origin of HIV-1 in the chimpanzee Pan troglodytes troglodytes. *Nature,* 397**,** 436-41.

GARCIA-CALLEJA, J. M., GOUWS, E. & GHYS, P. D. (2006) National population based HIV prevalence surveys in sub-Saharan Africa: results and implications for HIV and AIDS estimates. *Sex Transm Infect,* 82 Suppl 3**,** iii64-70.

GARCIA-RODRIGUEZ, M. J., CANALES, M. A., HERNANDEZ-MARAVER, D. & HERNANDEZ-NAVARRO, F. (2008) Late reactivation of resolved hepatitis B virus infection: An increasing complication post rituximab-based regimens treatment? *Am J Hematol,* 83**,** 673-675.

GAUFIN, T., PATTISON, M., GAUTAM, R., STOULIG, C., DUFOUR, J., MACFARLAND, J., MANDELL, D., TATUM, C., MARX, M. H., RIBEIRO, R. M., MONTEFIORI, D., APETREI, C. & PANDREA, I. (2009) Effect of B-cell depletion on viral replication and clinical outcome of simian immunodeficiency virus infection in a natural host. *J Virol,* 83**,** 10347-57.

GAZZARD, B. G., ANDERSON, J., BABIKER, A., BOFFITO, M., BROOK, G., BROUGH, G., CHURCHILL, D., CROMARTY, B., DAS, S., FISHER, M., FREEDMAN, A., GERETTI, A. M., JOHNSON, M., KHOO, S., LEEN, C., NAIR, D., PETERS, B., PHILLIPS, A., PILLAY, D., POZNIAK, A., WALSH, J., WILKINS, E., WILLIAMS, I., WILLIAMS, M. & YOULE, M. (2008) British HIV Association Guidelines for the treatment of HIV-1-infected adults with antiretroviral therapy 2008. *HIV Med,* 9**,** 563-608.

GEIJTENBEEK, T. B., KWON, D. S., TORENSMA, R., VAN VLIET, S. J., VAN DUIJNHOVEN, G. C., MIDDEL, J., CORNELISSEN, I. L., NOTTET, H. S., KEWALRAMANI, V. N., LITTMAN, D. R., FIGDOR, C. G. & VAN KOOYK, Y. (2000) DC-SIGN, a dendritic cell-specific HIV-1-binding protein that enhances trans-infection of T cells. *Cell,* 100**,** 587-97.

GELDERBLOM, H. R. (1991) Assembly and morphology of HIV: potential effect of structure on viral function. *AIDS,* 5**,** 617-37.

GEORGE, A. J., GALLOP, J. L. & RASHID, M. (1997) Kinetics of biomolecular interactions. *Exp. Opin. Ther. Patents,* 7**,** 947-963.

GHOSH, M., HOWARD, K. J., CAMERON, C. E., BENKOVIC, S. J., HUGHES, S. H. & LE GRICE, S. F. (1995) Truncating alpha-helix E' of p66 human immunodeficiency virus reverse transcriptase modulates RNase H function and impairs DNA strand transfer. *J Biol Chem,* 270**,** 7068-76.

GIORGI, J. V., HULTIN, L. E., MCKEATING, J. A., JOHNSON, T. D., OWENS, B., JACOBSON, L. P., SHIH, R., LEWIS, J., WILEY, D. J., PHAIR, J. P., WOLINSKY, S. M. & DETELS, R. (1999) Shorter survival in advanced human immunodeficiency virus type 1 infection is more closely associated with T lymphocyte activation than with plasma virus burden or virus chemokine coreceptor usage. *J Infect Dis,* 179**,** 859-70.

GONG, Q., OU, Q., YE, S., LEE, W. P., CORNELIUS, J., DIEHL, L., LIN, W. Y., HU, Z., LU, Y., CHEN, Y., WU, Y., MENG, Y. G., GRIBLING, P., LIN, Z., NGUYEN, K., TRAN, T., ZHANG, Y., ROSEN, H., MARTIN, F. & CHAN, A. C. (2005) Importance of cellular microenvironment and circulatory dynamics in B cell immunotherapy. *J Immunol,* 174**,** 817-26.

GOONETILLEKE, N., LIU, M. K., SALAZAR-GONZALEZ, J. F., FERRARI, G., GIORGI, E., GANUSOV, V. V., KEELE, B. F., LEARN, G. H., TURNBULL, E. L., SALAZAR, M. G., WEINHOLD, K. J., MOORE, S., LETVIN, N., HAYNES, B. F., COHEN, M. S., HRABER, P., BHATTACHARYA, T., BORROW, P., PERELSON, A. S., HAHN, B. H., SHAW, G. M., KORBER, B. T. & MCMICHAEL, A. J. (2009) The first T cell response to transmitted/founder virus contributes to the control of acute viremia in HIV-1 infection. *J Exp Med,* 206**,** 1253-72.

GORNY, M. K., REVESZ, K., WILLIAMS, C., VOLSKY, B., LOUDER, M. K., ANYANGWE, C. A., KRACHMAROV, C., KAYMAN, S. C., PINTER, A., NADAS, A., NYAMBI, P. N., MASCOLA, J. R. & ZOLLA-PAZNER, S. (2004) The V3 Loop Is Accessible on the Surface of Most Human Immunodeficiency Virus Type 1 Primary Isolates and Serves as a Neutralization Epitope. *Journal of Virology,* 78**,** 2394-2404.

GOTTLIEB, M. S. (2006) Pneumocystis pneumonia--Los Angeles. 1981. *Am J Public Health,* 96**,** 980-1; discussion 982-3.

GOTTLINGER, H. G. (Ed.) (2001) *HIV-1 Gag: a Molecular Machine Driving Viral Particle Assembly and Release*, Theoretical Biology and Biophysics Group, Los Alamos National Laboratory, Los Alamos.

GOTTLINGER, H. G., SODROSKI, J. G. & HASELTINE, W. A. (1989) Role of capsid precursor processing and myristoylation in morphogenesis and infectivity of human immunodeficiency virus type 1. *Proc Natl Acad Sci U S A,* 86**,** 5781-5.

GRAY, E. S., MOORE, P. L., CHOGE, I. A., DECKER, J. M., BIBOLLET-RUCHE, F., LI, H., LESEKA, N., TREURNICHT, F., MLISANA, K., SHAW, G. M., KARIM, S. S., WILLIAMSON, C. & MORRIS, L. (2007)

Neutralizing antibody responses in acute human immunodeficiency virus type 1 subtype C infection. *J Virol,* 81**,** 6187-96.

GREENSPAN, N. S. (Ed.) (2001) *Affinity, Complementarity, Cooperativity, and Specificity in Antibody Recognition. In Antibodies in Viral Infection*, Springer.

HAASE, A. T. Targeting early infection to prevent HIV-1 mucosal transmission. *Nature, 2010,* 464**,** 217-223.

HAIGWOOD, N. L., MONTEFIORI, D. C., SUTTON, W. F., MCCLURE, J., WATSON, A. J., VOSS, G., HIRSCH, V. M., RICHARDSON, B. A., LETVIN, N. L., HU, S. L. & JOHNSON, P. R. (2004) Passive immunotherapy in simian immunodeficiency virus-infected macaques accelerates the development of neutralizing antibodies. *J Virol,* 78**,** 5983-95.

HALLENBERGER, S., BOSCH, V., ANGLIKER, H., SHAW, E., KLENK, H. D. & GARTEN, W. (1992) Inhibition of furin-mediated cleavage activation of HIV-1 glycoprotein gp160. *Nature,* 360**,** 358-61.

HARE, C. B., PAPPALARDO, B. L., BUSCH, M. P., KARLSSON, A. C., PHELPS, B. H., ALEXANDER, S. S., BENTSEN, C., RAMSTEAD, C. A., NIXON, D. F., LEVY, J. A. & HECHT, F. M. (2006) Seroreversion in subjects receiving antiretroviral therapy during acute/early HIV infection. *Clin Infect Dis,* 42**,** 700-8.

HART, M., STEEL, A., CLARK, S. A., MOYLE, G., NELSON, M., HENDERSON, D. C., WILSON, R., GOTCH, F., GAZZARD, B. & KELLEHER, P. (2007) Loss of discrete memory B cell subsets is associated with impaired immunization responses in HIV-1 infection and may be a risk factor for invasive pneumococcal disease. *J Immunol,* 178**,** 8212-20.

HAYNES, B. F. & MONTEFIORI, D. C. (2006) Aiming to induce broadly reactive neutralizing antibody responses with HIV-1 vaccine candidates. *Expert Rev Vaccines,* 5**,** 347-63.

HECHT, F. M., WANG, L., COLLIER, A., LITTLE, S., MARKOWITZ, M., MARGOLICK, J., KILBY, J. M., DAAR, E., CONWAY, B. & HOLTE, S. (2006) A multicenter observational study of the potential benefits of initiating combination antiretroviral therapy during acute HIV infection. *J Infect Dis,* 194**,** 725-33.

HENDERSON, L. E., BOWERS, M. A., SOWDER, R. C., 2ND, SERABYN, S. A., JOHNSON, D. G., BESS, J. W., JR., ARTHUR, L. O., BRYANT, D. K. & FENSELAU, C. (1992) Gag proteins of the highly replicative MN strain of human immunodeficiency virus type 1: posttranslational modifications, proteolytic processings, and complete amino acid sequences. *J Virol,* 66**,** 1856-65.

HERRERA, C., SPENLEHAUER, C., FUNG, M. S., BURTON, D. R., BEDDOWS, S. & MOORE, J. P. (2003) Nonneutralizing Antibodies to the CD4-Binding Site on the gp120 Subunit of Human Immunodeficiency Virus Type 1 Do Not Interfere with the Activity of a Neutralizing Antibody against the Same Site. *J. Virol.,* 77**,** 1084-1091.

HESSELL, A. J., HANGARTNER, L., HUNTER, M., HAVENITH, C. E., BEURSKENS, F. J., BAKKER, J. M., LANIGAN, C. M., LANDUCCI, G., FORTHAL, D. N., PARREN, P. W., MARX, P. A. & BURTON, D. R. (2007) Fc receptor but not complement binding is important in antibody protection against HIV. *Nature,* 449**,** 101-4.

HEYNDRICKX, L., VERMOESEN, T., VEREECKEN, K., KURTH, J., COPPENS, S., AERTS, L., OHAGEN, A., VAN HERREWEGE, Y., LEWI, P. & VANHAM, G. (2008) Antiviral compounds show enhanced activity in HIV-1 single cycle pseudovirus assays as compared to classical PBMC assays. *J Virol Methods,* 148**,** 166-73.

HIOE, C. E., BASTIANI, L., HILDRETH, J. E. & ZOLLA-PAZNER, S. (1998) Role of cellular adhesion molecules in HIV type 1 infection and their impact on virus neutralization. *AIDS Res Hum Retroviruses,* 14 Suppl 3**,** S247-54.

HO, D. D. (1995) Time to hit HIV, early and hard. *N Engl J Med,* 333**,** 450-1.

HO, D. D., NEUMANN, A. U., PERELSON, A. S., CHEN, W., LEONARD, J. M. & MARKOWITZ, M. (1995) Rapid turnover of plasma virions and CD4 lymphocytes in HIV-1 infection. *Nature,* 373**,** 123-6.

HO, J., MOIR, S., MALASPINA, A., HOWELL, M. L., WANG, W., DIPOTO, A. C., O'SHEA, M. A., ROBY, G. A., KWAN, R., MICAN, J. M., CHUN, T. W. & FAUCI, A. S. (2006) Two overrepresented B cell populations in HIV-infected individuals undergo apoptosis by different mechanisms. *Proc Natl Acad Sci U S A,* 103**,** 19436-41.

HOEN, B., COOPER, D. A., LAMPE, F. C., PERRIN, L., CLUMECK, N., PHILLIPS, A. N., GOH, L. E., LINDBACK, S., SERENI, D., GAZZARD, B., MONTANER, J., STELLBRINK, H. J., LAZZARIN, A., PONSCARME, D., STASZEWSKI, S., MATHIESEN, L., SMITH, D., FINLAYSON, R., WEBER, R., WEGMANN, L., JANOSSY, G. & KINLOCH-DE LOES, S. (2007) Predictors of virological outcome and safety in primary HIV type 1-infected patients initiating quadruple antiretroviral therapy: QUEST GW PROB3005. *Clin Infect Dis,* 45**,** 381-90.

HOGERVORST, E., JURRIAANS, S., WOLF, F. D., WIJK, A. V., WIERSMA, A., VALK, M., ROOS, M., GEMEN, B. V., COUTINHO, R., MIEDEMA, F. & GOUDSMIT, J. (1995) Predictors for Non- and Slow Progression in Human Immunodeficiency Virus (HIV) Type 1 Infection: Low Viral RNA Copy Numbers in Serum and Maintenance of High HIV-1 p24-Specific but Not V3-Specific Antibody Levels. *The Journal of Infectious Diseases,* 171**,** 811-821.

HOGG, R. S., YIP, B., CHAN, K. J., WOOD, E., CRAIB, K. J., O'SHAUGHNESSY, M. V. & MONTANER, J. S. (2001) Rates of disease progression by baseline CD4 cell count and viral load after initiating triple-drug therapy. *JAMA,* 286**,** 2568-77.

HOLL, V., HEMMERTER, S., BURRER, R., SCHMIDT, S., BOHBOT, A., AUBERTIN, A. M. & MOOG, C. (2004) Involvement of Fc gamma RI (CD64) in the mechanism of HIV-1 inhibition by polyclonal IgG purified from infected patients in cultured monocyte-derived macrophages. *J Immunol,* 173**,** 6274-83.

HOLL, V., PERESSIN, M., SCHMIDT, S., DECOVILLE, T., ZOLLA-PAZNER, S., AUBERTIN, A. M. & MOOG, C. (2006) Efficient inhibition of HIV-1 replication in human immature monocyte-derived dendritic cells by purified anti-HIV-1 IgG without induction of maturation. *Blood,* 107**,** 4466-74.

HOLLINGSWORTH, T. D. I., LAEYENDECKER, O., SHIRREFF, G., DONNELLY, C. A., SERWADDA, D., WAWER, M. J., KIWANUKA, N., NALUGODA, F., COLLINSON-STRENG, A., SSEMPIJJA, V., HANAGE, W. P., QUINN, T. C., GRAY, R. H. & FRASER, C. HIV-1 Transmitting Couples Have Similar Viral Load Set-Points in Rakai, Uganda. *PLoS Pathog, 2010,* 6**,** e1000876.

HORWITZ J.P., C. J., NOEL M.J., (1964) The monomesylates of 1-(2'-Deoxy-beta-Dlyxofuranosylthymine. *Journal of Organic Chemistry,* 29**,** 2076-2078.

HUANG, C.-C., VENTURI, M., MAJEED, S., MOORE, M. J., PHOGAT, S., ZHANG, M.-Y., DIMITROV, D. S., HENDRICKSON, W. A., ROBINSON, J., SODROSKI, J., WYATT, R., CHOE, H., FARZAN, M. & KWONG, P. D. (2004) Structural basis of tyrosine sulfation and VH-gene usage in antibodies that recognize the HIV type 1 coreceptor-binding site on gp120. *Proceedings of the National Academy of Sciences of the United States of America,* 101**,** 2706-2711.

HUANG, C. C., TANG, M., ZHANG, M. Y., MAJEED, S., MONTABANA, E., STANFIELD, R. L., DIMITROV, D. S., KORBER, B., SODROSKI, J., WILSON, I. A., WYATT, R. & KWONG, P. D. (2005) Structure of a V3-containing HIV-1 gp120 core. *Science,* 310**,** 1025-8.

HUBER, M., FISCHER, M., MISSELWITZ, B., MANRIQUE, A., KUSTER, H., NIEDEROST, B., WEBER, R., VON WYL, V., GUNTHARD, H. F. & TRKOLA, A. (2006) Complement lysis activity in autologous plasma is associated with lower viral loads during the acute phase of HIV-1 infection. *PLoS Med,* 3**,** e441.

HUBNER, W., MCNERNEY, G. P., CHEN, P., DALE, B. M., GORDON, R. E., CHUANG, F. Y., LI, X. D., ASMUTH, D. M., HUSER, T. & CHEN, B. K. (2009) Quantitative 3D video microscopy of HIV transfer across T cell virological synapses. *Science,* 323**,** 1743-7.

HUTNICK, N. A., CARNATHAN, D. G., DUBEY, S. A., MAKEDONAS, G., COX, K. S., KIERSTEAD, L., RATCLIFFE, S. J., ROBERTSON, M. N., CASIMIRO, D. R., ERTL, H. C. J. & BETTS, M. R. (2009) Baseline Ad5

serostatus does not predict Ad5 HIV vaccine-induced expansion of adenovirus-specific CD4+ T cells. *Nat Med,* 15**,** 876-878.

HUTTO, C., ZHOU, Y., HE, J., GEFFIN, R., HILL, M., SCOTT, W. & WOOD, C. (1996) Longitudinal studies of viral sequence, viral phenotype, and immunologic parameters of human immunodeficiency virus type 1 infection in perinatally infected twins with discordant disease courses. *J Virol,* 70**,** 3589-98.

INOUE, H., NOJIMA, H. & OKAYAMA, H. (1990) High efficiency transformation of Escherichia coli with plasmids. *Gene,* 96**,** 23-8.

JACKSON, J. B., COOMBS, R. W., SANNERUD, K., RHAME, F. S. & BALFOUR, H. H., JR. (1988) Rapid and sensitive viral culture method for human immunodeficiency virus type 1. *J Clin Microbiol,* 26**,** 1416-8.

JAHN, A., FLOYD, S., CRAMPIN, A. C., MWAUNGULU, F., MVULA, H., MUNTHALI, F., MCGRATH, N., MWAFILASO, J., MWINUKA, V., MANGONGO, B., FINE, P. E., ZABA, B. & GLYNN, J. R. (2008) Population-level effect of HIV on adult mortality and early evidence of reversal after introduction of antiretroviral therapy in Malawi. *Lancet,* 371**,** 1603-11.

JETZT, A. E., YU, H., KLARMANN, G. J., RON, Y., PRESTON, B. D. & DOUGHERTY, J. P. (2000) High rate of recombination throughout the human immunodeficiency virus type 1 genome. *J Virol,* 74**,** 1234-40.

JIN, X., BAUER, D. E., TUTTLETON, S. E., LEWIN, S., GETTIE, A., BLANCHARD, J., IRWIN, C. E., SAFRIT, J. T., MITTLER, J., WEINBERGER, L., KOSTRIKIS, L. G., ZHANG, L., PERELSON, A. S. & HO, D. D. (1999) Dramatic Rise in Plasma Viremia after CD8+ T Cell Depletion in Simian Immunodeficiency Virusâ€“infected Macaques. *The Journal of Experimental Medicine,* 189**,** 991-998.

JOHNSON, P. R., SCHNEPP, B. C., ZHANG, J., CONNELL, M. J., GREENE, S. M., YUSTE, E., DESROSIERS, R. C. & REED CLARK, K. (2009) Vector-mediated gene transfer engenders long-lived neutralizing activity and protection against SIV infection in monkeys. *Nat Med,* 15**,** 901-906.

JUKES, T. H. C. C. (1969) Evolution of Protein Molecules. *Mammalian Protein Metabolism pp 21-132*.

KARN, J. (1999) Tackling Tat. *J Mol Biol,* 293**,** 235-54.

KARNASUTA, C., PARIS, R. M., COX, J. H., NITAYAPHAN, S., PITISUTTITHUM, P., THONGCHAROEN, P., BROWN, A. E., GURUNATHAN, S., TARTAGLIA, J., HEYWARD, W. L., MCNEIL, J. G., BIRX, D. L. & DE SOUZA, M. S. (2005) Antibody-dependent cell-mediated cytotoxic responses in participants enrolled in a phase I/II ALVAC-HIV/AIDSVAX B/E prime-boost HIV-1 vaccine trial in Thailand. *Vaccine,* 23**,** 2522-9.

KARPAS, A., HILL, F., YOULE, M., CULLEN, V., GRAY, J., BYRON, N., HAYHOE, F., TENANT-FLOWERS, M., HOWARD, L., GILGEN, D. & ET AL. (1988) Effects of passive immunization in patients with the acquired immunodeficiency syndrome-related complex and acquired immunodeficiency syndrome. *Proc Natl Acad Sci U S A,* 85**,** 9234-7.

KEELE, B. F., GIORGI, E. E., SALAZAR-GONZALEZ, J. F., DECKER, J. M., PHAM, K. T., SALAZAR, M. G., SUN, C., GRAYSON, T., WANG, S., LI, H., WEI, X., JIANG, C., KIRCHHERR, J. L., GAO, F., ANDERSON, J. A., PING, L. H., SWANSTROM, R., TOMARAS, G. D., BLATTNER, W. A., GOEPFERT, P. A., KILBY, J. M., SAAG, M. S., DELWART, E. L., BUSCH, M. P., COHEN, M. S., MONTEFIORI, D. C., HAYNES, B. F., GASCHEN, B., ATHREYA, G. S., LEE, H. Y., WOOD, N., SEOIGHE, C., PERELSON, A. S., BHATTACHARYA, T., KORBER, B. T., HAHN, B. H. & SHAW, G. M. (2008) Identification and characterization of transmitted and early founder virus envelopes in primary HIV-1 infection. *Proc Natl Acad Sci U S A,* 105**,** 7552-7.

KIEPIELA, P., LESLIE, A. J., HONEYBORNE, I., RAMDUTH, D., THOBAKGALE, C., CHETTY, S., RATHNAVALU, P., MOORE, C., PFAFFEROTT, K. J., HILTON, L., ZIMBWA, P., MOORE, S., ALLEN, T., BRANDER, C., ADDO, M. M., ALTFELD, M., JAMES, I., MALLAL, S., BUNCE, M., BARBER, L. D., SZINGER, J., DAY, C., KLENERMAN, P., MULLINS, J., KORBER, B., COOVADIA, H. M., WALKER, B. D. & GOULDER, P. J.

(2004) Dominant influence of HLA-B in mediating the potential co-evolution of HIV and HLA. *Nature,* 432**,** 769-75.

KINTER, A. L., OSTROWSKI, M., GOLETTI, D., OLIVA, A., WEISSMAN, D., GANTT, K., HARDY, E., JACKSON, R., EHLER, L. & FAUCI, A. S. (1996) HIV replication in CD4+ T cells of HIV-infected individuals is regulated by a balance between the viral suppressive effects of endogenous Î²-chemokines and the viral inductive effects of other endogenousâ€‰cytokines. *Proceedings of the National Academy of Sciences of the United States of America,* 93**,** 14076-14081.

KIRCHHERR, J. L., LU, X., KASONGO, W., CHALWE, V., MWANANYANDA, L., MUSONDA, R. M., XIA, S.-M., SCEARCE, R. M., LIAO, H.-X., MONTEFIORI, D. C., HAYNES, B. F. & GAO, F. (2007) High throughput functional analysis of HIV-1 env genes without cloning. *Journal of Virological Methods,* 143**,** 104-111.

KIRSCHNER, M., MONROSE, V., PALUCH, M., TECHODAMRONGSIN, N., RETHWILM, A. & MOORE, J. P. (2006) The production of cleaved, trimeric human immunodeficiency virus type 1 (HIV-1) envelope glycoprotein vaccine antigens and infectious pseudoviruses using linear polyethylenimine as a transfection reagent. *Protein Expression and Purification,* 48**,** 61-68.

KITAHATA, M. M., GANGE, S. J., ABRAHAM, A. G., MERRIMAN, B., SAAG, M. S., JUSTICE, A. C., HOGG, R. S., DEEKS, S. G., ERON, J. J., BROOKS, J. T., ROURKE, S. B., GILL, M. J., BOSCH, R. J., MARTIN, J. N., KLEIN, M. B., JACOBSON, L. P., RODRIGUEZ, B., STERLING, T. R., KIRK, G. D., NAPRAVNIK, S., RACHLIS, A. R., CALZAVARA, L. M., HORBERG, M. A., SILVERBERG, M. J., GEBO, K. A., GOEDERT, J. J., BENSON, C. A., COLLIER, A. C., VAN ROMPAEY, S. E., CRANE, H. M., MCKAIG, R. G., LAU, B., FREEMAN, A. M. & MOORE, R. D. (2009) Effect of early versus deferred antiretroviral therapy for HIV on survival. *N Engl J Med,* 360**,** 1815-26.

KLARMANN, G. J., YU, H., CHEN, X., DOUGHERTY, J. P. & PRESTON, B. D. (1997) Discontinuous plus-strand DNA synthesis in human immunodeficiency virus type 1-infected cells and in a partially reconstituted cell-free system. *J Virol,* 71**,** 9259-69.

KLASSE, P. J. & MOORE, J. P. (2004) Is there enough gp120 in the body fluids of HIV-1-infected individuals to have biologically significant effects? *Virology,* 323**,** 1-8.

KLATT, N. R., SHUDO, E., ORTIZ, A. M., ENGRAM, J. C., PAIARDINI, M., LAWSON, B., MILLER, M. D., ELSE, J., PANDREA, I., ESTES, J. D., APETREI, C., SCHMITZ, J. E., RIBEIRO, R. M., PERELSON, A. S. & SILVESTRI, G. CD8+ lymphocytes control viral replication in SIVmac239-infected rhesus macaques without decreasing the lifespan of productively infected cells. *PLoS Pathog, 2010,* 6**,** e1000747.

KLATZMANN, D., CHAMPAGNE, E., CHAMARET, S., GRUEST, J., GUETARD, D., HERCEND, T., GLUCKMAN, J. C. & MONTAGNIER, L. (1984) T-lymphocyte T4 molecule behaves as the receptor for human retrovirus LAV. *Nature,* 312**,** 767-8.

KOCH, M., PANCERA, M., KWONG, P. D., KOLCHINSKY, P., GRUNDNER, C., WANG, L., HENDRICKSON, W. A., SODROSKI, J. & WYATT, R. (2003) Structure-based, targeted deglycosylation of HIV-1 gp120 and effects on neutralization sensitivity and antibody recognition. *Virology,* 313**,** 387-400.

KWONG, P. D., DOYLE, M. L., CASPER, D. J., CICALA, C., LEAVITT, S. A., MAJEED, S., STEENBEKE, T. D., VENTURI, M., CHAIKEN, I., FUNG, M., KATINGER, H., PARREN, P. W., ROBINSON, J., VAN RYK, D., WANG, L., BURTON, D. R., FREIRE, E., WYATT, R., SODROSKI, J., HENDRICKSON, W. A. & ARTHOS, J. (2002) HIV-1 evades antibody-mediated neutralization through conformational masking of receptor-binding sites. *Nature,* 420**,** 678-82.

KWONG, P. D., WYATT, R., MAJEED, S., ROBINSON, J., SWEET, R. W., SODROSKI, J. & HENDRICKSON, W. A. (2000) Structures of HIV-1 gp120 envelope glycoproteins from laboratory-adapted and primary isolates. *Structure,* 8**,** 1329-39.

KWONG, P. D., WYATT, R., ROBINSON, J., SWEET, R. W., SODROSKI, J. & HENDRICKSON, W. A. (1998) Structure of an HIV gp120 envelope glycoprotein in complex with the CD4 receptor and a neutralizing human antibody. *Nature,* 393**,** 648-59.

LABRIJN, A. F., POIGNARD, P., RAJA, A., ZWICK, M. B., DELGADO, K., FRANTI, M., BINLEY, J., VIVONA, V., GRUNDNER, C., HUANG, C. C., VENTURI, M., PETROPOULOS, C. J., WRIN, T., DIMITROV, D. S., ROBINSON, J., KWONG, P. D., WYATT, R. T., SODROSKI, J. & BURTON, D. R. (2003) Access of antibody molecules to the conserved coreceptor binding site on glycoprotein gp120 is sterically restricted on primary human immunodeficiency virus type 1. *J Virol,* 77**,** 10557-65.

LAMBOTTE, O., BOUFASSA, F., MADEC, Y., NGUYEN, A., GOUJARD, C., MEYER, L., ROUZIOUX, C., VENET, A. & DELFRAISSY, J. F. (2005) HIV controllers: a homogeneous group of HIV-1-infected patients with spontaneous control of viral replication. *Clin Infect Dis,* 41**,** 1053-6.

LAMBOTTE, O., FERRARI, G., MOOG, C., YATES, N. L., LIAO, H.-X., PARKS, R. J., HICKS, C. B., OWZAR, K., TOMARAS, G. D., MONTEFIORI, D. C., HAYNES, B. F. & DELFRAISSY, J.-F. O. (2009) Heterogeneous neutralizing antibody and antibody-dependent cell cytotoxicity responses in HIV-1 elite controllers. *AIDS,* 23**,** 897-906 10.1097/QAD.0b013e328329f97d.

LAPENTA, C., SANTINI, S. M., PROIETTI, E., RIZZA, P., LOGOZZI, M., SPADA, M., PARLATO, S., FAIS, S., PITHA, P. M. & BELARDELLI, F. (1999) Type I Interferon Is a Powerful Inhibitor of in Vivo HIV-1 Infection and Preserves Human CD4+ T Cells from Virus-Induced Depletion in SCID Mice Transplanted with Human Cells. *Virology,* 263**,** 78-88.

LAWRENCE, M. C. & COLMAN, P. M. (1993) Shape Complementarity at Protein/Protein Interfaces. *Journal of Molecular Biology,* 234**,** 946-950.

LEHMANN-CHE, J. & SAIB, A. (2004) Early stages of HIV replication: how to hijack cellular functions for a successful infection. *AIDS Rev,* 6**,** 199-207.

LEMEY, P., PYBUS, O. G., WANG, B., SAKSENA, N. K., SALEMI, M. & VANDAMME, A. M. (2003) Tracing the origin and history of the HIV-2 epidemic. *Proc Natl Acad Sci U S A,* 100**,** 6588-92.

LEVESQUE, M. C., MOODY, M. A., HWANG, K. K., MARSHALL, D. J., WHITESIDES, J. F., AMOS, J. D., GURLEY, T. C., ALLGOOD, S., HAYNES, B. B., VANDERGRIFT, N. A., PLONK, S., PARKER, D. C., COHEN, M. S., TOMARAS, G. D., GOEPFERT, P. A., SHAW, G. M., SCHMITZ, J. E., ERON, J. J., SHAHEEN, N. J., HICKS, C. B., LIAO, H. X., MARKOWITZ, M., KELSOE, G., MARGOLIS, D. M. & HAYNES, B. F. (2009) Polyclonal B cell differentiation and loss of gastrointestinal tract germinal centers in the earliest stages of HIV-1 infection. *PLoS Med,* 6**,** e1000107.

LEWIN, A., MAYER, M., CHUSAINOW, J., JACOB, D. & APPEL, B. (2005) Viral promoters can initiate expression of toxin genes introduced into Escherichia coli. *BMC Biotechnol,* 5**,** 19.

LI, B., DECKER, J. M., JOHNSON, R. W., BIBOLLET-RUCHE, F., WEI, X., MULENGA, J., ALLEN, S., HUNTER, E., HAHN, B. H., SHAW, G. M., BLACKWELL, J. L. & DERDEYN, C. A. (2006a) Evidence for Potent Autologous Neutralizing Antibody Titers and Compact Envelopes in Early Infection with Subtype C Human Immunodeficiency Virus Type 1. *Journal of Virology,* 80**,** 5211-5218.

LI, M., GAO, F., MASCOLA, J. R., STAMATATOS, L., POLONIS, V. R., KOUTSOUKOS, M., VOSS, G., GOEPFERT, P., GILBERT, P., GREENE, K. M., BILSKA, M., KOTHE, D. L., SALAZAR-GONZALEZ, J. F., WEI, X., DECKER, J. M., HAHN, B. H. & MONTEFIORI, D. C. (2005) Human immunodeficiency virus type 1 env clones from acute and early subtype B infections for standardized assessments of vaccine-elicited neutralizing antibodies. *J Virol,* 79**,** 10108-25.

LI, Q., ESTES, J. D., SCHLIEVERT, P. M., DUAN, L., BROSNAHAN, A. J., SOUTHERN, P. J., REILLY, C. S., PETERSON, M. L., SCHULTZ-DARKEN, N., BRUNNER, K. G., NEPHEW, K. R., PAMBUCCIAN, S., LIFSON, J. D., CARLIS, J. V. & HAASE, A. T. (2009a) Glycerol monolaurate prevents mucosal SIV transmission. *Nature,* 458**,** 1034-8.

LI, Y., CLEVELAND, B., KLOTS, I., TRAVIS, B., RICHARDSON, B. A., ANDERSON, D., MONTEFIORI, D., POLACINO, P. & HU, S.-L. (2008) Removal of a Single N-Linked Glycan in Human

Immunodeficiency Virus Type 1 gp120 Results in an Enhanced Ability To Induce Neutralizing Antibody Responses. *J. Virol.,* 82**,** 638-651.

LI, Y., MIGUELES, S. A., WELCHER, B., SVEHLA, K., PHOGAT, A., LOUDER, M. K., WU, X., SHAW, G. M., CONNORS, M., WYATT, R. T. & MASCOLA, J. R. (2007) Broad HIV-1 neutralization mediated by CD4-binding site antibodies. *Nat Med,* 13**,** 1032-1034.

LI, Y., SVEHLA, K., LOUDER, M. K., WYCUFF, D., PHOGAT, S., TANG, M., MIGUELES, S. A., WU, X., PHOGAT, A., SHAW, G. M., CONNORS, M., HOXIE, J., MASCOLA, J. R. & WYATT, R. (2009b) Analysis of neutralization specificities in polyclonal sera derived from human immunodeficiency virus type 1-infected individuals. *J Virol,* 83**,** 1045-59.

LI, Y., SVEHLA, K., MATHY, N. L., VOSS, G., MASCOLA, J. R. & WYATT, R. (2006b) Characterization of antibody responses elicited by human immunodeficiency virus type 1 primary isolate trimeric and monomeric envelope glycoproteins in selected adjuvants. *J Virol,* 80**,** 1414-26.

LIAO, Z., CIMAKASKY, L. M., HAMPTON, R., NGUYEN, D. H. & HILDRETH, J. E. (2001) Lipid rafts and HIV pathogenesis: host membrane cholesterol is required for infection by HIV type 1. *AIDS Res Hum Retroviruses,* 17**,** 1009-19.

LIFSON, J. D., ROSSIO, J. L., PIATAK, M., JR., PARKS, T., LI, L., KISER, R., COALTER, V., FISHER, B., FLYNN, B. M., CZAJAK, S., HIRSCH, V. M., REIMANN, K. A., SCHMITZ, J. E., GHRAYEB, J., BISCHOFBERGER, N., NOWAK, M. A., DESROSIERS, R. C. & WODARZ, D. (2001) Role of CD8+ Lymphocytes in Control of Simian Immunodeficiency Virus Infection and Resistance to Rechallenge after Transient Early Antiretroviral Treatment. *J. Virol.,* 75**,** 10187-10199.

LITTLE, S. J., MCLEAN, A. R., SPINA, C. A., RICHMAN, D. D. & HAVLIR, D. V. (1999) Viral dynamics of acute HIV-1 infection. *J Exp Med,* 190**,** 841-50.

LITTMAN, D. R., MADDON, P. J. & AXEL, R. (1988) Corrected CD4 sequence. *Cell,* 55**,** 541.

LIU, J., BARTESAGHI, A., BORGNIA, M. J., SAPIRO, G. & SUBRAMANIAM, S. (2008) Molecular architecture of native HIV-1 gp120 trimers. *Nature,* 455**,** 109-13.

LOOMIS-PRICE, L. D., COX, J. H., MASCOLA, J. R., VANCOTT, T. C., MICHAEL, N. L., FOUTS, T. R., REDFIELD, R. R., ROBB, M. L., WAHREN, B., SHEPPARD, H. W. & BIRX, D. L. (1998) Correlation between humoral responses to human immunodeficiency virus type 1 envelope and disease progression in early-stage infection. *J Infect Dis,* 178**,** 1306-16.

LOPEZ-VERGES, S., CAMUS, G., BLOT, G., BEAUVOIR, R., BENAROUS, R. & BERLIOZ-TORRENT, C. (2006) Tail-interacting protein TIP47 is a connector between Gag and Env and is required for Env incorporation into HIV-1 virions. *Proc Natl Acad Sci U S A,* 103**,** 14947-52.

LOSIER, M., FORTIN, J. F., CANTIN, R., BERGERON, M. G. & TREMBLAY, M. J. (2003) Virion-bound ICAM-1 and activated LFA-1: a combination of factors conferring resistance to neutralization by sera from human immunodeficiency virus type 1-infected individuals independently of the disease status and phase. *Clin Immunol,* 108**,** 111-8.

LOUDER, M. K., SAMBOR, A., CHERTOVA, E., HUNTE, T., BARRETT, S., OJONG, F., SANDERS-BUELL, E., ZOLLA-PAZNER, S., MCCUTCHAN, F. E., ROSER, J. D., GABUZDA, D., LIFSON, J. D. & MASCOLA, J. R. (2005) HIV-1 envelope pseudotyped viral vectors and infectious molecular clones expressing the same envelope glycoprotein have a similar neutralization phenotype, but culture in peripheral blood mononuclear cells is associated with decreased neutralization sensitivity. *Virology,* 339**,** 226-38.

LU, M., BLACKLOW, S. C. & KIM, P. S. (1995) A trimeric structural domain of the HIV-1 transmembrane glycoprotein. *Nat Struct Biol,* 2**,** 1075-82.

LUND, F. E. & RANDALL, T. D. Effector and regulatory B cells: modulators of CD4(+) T cell immunity. *Nat Rev Immunol,* 10**,** 236-47.

MADDON, P. J., LITTMAN, D. R., GODFREY, M., MADDON, D. E., CHESS, L. & AXEL, R. (1985) The isolation and nucleotide sequence of a cDNA encoding the T cell surface protein T4: a new member of the immunoglobulin gene family. *Cell,* 42**,** 93-104.

MADEC, Y., BOUFASSA, F., PORTER, K. & MEYER, L. (2005a) Spontaneous control of viral load and CD4 cell count progression among HIV-1 seroconverters. *AIDS,* 19**,** 2001-7.

MAERTENS, G., CHEREPANOV, P., PLUYMERS, W., BUSSCHOTS, K., DE CLERCQ, E., DEBYSER, Z. & ENGELBORGHS, Y. (2003) LEDGF/p75 Is Essential for Nuclear and Chromosomal Targeting of HIV-1 Integrase in Human Cells. *Journal of Biological Chemistry,* 278**,** 33528-33539.

MAHALANABIS, M., JAYARAMAN, P., MIURA, T., PEREYRA, F., CHESTER, E. M., RICHARDSON, B., WALKER, B. & HAIGWOOD, N. L. (2009a) Continuous viral escape and selection by autologous neutralizing antibodies in drug-naive human immunodeficiency virus controllers. *J Virol,* 83**,** 662-72.

MAK, J., JIANG, M., WAINBERG, M. A., HAMMARSKJOLD, M. L., REKOSH, D. & KLEIMAN, L. (1994) Role of Pr160gag-pol in mediating the selective incorporation of tRNA(Lys) into human immunodeficiency virus type 1 particles. *J Virol,* 68**,** 2065-72.

MALENBAUM, S. E., YANG, D., CAVACINI, L., POSNER, M., ROBINSON, J. & CHENG-MAYER, C. (2000) The N-terminal V3 loop glycan modulates the interaction of clade A and B human immunodeficiency virus type 1 envelopes with CD4 and chemokine receptors. *J Virol,* 74**,** 11008-16.

MALHOTRA, U., BERREY, M. M., HUANG, Y., MARKEE, J., BROWN, D. J., AP, S., MUSEY, L., SCHACKER, T., COREY, L. & MCELRATH, M. J. (2000) Effect of combination antiretroviral therapy on T-cell immunity in acute human immunodeficiency virus type 1 infection. *J Infect Dis,* 181**,** 121-31.

MALIM, M. H., TILEY, L. S., MCCARN, D. F., RUSCHE, J. R., HAUBER, J. & CULLEN, B. R. (1990) HIV-1 structural gene expression requires binding of the Rev trans-activator to its RNA target sequence. *Cell,* 60**,** 675-83.

MARKOSYAN, R. M., COHEN, F. S. & MELIKYAN, G. B. (2003) HIV-1 envelope proteins complete their folding into six-helix bundles immediately after fusion pore formation. *Mol Biol Cell,* 14**,** 926-38.

MARKOWITZ, M., LOUIE, M., HURLEY, A., SUN, E., DI MASCIO, M., PERELSON, A. S. & HO, D. D. (2003) A novel antiviral intervention results in more accurate assessment of human immunodeficiency virus type 1 replication dynamics and T-cell decay in vivo. *J Virol,* 77**,** 5037-8.

MARSCHANG, P., SODROSKI, J., WURZNER, R. & DIERICH, M. P. (1995) Decay-accelerating factor (CD55) protects human immunodeficiency virus type 1 from inactivation by human complement. *Eur J Immunol,* 25**,** 285-90.

MARTIN, L., STRICHER, F., MISSE, D., SIRONI, F., PUGNIERE, M., BARTHE, P., PRADO-GOTOR, R., FREULON, I., MAGNE, X., ROUMESTAND, C., MENEZ, A., LUSSO, P., VEAS, F. & VITA, C. (2003) Rational design of a CD4 mimic that inhibits HIV-1 entry and exposes cryptic neutralization epitopes. *Nat Biotechnol,* 21**,** 71-6.

MARTIN, N., WELSCH, S., JOLLY, C., BRIGGS, J. A. G., VAUX, D. & SATTENTAU, Q. J. Virological Synapse-Mediated Spread of Human Immunodeficiency Virus Type 1 between T Cells Is Sensitive to Entry Inhibition. *J. Virol, 2010,* 84**,** 3516-3527.

MASCOLA, J. R. (1999) Neutralization of HIV-1 infection of human peripheral blood mononuclear cells (PBMC). *In HIV Protocols (M. Nelson and J.H. Kim, eds.)***,** 309-315.

MASCOLA, J. R. & BURKE, D. S. (1993) Antigen detection in neutralization assays: high levels of interfering anti-p24 antibodies in some plasma. *AIDS Res Hum Retroviruses,* 9**,** 1173-4.

MASCOLA, J. R., D'SOUZA, P., GILBERT, P., HAHN, B. H., HAIGWOOD, N. L., MORRIS, L., PETROPOULOS, C. J., POLONIS, V. R., SARZOTTI, M. & MONTEFIORI, D. C. (2005) Recommendations for the Design and Use of Standard Virus Panels To Assess Neutralizing Antibody Responses Elicited by Candidate Human Immunodeficiency Virus Type 1 Vaccines. *Journal of Virology,* 79**,** 10103-10107.

MASCOLA, J. R., LEWIS, M. G., STIEGLER, G., HARRIS, D., VANCOTT, T. C., HAYES, D., LOUDER, M. K., BROWN, C. R., SAPAN, C. V., FRANKEL, S. S., LU, Y., ROBB, M. L., KATINGER, H. & BIRX, D. L. (1999) Protection of Macaques against pathogenic simian/human immunodeficiency virus 89.6PD by passive transfer of neutralizing antibodies. *J Virol,* 73**,** 4009-18.

MASCOLA, J. R., LEWIS, M. G., VANCOTT, T. C., STIEGLER, G., KATINGER, H., SEAMAN, M., BEAUDRY, K., BAROUCH, D. H., KORIOTH-SCHMITZ, B., KRIVULKA, G., SAMBOR, A., WELCHER, B., DOUEK, D. C., MONTEFIORI, D. C., SHIVER, J. W., POIGNARD, P., BURTON, D. R. & LETVIN, N. L. (2003) Cellular immunity elicited by human immunodeficiency virus type 1/ simian immunodeficiency virus DNA vaccination does not augment the sterile protection afforded by passive infusion of neutralizing antibodies. *J Virol,* 77**,** 10348-56.

MASCOLA, J. R., STIEGLER, G., VANCOTT, T. C., KATINGER, H., CARPENTER, C. B., HANSON, C. E., BEARY, H., HAYES, D., FRANKEL, S. S., BIRX, D. L. & LEWIS, M. G. (2000) Protection of macaques against vaginal transmission of a pathogenic HIV-1/SIV chimeric virus by passive infusion of neutralizing antibodies. *Nat Med,* 6**,** 207-10.

MATTAPALLIL, J. J., DOUEK, D. C., HILL, B., NISHIMURA, Y., MARTIN, M. & ROEDERER, M. (2005) Massive infection and loss of memory CD4+ T cells in multiple tissues during acute SIV infection. *Nature,* 434**,** 1093-7.

MAUDRU, T. & PEDEN, K. (1997) Elimination of background signals in a modified polymerase chain reaction-based reverse transcriptase assay. *J Virol Methods,* 66**,** 247-61.

MCCLURE, M. O., MARSH, M. & WEISS, R. A. (1988) Human immunodeficiency virus infection of CD4-bearing cells occurs by a pH-independent mechanism. *EMBO J,* 7**,** 513-8.

MCCOY, A. J., CHANDANA EPA, V. & COLMAN, P. M. (1997) Electrostatic complementarity at protein/protein interfaces. *J Mol Biol,* 268**,** 570-84.

MCDONALD, R. & BURNETT, V. (2005) Novel single-round PCR and cloning of full-length envelope genes of HIV-1 may yield new insight into biomolecular antibacterial drug development. *Journal of Virological Methods,* 126**,** 111-118.

MCDOUGAL, J. S., KENNEDY, M. S., SLIGH, J. M., CORT, S. P., MAWLE, A. & NICHOLSON, J. K. (1986) Binding of HTLV-III/LAV to T4+ T cells by a complex of the 110K viral protein and the T4 molecule. *Science,* 231**,** 382-5.

MELIKYAN, G. B., MARKOSYAN, R. M., HEMMATI, H., DELMEDICO, M. K., LAMBERT, D. M. & COHEN, F. S. (2000) Evidence that the transition of HIV-1 gp41 into a six-helix bundle, not the bundle configuration, induces membrane fusion. *J Cell Biol,* 151**,** 413-23.

MELLORS, J. W., KINGSLEY, L. A., RINALDO, C. R., JR., TODD, J. A., HOO, B. S., KOKKA, R. P. & GUPTA, P. (1995) Quantitation of HIV-1 RNA in plasma predicts outcome after seroconversion. *Ann Intern Med,* 122**,** 573-9.

MERVIS, R. J., AHMAD, N., LILLEHOJ, E. P., RAUM, M. G., SALAZAR, F. H., CHAN, H. W. & VENKATESAN, S. (1988) The gag gene products of human immunodeficiency virus type 1: alignment within the gag open reading frame, identification of posttranslational modifications, and evidence for alternative gag precursors. *J Virol,* 62**,** 3993-4002.

METZNER, K. J., JIN, X., LEE, F. V., GETTIE, A., BAUER, D. E., DI MASCIO, M., PERELSON, A. S., MARX, P. A., HO, D. D., KOSTRIKIS, L. G. & CONNOR, R. I. (2000) Effects of in Vivo Cd8+ T Cell Depletion on Virus Replication in Rhesus Macaques Immunized with a Live, Attenuated Simian Immunodeficiency Virus Vaccine. *The Journal of Experimental Medicine,* 191**,** 1921-1932.

MIGUELES, S. A., LABORICO, A. C., SHUPERT, W. L., SABBAGHIAN, M. S., RABIN, R., HALLAHAN, C. W., BAARLE, D. V., KOSTENSE, S., MIEDEMA, F., MCLAUGHLIN, M., EHLER, L., METCALF, J., LIU, S. & CONNORS, M. (2002) HIV-specific CD8+ T cell proliferation is coupled to perforin expression and is maintained in nonprogressors. *Nat Immunol,* 3**,** 1061-1068.

MILLER, C. J., GENESCA, M., ABEL, K., MONTEFIORI, D., FORTHAL, D., BOST, K., LI, J., FAVRE, D. & MCCUNE, J. M. (2007) Antiviral antibodies are necessary for control of simian immunodeficiency virus replication. *J Virol,* 81**,** 5024-35.

MILLER, C. J., LI, Q., ABEL, K., KIM, E. Y., MA, Z. M., WIETGREFE, S., LA FRANCO-SCHEUCH, L., COMPTON, L., DUAN, L., SHORE, M. D., ZUPANCIC, M., BUSCH, M., CARLIS, J., WOLINSKY, S. & HAASE, A. T. (2005) Propagation and dissemination of infection after vaginal transmission of simian immunodeficiency virus. *J Virol,* 79**,** 9217-27.

MILLER, M. A., CLOYD, M. W., LIEBMANN, J., RINALDO, C. R., ISLAM, K. R., WANG, S. Z. S., MIETZNER, T. A. & MONTELARO, R. C. (1993) Alterations in Cell Membrane Permeability by the Lentivirus Lytic Peptide (LLP-1) of HIV-1 Transmembrane Protein. *Virology,* 196**,** 89-100.

MILLER, M. D., FARNET, C. M. & BUSHMAN, F. D. (1997) Human immunodeficiency virus type 1 preintegration complexes: studies of organization and composition. *J Virol,* 71**,** 5382-90.

MIYAUCHI, K., KIM, Y., LATINOVIC, O., MOROZOV, V., MELIKYAN, G.B. (2009) HIV enters cells via endocytosis and dynamin-dependent fusion with endosomes. *Cell*, 137, 433-44

MOIR, S. & FAUCI, A. S. (2009a) B cells in HIV infection and disease. *Nat Rev Immunol,* 9**,** 235-45.

MOIR, S., HO, J., MALASPINA, A., WANG, W., DIPOTO, A. C., O'SHEA, M. A., ROBY, G., KOTTILIL, S., ARTHOS, J., PROSCHAN, M. A., CHUN, T. W. & FAUCI, A. S. (2008a) Evidence for HIV-associated B cell exhaustion in a dysfunctional memory B cell compartment in HIV-infected viremic individuals. *J Exp Med,* 205**,** 1797-805.

MOIR, S., MALASPINA, A., HO, J., WANG, W., DIPOTO, A. C., O'SHEA, M. A., ROBY, G., MICAN, J. M., KOTTILIL, S., CHUN, T. W., PROSCHAN, M. A. & FAUCI, A. S. (2008b) Normalization of B cell counts and subpopulations after antiretroviral therapy in chronic HIV disease. *J Infect Dis,* 197**,** 572-9.

MOIR, S., MALASPINA, A., PICKERAL, O. K., DONOGHUE, E. T., VASQUEZ, J., MILLER, N. J., KRISHNAN, S. R., PLANTA, M. A., TURNEY, J. F., JUSTEMENT, J. S., KOTTILIL, S., DYBUL, M., MICAN, J. M., KOVACS, C., CHUN, T. W., BIRSE, C. E. & FAUCI, A. S. (2004) Decreased survival of B cells of HIV-viremic patients mediated by altered expression of receptors of the TNF superfamily. *J Exp Med,* 200**,** 587-99.

MONDOR, I., UGOLINI, S. & SATTENTAU, Q. J. (1998) Human immunodeficiency virus type 1 attachment to HeLa CD4 cells is CD4 independent and gp120 dependent and requires cell surface heparans. *J Virol,* 72**,** 3623-34.

MONTEFIORI, D. C. (2005) Evaluating neutralizing antibodies against HIV, SIV, and SHIV in luciferase reporter gene assays. *Curr Protoc Immunol,* Chapter 12**,** Unit 12 11.

MONTEFIORI, D. C. (2009) Measuring HIV neutralization in a luciferase reporter gene assay. *Methods Mol Biol,* 485**,** 395-405.

MONTEFIORI, D. C., ALTFELD, M., LEE, P. K., BILSKA, M., ZHOU, J., JOHNSTON, M. N., GAO, F., WALKER, B. D. & ROSENBERG, E. S. (2003) Viremia control despite escape from a rapid and potent autologous neutralizing antibody response after therapy cessation in an HIV-1-infected individual. *J Immunol,* 170**,** 3906-14.

MONTEFIORI, D. C., HILL, T. S., VO, H. T., WALKER, B. D. & ROSENBERG, E. S. (2001) Neutralizing antibodies associated with viremia control in a subset of individuals after treatment of acute human immunodeficiency virus type 1 infection. *J Virol,* 75**,** 10200-7.

MOORE, J. P., CAO, Y., HO, D. D. & KOUP, R. A. (1994) Development of the anti-gp120 antibody response during seroconversion to human immunodeficiency virus type 1. *J. Virol.,* 68**,** 5142-5155.

MOORE, J. P., CAO, Y., QING, L., SATTENTAU, Q. J., PYATI, J., KODURI, R., ROBINSON, J., BARBAS, C. F., 3RD, BURTON, D. R. & HO, D. D. (1995) Primary isolates of human immunodeficiency virus type 1 are relatively resistant to neutralization by monoclonal antibodies to gp120, and their neutralization is not predicted by studies with monomeric gp120. *J Virol,* 69**,** 101-9.

MOORE, P. L., CROOKS, E. T., PORTER, L., ZHU, P., CAYANAN, C. S., GRISE, H., CORCORAN, P., ZWICK, M. B., FRANTI, M., MORRIS, L., ROUX, K. H., BURTON, D. R. & BINLEY, J. M. (2006) Nature of Nonfunctional Envelope Proteins on the Surface of Human Immunodeficiency Virus Type 1. *J. Virol.,* 80**,** 2515-2528.

MORCOCK, D. R., THOMAS, J. A., SOWDER, R. C., 2ND, HENDERSON, L. E., CRISE, B. J. & GORELICK, R. J. (2008) HIV-1 inactivation by 4-vinylpyridine is enhanced by dissociating Zn(2+) from nucleocapsid protein. *Virology,* 375**,** 148-58.

MORELL, A., TERRY, W. D. & WALDMANN, T. A. (1970) Metabolic properties of IgG subclasses in man. *The Journal of Clinical Investigation,* 49**,** 673-680.

MORRIS, L., BINLEY, J. M., CLAS, B. A., BONHOEFFER, S., ASTILL, T. P., KOST, R., HURLEY, A., CAO, Y., MARKOWITZ, M., HO, D. D. & MOORE, J. P. (1998) HIV-1 antigen-specific and -nonspecific B cell responses are sensitive to combination antiretroviral therapy. *J Exp Med,* 188**,** 233-45.

MOULARD, M., LORTAT-JACOB, H., MONDOR, I., ROCA, G., WYATT, R., SODROSKI, J., ZHAO, L., OLSON, W., KWONG, P. D. & SATTENTAU, Q. J. (2000) Selective interactions of polyanions with basic surfaces on human immunodeficiency virus type 1 gp120. *J Virol,* 74**,** 1948-60.

MOULARD, M., PHOGAT, S. K., SHU, Y., LABRIJN, A. F., XIAO, X., BINLEY, J. M., ZHANG, M. Y., SIDOROV, I. A., BRODER, C. C., ROBINSON, J., PARREN, P. W., BURTON, D. R. & DIMITROV, D. S. (2002) Broadly cross-reactive HIV-1-neutralizing human monoclonal Fab selected for binding to gp120-CD4-CCR5 complexes. *Proc Natl Acad Sci U S A,* 99**,** 6913-8.

MULLER, H.J. (1964). The relation of recombination to mutational advance. *Mutat Res,* 106, 2–9

MURIAUX, D., MIRRO, J., HARVIN, D. & REIN, A. (2001) RNA is a structural element in retrovirus particles. *Proc Natl Acad Sci U S A,* 98**,** 5246-51.

NALDINI, L., BLOMER, U., GALLAY, P., ORY, D., MULLIGAN, R., GAGE, F. H., VERMA, I. M. & TRONO, D. (1996) In vivo gene delivery and stable transduction of nondividing cells by a lentiviral vector. *Science,* 272**,** 263-7.

NAVIS, M., EDO MATAS, D., RACHINGER, A., KONING, F. A., VAN SWIETEN, P., KOOTSTRA, N. A. & SCHUITEMAKER, H. (2008) Molecular Evolution of Human Immunodeficiency Virus Type 1 upon Transmission between Human Leukocyte Antigen Disparate Donor-Recipient Pairs. *PLoS ONE,* 3**,** e2422.

NICKLE, D. C., JENSEN, M. A., SHRINER, D., BRODIE, S. J., FRENKEL, L. M., MITTLER, J. E. & MULLINS, J. I. (2003) Evolutionary indicators of human immunodeficiency virus type 1 reservoirs and compartments. *J Virol,* 77**,** 5540-6.

NORA, T., BOUCHONNET, F., LABROSSE, B., CHARPENTIER, C., MAMMANO, F., CLAVEL, F. & HANCE, A. (2008) Functional diversity of HIV-1 envelope proteins expressed by contemporaneous plasma viruses. *Retrovirology,* 5**,** 23.

OELRICHS, R. B., LAWSON, V. A., COATES, K. M., CHATFIELD, C., DEACON, N. J. & MCPHEE, D. A. (2000) Rapid full-length genomic sequencing of two cytopathically heterogeneous Australian primary HIV-1 isolates. *J Biomed Sci,* 7**,** 128-35.

OGERT, R. A., BA, L., HOU, Y., BUONTEMPO, C., QIU, P., DUCA, J., MURGOLO, N., BUONTEMPO, P., RALSTON, R. & HOWE, J. A. (2009) Structure-Function Analysis of Human Immunodeficiency Virus Type 1 gp120 Amino Acid Mutations Associated with Resistance to the CCR5 Coreceptor Antagonist Vicriviroc. *J. Virol.,* 83**,** 12151-12163.

OSMANOV, S., PATTOU, C., WALKER, N., SCHWARDLANDER, B., ESPARZA, J., ISOLATION, W.-U. N. F. H. & CHARACTERIZATION (2002) Estimated global distribution and regional spread of HIV-1 genetic subtypes in the year 2000. *J Acquir Immune Defic Syndr,* 29**,** 184-90.

PANCERA, M., MCLELLAN, J. S., WU, X., ZHU, J., CHANGELA, A., SCHMIDT, S. D., YANG, Y., ZHOU, T., PHOGAT, S., MASCOLA, J. R. & KWONG, P. D. Crystal structure of PG16 and chimeric dissection

with somatically related PG9: Structure-function analysis of two quaternary-specific antibodies that effectively neutralize HIV-1. *J Virol, 2010*.

PARKER, D. C. (1993) T cell-dependent B cell activation. *Annu Rev Immunol,* 11**,** 331-60.

PARREN, P. W., MONDOR, I., NANICHE, D., DITZEL, H. J., KLASSE, P. J., BURTON, D. R. & SATTENTAU, Q. J. (1998) Neutralization of human immunodeficiency virus type 1 by antibody to gp120 is determined primarily by occupancy of sites on the virion irrespective of epitope specificity. *J Virol,* 72**,** 3512-9.

PARREN, P. W., MOORE, J. P., BURTON, D. R. & SATTENTAU, Q. J. (1999) The neutralizing antibody response to HIV-1: viral evasion and escape from humoral immunity. *AIDS,* 13 Suppl A**,** S137-62.

PASTORE, C., NEDELLEC, R., RAMOS, A., PONTOW, S., RATNER, L. & MOSIER, D. E. (2006) Human Immunodeficiency Virus Type 1 Coreceptor Switching: V1/V2 Gain-of-Fitness Mutations Compensate for V3 Loss-of-Fitness Mutations. *J. Virol.,* 80**,** 750-758.

PASTORE, C., RAMOS, A. & MOSIER, D. E. (2004) Intrinsic Obstacles to Human Immunodeficiency Virus Type 1 Coreceptor Switching. *J. Virol.,* 78**,** 7565-7574.

PATIRIS, P. & HANSON, C. (2005) Single-round HIV type 1 neutralization measured by ELISPOT technique in primary human cells. *AIDS Res Hum Retroviruses,* 21**,** 784-90.

PENSIEROSO, S., CAGIGI, A., PALMA, P., NILSSON, A., CAPPONI, C., FREDA, E., BERNARDI, S., THORSTENSSON, R., CHIODI, F. & ROSSI, P. (2009) Timing of HAART defines the integrity of memory B cells and the longevity of humoral responses in HIV-1 vertically-infected children. *Proceedings of the National Academy of Sciences,* 106**,** 7939-7944.

PEPIN, J., MORGAN, G., DUNN, D., GEVAO, S., MENDY, M., GAYE, I., SCOLLEN, N., TEDDER, R. & WHITTLE, H. (1991) HIV-2-induced immunosuppression among asymptomatic West African prostitutes: evidence that HIV-2 is pathogenic, but less so than HIV-1. *AIDS,* 5**,** 1165-72.

PERELSON, A. S., NEUMANN, A. U., MARKOWITZ, M., LEONARD, J. M. & HO, D. D. (1996) HIV-1 Dynamics in Vivo: Virion Clearance Rate, Infected Cell Life-Span, and Viral Generation Time. *Science,* 271**,** 1582-1586.

PEREYRA, F., ADDO, M. M., KAUFMANN, D. E., LIU, Y., MIURA, T., RATHOD, A., BAKER, B., TROCHA, A., ROSENBERG, R., MACKEY, E., UEDA, P., LU, Z., COHEN, D., WRIN, T., PETROPOULOS, C. J., ROSENBERG, E. S. & WALKER, B. D. (2008a) Genetic and immunologic heterogeneity among persons who control HIV infection in the absence of therapy. *J Infect Dis,* 197**,** 563-71.

PEREYRA, F., PALMER, S., MIURA, T., BLOCK, B. L., WIEGAND, A., ROTHCHILD, A. C., BAKER, B., ROSENBERG, R., CUTRELL, E., SEAMAN, M. S., COFFIN, J. M. & WALKER, B. D. (2009) Persistent low-level viremia in HIV-1 elite controllers and relationship to immunologic parameters. *J Infect Dis,* 200**,** 984-90.

PETERSEN-MAHRT, S. K., HARRIS, R. S. & NEUBERGER, M. S. (2002) AID mutates E. coli suggesting a DNA deamination mechanism for antibody diversification. *Nature,* 418**,** 99-103.

PETROPOULOS, C. J., PARKIN, N. T., LIMOLI, K. L., LIE, Y. S., WRIN, T., HUANG, W., TIAN, H., SMITH, D., WINSLOW, G. A., CAPON, D. J. & WHITCOMB, J. M. (2000) A novel phenotypic drug susceptibility assay for human immunodeficiency virus type 1. *Antimicrob Agents Chemother,* 44**,** 920-8.

PHILLIPS, A. N., GAZZARD, B., GILSON, R., EASTERBROOK, P., JOHNSON, M., WALSH, J., LEEN, C., FISHER, M., ORKIN, C., ANDERSON, J., PILLAY, D., DELPECH, V., SABIN, C., SCHWENK, A., DUNN, D., GOMPELS, M., HILL, T., PORTER, K. & BABIKER, A. (2007) Rate of AIDS diseases or death in HIV-infected antiretroviral therapy-naive individuals with high CD4 cell count. *AIDS,* 21**,** 1717-21.

PIANTADOSI, A., PANTELEEFF, D., BLISH, C. A., BAETEN, J. M., JAOKO, W., MCCLELLAND, R. S. & OVERBAUGH, J. (2009) Breadth of Neutralizing Antibody Response to Human Immunodeficiency Virus Type 1 Is Affected by Factors Early in Infection but Does Not Influence Disease Progression. *Journal of Virology,* 83**,** 10269-10274.

PILGRIM, A. K., PANTALEO, G., COHEN, O. J., FINK, L. M., ZHOU, J. Y., ZHOU, J. T., BOLOGNESI, D. P., FAUCI, A. S. & MONTEFIORI, D. C. (1997) Neutralizing antibody responses to human immunodeficiency virus type 1 in primary infection and long-term-nonprogressive infection. *J Infect Dis,* 176**,** 924-32.

PIZZATO, M., ERLWEIN, O., BONSALL, D., KAYE, S., MUIR, D. & MCCLURE, M. O. (2009) A one-step SYBR Green I-based product-enhanced reverse transcriptase assay for the quantitation of retroviruses in cell culture supernatants. *J Virol Methods,* 156**,** 1-7.

PLANTIER, J.-C., LEOZ, M., DICKERSON, J. E., DE OLIVEIRA, F., CORDONNIER, F., LEMEE, V., DAMOND, F., ROBERTSON, D. L. & SIMON, F. (2009) A new human immunodeficiency virus derived from gorillas. *Nat Med,* 15**,** 871-872.

PLATT, E. J., WEHRLY, K., KUHMANN, S. E., CHESEBRO, B. & KABAT, D. (1998a) Effects of CCR5 and CD4 Cell Surface Concentrations on Infections by Macrophagetropic Isolates of Human Immunodeficiency Virus Type 1. *J. Virol.,* 72**,** 2855-2864.

POIGNARD, P., FOUTS, T., NANICHE, D., MOORE, J. P. & SATTENTAU, Q. J. (1996) Neutralizing antibodies to human immunodeficiency virus type-1 gp120 induce envelope glycoprotein subunit dissociation. *J Exp Med,* 183**,** 473-84.

POIGNARD, P., SABBE, R., PICCHIO, G. R., WANG, M., GULIZIA, R. J., KATINGER, H., PARREN, P. W., MOSIER, D. E. & BURTON, D. R. (1999) Neutralizing antibodies have limited effects on the control of established HIV-1 infection in vivo. *Immunity,* 10**,** 431-8.

POLONIS, V. R., BROWN, B. K., ROSA BORGES, A., ZOLLA-PAZNER, S., DIMITROV, D. S., ZHANG, M. Y., BARNETT, S. W., RUPRECHT, R. M., SCARLATTI, G., FENYO, E. M., MONTEFIORI, D. C., MCCUTCHAN, F. E. & MICHAEL, N. L. (2008) Recent advances in the characterization of HIV-1 neutralization assays for standardized evaluation of the antibody response to infection and vaccination. *Virology,* 375**,** 315-20.

POLONIS, V. R. A., SCHUITEMAKER, H. B., BUNNIK, E. M. B., BROWN, B. K. C. & SCARLATTI, G. D. (2009) Impact of host cell variation on the neutralization of HIV-1 in vitro. *Current Opinion in HIV & AIDS,* 4**,** 400-407.

POPOFF, I. J., SAVAGE, J. A., BLAKE, J., JOHNSON, P. & DEANS, J. P. (1998) The association between CD20 and Src-family Tyrosine kinases requires an additional factor. *Mol Immunol,* 35**,** 207-14.

POPOVIC, M., SARNGADHARAN, M. G., READ, E. & GALLO, R. C. (1984) Detection, isolation, and continuous production of cytopathic retroviruses (HTLV-III) from patients with AIDS and pre-AIDS. *Science,* 224**,** 497-500.

POPPER, K. (1962) Conjectures and Refutations. *NY: Basic Books*, 36-37

POTTER, S. J., LACABARATZ, C., LAMBOTTE, O., PEREZ-PATRIGEON, S., VINGERT, B., SINET, M., COLLE, J.-H., URRUTIA, A., SCOTT-ALGARA, D., BOUFASSA, F., DELFRAISSY, J.-F., THEZE, J., VENET, A. & CHAKRABARTI, L. A. (2007) Preserved Central Memory and Activated Effector Memory CD4+ T-Cell Subsets in Human Immunodeficiency Virus Controllers: an ANRS EP36 Study. *J. Virol.,* 81**,** 13904-13915.

PRABAKARAN, P., GAN, J., WU, Y. Q., ZHANG, M. Y., DIMITROV, D. S. & JI, X. (2006) Structural mimicry of CD4 by a cross-reactive HIV-1 neutralizing antibody with CDR-H2 and H3 containing unique motifs. *J Mol Biol,* 357**,** 82-99.

PRESTON, B. D., POIESZ, B. J. & LOEB, L. A. (1988) Fidelity of HIV-1 reverse transcriptase. *Science,* 242**,** 1168-71.

PROVINE, N. M., PURYEAR, W. B., WU, X., OVERBAUGH, J. & HAIGWOOD, N. L. (2009) The infectious molecular clone and pseudotyped virus models of human immunodeficiency virus type 1 exhibit significant differences in virion composition with only moderate differences in infectivity and inhibition sensitivity. *J Virol,* 83**,** 9002-7.

PUTKONEN, P., THORSTENSSON, R., GHAVAMZADEH, L., ALBERT, J., HILD, K., BIBERFELD, G. & NORRBY, E. (1991) Prevention of HIV-2 and SIVsm infection by passive immunization in cynomolgus monkeys. *Nature,* 352**,** 436-8.

REEVES, J. D., GALLO, S. A., AHMAD, N., MIAMIDIAN, J. L., HARVEY, P. E., SHARRON, M., PÃ¶HLMANN, S., SFAKIANOS, J. N., DERDEYN, C. A., BLUMENTHAL, R., HUNTER, E. & DOMS, R. W. (2002) Sensitivity of HIV-1 to entry inhibitors correlates with envelope/coreceptor affinity, receptor density, and fusion kinetics. *Proceedings of the National Academy of Sciences of the United States of America,* 99**,** 16249-16254.

RERKS-NGARM, S., PITISUTTITHUM, P., NITAYAPHAN, S., KAEWKUNGWAL, J., CHIU, J., PARIS, R., PREMSRI, N., NAMWAT, C., DE SOUZA, M., ADAMS, E., BENENSON, M., GURUNATHAN, S., TARTAGLIA, J., MCNEIL, J. G., FRANCIS, D. P., STABLEIN, D., BIRX, D. L., CHUNSUTTIWAT, S., KHAMBOONRUANG, C., THONGCHAROEN, P., ROBB, M. L., MICHAEL, N. L., KUNASOL, P. & KIM, J. H. (2009) Vaccination with ALVAC and AIDSVAX to prevent HIV-1 infection in Thailand. *N Engl J Med,* 361**,** 2209-20.

RICHMAN, D. D., WRIN, T., LITTLE, S. J. & PETROPOULOS, C. J. (2003) Rapid evolution of the neutralizing antibody response to HIV type 1 infection. *Proc Natl Acad Sci U S A,* 100**,** 4144-9.

ROBERT-GUROFF, M., BROWN, M. & GALLO, R. C. (1985) HTLV-III-neutralizing antibodies in patients with AIDS and AIDS-related complex. *Nature,* 316**,** 72-74.

ROBERTSON, C. A., MOK, J. Y. Q., FROEBEL, K. S., SIMMONDS, P., BURNS, S. M., MARSDEN, H. S. & GRAHAM, S. (1992) Maternal Antibodies to gpl20 V3 Sequence Do Not Correlate with Protection against Vertical Transmission of Human Immunodeficiency Virus. *The Journal of Infectious Diseases,* 166**,** 704-709.

ROBERTSON, M., CASIMIRO, D, DE ROSA, S, ET AL (2008a) Immunological characterization of subjects from the STEP Study: a phase IIB test of Concept Trial of the MRKAd5 HIV-1 Gag/Pol/Nef Trivalent vaccine. *15th Conference on Retroviruses and Opportunistic Infections.* Boston, MA.

ROBERTSON, M., MEHROTRA, D, FITZGERALD, D, ET AL (2008b) Efficacy results from the STEP Study: A phase II Test of Concept trial of the MRKAd5 HIV-1 Gag/Pol/Nef Trivalent vaccin. *Presented at the 15th Conference on Retroviruses and Opportunistic Infections.* Boston, MA.

ROCKSTROH, J. K. (2006) Influence of viral hepatitis on HIV infection. *J Hepatol,* 44**,** S25-7.

RODRIGUEZ, B., SETHI, A. K., CHERUVU, V. K., MACKAY, W., BOSCH, R. J., KITAHATA, M., BOSWELL, S. L., MATHEWS, W. C., BANGSBERG, D. R., MARTIN, J., WHALEN, C. C., SIEG, S., YADAVALLI, S., DEEKS, S. G. & LEDERMAN, M. M. (2006) Predictive value of plasma HIV RNA level on rate of CD4 T-cell decline in untreated HIV infection. *JAMA,* 296**,** 1498-506.

RONG, R., LI, B., LYNCH, R. M., HAALAND, R. E., MURPHY, M. K., MULENGA, J., ALLEN, S. A., PINTER, A., SHAW, G. M., HUNTER, E., ROBINSON, J. E., GNANAKARAN, S. & DERDEYN, C. A. (2009) Escape from Autologous Neutralizing Antibodies in Acute/Early Subtype C HIV-1 Infection Requires Multiple Pathways. *PLoS Pathog,* 5**,** e1000594.

ROWLAND-JONES, S. & DE SILVA, T. (2008) Resisting immune exhaustion in HIV-1 infection. *PLoS Med,* 5**,** e103.

RUFF, C. T., RAY, S. C., KWON, P., ZINN, R., PENDLETON, A., HUTTON, N., ASHWORTH, R., GANGE, S., QUINN, T. C., SILICIANO, R. F. & PERSAUD, D. (2002) Persistence of wild-type virus and lack of temporal structure in the latent reservoir for human immunodeficiency virus type 1 in pediatric patients with extensive antiretroviral exposure. *J Virol,* 76**,** 9481-92.

SAAD, J. S., MILLER, J., TAI, J., KIM, A., GHANAM, R. H. & SUMMERS, M. F. (2006) Structural basis for targeting HIV-1 Gag proteins to the plasma membrane for virus assembly. *Proc Natl Acad Sci U S A,* 103**,** 11364-9.

SAADOUN, D., RESCHE-RIGON, M., SENE, D., PERARD, L., KARRAS, A. & CACOUB, P. (2008) Rituximab combined with Peg-interferon-ribavirin in refractory hepatitis C virus-associated cryoglobulinaemia vasculitis. *Ann Rheum Dis,* 67**,** 1431-6.

SAAG, M., GOODRICH, J., FATKENHEUER, G., CLOTET, B., CLUMECK, N., SULLIVAN, J., WESTBY, M., VAN DER RYST, E., MAYER, H. & GROUP, A. S. (2009) A double-blind, placebo-controlled trial of maraviroc in treatment-experienced patients infected with non-R5 HIV-1. *J Infect Dis,* 199**,** 1638-47.

SAIFUDDIN, M., HEDAYATI, T., ATKINSON, J., HOLGUIN, M., PARKER, C. & SPEAR, G. (1997) Human immunodeficiency virus type 1 incorporates both glycosyl phosphatidylinositol-anchored CD55 and CD59 and integral membrane CD46 at levels that protect from complement-mediated destruction. *J Gen Virol,* 78**,** 1907-1911.

SAIFUDDIN, M., PARKER, C. J., PEEPLES, M. E., GORNY, M. K., ZOLLA-PAZNER, S., GHASSEMI, M., ROONEY, I. A., ATKINSON, J. P. & SPEAR, G. T. (1995) Role of virion-associated glycosylphosphatidylinositol-linked proteins CD55 and CD59 in complement resistance of cell line-derived and primary isolates of HIV-1. *The Journal of Experimental Medicine,* 182**,** 501-509.

SALAZAR-GONZALEZ, J. F., SALAZAR, M. G., KEELE, B. F., LEARN, G. H., GIORGI, E. E., LI, H., DECKER, J. M., WANG, S., BAALWA, J., KRAUS, M. H., PARRISH, N. F., SHAW, K. S., GUFFEY, M. B., BAR, K. J., DAVIS, K. L., OCHSENBAUER-JAMBOR, C., KAPPES, J. C., SAAG, M. S., COHEN, M. S., MULENGA, J., DERDEYN, C. A., ALLEN, S., HUNTER, E., MARKOWITZ, M., HRABER, P., PERELSON, A. S., BHATTACHARYA, T., HAYNES, B. F., KORBER, B. T., HAHN, B. H. & SHAW, G. M. (2009) Genetic identity, biological phenotype, and evolutionary pathways of transmitted/founder viruses in acute and early HIV-1 infection. *J Exp Med,* 206**,** 1273-89.

SAPHIRE, E. O., PARREN, P. W., PANTOPHLET, R., ZWICK, M. B., MORRIS, G. M., RUDD, P. M., DWEK, R. A., STANFIELD, R. L., BURTON, D. R. & WILSON, I. A. (2001) Crystal structure of a neutralizing human IGG against HIV-1: a template for vaccine design. *Science,* 293**,** 1155-9.

SAREZ-CIRION, A., LACABARATZ, C., LAMBOTTE, O., VERSMISSE, P., URRUTIA, A., BOUFASSA, F., BARRÃ©-SINOUSSI, F. O., DELFRAISSY, J.-F. O., SINET, M., PANCINO, G. & VENET, A. (2007) HIV controllers exhibit potent CD8 T cell capacity to suppress HIV infection ex vivo and peculiar cytotoxic T lymphocyte activation phenotype. *Proceedings of the National Academy of Sciences,* 104**,** 6776-6781.

SATHER, D. N., ARMANN, J., CHING, L. K., MAVRANTONI, A., SELLHORN, G., CALDWELL, Z., YU, X., WOOD, B., SELF, S., KALAMS, S. & STAMATATOS, L. (2009) Factors associated with the development of cross-reactive neutralizing antibodies during human immunodeficiency virus type 1 infection. *J Virol,* 83**,** 757-69.

SATTENTAU, Q. J. & KLASSE, P. J. (Eds.) (2001) *Mechanisms of Virus Neutralization by Antibodies. In Antibodies in Virus Infection*, Springer.

SATTENTAU, Q. J., MOORE, J. P., VIGNAUX, F., TRAINCARD, F. & POIGNARD, P. (1993) Conformational changes induced in the envelope glycoproteins of the human and simian immunodeficiency viruses by soluble receptor binding. *Journal of Virology,* 67**,** 7383-7393.

SCANLAN, C. N., PANTOPHLET, R., WORMALD, M. R., OLLMANN SAPHIRE, E., STANFIELD, R., WILSON, I. A., KATINGER, H., DWEK, R. A., RUDD, P. M. & BURTON, D. R. (2002) The broadly neutralizing anti-human immunodeficiency virus type 1 antibody 2G12 recognizes a cluster of alpha1-->2 mannose residues on the outer face of gp120. *J Virol,* 76**,** 7306-21.

SCARLATTI, G., LEITNER, T., HODARA, V., JANSSON, M., KARLSSON, A., WAHLBERG, J., ROSSI, P., UHLEN, M., FENYO, E. M. & ALBERT, J. (1996) Interplay of HIV-1 phenotype and neutralizing antibody response in pathogenesis of AIDS. *Immunol Lett,* 51**,** 23-8.

SCHACKER, T., COLLIER, A. C., HUGHES, J., SHEA, T. & COREY, L. (1996) Clinical and epidemiologic features of primary HIV infection. *Ann Intern Med,* 125**,** 257-64.

SCHARF, O., GOLDING, H., KING, L. R., ELLER, N., FRAZIER, D., GOLDING, B. & SCOTT, D. E. (2001) Immunoglobulin G3 from Polyclonal Human Immunodeficiency Virus (HIV) Immune Globulin Is More Potent than Other Subclasses in Neutralizing HIV Type 1. *J. Virol.,* 75**,** 6558-6565.

SCHEID, J. F., MOUQUET, H., FELDHAHN, N., SEAMAN, M. S., VELINZON, K., PIETZSCH, J., OTT, R. G., ANTHONY, R. M., ZEBROSKI, H., HURLEY, A., PHOGAT, A., CHAKRABARTI, B., LI, Y., CONNORS, M., PEREYRA, F., WALKER, B. D., WARDEMANN, H., HO, D., WYATT, R. T., MASCOLA, J. R., RAVETCH, J. V. & NUSSENZWEIG, M. C. (2009) Broad diversity of neutralizing antibodies isolated from memory B cells in HIV-infected individuals. *Nature,* 458**,** 636-40.

SCHMITZ, J. E., KURODA, M. J., SANTRA, S., SASSEVILLE, V. G., SIMON, M. A., LIFTON, M. A., RACZ, P., TENNER-RACZ, K., DALESANDRO, M., SCALLON, B. J., GHRAYEB, J., FORMAN, M. A., MONTEFIORI, D. C., RIEBER, E. P., LETVIN, N. L. & REIMANN, K. A. (1999) Control of viremia in simian immunodeficiency virus infection by CD8+ lymphocytes. *Science,* 283**,** 857-60.

SCHWARTZ, O., MARECHAL, V., FRIGUET, B., ARENZANA-SEISDEDOS, F. & HEARD, J. M. (1998) Antiviral activity of the proteasome on incoming human immunodeficiency virus type 1. *J Virol,* 72**,** 3845-50.

SCHWICKERT, T. A., LINDQUIST, R. L., SHAKHAR, G., LIVSHITS, G., SKOKOS, D., KOSCO-VILBOIS, M. H., DUSTIN, M. L. & NUSSENZWEIG, M. C. (2007) In vivo imaging of germinal centres reveals a dynamic open structure. *Nature*.

SEAMAN, M. S., JANES, H., HAWKINS, N., GRANDPRE, L. E., DEVOY, C., GIRI, A., COFFEY, R. T., HARRIS, L., WOOD, B., DANIELS, M. G., BHATTACHARYA, T., LAPEDES, A., POLONIS, V. R., MCCUTCHAN, F. E., GILBERT, P. B., SELF, S. G., KORBER, B. T., MONTEFIORI, D. C. & MASCOLA, J. R. Tiered categorization of a diverse panel of HIV-1 Env pseudoviruses for assessment of neutralizing antibodies. *J Virol,* 84**,** 1439-52.

SEKALY, R.-P. (2008) The failed HIV Merck vaccine study: a step back or a launching point for future vaccine development? *The Journal of Experimental Medicine,* 205**,** 7-12.

SHRINER, D., SHANKARAPPA, R., JENSEN, M. A., NICKLE, D. C., MITTLER, J. E., MARGOLICK, J. B. & MULLINS, J. I. (2004) Influence of Random Genetic Drift on Human Immunodeficiency Virus Type 1 env Evolution During Chronic Infection. *Genetics,* 166**,** 1155-1164.

SILICIANO, J. D., KAJDAS, J., FINZI, D., QUINN, T. C., CHADWICK, K., MARGOLICK, J. B., KOVACS, C., GANGE, S. J. & SILICIANO, R. F. (2003) Long-term follow-up studies confirm the stability of the latent reservoir for HIV-1 in resting CD4+ T cells. *Nat Med,* 9**,** 727-728.

SILVER, J., MAUDRU, T., FUJITA, K. & REPASKE, R. (1993) An RT-PCR assay for the enzyme activity of reverse transcriptase capable of detecting single virions. *Nucl. Acids Res.,* 21**,** 3593-3594.

SIMEK, M. D., RIDA, W., PRIDDY, F. H., PUNG, P., CARROW, E., LAUFER, D. S., LEHRMAN, J. K., BOAZ, M., TARRAGONA-FIOL, T., MIIRO, G., BIRUNGI, J., POZNIAK, A., MCPHEE, D. A., MANIGART, O., KARITA, E., INWOLEY, A., JAOKO, W., DEHOVITZ, J., BEKKER, L. G., PITISUTTITHUM, P., PARIS, R., WALKER, L. M., POIGNARD, P., WRIN, T., FAST, P. E., BURTON, D. R. & KOFF, W. C. (2009) Human immunodeficiency virus type 1 elite neutralizers: individuals with broad and potent neutralizing activity identified by using a high-throughput neutralization assay together with an analytical selection algorithm. *J Virol,* 83**,** 7337-48.

SIMMONDS, P., ZHANG, L. Q., MCOMISH, F., BALFE, P., LUDLAM, C. A. & BROWN, A. J. (1991) Discontinuous sequence change of human immunodeficiency virus (HIV) type 1 env sequences in plasma viral and lymphocyte-associated proviral populations in vivo: implications for models of HIV pathogenesis. *J. Virol.,* 65**,** 6266-6276.

SMITH-FRANKLIN, B. A., KEELE, B. F., TEW, J. G., GARTNER, S., SZAKAL, A. K., ESTES, J. D., THACKER, T. C. & BURTON, G. F. (2002) Follicular Dendritic Cells and the Persistence of HIV Infectivity: The Role of Antibodies and Fc{gamma} Receptors. *J Immunol,* 168**,** 2408-2414.

SPIRA, A. & HO, D. (1995) Effect of different donor cells on human immunodeficiency virus type 1 replication and selection in vitro. *J. Virol.,* 69**,** 422-429.

STACEY, A. R., NORRIS, P. J., QIN, L., HAYGREEN, E. A., TAYLOR, E., HEITMAN, J., LEBEDEVA, M., DECAMP, A., LI, D., GROVE, D., SELF, S. G. & BORROW, P. (2009) Induction of a striking systemic cytokine cascade prior to peak viremia in acute human immunodeficiency virus type 1 infection, in contrast to more modest and delayed responses in acute hepatitis B and C virus infections. *J Virol,* 83**,** 3719-33.

STANFIELD, R. L., GORNY, M. K., WILLIAMS, C., ZOLLA-PAZNER, S. & WILSON, I. A. (2004) Structural rationale for the broad neutralization of HIV-1 by human monoclonal antibody 447-52D. *Structure,* 12**,** 193-204.

STARCICH, B. R., HAHN, B. H., SHAW, G. M., MCNEELY, P. D., MODROW, S., WOLF, H., PARKS, E. S., PARKS, W. P., JOSEPHS, S. F., GALLO, R. C. & ET AL. (1986) Identification and characterization of conserved and variable regions in the envelope gene of HTLV-III/LAV, the retrovirus of AIDS. *Cell,* 45**,** 637-48.

STASI, R., DEL POETA, G., STIPA, E., EVANGELISTA, M. L., TRAWINSKA, M. M., COOPER, N. & AMADORI, S. (2007) Response to B-cell depleting therapy with rituximab reverts the abnormalities of T-cell subsets in patients with idiopathic thrombocytopenic purpura. *Blood,* 110**,** 2924-30.

STAVNEZER, J. (1996) Immunoglobulin class switching. *Curr Opin Immunol,* 8**,** 199-205.

STEIN, D. S., KORVICK, J. A. & VERMUND, S. H. (1992) CD4+ lymphocyte cell enumeration for prediction of clinical course of human immunodeficiency virus disease: a review. *J Infect Dis,* 165**,** 352-63.

STEINGROVER, R., GARCIA, E. F., VAN VALKENGOED, I. G. M., BEKKER, V., BEZEMER, D., KROON, F. P., DEKKER, L., PRINS, M., DE WOLF, F., LANGE, J. M. A. & PRINS, J. M. Transient Lowering of the Viral Set Point After Temporary Antiretroviral Therapy of Primary HIV Type 1 Infection. *AIDS Research and Human Retroviruses, 2009,* 26**,** 379-387.

STREECK, H., BRUMME, Z. L., ANASTARIO, M., COHEN, K. W., JOLIN, J. S., MEIER, A., BRUMME, C. J., ROSENBERG, E. S., ALTER, G., ALLEN, T. M., WALKER, B. D. & ALTFELD, M. (2008) Antigen Load and Viral Sequence Diversification Determine the Functional Profile of HIV-1â€“Specific CD8⁺ T Cells. *PLoS Med,* 5**,** e100.

SULLIVAN, N., SUN, Y., LI, J., HOFMANN, W. & SODROSKI, J. (1995) Replicative function and neutralization sensitivity of envelope glycoproteins from primary and T-cell line-passaged human immunodeficiency virus type 1 isolates. *Journal of Virology,* 69**,** 4413-4422.

TAKAI, T. (2002) Roles of Fc receptors in autoimmunity. *Nat Rev Immunol,* 2**,** 580-92.

TAKEHISA, J., KRAUS, M. H., AYOUBA, A., BAILES, E., VAN HEUVERSWYN, F., DECKER, J. M., LI, Y., RUDICELL, R. S., LEARN, G. H., NEEL, C., NGOLE, E. M., SHAW, G. M., PEETERS, M., SHARP, P. M. & HAHN, B. H. (2009) Origin and Biology of Simian Immunodeficiency Virus in Wild-Living Western Gorillas. *J. Virol.,* 83**,** 1635-1648.

TAYLOR, J. M., SY, J. P., VISSCHER, B. & GIORGI, J. V. (1995) CD4+ T-cell number at the time of acquired immunodeficiency syndrome. *Am J Epidemiol,* 141**,** 645-51.

TAYLOR, R. P. & LINDORFER, M. A. (2008) Immunotherapeutic mechanisms of anti-CD20 monoclonal antibodies. *Curr Opin Immunol,* 20**,** 444-9.

TELESNITSKY, A. & GOFF, S. P. (1997) *Reverse Transcriptase and the Generation of Retroviral DNA*.

TENCZA, S., MILLER, M., ISLAM, K., MIETZNER, T. & MONTELARO, R. (1995) Effect of amino acid substitutions on calmodulin binding and cytolytic properties of the LLP-1 peptide segment of human immunodeficiency virus type 1 transmembrane protein. *Journal of Virology,* 69**,** 5199-5202.

TENCZA, S. B., MIETZNER, T. A. & MONTELARO, R. C. (1997) Calmodulin-binding function of LLP segments from the HIV type 1 transmembrane protein is conserved among natural sequence variants. *AIDS Res Hum Retroviruses,* 13**,** 263-9.

TITANJI, K., CHIODI, F., BELLOCCO, R., SCHEPIS, D., OSORIO, L., TASSANDIN, C., TAMBUSSI, G., GRUTZMEIER, S., LOPALCO, L. & DE MILITO, A. (2005) Primary HIV-1 infection sets the stage for important B lymphocyte dysfunctions. *AIDS,* 19**,** 1947-55.

TOMARAS, G. D., YATES, N. L., LIU, P., QIN, L., FOUDA, G. G., CHAVEZ, L. L., DECAMP, A. C., PARKS, R. J., ASHLEY, V. C., LUCAS, J. T., COHEN, M., ERON, J., HICKS, C. B., LIAO, H. X., SELF, S. G., LANDUCCI, G., FORTHAL, D. N., WEINHOLD, K. J., KEELE, B. F., HAHN, B. H., GREENBERG, M. L., MORRIS, L., KARIM, S. S., BLATTNER, W. A., MONTEFIORI, D. C., SHAW, G. M., PERELSON, A. S. & HAYNES, B. F. (2008) Initial B-cell responses to transmitted human immunodeficiency virus type 1: virion-binding immunoglobulin M (IgM) and IgG antibodies followed by plasma anti-gp41 antibodies with ineffective control of initial viremia. *J Virol,* 82**,** 12449-63.

TREMBLAY, C. L., GIGUEL, F., KOLLMANN, C., GUAN, Y., CHOU, T. C., BAROUDY, B. M. & HIRSCH, M. S. (2002) Anti-human immunodeficiency virus interactions of SCH-C (SCH 351125), a CCR5 antagonist, with other antiretroviral agents in vitro. *Antimicrob Agents Chemother,* 46**,** 1336-9.

TRKOLA, A., KUSTER, H., LEEMANN, C., OXENIUS, A., FAGARD, C., FURRER, H., BATTEGAY, M., VERNAZZA, P., BERNASCONI, E., WEBER, R., HIRSCHEL, B., BONHOEFFER, S. & GUNTHARD, H. F. (2004) Humoral immunity to HIV-1: kinetics of antibody responses in chronic infection reflects capacity of immune system to improve viral set point. *Blood,* 104**,** 1784-92.

TRKOLA, A., KUSTER, H., RUSERT, P., JOOS, B., FISCHER, M., LEEMANN, C., MANRIQUE, A., HUBER, M., REHR, M., OXENIUS, A., WEBER, R., STIEGLER, G., VCELAR, B., KATINGER, H., ACETO, L. & GUNTHARD, H. F. (2005) Delay of HIV-1 rebound after cessation of antiretroviral therapy through passive transfer of human neutralizing antibodies. *Nat Med,* 11**,** 615-22.

TUEN, M., VISCIANO, M. L., CHIEN, P. C., JR., COHEN, S., CHEN, P. D., ROBINSON, J., HE, Y., PINTER, A., GORNY, M. K. & HIOE, C. E. (2005) Characterization of antibodies that inhibit HIV gp120 antigen processing and presentation. *Eur J Immunol,* 35**,** 2541-51.

VAN VALEN, L. (1973) A New Evolutionary Law. *Evolutionary Theory,* 1**,** 1-30.

VERONESE, F. D., DEVICO, A. L., COPELAND, T. D., OROSZLAN, S., GALLO, R. C. & SARNGADHARAN, M. G. (1985) Characterization of gp41 as the transmembrane protein coded by the HTLV-III/LAV envelope gene. *Science,* 229**,** 1402-5.

VIRGIN, H. W. & WALKER, B. D. Immunology and the elusive AIDS vaccine. *Nature, 2010,* 464**,** 224-231.

VORONIN, Y., CHOHAN, B., EMERMAN, M. & OVERBAUGH, J. (2007) Primary Isolates of Human Immunodeficiency Virus Type 1 Are Usually Dominated by the Major Variants Found in Blood. *J. Virol.,* 81**,** 10232-10241.

VOULGAROPOULOU, F., TAN, B., SOARES, M., HAHN, B. & RATNER, L. (1999) Distinct Human Immunodeficiency Virus Strains in the Bone Marrow Are Associated with the Development of Thrombocytopenia. *Journal of Virology,* 73**,** 3497-3504.

WALKER, L. M., PHOGAT, S. K., CHAN-HUI, P.-Y., WAGNER, D., PHUNG, P., GOSS, J. L., WRIN, T., SIMEK, M. D., FLING, S., MITCHAM, J. L., LEHRMAN, J. K., PRIDDY, F. H., OLSEN, O. A., FREY, S. M., HAMMOND, P. W., PROTOCOL G PRINCIPAL INVESTIGATORS, KAMINSKY, S., ZAMB, T., MOYLE, M., KOFF, W. C., POIGNARD, P. & BURTON, D. R. (2009) Broad and Potent Neutralizing Antibodies from an African Donor Reveal a New HIV-1 Vaccine Target. *Science,* 326**,** 285-289.

WANG, J., SMERDON, S. J., JAGER, J., KOHLSTAEDT, L. A., RICE, P. A., FRIEDMAN, J. M. & STEITZ, T. A. (1994) Structural basis of asymmetry in the human immunodeficiency virus type 1 reverse transcriptase heterodimer. *Proc Natl Acad Sci U S A,* 91**,** 7242-6.

WAWER, M. J., GRAY, R. H., SEWANKAMBO, N. K., SERWADDA, D., LI, X., LAEYENDECKER, O., KIWANUKA, N., KIGOZI, G., KIDDUGAVU, M., LUTALO, T., NALUGODA, F., WABWIRE-MANGEN, F., MEEHAN, M. P. & QUINN, T. C. (2005) Rates of HIV-1 transmission per coital act, by stage of HIV-1 infection, in Rakai, Uganda. *J Infect Dis,* 191**,** 1403-9.

WEI, X., DECKER, J. M., LIU, H., ZHANG, Z., ARANI, R. B., KILBY, J. M., SAAG, M. S., WU, X., SHAW, G. M. & KAPPES, J. C. (2002) Emergence of Resistant Human Immunodeficiency Virus Type 1 in Patients Receiving Fusion Inhibitor (T-20) Monotherapy. *Antimicrob. Agents Chemother.,* 46**,** 1896-1905.

WEI, X., DECKER, J. M., WANG, S., HUI, H., KAPPES, J. C., WU, X., SALAZAR-GONZALEZ, J. F., SALAZAR, M. G., KILBY, J. M., SAAG, M. S., KOMAROVA, N. L., NOWAK, M. A., HAHN, B. H., KWONG, P. D. & SHAW, G. M. (2003) Antibody neutralization and escape by HIV-1. *Nature,* 422**,** 307-12.

WEISS, C. D., LEVY, J. A. & WHITE, J. M. (1990) Oligomeric organization of gp120 on infectious human immunodeficiency virus type 1 particles. *J Virol,* 64**,** 5674-7.

WEISSENHORN, W., DESSEN, A., HARRISON, S. C., SKEHEL, J. J. & WILEY, D. C. (1997) Atomic structure of the ectodomain from HIV-1 gp41. *Nature,* 387**,** 426-30.

WILKINSON, R. A., PISCITELLI, C., TEINTZE, M., CAVACINI, L. A., POSNER, M. R. & LAWRENCE, C. M. (2005) Structure of the Fab fragment of F105, a broadly reactive anti-human immunodeficiency virus (HIV) antibody that recognizes the CD4 binding site of HIV type 1 gp120. *J Virol,* 79**,** 13060-9.

WOHRL, B. M. & MOELLING, K. (1990) Interaction of HIV-1 ribonuclease H with polypurine tract containing RNA-DNA hybrids. *Biochemistry,* 29**,** 10141-7.

WONG, J. K., STRAIN, M. C., PORRATA, R., REAY, E., SANKARAN-WALTERS, S., IGNACIO, C. C., RUSSELL, T., PILLAI, S. K., LOONEY, D. J. & DANDEKAR, S. In vivo CD8+ T-cell suppression of siv viremia is not mediated by CTL clearance of productively infected cells. *PLoS Pathog, 2010,* 6**,** e1000748.

WOROBEY, M., GEMMEL, M., TEUWEN, D. E., HASELKORN, T., KUNSTMAN, K., BUNCE, M., MUYEMBE, J. J., KABONGO, J. M., KALENGAYI, R. M., VAN MARCK, E., GILBERT, M. T. & WOLINSKY, S. M. (2008) Direct evidence of extensive diversity of HIV-1 in Kinshasa by 1960. *Nature,* 455**,** 661-4.

WU, H., KWONG, P. D. & HENDRICKSON, W. A. (1997) Dimeric association and segmental variability in the structure of human CD4. *Nature,* 387**,** 527-30.

WU, X., ZHOU, T., O'DELL, S., WYATT, R. T., KWONG, P. D. & MASCOLA, J. R. (2009) Mechanism of human immunodeficiency virus type 1 resistance to monoclonal antibody B12 that effectively targets the site of CD4 attachment. *J Virol,* 83**,** 10892-907.

XIANG, S. H., DOKA, N., CHOUDHARY, R. K., SODROSKI, J. & ROBINSON, J. E. (2002) Characterization of CD4-induced epitopes on the HIV type 1 gp120 envelope glycoprotein recognized by neutralizing human monoclonal antibodies. *AIDS Res Hum Retroviruses,* 18**,** 1207-17.

YANG, X., KURTEVA, S., LEE, S. & SODROSKI, J. (2005) Stoichiometry of Antibody Neutralization of Human Immunodeficiency Virus Type 1. *J. Virol.,* 79**,** 3500-3508.

YANG, X., LIPCHINA, I., COCKLIN, S., CHAIKEN, I. & SODROSKI, J. (2006) Antibody Binding Is a Dominant Determinant of the Efficiency of Human Immunodeficiency Virus Type 1 Neutralization. *J. Virol.,* 80**,** 11404-11408.

YANG, Z., NIELSEN, R., GOLDMAN, N. & PEDERSEN, A. M. (2000) Codon-substitution models for heterogeneous selection pressure at amino acid sites. *Genetics,* 155**,** 431-49.

YORK, J., FOLLIS, K. E., TRAHEY, M., NYAMBI, P. N., ZOLLA-PAZNER, S. & NUNBERG, J. H. (2001) Antibody Binding and Neutralization of Primary and T-Cell Line-Adapted Isolates of Human Immunodeficiency Virus Type 1. *Journal of Virology,* 75**,** 2741-2752.

ZENNOU, V., MAMMANO, F., PAULOUS, S., MATHEZ, D. & CLAVEL, F. (1998) Loss of viral fitness associated with multiple Gag and Gag-Pol processing defects in human immunodeficiency virus type 1 variants selected for resistance to protease inhibitors in vivo. *J Virol,* 72**,** 3300-6.

ZHANG, H., DORNADULA, G., ORENSTEIN, J. & POMERANTZ, R. J. (2000) Morphologic changes in human immunodeficiency virus type 1 virions secondary to intravirion reverse transcription: evidence indicating that reverse transcription may not take place within the intact viral core. *J Hum Virol,* 3**,** 165-72.

ZHANG, L., RIBEIRO, R. M., MASCOLA, J. R., LEWIS, M. G., STIEGLER, G., KATINGER, H., PERELSON, A. S. & DAVENPORT, M. P. (2004a) Effects of antibody on viral kinetics in simian/human immunodeficiency virus infection: implications for vaccination. *J Virol,* 78**,** 5520-2.

ZHANG, M. Y., XIAO, X., SIDOROV, I. A., CHOUDHRY, V., CHAM, F., ZHANG, P. F., BOUMA, P., ZWICK, M., CHOUDHARY, A., MONTEFIORI, D. C., BRODER, C. C., BURTON, D. R., QUINNAN, G. V., JR. & DIMITROV, D. S. (2004b) Identification and characterization of a new cross-reactive human immunodeficiency virus type 1-neutralizing human monoclonal antibody. *J Virol,* 78**,** 9233-42.

ZHANG, Y. J., FRACASSO, C., FIORE, J. R., BJORNDAL, A., ANGARANO, G., GRINGERI, A. & FENYO, E. M. (1997) Augmented serum neutralizing activity against primary human immunodeficiency virus type 1 (HIV-1) isolates in two groups of HIV-1-infected long-term nonprogressors. *J Infect Dis,* 176**,** 1180-7.

ZHOU, T., GEORGIEV, I., WU, X., YANG, Z.-Y., DAI, K., FINZI, A., DO KWON, Y., SCHEID, J., SHI, W., XU, L., YANG, Y., ZHU, J., NUSSENZWEIG, M. C., SODROSKI, J., SHAPIRO, L., NABEL, G. J., MASCOLA, J. R. & KWONG, P. D. Structural Basis for Broad and Potent Neutralization of HIV-1 by Antibody VRC01. *Science, 2010***,** science.1192819.

ZHOU, T., XU, L., DEY, B., HESSELL, A. J., VAN RYK, D., XIANG, S. H., YANG, X., ZHANG, M. Y., ZWICK, M. B., ARTHOS, J., BURTON, D. R., DIMITROV, D. S., SODROSKI, J., WYATT, R., NABEL, G. J. & KWONG, P. D. (2007) Structural definition of a conserved neutralization epitope on HIV-1 gp120. *Nature,* 445**,** 732-7.

ZOLLA-PAZNER, S., ZHONG, P., REVESZ, K., VOLSKY, B., WILLIAMS, C., NYAMBI, P. & GORNY, M. K. (2004) The cross-clade neutralizing activity of a human monoclonal antibody is determined by the GPGR V3 motif of HIV type 1. *AIDS Res Hum Retroviruses,* 20**,** 1254-8.

Journal of Virological Methods 156 (2009) 1–7

Contents lists available at ScienceDirect

Journal of Virological Methods

journal homepage: www.elsevier.com/locate/jviromet

Protocol

A one-step SYBR Green I-based product-enhanced reverse transcriptase assay for the quantitation of retroviruses in cell culture supernatants

Massimo Pizzato[a,*], Otto Erlwein[a], David Bonsall[a], Stephen Kaye[a], David Muir[b], Myra O. McClure[a]

[a] Jefferiss Trust Laboratories, Wright-Fleming Institute, Imperial College, London W2 1PG, United Kingdom
[b] Department of Clinical Virology, Imperial College Health Trust, St. Mary's Campus, London W2 1NY, United Kingdom

Article history:
Received 15 April 2008
Received in revised form 6 October 2008
Accepted 13 October 2008
Available online 5 December 2008

Keywords:
Reverse transcriptase assay
Retrovirus
HIV
Real-time PCR

A B S T R A C T

PCR-enhanced reverse transcriptase assays (PERT) are sensitive tools for the detection of retroviruses in biological samples. The adaptation of real-time PCR techniques based on fluorescent probes (F-PERT) has added a reliable quantitative capacity to the assay. In the interest of economy and time, the SYBR Green I-based real-time detection system was used to establish a convenient one-step PERT assay (SG-PERT). This assay can be completed in 2 h, is linear over six orders of magnitude and can be used to quantify retroviruses belonging to divergent species, such as the human immunodeficiency virus type 1 (HIV-1), murine leukemia virus (MLV) and prototypic foamy virus (PFV).

© 2008 Elsevier B.V. All rights reserved.

1. Type of research

Assays for the routine quantitation of retrovirus particles are essential tools in research areas addressing the biology of retroviruses and the development and use of viral vectors for gene transfer. To this end, ELISA-based techniques for the quantitation of retroviral Gag proteins are often expensive and require extensive sample dilution, because they are linear only over a limited range of antigen concentration. RT-PCR strategies to detect and quantify virion-associated retrovirus genomes rely on sequence-specific primer design and require RNA isolation procedures which make it expensive and labour intensive. In contrast, biochemical assays which estimate the amount of virion-associated reverse transcriptase (RT-assays) can universally detect and quantify retrovirus particles. The enzymatic activity of RT, present in all retroviruses, is measured using an RNA template which is reverse transcribed *in vitro* by the retroviral enzyme. The resulting DNA product (cDNA) is then quantified as a measure of the amount of virions present. Conventionally, quantitation of the cDNA is achieved by measuring the amount of nucleotides incorporated using radioactively labelled reagents or colorimetric techniques. However, during the last 15 years product-enhanced RT (PERT) assays have been developed using PCR techniques to amplify the cDNA and to allow the detection of even single retrovirus particles (Chang et al., 1997; Fan et al., 2006; Heneine et al., 1995; Pyra et al., 1994; Silver et al., 1993; Yamamoto et al., 1996). Furthermore, the adaptation of real-time PCR techniques based on the fluorogenic 5′-nuclease chemistry (F-PERT) to one- or two-step assays has coupled the high sensitivity given by the PCR to the quantitative capacity given by real-time analysis of product amplification, making it linear over six orders of magnitude (Arnold et al., 1998; Lovatt et al., 1999; Maudru and Peden, 1998; Sears and Khan, 2003). PERT and F-PERT assays can be used to detect low amounts of retroviruses in biological products (Brorson et al., 2001, 2002; Lovatt et al., 1999), HIV in serum samples (Garcia Lerma et al., 1998; Pyra et al., 1994), replication competent recombinant retroviruses in cultures producing vectors for gene transfer (Sastry et al., 2005) and endogenous retroviruses (Bisset et al., 2007; Khan and Sears, 2001).

SYBR Green I-based systems offer a popular alternative to fluorescent probe-based real-time PCR techniques and are based on its ability to produce a 100-fold increase of fluorescence when bound to double-stranded DNA. Because the binding of SYBR Green I to nucleic acid is not sequence-specific, the fluorescent signal produced when in complex with DNA is directly proportional to the length and amount of DNA copies synthesized during the reaction, making this technique very precise and sensitive. Given the popularity of the SYBR Green I-based systems and their cost efficiency, the SYBR Green I chemistry has been adapted to a one-step PERT (SG-PERT). Several attempts were required in order to identify crucial reaction conditions and develop a robust and sensitive

* Corresponding author at: Imperial College London, Jefferiss Research Trust Laboratories, St. Mary's Campus, Norfolk Place, London W2 1PG, United Kingdom. Tel.: +44 20 7594 3918; fax: +44 20 7594 3906.
E-mail address: m.pizzato@imperial.ac.uk (M. Pizzato).

0166-0934/$ – see front matter © 2008 Elsevier B.V. All rights reserved.
doi:10.1016/j.jviromet.2008.10.012

assay, which is proposed as a fast and economic tool for the routine quantitation of divergent retroviruses.

2. Time required for a 20 sample experiment: 1 h 50 min

(i) Sample preparation: 20 min
(ii) Reaction set-up: 10 min
(iii) RT and PCR reactions: 1 h 10 min
(iv) Data analysis: 10 min

3. Materials

3.1. Cells and viruses

Human endothelial cells HEK 293T, human fibrosarcoma cells HT1080 and Hela-derived TZM-BL indicator cells were grown in DMEM (Invitrogen, Paisley, UK). Human lymphoblastoid Jurkat E6.1 cells were grown in RPMI (Invitrogen, Paisley, UK). Media were supplemented with 10% fetal calf serum (Invitrogen, Paisley, UK) and cell cultures were maintained at 37 °C and 5% CO_2.

HIV-1 was generated using the proviral construct pNL4-3 (Adachi et al., 1986). Recombinant murine leukemia virus (MLV) vector was produced using the gag-pol expression plasmid, pHIT-60 (Soneoka et al., 1995), the VSV-G (G protein from the vesicular stomatitis virus) expression plasmid, pMDG (Naldini et al., 1996) and the retroviral vector, pCNCG-GFP (Neil et al., 2001). Recombinant PFV vector was produced using the vector plasmid, pMH71 (Heinkelein et al., 2003) and pczHFVenv encoding the HFV (human foamy virus) envelope glycoprotein (Pietschmann et al., 1999).

3.2. Special equipment and software

- LightCycler 2.0 (Roche Diagnostics, Burgess Hill, UK).
- LightCycler software 4.0 (Roche Diagnostics, Burgess Hill, UK).
- 7900HT Real-Time PCR system and software (Applied Biosystems, Warrington, UK).

3.3. Chemicals and reagents

- 1 kb plus DNA molecular weight marker, Sybr Green I, deoxynucleotides and Platinum Taq (Invitrogen, Paisley, UK).
- Recombinant HIV-1 reverse transcriptase and AmpliTaq Gold polymerase (Ambion/Applied Biosystems, Warrington, UK).
- Ammonium sulphate, potassium chloride, magnesium chloride, manganese chloride, Tris–HCl, dithiothreitol, Triton X-100, DNase and RNase-free water, glycerol, 1,4-dithioerythritol (DTT) and agarose (Sigma–Aldrich, Gillingham, UK).
- Bovine serum albumin (New England Biolabs, Hitchin, UK).
- Hot-start Taq polymerase (MBI Fermentas, York, UK).
- Brome mosaic virus RNA and RNAsin ribonuclease inhibitor (Promega, Southampton, UK).
- Forward (5′-GGTCTCTTTTAGAGATTTACAGTG-3′) and reverse (5′-CGTGGTTGACACGCAGACCTCTTAC-3′) primer oligonucleotides (Invitrogen, Paisley, UK).
- LightCycler 20 μl capillaries (Roche Diagnostics, Burgess Hill, UK).
- Saquinavir (NIBSC, Potters Bar, UK)
- PFU ultra, PFU turbo and EasyA (Stratagene, Amsterdam Zuidoost, The Netherlands)
- Murex HIV antigen mAB ELISA assay kit (Abbott Murex, Maidenhead, UK).
- X-Gal (5-bromo-4-chloro-3-indolyl-b-galactopyranoside) (Melford, Chelsworth UK).

4. Detailed procedure

4.1. Sample preparation

4.1.1. Production of viruses and recombinant retrovirus vectors

Jurkat E6.1 cells were infected with HIV-1 NL4-3, previously generated by transfection of HEK 293T cells with pNL4-3 and passaged for more than 2 weeks to establish chronic infection.

Recombinant MLV and PFV (prototypic foamy virus) vectors were produced by transfection of HEK 293T cells. Briefly, 1.5 million cells, seeded in T25 flasks 1 day earlier, were transfected using Lipofectamine 2000 (Invitrogen) according to the manufacturer's instructions with pHIT-60, pMDG and pCNCG-GFP (MLV) and pMH71 and pczHFVenv (PFV). Vector-containing supernatants were harvested 48 h after transfection. After clarification by low-speed centrifugation, supernatants were prepared for infectivity assay and SG-PERT analyses by filtering through a 0.45 μm pore filter.

4.1.2. Infectivity assays

TZM-BL or HT1080 target cells were seeded onto 48-well plates (2×10^4 cells/well) 1 day before infection or transduction. Virus and vector supernatants were serially diluted 10-fold in triplicate in culture medium and target cells inoculated with 0.4 ml of each dilution. Virus supernatant was replaced with fresh medium 24 h later and end-point titers evaluated 72 h post-infection (TZM-bl cells) or post-transduction (HT1080 cells). To ensure that HIV-1 infection of TZM-bl resulted in a single cycle of replication, target cells were treated with 1 μM of the protease inhibitor saquinavir. HIV-1 infection of TZM-bl cells was evaluated by staining infected cells with X-Gal as previously described (Pizzato et al., 2001) The infectivities of MLV and PFV GFP vectors were evaluated by counting fluorescent foci by fluorescence microscopy in transduced HT1080 cells. Clusters of stained cells were attributed to a single infection event and titre was expressed as infectious units (i.u.).

4.1.3. Measurements of p24 and HIV-1 RNA in virus supernatants

P24 antigen was measured in cell culture supernatants using the Murex HIV antigen mAB ELISA assay kit following the manufacturer's guidelines. HIV-1 RNA was quantified by Siemens Versant HIV-1 bDNA (branched-chain DNA) assay, after the sample was diluted 10^5-fold in normal human plasma to obtain a concentration falling within the range of the assay.

4.1.4. Preparation and storage of SG-PERT assay buffers

All buffers were prepared using RNAse-free reagents:

2× virus lysis buffer (0.25% Triton X-100, 50 mM KCl, 100 mM TrisHCl pH7.4, 40% glycerol) was stored at −20 °C. RNAse inhibitor (0.4 U/μl) was added to the volume of buffer needed for virus disruption immediately before use.

10× sample dilution buffer (50 mM $(NH_4)_2SO_4$, 200 mM KCl and 200 mM Tris–HCl pH 8.3) was stored in aliquots at −20 °C.

2× reaction mix (10 mM $(NH_4)_2SO_4$, 40 mM KCl and 40 mM Tris–Cl pH 0.3, 10 mM $MgCl_2$, 0.2 mg/ml BSA, 1/10,000 SYBR Green I, 400 μM dNTPs, 1 μM forward primer,1 μM reverse primer, 1.2 μg/ml BMV RNA) was stored in aliquots at −80 °C. Hotstart Taq was added (0.2 U/reaction) immediately before use.

4.1.5. Preparation of virus lysates

Five microliters of undiluted or diluted virus supernatant, or 5 μl of recombinant HIV-1 RT diluted in sample dilution buffer, were mixed with 5 μl of 2× virus lysis buffer in a 1.5 ml microfuge tube. After 10 min incubation at room temperature, 90 μl of sample dilution buffer were added and the tube vortexed to obtain a 10-fold dilution.

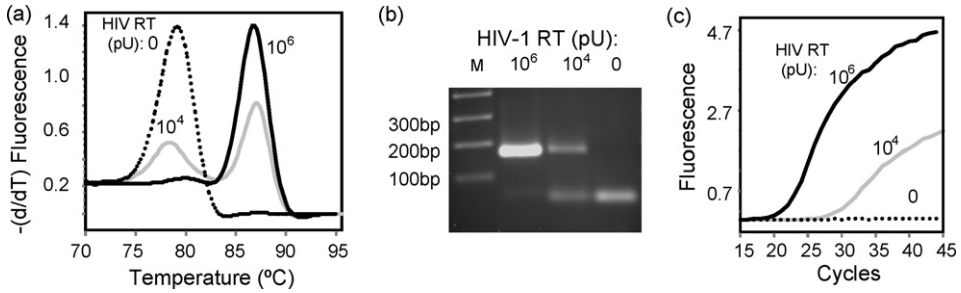


Fig. 1. The SG-PERT assay. (a) Melting curve of PCR products obtained by testing the indicated amount of recombinant HIV-1 RT with SG-PERT. (b) Agarose gel visualizing the DNA products in the SG-PERT reactions analyzed in (a). M: molecular weight marker with indicated molecular sizes. (c) Real-time amplification curves of the reactions visualized in (a) and obtained by acquiring the fluorescence at 83 °C.

4.2. Reaction set-up

Ten microliters of the diluted virus lysate samples were mixed immediately with 10 μl of 2× reaction mix already aliquoted into the reservoir of pre-chilled 20 μl capillaries (lightcycler) or optical tubes (HT7900). The capillaries or tubes were briefly centrifuged to sediment the reaction components and applied to real-time platforms. Thermal cycler conditions used were: 30 min RT reaction at 37 °C, 5 min hot-start Taq activation at 95 °C and 45 cycles of amplification. Each amplification cycle was composed of 5 s denaturation at 95 °C, 5 s annealing at 55 °C, 15 s extension at 72 °C, 7 s acquisition at 83 °C, using the lightcycler; 5 s denaturation at 95 °C, 5 s annealing at 55 °C, 20 s extension at 72 °C, 11 s acquisition at 83 °C, using the 7900HT platform.

Where indicated, the 20 μl PCR products were visualized after electrophoretic separation in 1.8% agarose gel and stained with ethidium bromide.

4.3. Data analysis

Amplification curves and melting temperatures were generated by recording fluorescence at 530 nm and analyzed using the LightCycler software 4. For each amplification curve the software calculates the crossing point, defined as the cycle number at which the fluorescence of a sample rises above the background fluorescence. The fit points method with arithmetic background correction was used to calculate the crossing points and generate the standard curves following the operator's manual. First, the noise band was adjusted using the software automatic option. The maximum number of fit points fitting the linear portion of the curve was then added. The software option "minimize errors" was chosen to automatically adjust the threshold line for the calculation of crossing points. The regression analysis of crossing points versus dilution factors of virus supernatants or recombinant RT was automatically calculated by the software. The slope of the curve, which is referred to as the efficiency of the reaction, indicates the efficiency of the amplification, the perfect value being 2. Melting peaks were calculated automatically by the software.

For data acquired with the 7900HT system, crossing points were calculated automatically by the software.

5. Results

5.1. SG-PERT reaction conditions

A one step real-time based PERT assay was established using the BMV RNA template and primer set which have already been described (Silver et al., 1993) and which amplify a 168 bp fragment at the 3′ end of the BMV genome. After screening several thermophilic DNA polymerases, the hot-start Taq-polymerase from MBI Fermentas was chosen for the PCR amplification because it was found to lack significant RT activity (not shown), as already suggested (Fan et al., 2006; Maudru and Peden, 1997).

Since the binding of SYBR Green I to DNA is sequence-independent, non-specific PCR fragments can contribute to the fluorescent signal recorded by the instrument. A melting curve analysis of the PCR products obtained was, therefore, performed to confirm the presence of the specific DNA fragment which correlates with a distinct melting peak at 86 °C (Fig. 1a). Accordingly, agarose gel electrophoresis analyses of the PCR product obtained in the light cycler confirmed the presence of the predicted 168 bp specific fragment and the absence of non-specific products (Fig. 1b). Primer–dimer formation was often detected in negative or weakly positive samples, characterized by a melting peak at 79 °C (Fig. 1b

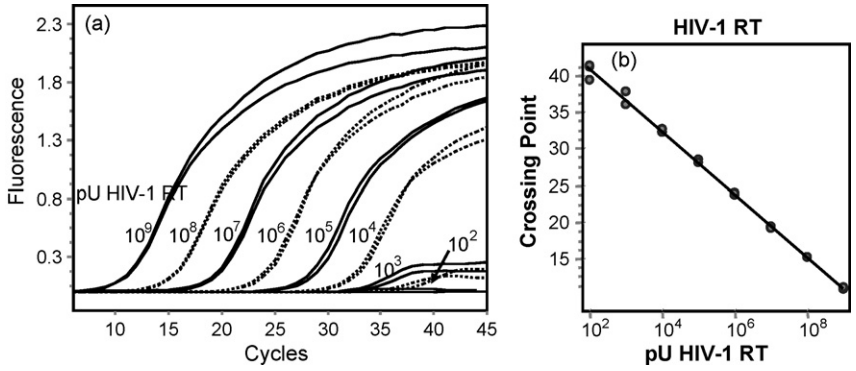


Fig. 2. SG-PERT detection of recombinant HIV-1 RT. (a) Amplification curves obtained with 10-fold serial dilutions of recombinant HIV-1 RT, performed in duplicate. (b) Standard curve showing the input of recombinant HIV-1 RT against the respective crossing points of amplification curves shown in (a) and calculated by the LightCycler software 4. Reaction efficiency is shown.

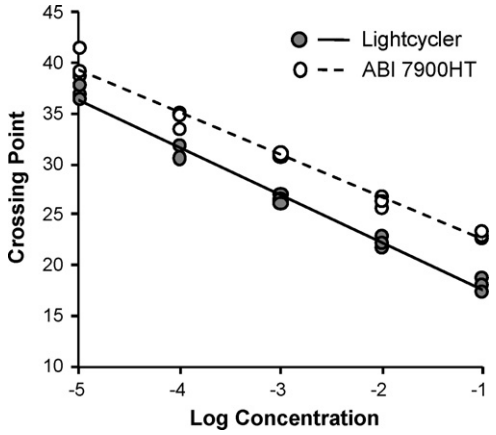


Fig. 3. SG-PERT detection of HIV-1 with two different real-time PCR platforms. Crossing points obtained with the lightcycler and the ABI 7900HT using 10-fold serial dilutions of HIV-$1_{NL4.3}$ retroviral supernatants containing 3×10^5 i.u./ml. Results of triplicate samples and linear regression are shown.

and 1c). To avoid non-specific signal detection of primer dimers, fluorescence was acquired at 83 °C (Fig. 1c). The melting temperature of the PCR product was found to remain constant when recombinant MLV RT or different virus supernatants were tested (not shown), indicating no need to adjust the acquisition temperature.

5.2. Sensitivity of the assay

The sensitivity of the SG-PERT was tested with the lightcycler using 10-fold serial dilutions of recombinant HIV-1 RT, starting from 1 mU. The assay provided a detectable and reproducible signal down to the 10^{-7} dilution equivalent to 100 pU of HIV-1 RT (Fig. 2a), indicating a sensitivity close to that reported by other real-time PCR-based RT-assays for the detection of HIV-1 RT (Arnold et al., 1998; Lovatt et al., 1999; Maudru and Peden, 1997). The diagram generated by plotting the crossing points against the enzyme dilution factor shows linearity over six orders of magnitude (Fig. 2b).

The ability of SG-PERT to detect HIV-1 virus particles in cell culture supernatants was then tested in the lightcycler using cell culture medium derived from Jurkat E6.1 producing HIV-$1_{NL4.3}$. This virus suspension had an infectious titre of 3×10^5 i.u./ml, a p24 content of 355 ng/ml and a virus load of 11.6×10^9 HIV-1 RNA copies/ml. The SG-PERT could detect RT activity down to the 10^{-5} dilution (Fig. 3). Because only 0.5 μl of virus sample is added to the 20 μl reactions, it can be concluded that the assay detects RT activity associated with six HIV RNA copies (three virions) or 1.7×10^{-3} pg of p24. To establish whether SG-PERT can be performed with equal sensitivity using different real-time PCR platforms, the same virus supernatant was tested using the 7900HT apparatus. As shown in Fig. 3, the sensitivity and linear range of the assay remain similar using both real-time PCR platforms.

5.3. Specificity of the assay

The performance of SG-PERT was evaluated for the quantitation and detection of virus particles and recombinant retroviral vectors based on divergent retroviruses. For this purpose, serial dilutions of cell culture supernatants from cells producing HIV and recombinant MLV or PFV GFP transducing vectors were tested in parallel and in triplicate using the lightcycler. End-point infectious titres were first determined to be 4.0×10^6 i.u./ml for the HIV-1 sample, 7.4×10^5 i.u./ml for the PFV sample and 4.2×10^6 i.u./ml for the MLV sample. Results show that for all three types of retrovirus the assay is linear over five to six orders of magnitude and

Table 1
Detection of divergent retrovirus particles and intra-assay variation with SG-PERT.

Virus dilution	Crossing point and coefficient of variation[a]		
	HIV-1	MLV	PFV
Neat	13.47 (0.28%)	17.08 (1.00%)	18.15 (1.26%)
10^{-1}	16.12 (0.31%)	19.18 (0.64%)	21.64 (0.70%)
10^{-2}	19.33 (0.26%)	22.52 (0.76%)	25.09 (0.74%)
10^{-3}	22.92 (0.64%)	26.13 (0.61%)	28.71 (0.98%)
10^{-4}	26.20 (0.19%)	29.70 (1.07%)	32.45 (0.30%)
10^{-5}	29.79 (1.19%)	33.48 (0.66%)	35.64 (2.08%)
10^{-6}	33.10 (0.68%)	36.32 (1.97%)	n.d.
10^{-7}	n.d.	n.d.	n.d.

n.d.: not detected.
[a] Crossing point calculated with the fit points methods. Values are average of triplicate dilutions values. Intraexperimental coefficient of variation is indicated in parenthesis.

detects RT-activity in supernatants containing less than 10 i.u./ml (Fig. 4). As shown in Table 1, for all three types of virus and for all dilutions tested, the coefficient of variation ranges between 0.19% and 2.08%. Reaction efficiencies of 1.995, 1.997 and 1.894 for HIV-1, MLV and PFV, respectively indicate that SG-PERT can be reliably used as a tool for the quantitation of divergent retroviruses.

Retrovirus-free supernatants from uninfected cell cultures were used as negative controls. Rarely and randomly was a weak signal detected with crossing point above 39 PCR cycles. This signal most likely results from the activity of eukaryotic polymerases associated with cellular debris, as reported elsewhere (Voisset et al., 2001). Only samples generating a signal at an earlier PCR cycle than the virus-free control are, therefore, considered positive in these cases.

5.4. Reproducibility of the assay

Reproducibility of the assay was evaluated by testing serial dilutions of the same HIV-1 virus suspension in independent experiments using the lightcycler. Four serial dilutions of an HIV-1 virus supernatant were tested in 18 experiments performed using stocks of lysis buffers and reaction mixtures prepared in three independent occasions. The coefficient of variation ranged from 4.1% to 7.6% (Fig. 5).

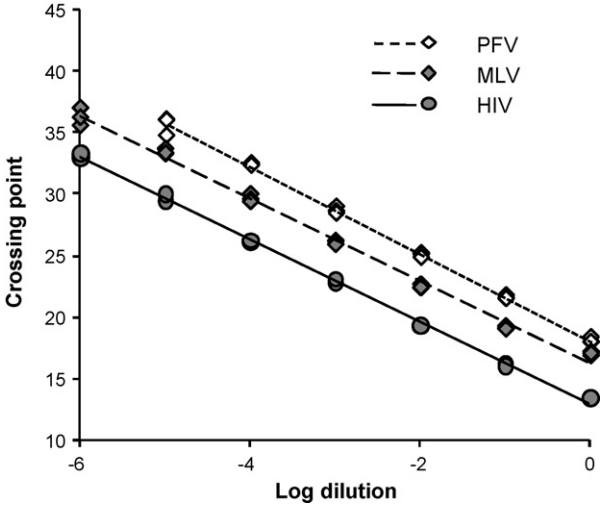


Fig. 4. Detection of divergent retroviruses by SG-PERT. Crossing points and linear regressions obtained with 10-fold serial dilutions of retroviral supernatants performed in triplicate in the lightcycler, using HIV-1_{NL4-3} (infectious titre 4×10^6 i.u./ml), MLV GFP vector (transducing titre of 4.2×10^6 i.u./ml) and PFV GFP vector (transducing titre of 7.4×10^5 i.u./ml).

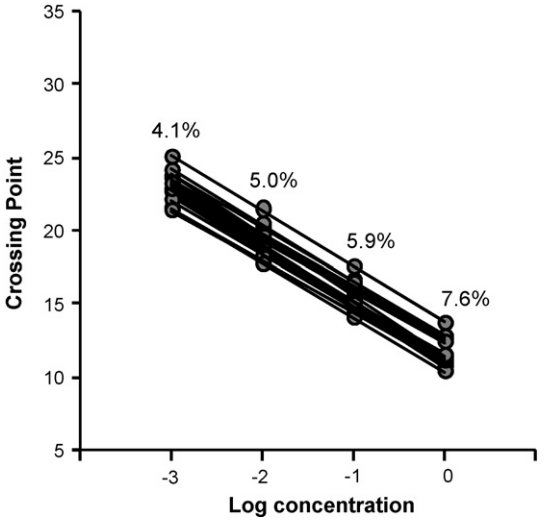


Fig. 5. Intraexperimental variation. Results of 18 SG-PERT independent experiments performed with the lightcycler using the same four HIV-$1_{NL4.3}$ dilutions and three independent lysis and reaction buffer stocks. Coefficient of variation is indicated as percentage of the respective mean crossing point value.

6. Discussion

A SYBR green I-based real-time PERT assay (SG-PERT) for the quantitation and detection of HIV-1 and other divergent retroviruses is described. The assay is linear over six orders of magnitude and requires less than 2 h from sample preparation to data analysis when performed using the lightcycler.

Although PERT was originally established as a two-step assay (Heneine et al., 1995; Lovatt et al., 1999; Maudru and Peden, 1998; Pyra et al., 1994; Yamamoto et al., 1996) the one-step assay, previously proposed using the fluorescent probes techniques (Arnold et al., 1998), adds convenience and minimizes sample handling, which may cause cross-contaminations and decreases quantitative reliability.

Based on the quantitation of viral RNA copies in a cell culture supernatant containing HIV-1 particles, a 1/1500 ratio of infectious units/total HIV-1 particles was established, a value within the range reported in literature (Dimitrov et al., 1993; Kimpton and Emerman, 1992). It was therefore estimated that the SG-PERT assay can detect the presence of three HIV-1 particles in the reaction tube. Because the virus sample represents only 5% of the 20 μl reaction, the assay can reveal RT-activity in HIV-1 supernatants containing 6000 virions or 4 i.u./ml. While this satisfies most needs of a retrovirus research laboratory, the detection capacity of the assay can be increased by the addition of an ultracentrifugation step to concentrate the virus before performing SG-PERT.

The reaction conditions were originally optimised for use with glass capillaries in the lightcycler, which requires the presence of BSA to prevent abstraction of reagents on the glass surface (Teo et al., 2002). However, the same reaction formulation has allowed efficient and quantitative detection of RT activity also with the 7900HT platform, indicating that the protocol described here can be performed with real-time PCR platforms which use plastic tubes instead of glass capillaries. Because the buffers used in this study are entirely home-made, stocks prepared on different occasions might contain small differences which could affect assay efficiency. However, the small inter-assay variation observed between experiments performed using different stocks of lysis and reaction buffers shows that the SG-PERT is reproducible.

While the use of PERT was proposed originally for the detection of retroviruses in clinical specimens (Garcia Lerma et al., 1998; Pyra et al., 1994), undiluted human plasma was found to inhibit potently the one-step SG-PERT (data not shown), suggesting that the assay might not be suitable for analyses of some complex biological samples. However, given its linearity over six orders of magnitude, the simple set-up, the rapid procedure and the low intra- and inter-assay variation, SG-PERT represents an ideal tool for the routine quantitation of retroviruses in cell culture samples. The assay proved also to be a useful tool with which to screen cell lines for retrovirus contamination of tissue cultures (Takeuchi et al., 2008).

This report provides all the information required to perform SG-PERT without the need of acquiring expensive buffers with proprietary formulations. Because the SYBR Green I reagent is relatively inexpensive, the assay described allows significant cost savings compared with the use of most alternative techniques.

6.1. Trouble-shooting

The effects of several chemicals and reagents on the performance of the assay were investigated and are discussed here.

6.1.1. BSA requirement

SYBR Green I is offered currently by different providers in ready-to-use real-time PCR and RT-PCR kits. As the formulation of the reaction mixtures is generally proprietary and, therefore, unavailable, the optimal reaction conditions for the reverse transcription and amplification of BMV RNA in glass capillaries were first investigated using 1 mU of recombinant HIV-1 RT, 5 mM $MgCl_2$ and a 1:20,000 dilution of SYBR Green I, already reported to be compatible with a real-time PCR system (Karsai et al., 2002). After testing numerous buffer formulations, it was established that efficient PCR amplification requires BSA at a final concentration of 0.1 mg/ml (Fig. 6a).

The importance of BSA for the reaction in glass capillaries has been linked to the propensity of the glass surface to sequester some reaction components, such as the taq polymerase (Teo et al., 2002). As shown in Fig. 1, the reaction buffer containing BSA can be successfully used in a real-time PCR platform accepting plastic tubes.

6.1.2. The use of different thermophilic polymerases

Several polymerases from different suppliers were tested. PFU Ultra and PFU Turbo, which are reported to lack RT activity ((Arezi et al., 2003) and products specification from suppliers) could not be adapted to real-time PCR in the light cycler (not shown). Platinum Taq, AmpliTaq Gold, Easy-A performed very efficiently in the light cycler with SYBR Green I, but generated a strong background signal arising early between cycle 20 and 30 in the absence of added retroviral RT activity. Hot-start Taq-polymerase from MBI Fermentas was selected because it consistently failed to reverse transcribe the BMV RNA in 45-cycle PCR reactions.

6.1.3. Concentration and storage of SYBR Green I

Repeated freeze-thaw cycles were avoided by storing multiple aliquots of the SYBR Green I concentrated stock and the 1/100 diluted aliquots used to make the master mix at −80 °C. The reagent was diluted in TE buffer, pH 8.0, as suggested elsewhere (Karsai et al., 2002). More than two freeze-thawing cycles of the 1/100 diluted SYBR Green I aliquots resulted in a significant loss of assay sensitivity (not shown). The assay sensitivity and strength depend on the SYBR Green I concentration. The effects of different dilutions of the dye ranging from 1/60,000 to 1/10,000 (Fig. 6b) were tested. The 1:20,000 dilution was chosen because it combines high sensitivity with a robust signal.

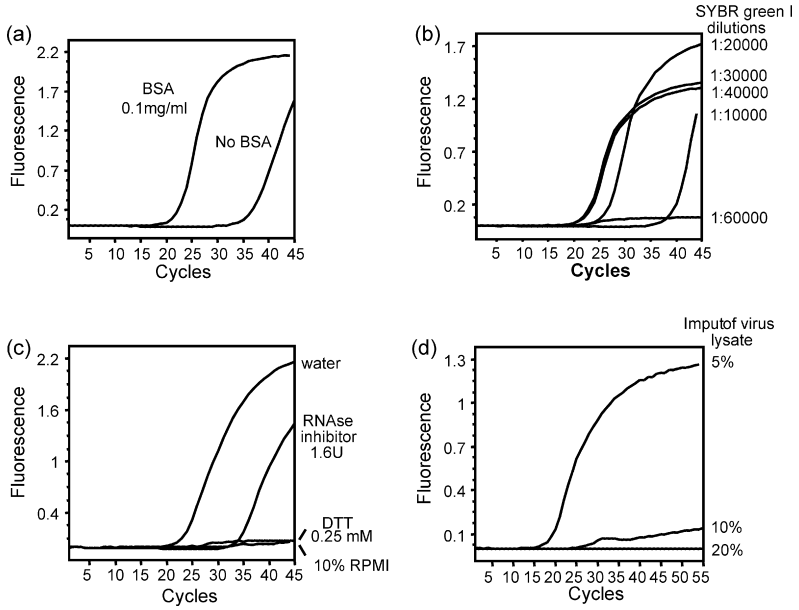


Fig. 6. Crucial effects of different reagents on the assay performance. (a) Positive effect of BSA on the SG-PERT reaction. (b) Performance of the assay with varying SYBR Green I concentrations, as indicated. (c) Inhibitory effects of different components of the virus lysate. (a), (b) and (c) were obtained by testing 1 μU of recombinant HIV-1 RT. (d) Effects of varying amount of virus lysate on the assay performance using HIV-1 NL4-3 containing supernatant. Percentages in (c) and (d) indicate the reagent volume as a proportion of the total reaction volume.

6.1.4. The effect of different components of the virus lysate on the outcome of the assay

After optimising the reaction using recombinant HIV-1 RT, based on previously described protocols (Heneine et al., 1995; Lovatt et al., 1999; Maudru and Peden, 1998; Pyra et al., 1994; Yamamoto et al., 1996), the assay was tested with a suspension of HIV-1 virions lysed in a buffer supplemented with 0.2 U/μl RNAse inhibitor, 1 mM DTT. The assay repeatedly failed to generate any signal, indicating that the virus lysate could contain inhibitory reagents. We tested the effects of single components of the virus lysate on the SG-PERT efficiency using 1 μU of recombinant HIV-1 RT (Fig. 6c). We established that 0.1 mM DTT acts as a powerful inhibitor, in line with previous reports indicating a negative interference with SYBR Green I-based RT-PCR (Lekanne Deprez et al., 2002; Pastorino et al., 2005; Pierce et al., 2002; Varga and James, 2005). The presence of RPMI culture medium in the reaction was also found to affect negatively the assay when it represented 10% of the final reaction volume. Similarly, when 1.6 U of the RNAse inhibitor was present in the 20 μl reaction the assay failed. In contrast, other components of the virus lysates did not significantly affect the performance of SG-PERT. While DTT can be omitted from the RT reaction without loss of enzyme activity (data not shown and Lekanne Deprez et al., 2002), the inhibitory effects of culture medium and RNase inhibitor were avoided by minimizing the amount of virion lysate added to the reaction mix. Given that the presence of RNAse inhibitor is strictly essential, its negative effects were minimized by treating the virion lysate (which represents the main source of RNAses) rather than the total reaction with a concentrated formulation of RNase inhibitor. A robust signal was, therefore, obtained only when the virus lysate was not exceeding 5% of the final reaction volume (Fig. 6d).

6.1.5. Divalent cations

Since efficient reverse transcriptase activity is known to require Mg^{2+}, $MgCl_2$ concentrations ranging from 1.25 to 10 mM were tested and found to have no significant effects on the assay sensitivity (not shown). Although gamma-retroviruses are known to prefer Mn^{2+}, addition of 2 mM $MnCl_2$ to the reaction assay resulted in 100-fold lower efficiency of detection of MLV virus suspensions (not shown).

6.1.6. Absolute quantitation of virus suspensions

For experimental purposes, absolute values of the virus suspensions tested can be retrieved from a standard curve created using known amounts of recombinant RT or serial dilutions of a previously characterized virus stock.

6.1.7. Improved primer design

An alternative set of oligonucleotides (forward: 5′-TAGTTGTTGGGCTTCGCTTT-3′; reverse:5′-TTGTCGGCTTTACCTGCTTT3′) was designed to avoid primer-dimer formation with SG-PERT under the same conditions described in the article. While this modification does not alter the properties of the assay, it further improves the signal generated by low levels of RT activity.

Essential literature references:

- Arnold et al. (1998)
- Chang et al. (1997)
- Lovatt et al. (1999)
- Maudru and Peden (1998)
- Pyra et al. (1994)
- Silver et al. (1993)
- Sears and Khan (2003)

7. Quick procedure

7.1. Sample preparation

- Virus supernatants are harvested, clarified by low-speed centrifugation (400 g) for 10 min and filtered through a 0.45 μm pore filter.
- RNAse inhibitor (0.4 U/μl) is added to 2× virus lysis buffer.
- 5 μl aliquots of 2× lysis buffer are immediately dispensed into 1.5 ml microfuge tubes.

- 5 μl of virus suspensions are added to the tubes and mixed with the 2× lysis buffer.
- Samples are incubated at room temperature for 10 min.

7.2. Reaction set-up (for lightcycler)

- Taq polymerase (0.2 U/reaction) is added to 2× reaction mix.
- Ten microliters aliquots of 2× reaction mix are placed into the reservoir of pre-chilled glass capillaries.
- Virus lysates (10 μl) are diluted with the addition of 90 μl of sample dilution buffer and vortexed.
- Ten microliters of each diluted sample is immediately mixed with the reaction buffer in glass capillaries.
- Capillaries are centrifuged in a microfuge at 3000 rpm for 15 s and inserted into the LightCycler carousel.
- Reaction is performed in the LightCycler using the following parameters:
  - o 30 min RT reaction at 37 °C.
  - o 5 min hot-start Taq activation at 95 °C.
  - o 45 cycles of amplification (5 s denaturation at 95 °C, 5 s annealing at 55 °C, 15 s extension at 72 °C, 7 s acquisition at 83 °C).
  - o Optional melting analysis of PCR products from 60 to 95 °C.

7.3. Data analysis

- Arithmetic background correction and automatic noise band adjustment are performed.
- The maximum number of fit points fitting the linear portion of the curve is added for the calculation of crossing points.
- A standard curve may be obtained using known concentrations of recombinant RT or defined dilutions of a virus suspension to allow absolute quantitation or data comparison between experiments:
  - o A minimum of four standard samples are included in the RT assay.
  - o The threshold line for crossing point calculation is automatically defined by the software in order to minimize errors of the standard curve.

Acknowledgements

We thank Peter Cherepanov and Anna Helander for helpful discussions. The following reagent was obtained through the AIDS Research and Reference Reagent Program, Division of AIDS, NIAID, NIH: TZM-bl from Dr. John C. Kappes, Dr. Xiaoyun Wu and Tranzyme Inc.

References

Adachi, A., Gendelman, H.E., Koenig, S., Folks, T., Willey, R., Rabson, A., Martin, M.A., 1986. Production of acquired immunodeficiency syndrome-associated retrovirus in human and nonhuman cells transfected with an infectious molecular clone. J. Virol. 59, 284–291.

Arezi, B., Xing, W., Sorge, J.A., Hogrefe, H.H., 2003. Amplification efficiency of thermostable DNA polymerases. Anal. Biochem. 321, 226–235.

Arnold, B.A., Hepler, R.W., Keller, P.M., 1998. One-step fluorescent probe product-enhanced reverse transcriptase assay. Biotechniques 25, 98–106.

Bisset, L.R., Boni, J., Lutz, H., Schupbach, J., 2007. Lack of evidence for PERV expression after apoptosis-mediated horizontal gene transfer between porcine and human cells. Xenotransplantation 14, 13–24.

Brorson, K., Swann, P.G., Lizzio, E., Maudru, T., Peden, K., Stein, K.E., 2001. Use of a quantitative product-enhanced reverse transcriptase assay to monitor retrovirus levels in mAb cell-culture and downstream processing. Biotechnol. Prog. 17, 188–196.

Brorson, K., Xu, Y., Swann, P.G., Hamilton, E., Mustafa, M., de Wit, C., Norling, L.A., Stein, K.E., 2002. Evaluation of a quantitative product-enhanced reverse transcriptase assay to monitor retrovirus in mAb cell-culture. Biologicals 30, 15–26.

Chang, A., Ostrove, J.M., Bird, R.E., 1997. Development of an improved product enhanced reverse transcriptase assay. J. Virol. Methods 65, 45–54.

Dimitrov, D.S., Willey, R.L., Sato, H., Chang, L.J., Blumenthal, R., Martin, M.A., 1993. Quantitation of human immunodeficiency virus type 1 infection kinetics. J. Virol. 67, 2182–2190.

Fan, X.Y., Lu, G.Z., Wu, L.N., Chen, J.H., Xu, W.Q., Zhao, C.N., Guo, S.Q., 2006. A modified single-tube one-step product-enhanced reverse transcriptase (mSTOS-PERT) assay with heparin as DNA polymerase inhibitor for specific detection of RTase activity. J. Clin. Virol. 37, 305–312.

Garcia Lerma, J.G., Yamamoto, S., Gomez-Cano, M., Soriano, V., Green, T.A., Busch, M.P., Folks, T.M., Heneine, W., 1998. Measurement of human immunodeficiency virus type 1 plasma virus load based on reverse transcriptase (RT) activity: evidence of variabilities in levels of virion-associated RT. J. Infect. Dis. 177, 1221–1229.

Heinkelein, M., Rammling, M., Juretzek, T., Lindemann, D., Rethwilm, A., 2003. Retrotransposition and cell-to-cell transfer of foamy viruses. J. Virol. 77, 11855–11858.

Heneine, W., Yamamoto, S., Switzer, W.M., Spira, T.J., Folks, T.M., 1995. Detection of reverse transcriptase by a highly sensitive assay in sera from persons infected with human immunodeficiency virus type 1. J. Infect. Dis. 171, 1210–1216.

Karsai, A., Muller, S., Platz, S., Hauser, M.T., 2002. Evaluation of a homemade SYBR green I reaction mixture for real-time PCR quantification of gene expression. Biotechniques 32 (790–792), 794–796.

Khan, A.S., Sears, J.F., 2001. Pert analysis of endogenous retroviruses induced from K-BALB mouse cells treated with 5-iododeoxyuridine: a potential strategy for detection of inducible retroviruses from vaccine cell substrates. Dev. Biol. (Basel) 106 (387–392), 392–393.

Kimpton, J., Emerman, M., 1992. Detection of replication-competent and pseudotyped human immunodeficiency virus with a sensitive cell line on the basis of activation of an integrated beta-galactosidase gene. J. Virol. 66, 2232–2239.

Lekanne Deprez, R.H., Fijnvandraat, A.C., Ruijter, J.M., Moorman, A.F., 2002. Sensitivity and accuracy of quantitative real-time polymerase chain reaction using SYBR green I depends on cDNA synthesis conditions. Anal. Biochem. 307, 63–69.

Lovatt, A., Black, J., Galbraith, D., Doherty, I., Moran, M.W., Shepherd, A.J., Griffen, A., Bailey, A., Wilson, N., Smith, K.T., 1999. High throughput detection of retrovirus-associated reverse transcriptase using an improved fluorescent product enhanced reverse transcriptase assay and its comparison to conventional detection methods. J. Virol. Methods 82, 185–200.

Maudru, T., Peden, K., 1997. Elimination of background signals in a modified polymerase chain reaction-based reverse transcriptase assay. J. Virol. Methods 66, 247–261.

Maudru, T., Peden, K.W., 1998. Adaptation of the fluorogenic 5′-nuclease chemistry to a PCR-based reverse transcriptase assay. Biotechniques 25, 972–975.

Naldini, L., Blomer, U., Gallay, P., Ory, D., Mulligan, R., Gage, F.H., Verma, I.M., Trono, D., 1996. In vivo gene delivery and stable transduction of nondividing cells by a lentiviral vector [see comments]. Science 272, 263–267.

Neil, S., Martin, F., Ikeda, Y., Collins, M., 2001. Postentry restriction to human immunodeficiency virus-based vector transduction in human monocytes. J. Virol. 75, 5448–5456.

Pastorino, B., Bessaud, M., Grandadam, M., Murri, S., Tolou, H.J., Peyrefitte, C.N., 2005. Development of a TaqMan RT-PCR assay without RNA extraction step for the detection and quantification of African Chikungunya viruses. J. Virol. Methods 124, 65–71.

Pierce, K.E., Rice, J.E., Sanchez, J.A., Wangh, L.J., 2002. QuantiLyse: reliable DNA amplification from single cells. Biotechniques 32, 1106–1111.

Pietschmann, T., Heinkelein, M., Heldmann, M., Zentgraf, H., Rethwilm, A., Lindemann, D., 1999. Foamy virus capsids require the cognate envelope protein for particle export. J. Virol. 73, 2613–2621.

Pizzato, M., Blair, E.D., Fling, M., Kopf, J., Tomassetti, A., Weiss, R.A., Takeuchi, Y., 2001. Evidence for nonspecific adsorption of targeted retrovirus vector particles to cells. Gene Ther. 8, 1088–1096.

Pyra, H., Boni, J., Schupbach, J., 1994. Ultrasensitive retrovirus detection by a reverse transcriptase assay based on product enhancement. Proc. Natl. Acad. Sci. U. S. A. 91, 1544–1548.

Sastry, L., Xu, Y., Duffy, L., Koop, S., Jasti, A., Roehl, H., Jolly, D., Cornetta, K., 2005. Product-enhanced reverse transcriptase assay for replication-competent retrovirus and lentivirus detection. Hum. Gene Ther. 16, 1227–1236.

Sears, J.F., Khan, A.S., 2003. Single-tube fluorescent product-enhanced reverse transcriptase assay with Ampliwax (STF-PERT) for retrovirus quantitation. J. Virol. Methods 108, 139–142.

Silver, J., Maudru, T., Fujita, K., Repaske, R., 1993. An RT-PCR assay for the enzyme activity of reverse transcriptase capable of detecting single virions. Nucleic Acids Res. 21, 3593–3594.

Soneoka, Y., Cannon, P.M., Ramsdale, E.E., Griffiths, J.C., Romano, G., Kingsman, S.M., Kingsman, A.J., 1995. A transient three-plasmid expression system for the production of high titer retroviral vectors. Nucleic Acids Res. 23, 628–633.

Takeuchi, Y., McClure, M.O., Pizzato, M, 2008. Identification of gamma-retroviruses constitutively released from cell lines used for HIV research. J. Virol. 82 (24).

Teo, I.A., Choi, J.W., Morlese, J., Taylor, G., Shaunak, S., 2002. LightCycler qPCR optimisation for low copy number target DNA. J. Immunol. Methods 270, 119–133.

Varga, A., James, D., 2005. Detection and differentiation of Plum pox virus using real-time multiplex PCR with SYBR Green and melting curve analysis: a rapid method for strain typing. J. Virol. Methods 123, 213–220.

Voisset, C., Tonjes, R.R., Breyton, P., Mandrand, B., Paranhos-Baccala, G., 2001. Specific detection of RT activity in culture supernantants of retrovirus-producing cells, using synthetic DNA as competitor in polymerase enhanced reverse transcriptase assay. J. Virol. Methods 94, 187–193.

Yamamoto, S., Folks, T.M., Heneine, W., 1996. Highly sensitive qualitative and quantitative detection of reverse transcriptase activity: optimization, validation, and comparative analysis with other detection systems. J. Virol. Methods 61, 135–143.

nature COMMUNICATIONS

OPEN

ARTICLE

Received 20 Apr 2010 | Accepted 23 Sep 2010 | Published 19 Oct 2010

DOI: 10.1038/ncomms1100

B-cell depletion reveals a role for antibodies in the control of chronic HIV-1 infection

Kuan-Hsiang G. Huang[1,*], David Bonsall[2,*], Aris Katzourakis[3], Emma C. Thomson[2], Sarah J. Fidler[2], Janice Main[2], David Muir[2], Jonathan N. Weber[2], Alexander J. Frater[1], Rodney E. Phillips[1], Oliver G. Pybus[3], Philip J.R. Goulder[1], Myra O. McClure[2], Graham S. Cooke[2,†] & Paul Klenerman[1,†]

HIV can be partially contained by host immunity and understanding the basis of this may inform vaccine design. The importance of B-cell function in long-term control is poorly understood. One method of investigating this is *in vivo* cellular depletion. In this study, we take advantage of a unique opportunity to investigate the role of B cells in an HIV-infected patient. The HIV-1$^+$ patient studied here was not taking antiretroviral drugs and was treated for pre-existing low-grade lymphoplasmacytoid lymphoma by depletion of CD20+ B cells using rituximab. We demonstrate that B-cell depletion results in a decline in autologous neutralizing antibody (NAb) responses and a 1.7 $\log_{10}$ rise in HIV-1 plasma viral load (pVL). The recovery of NAbs results in a decline in pVL. The HIV-1 sequences diversify and NAb-resistant mutants are subsequently selected. These data suggest that B-cell function can contribute to the long-term control of pVL, and that NAbs may be more important in controlling chronic HIV-1 infection than previously suspected.

[1] Nuffield Department of Medicine and NIHR Biomedical Research Centre, Oxford Martin School, Peter Medawar Building for Pathogen Research, University of Oxford, South Parks Road, Oxford OX1 3SY, UK. [2] Jefferiss Research laboratories, Faculty of Medicine, Imperial College London, St Mary's Campus, Norfolk Place, London W2 1PG, UK. [3] Department of Zoology, University of Oxford, South Parks Road, Oxford OX1 3SY, UK. *These authors contributed equally to this work. †These authors contributed equally to this work. Correspondence and requests for materials should be addressed to P.K. (email: paul.klenerman@ndm.ox.ac.uk).

© 2010 Macmillan Publishers Limited. All rights reserved.

HIV-1 is readily able to evade host defence and establish persistent infection. The virus may, however, be partially contained by host adaptive immunity, including both B- and T-cell responses. There is good evidence that CD8+ T-cell responses have a role in viral suppression. For example, there are strong HLA class I associations with clinical outcome[1], and in the SIV model, macaques in whom CD8+ T cells are depleted show significant increases in their viral load[2]. These findings have led to a major initiative to develop T-cell-based vaccines, and much work to define the correlates of protection based on assays of T-cell function[3,4]. However, as a leading HIV vaccine candidate failed to induce protective T-cell responses[5] and recent trial data suggest partial protection from a vaccine including a gp120 component[6], the incentive to understand the role of neutralizing antibodies (NAbs) and of B cells in HIV infection has increased considerably[7–9].

B cells have a multifaceted role in humoral and cellular responses to HIV-1, yet their impact in containing the virus remains unclear. This is partly because of the complex nature of the antigenic target (gp120)[10]. Key obstacles to the development of both T- and B-cell defence are the abilities of the HIV-1 genome to integrate and also evolve rapidly in the face of immune selection pressure: the latter feature results from both the high replication rate of the virus and the error-prone nature of the HIV-1 reverse transcriptase, which lacks proofreading capacity[11]. These mutations are readily accommodated within gp120 because of plasticity of the structure and the capacity to acquire glycosylation sequons that provide a 'glycan shield'[12]. Therefore, emerging NAbs repeatedly select mutant viruses that are resistant to neutralization[13]. The NAb response also evolves through somatic recombination and affinity maturation of proliferating B cells, but is only partially effective against concurrently circulating viruses, while retaining potent activity against strains previously circulating within the patient[13–15]. Such data have cast doubt on the contribution of NAbs to the control of virus load, despite the counterargument that NAbs must inhibit virus replication to drive the selection of resistant variants.

Monoclonal antibodies have been identified that both cross-recognize and potently neutralize a variety of HIV-1 strains[16–19]. The targets for these are well defined and include, among others, CD4 and co-receptor binding sites and epitopes within the gp41 fusion subunit[20]. These areas are under some structural constraint compared with other epitopes, such as in the exposed variable loops. Few potent monoclonal antibodies have been isolated, yet the proportion of gp120-specific antibodies capable of neutralization may be greater than once believed[8,21]. Recent studies indicate that some individuals possess NAbs that exhibit broad and potent neutralization capacity[18,21,22], but functional data to causally link such antibodies to the control of viremia are lacking. Furthermore, the contribution of B-cell responses to the containment of plasma viral load (pVL) has been difficult to determine, because of other important factors that limit virus replication, such as T-cell response, virus fitness and host genetics[23].

Historically, functional importance has been confidently attributed to specific arms of the immune response by means of experiments that deplete or transfer that effector arm. Although such data are readily available in animal models, they are rarely available in humans. As recent vaccine studies have highlighted substantial differences between SIV models and HIV, it is important to seek such evidence in human studies.

Rituximab (Rituxan, MabThera; Roche) is a monoclonal antibody targeting CD20 antigen expressed on most B cells, with the exception of the terminally differentiated plasma cells. It has become widely used for treatment of lymphoma and also of antibody-mediated autoimmune diseases[24]. We report a unique case in which rituximab monotherapy was used in a patient with stable viraemia, in the absence of antiretroviral therapy (ART).

By combined analyses of viral dynamics, viral evolution and autologous NAb responses, we show reversible loss of HIV-1 control following rituximab monotherapy. Loss of control was associated with reduction in titres of NAbs targeting the CD4 binding site, as well as with an increase in genetic diversity and transient reversion to NAb-sensitive virus. As NAb levels later increased, pVL was once more controlled and this was accompanied by further immune selection of NAb-resistant viruses. These data suggest that despite ongoing immune escape, NAbs secreted by CD20+ B cells may have a significant role in control of pVL during chronic HIV-1 infection, a finding of significance for HIV-1 immunotherapies and vaccines.

Results

Clinical course of the study subject. The patient, a Caucasian man, was diagnosed with HIV seroconversion illness at the age of 58 years. Three years earlier, he was diagnosed with low-grade lymphoplasmacytoid lymphoma, for which he did not receive treatment[25]. Histologically, this was defined as a small lymphocytic B-cell lymphoma with plasmacytoid differentiation mostly expressing CD20 and CD79. The tumour was IgM secreting. His only other medical history of note was an acute hepatitis B infection approximately 30 years earlier. Following HIV-1 seroconversion, the patient was recruited into a prospective, non-randomized observational study of early treatment and received 3 months of highly active antiretroviral therapy[26]. After 30 months, he developed a rising paraproteinaemia, attributed to his lymphoma, and received thalidomide treatment without clinical effect. He initiated rituximab therapy 1,075 days after HIV seroconversion and received four weekly doses (375 mg m^{-2}). He felt unwell 20 weeks after the first dose of rituximab with malaise and fever associated with a marked rise in HIV pVL (increase of 1.7 log_{10}; Fig. 1). In addition, he developed

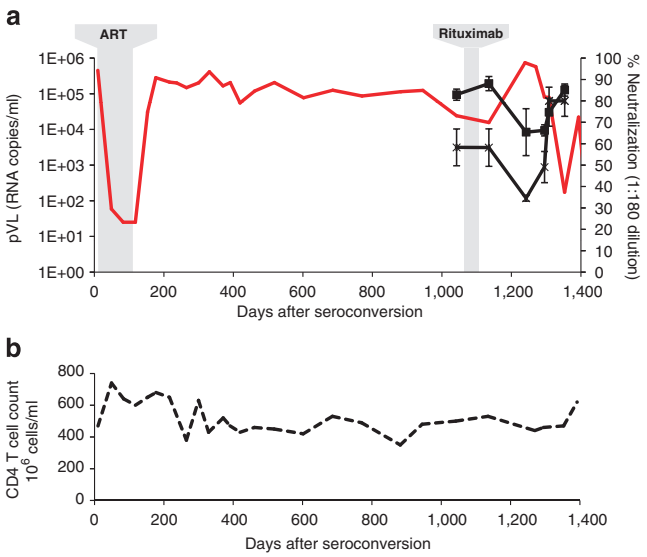


Figure 1 | Autologous neutralizing antibody titres over time. (**a**) Pseudotyped virus particles were constructed using full-length envelope clones that represent majority quasi-species at 336 or 1,042 days after seroconversion. Plasma VL over time is indicated (red line). The brief dip in viral load over the first 100 days represents the period of initial ART as part of the short-course ART trial (shaded grey). The neutralizing effects (%; right *y* axis) of patient sera are shown for autologous viruses constructed with cloned *env* genes derived 336 days (black squares) and 1,042 days (crosses) after seroconversion. Results from a single clone (tested in triplicate) representative of three clones are shown. Serum was sampled sequentially before and after rituximab therapy (1,075–1,106 days, shaded grey), and assayed at concentrations ranging from 1:20 to 1:4,370; the neutralizing effects of sera diluted 1:180 are shown here. Error bars show standard deviations of triplicate tests. (**b**) CD4 T lymphocyte count (dashed line) is shown over time.

© 2010 Macmillan Publishers Limited. All rights reserved.

biochemical hepatitis (attributed to reactivation of hepatitis B) that resolved with only supportive treatment. Antiretrovirals were initiated 1,392 days after seroconversion.

Impact of B-cell depletion on NAb titres. Following rituximab therapy, the subject's HIV-1 pVL, previously stable, increased by more than 1.7 $\log_{10}$, peaking at 737,400 copies per ml 4 months after the final dose of rituximab (Fig. 1). The pVL subsequently returned to baseline levels in the absence of ART. We therefore analysed the impact of rituximab therapy on NAb titres in relation to viral dynamics.

Rituximab therapy led to a 30% reduction in total IgG levels, which reached their lowest point at the peak of virus load (10.8 $g\,l^{-1}$; normal range 8–16 $g\,l^{-1}$) and returned to pre-rituximab levels thereafter (Supplementary Table S1). To evaluate NAb activity throughout this period, we generated pseudoviruses derived from autologous *envelope* (*env*) sequences. Serum obtained before the first dose of rituximab potently neutralized virus pseudotyped with autologous envelope derived from plasma acquired 2 years previously (day 336 after seroconversion) (Table 1). The same serum neutralized contemporaneous autologous Env pseudotypes, although to a lesser extent, with 1:60 serum dilutions effectively blocking more than 90% infection. Heterologous NAb activity was also observed against HXB2 and 8/12 Tier 2/3 clade-B reference strains (NIH, AIDS) (Table 2). Following rituximab therapy, we observed a marked decrease in neutralizing activity characterized by a drop of more than threefold in IC_{50} serum titres against day 336 Env pseudotypes, which recovered over a 4-month period. Strikingly, these changes coincided with the increase in pVL. Recovery of NAb responses correlated with control of viraemia (Fig. 1).

Analysis of sequence evolution in HIV-1 envelope over time. To evaluate sequence evolution over this period, *env* products were generated by reverse transcription (RT)–PCR from plasma viral RNA, before and after rituximab therapy (days 1,075–1,392; Fig. 2a). We identified clear sequence diversification as the virus peaked during rituximab treatment (mean genetic distance = 0.02 versus 0.004; $P < 0.0001$). This diversification manifested as an increase in effective population size as measured using BEAST[27] (fivefold change; Fig. 2b). To assess whether these diverse strains represented a re-emergence of archived provirus, we used an identical sequencing strategy to analyse stored peripheral blood mononuclear cell (PBMC) samples available from the time of seroconversion up to day 1,042; these sequences were placed on a time-structured tree (Supplementary Fig. S1). Viruses detected after rituximab treatment did not represent re-emergence of early archived strains; those strains present as pVL peaked were most closely related to strains present in plasma at day 1,042, with a subset related to those archived in PBMC at day 1,042.

Immune selection and neutralization of HIV-1 envelope. The apparent *in vivo* impact of the NAbs in this individual prompted a search for the targets of binding. To identify potential NAb targets, we first analysed immune selection using CODEML, analysing the ratio of non-synonymous to synonymous mutations (dN/dS) at each site. We observed two sites under selection (Fig. 3; Supplementary Fig. S1)—position 339 ($dN/dS = 7.6$, $P < 0.0001$) and position 363 ($dN/dS = 6.977$, $P = 0.03$). Residue 363 lies between the β14 and β15 anti-parallel strands of gp120 and is exposed on the surface of the outer domain in close proximity to the CD4 binding loop[28]. Computational modelling of atomic level envelope structures has shown that mutations proximal to the CD4-binding loop are critical in conferring resistance to CD4bs antibodies[29]. Furthermore, site-directed mutagenesis of site 363 has previously been shown to affect neutralization of the CD4bs antibodies M-14 and b12[30,31]. Before the first dose of rituximab (day 1,042 after seroconversion), position 363 was occupied by an arginine in all viral RNA sequences, whereas all proviral DNA clones sampled up to and including day 1,042 had a glutamine at the same position. Following rituximab therapy, R363 variants were temporarily replaced with Q363 variants, which reverted to arginine residues as NAb titres rebounded and viraemia was controlled.

Before rituximab therapy, an asparagine at site 339 formed part of an *N*-linked glycosylation site. This residue is located within the α3 helix, which is exposed on the surface of the protein according to atomic level structures. A previous study showed that site 339 is involved in recognition by 2G12, a monoclonal antibody the binding of which is carbohydrate dependent[32]. However, in addition to this, mutations at site 339 have been reported to affect binding by monoclonal antibody b12: this effect is observed despite site 339 being some distance away from the CD4 binding site, and potentially occurs through conformational perturbation[32]. No other sites in the envelope were found to be under positive selection, indicating that mutations at these positions affected NAb binding.

To examine the effect of sequence changes on neutralization susceptibility, pseudoviruses mimicking Q363R and R339N/E were constructed by site-directed mutagenesis. The selected Q363/339E mutation reduced the IC_{50} titres of day 1,042 serum by more than twofold (IC_{50} from >775 to 300). Confirming previous data, the Q363R mutation was also shown to inhibit neutralization by fivefold by antibody b12[31], whereas N339E inhibited neutralization susceptibility by fourfold to the carbohydrate-specific antibody 2G12[12,32].

To further define the site of binding of the patient's NAbs, we performed a direct competition experiment using well-defined monoclonal antibodies and recombinant clade B envelope as the antigenic target (Fig. 4). This experiment showed strong binding competition between patient sera and antibodies b12, 4.8d (which targets an epitope overlapping with the co-receptor binding site) and 447-52D (which targets the V3 loop). No competition was observed against 2G12. The experiment also revealed a clear decline in competition for binding in samples taken during the peak of viraemia, which recovered as pVL declined, in good accordance with the data obtained from the neutralization experiments, but using an independent system of evaluation (Fig. 4b).

Table 1 | IC_{50} neutralizing titres against autologous viruses.

Serum (day)	D336 pseudovirus	D1042 pseudovirus	HXB2	VSV-G
1,042	>775	150	850	<20
1,135	>775	225	1000	N/T
1,239	220	<120*	875	20
1,295	250	150	325	20
1,308	360	375	1000	<20
1,353	600	425	3950	N/T
Negative serum	<20	<20	<20	N/T

Abbreviations: N/T, virus-serum combinations that were not tested because of limited availability of sera; VSV-G, vesicular stomatitis virus control.
The mean half maximal inhibitory concentrations of sera (IC_{50}, reciprocal dilutions) are given for three viruses pseudotyped with representative Env clones derived from d336 and d1042 plasma (autologous).
*1:120 was the highest concentration of day 1,239 serum that could be tested against day 1,042 virus due to limited serum availability.

© 2010 Macmillan Publishers Limited. All rights reserved.

Table 2 | IC_{50} neutralizing titres against heterologous viruses.

Serum (day)	HXB2	6535	QH0692	PVO	TRO	AC10.0	pREJO 4541	pTRJO 4551	pRHPA 4259
1,042	850	220	220	90	120	90	140	50	50
1,353	3950	300	170	90	130	160	220	140	120
Negative	<20	20*	<20	<20	<20	<20	20*	20*	<20

The mean half-maximal inhibitory concentrations of sera (IC_{50}, reciprocal dilutions) are given for pseudoviruses derived from a standardized reference panel (NIAID, NIH) (heterologous). Reductions in infected TZM-bl cells by pooled HIV-negative sera (*) were attributed to cellular toxicity which was not observed at concentrations below 1:20.

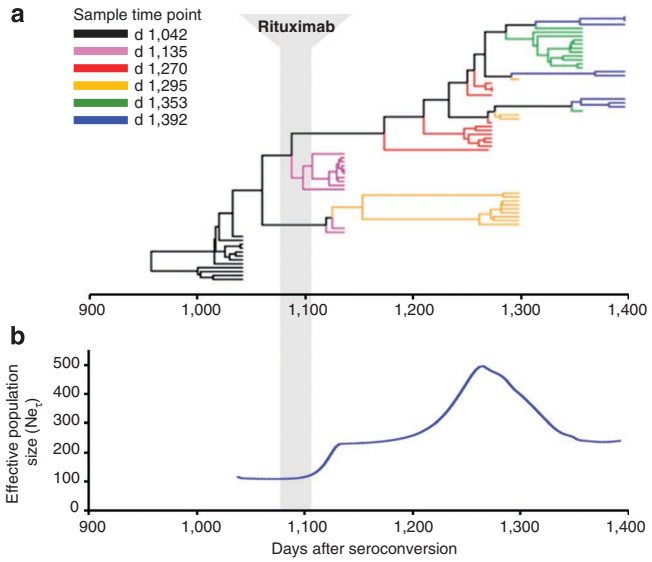


Figure 2 | Diversification of HIV-1 env sequences after rituximab therapy. (**a**) A time-structured tree, showing divergence-time estimates among intra-host plasma HIV-1 clonal sequences before and after rituximab therapy (shaded grey), based on a Bayesian relaxed molecular clock applied to 969 nucleotides[58]. The external nodes represent sequences taken from time points indicated by the colours given in the figure key (inset). The topology is of the highest likelihood calculated using BEAST, with branch lengths proportional to time estimates for the subtending nodes (summarizing 60 million Markov chain Monte Carlo (MCMC) simulations, generated after discarding 6 million as burn-in). All the parameters in the MCMC started from random values, except for substitution rates and population size, where the priors were imported from the combined proviral and plasma viral sequence data of the same host calculated by BEAST software. (**b**) The effective population sizes (Ne_t) were calculated using BEAST. The *x* axis (days after seroconversion) is the same as for Figure 2a[59].

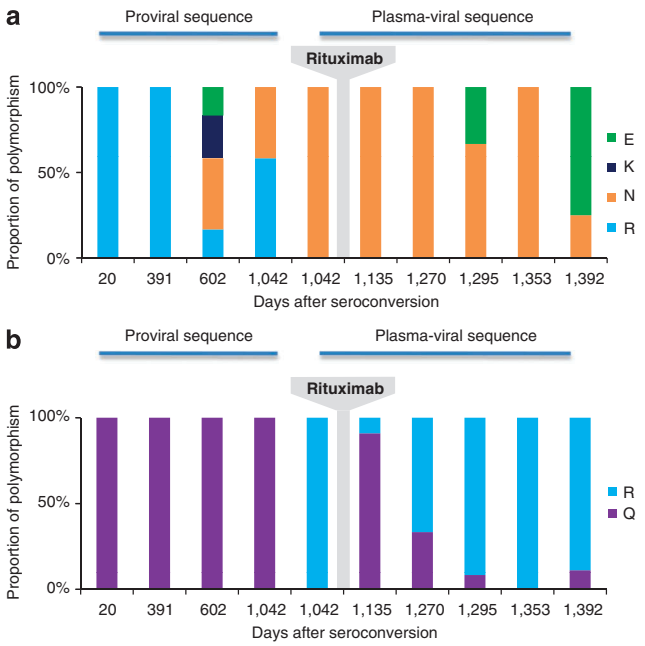


Figure 3 | Tracking of selected envelope mutants. This figure shows the relative frequencies of polymorphisms at sites (**a**) 339, $dN/dS = 7.61$ $P < 0.0001$ and (**b**) 363 $dN/dS = 6.98$ $P < 0.031$. The individual bars along the *x* axis represent the different time points of sequencing (comparable to Fig. 2; Supplementary Fig. S1): these are taken either from proviral DNA samples (days 20–1,042) or from plasma samples (days 1,042–1,392). The time of rituximab therapy is indicated. Each bar shows the frequency of mutations at these positions, the key depicts the different amino-acid residues detected.

Analysis of other potential effects of rituximab. We investigated other possible causes for the observations made, particularly the possibility of an indirect impact on cellular immunity[33]. We analysed the sequence of key CTL epitopes over time, and carried out interferon-γ (IFN-γ) ELISpot analyses. Although some mutations in pre-rituximab sequences were observed, the majority of the epitopes remained stable (Table 3). It is of importance that control over pVL was regained without further escape/reversion at these sites.

Second, immune activation through recrudescence of other infectious agents may have a role in this case. Concurrent with the pVL increase, the patient also developed elevated liver transaminases, associated with reactivation of previously controlled hepatitis B virus (HBV) infection[34]. However, control of HIV was observed at a time when HBV load was still high, suggesting that HBV replication *per se* was not driving HIV replication (up to day 1,389; Supplementary Fig. S2) in this patient. In the setting of acute illness, there was no evidence of EBV, HHV-6, HHV-8 or HCV in blood. Cytomegalovirus was present only at low copy number (50 copies per ml). A bronchoalveolar lavage was tested for a broad panel of relevant viruses, all of which were negative, including VZV and HSV1/2. Clearly, these data do not exclude reactivation of a further latent infection, or concurrent superinfection, although the major herpesvirus infections appear unlikely to be contributing significantly.

Discussion

In this study, B-cell depletion led to a decline in NAb titres against HIV, concurrent with rising pVL. Recovery of NAb titres coincided with control over viral load. Multiple analytical techniques were used to longitudinally characterize the distinct virus population that emerged as NAbs returned. The common ancestor of this new virus population was defined by polymorphisms at two residues exposed on the surface of the virus envelope, both of which showed evidence of positive selection, with mutations affecting binding of NAbs.

There are no published studies on the impact of rituximab alone on HIV viraemia in humans. Studies on acute SIV_{mac} infection in macaques treated with rituximab indicate a role for NAb responses in containing post-acute viral load[35,36]. In contrast, a recent study

© 2010 Macmillan Publishers Limited. All rights reserved.

using African Green monkeys did not reveal any effect of rituximab treatment during acute SIV_{agm} infection[37]; thus, data from human studies are important to resolve this issue.

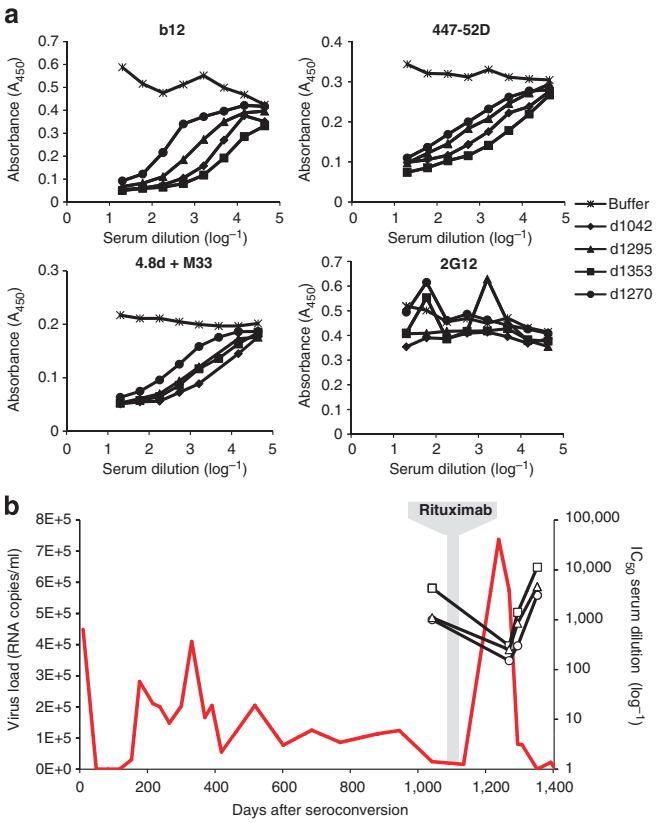


Figure 4 | Characterization of patient antibodies by competition ELISA. (**a**) Serial dilutions of patient serum (*x* axes) collected on days 1,042 (filled diamonds), 1,270 (filled circles), 1,295 (filled triangles) and 1,353 (filled squares) after seroconversion reduced gp120 binding with NAbs b12, 447-52D and 4.8d, thereby reducing colorimetric change and light absorption (A_{450nm}, *y* axes). Pooled serum collected from HIV-uninfected subjects (stars) did not compete with any NAb for gp120 binding. All sera failed to compete with 2G12 for gp120 binding. (**b**) The reciprocal dilutions of sera, sampled before and after rituximab therapy, which reduce gp120-NAb binding by 50% (IC_{50}, right *y* axis). Hundred percent binding was taken as that observed in microtitre wells containing IgGb12 (empty squares), 4.8d (empty triangles) or 447D (empty circles) in the absence of patient sera. Corresponding VLs are shown by the red line (left *y* axis).

It is possible that depletion of B cells had an indirect impact on viral load through modulation of CD4+ or CD8+ T-cell subsets. Although we cannot exclude this, the mechanism for such an indirect effect is not clear and, importantly, no impact on CD8+ T-cell responses has been observed in the SIV models quoted above[36]. The delay of several weeks that is observed between rituximab treatment and the change in viral load is much more consistent with the observed decline in antibody titres than a direct B-cell/T-cell interaction, which would be expected to take effect immediately. In addition, the changes in the prevailing sequence (reversion and subsequent re-selection of a mutated NAb epitope; Figs 2, 3; Supplementary Fig. S1) are consistent with relaxation and re-application of NAb-mediated selection pressure.

The impact of other reactivating viruses on HIV load is complex. As in this case, rituximab treatment is known to have the potential to reactivate HBV[38], even in those with previously controlled infection (HbsAg−, HBcoreAb+). This points to an important role for B cells in long-term control of HBV—a virus in which CD8+ T cells have an important role in acute disease[39]. The relationship between HBV pVL and HIV pVL is not fully understood, but overall these appear to be independent[40,41]. In this case, HBV and HIV pVL increased within a similar timeframe; however, control over HIV occurred spontaneously, whereas HBV load remained high, indicating that they were differentially regulated in this patient (Supplementary Fig. S2). However, this does not exclude a secondary impact of HBV through induction of liver inflammation or other consequences of immune activation. In addition, although we did not find other evidence of systemic reactivation of other major pathogens in this individual, it remains possible that local or low-level reactivation could also affect HIV pVL.

Overall, our findings support previous suggestions of an evolutionary balance between virus and NAbs[12,42]. At first sight, these findings appear at odds with previous studies that fail to confirm an association between long-term virus control and NAb response, especially in elite controllers[43]. However, as shown here, the dynamics of immune responses are critical to their interpretation; therefore complex relationships could easily be missed in cross-sectional studies, especially analyses of those with favourable CD8+ T-cell responses[1,43,44].

There is a clear relationship between the changes in NAb titre and pVL demonstrated in this study, although the mechanism of action of such NAbs *in vivo* may be complex. Studies using engineered antibodies in which Fc binding was disrupted have shown that interactions of NAbs with infected cells, leading to engagement of effector cells, may provide an important component of the protective capacity *in vivo*[45,46]. It is also possible that other non-NAb specificities not defined using *in vitro* NAb assays might have a role *in vivo*[47]. It is noteworthy that as B-cell responses to HIV envelope

Table 3 | Analysis of CD8+ T cell responses and epitope evolution over time.

Epitope	Autologous sequence	Response pre-rituximab Year 1	Response pre-rituximab Year 3	Mutation pre-rituximab	Mutation post-rituximab
A11 gag TK8	TLYCVHQK	1,200	—	K8N	Q7A
A11 pol AK11	ACQGVGGPGHK	300	—	—	G9A
A11 nef QK10	QVPLRPMTYK	—	—	—	—
A11 pol AK9	AIFQCSMTK	—	—	—	—
B8 gag p17 GK9	GGSKKYQLK	—	—	K3R/K7Q	K3R/K7Q
B8 gag p17 EV9	ELKSLYNTV	160	200	—	—
B8 gag p24 DI8	DIYKRWII	640	600	—	—
B8 gag p24 DL9	DCKTILKAL	—	—	—	—
B8 nef WM9	WPKVRERM	—	—	K3G/E6D	K3R
B8 nef FL8	FLKEKGGL	—	—	K5Q	K5Q
B57 gag TW10*	TSNLQEQIGW*	—	—	N3T (242)*	N3T (242)*

CD8+ T cell responses were analysed using *ex vivo* IFN-γ-ELISpot analysis (spot forming units/million PBMCs are shown). The HLA Class IA and Class IB genotypes are A0101, A1101 and B0801, B0801. Sequencing of the corresponding peptides was carried out at the time points shown, and mutating residues have been underlined.
*This epitope is a B57 escape mutant, transmitted to, but not recognized by the recipient, and which shows reversion pre-rituximab therapy.

© 2010 Macmillan Publishers Limited. All rights reserved.

may be poorly sustained, it has been proposed that long-term plasma cell pools may not be established (reviewed in refs 48,49). As plasma cells are spared the effects of rituximab[50] (and total IgG levels therefore remain relatively less affected), it is suggested that the antiviral NAbs identified here, and potentially elsewhere, are maintained by B-cell populations that express CD20.

In conclusion, this unique study suggests that B cells, and their secreted NAbs, can affect HIV viral load in chronic infection. This evidence, derived directly from observations in man, may inform the rational design of future immunotherapies and HIV vaccines.

Methods

Construction of HIV-1 *env* expression cassettes. The study was approved according to local ethical review (IRB Number 99/IA/161E). Full-length virus *env* was PCR amplified from cDNA obtained by RT of plasma-derived viral RNA collected 336 and 1,042 days after seroconversion for construction of pre-rituximab Env-pseudotyped virus. The latter time point represented virus present around the time of rituximab treatment. The primers used were *env*1A (outer sense, 5′-CACCGGCTTAGGCATCTCCTATGGCAGGAAGAA3′), *env*1M (outer antisense and RT, 5′-TAGCCCTTCCAGTCCCCCCTTTTCTTTTA-3′)[51], *env*F1/2 (inner sense, 5′-GGGCTCGAGACCGGTGAGCAGAAGACAGTGGCAATG(±A)-3′) and *env*R1/2 (inner antisense, 5′-AAATCTAGAGGGCCCCCATTGCCACCCATBTTA(±TAGC)-3′). Bulk PCR products were restriction-cloned into pcDNA3.1 (Invitrogen) using sites *Apa*I and *Xho*I to result in pcDNA3.1.*env*, followed by sequencing. Of 20 genetically distinct clones that were most representative of the consensus sequence, 3 were selected for neutralization experiments.

Site-directed mutagenesis. Where stated, 100 ng pcDNA3.1.*env* was used as a template for PCR amplification using PfuUltraII Fusion HS (Stratagene) in the supplied buffer supplemented with 250 μM dNTPs and 3% dimethylsulphoxide. Mutagenesis primers contained restriction sites inserted by synonymous mutation (underlined): R339Nf (5′-ATTGTAACATTTCTCGAGTAGAATGGAATGACACCTTAA-3′), R339Nr (5′-TTAAGGTGTCATTCCATTCTACTCGAGAAATGTTACAAT-3′), R339Ef (5′-ATTGTAACATTTCTAGAGTAGAATGGGAAGACACCTTAA-3′), R339Er (5′-TTAAGGTGTCTTCCCATTCTACTCTAGAAATGTTACAAT-3′), Q363Rf (5′-TAAAACAATAATCTTTAATCGATCCTCAGGA-3′) and Q363Rr (5′-TCCTGAGGATCGATTAAAGATTATTGTTTTA-3′). After 18 amplification cycles (95 °C for 50 s, 60 °C for 50 s and 68 °C for 9 min), *dam*-methylated PCR templates were eliminated by *Dpn*I restriction digestion. Mutant clones were identified by restriction analysis and confirmed by nucleotide sequencing. Double mutants were constructed by sequential PCR amplifications.

Construction and neutralization of Env-pseudotyped virus particles. Autologous *env* clones and a heterologous panel of subtype-B reference strains[52] were co-transfected with the HIV-1 backbone nl4.3Δ*env*[53] into 293T-17 human epithelial kidney cells using Lipofectamine 2000 (Invitrogen). At 48 h following transfection, supernatants were collected by 0.45-μm filtration and stored at −150 °C before titration onto the HIV-permissive reporter cell line, TZM-bl, which stably expresses *Escherichia coli* β-galactosidase under regulatory control of a Tat-responsive HIV-1 long terminal repeat. Cells were fixed with glutaraldehyde (0.2%) and stained with X-gal substrate 48 h after infection. After staining, infected cells formed 'blue' focus-forming units, which were counted under light microscopy to determine the virus titre. Autologous Env-pseudotyped virus was confirmed to be R5 tropic by titration onto $CD4^+CCR5^+$ and $CD4^+CXCR4^+$ GHOST cell lines, which express green fluorescence protein in response to viral Tat.

For neutralization experiments, pseudotyped virus was incubated for 1 h with a threefold dilution series of heat-inactivated serum, or with broadly specific NAbs (b12 or 2G12)[12]. After 48 h, fixed and stained cells were manually counted and neutralization was measured as the percentage reduction of focus-forming units relative to non-neutralized virus controls. Samples were prepared in triplicate microtitre wells and counts were verified by separate investigators (DB and ET).

Competitive binding assays. Antibody specificity was mapped using a competitive-binding enzyme-linked immunosorbent assay (ELISA). High-binding microtitre plates (Greiner) were coated overnight with recombinant Bal-strain gp120 and blocked with 2% milk powder to limit non-specific antibody binding. Each plate received threefold dilution series of patient sera and was incubated with 50% saturating titres of biotinylated NAbs (b12, 2G12, 447-52D). An additional plate was pre-incubated with the CD4 peptide mimic M33 before incubation with biotinylated NAb 4.8d[54]. Bound NAb was detected with streptavidin horseradish peroxidase and TMB chromogen substrate. Serum-mediated inhibition of NAb binding was determined as the percentage reduction in light absorbance ($A_{450\,nm}$) compared with wells that received dilution buffer (PBS 0.05% Tween 20, 1% bovine serum albumin) instead of serum.

ELISpot for interferon-γ secreting CD8+ T cells. This was performed using panels containing optimized HLA-matched peptides[55]. Fresh PBMCs were tested for T-cell responses using *ex vivo* Interferon-γ ELISpot assays. 96-well nitrocellulose plates (Millipore) were coated with 0.05 μg ml^{-1} recombinant anti-IFN-γ (Mabtech) in PBS overnight at 4 °C. Plates were then washed seven times with PBS and blocked with R10 for 2 h at 37 °C. PBMCs (2×10^5) were added to each well and then stimulated with peptide. The final concentration for peptide stimulation was 10 μg ml^{-1} and each peptide was tested in duplicate. Medium alone was used as a negative control and 1 μg ml^{-1} phytohemagglutinin was used as a positive control for all assays. The assay plates were incubated for 18 h at 37 °C and, after extensive washing with PBS, a biotinylated secondary mouse anti-human IFN-γ monoclonal antibody (0.05 μg ml^{-1}; Mabtech) was added. The plates were developed using an alkaline phosphatase-conjugating substrate AP colour reagent A + B (BioRad). After 15 min, the colorimetric reaction was stopped by washing with tap water. Plates were air dried and spots were counted using an automated ELISpot reader (AID ELISpot Reader System). IFN-γ-producing T cells were expressed as spot-forming units per 1×10^6 cells. The number of specific IFN-γ-secreting cells was calculated by subtracting the unstimulated control value from the stimulated sample.

Sequence evolution and bioinformatics software. For sequence evaluation in evolutionary studies, PCR amplification of HIV *env*, followed by cloning and sequencing, was performed as previously described[56]. Analyses of evolution and site-specific selection were performed using BEAST[27] and CODEML[57]. CODEML was used to identify sites that have been subjected to positive selection using site-specific codon models. These models allow dN/dS to vary among sites, with values significantly above 1 indicating sites that had been under positive selection. We compared the fit of models M7 (which does not allow any sites to have a d*N*/d*S* of above 1) with M8 (which fits a class of sites with a d*N*/d*S* of above 1), using a likelihood ratio rest. The empirical Bayesian approach implemented by CODEML was used to identify codons under positive selection, using a cut-off of >90%. BEAST was used to model the evolution of the viral sequences through time, using the log-normal relaxed clock distribution to accommodate rate variation among branches. The multiple alignments contained 969 nucleotides. BEAST was run for 60 million steps, with the first 10% discarded as burn-in, and convergence was checked using Tracer. All analyses were repeated to ensure convergence. A preliminary BEAST analysis was performed that included the proviral sequence data, as these samples spanned a longer period of time than just the sequences obtained from plasma samples. The rate of evolution and effective population size were estimated from these time-structured sequences, and used in an analysis including only sequences obtained from plasma samples.

References

1. Goulder, P. J. & Watkins, D. I. Impact of MHC class I diversity on immune control of immunodeficiency virus replication. *Nat. Rev. Immunol.* **8,** 619–30 (2008).
2. Schmitz, J. E. *et al.* Control of viremia in simian immunodeficiency virus infection by CD8+ lymphocytes. *Science* **283,** 857–860 (1999).
3. Hersperger, A. R. *et al.* Perforin expression directly *ex vivo* by HIV-specific CD8 T-cells is a correlate of HIV elite control. *PLoS Pathog.* **6,** e1000917 (2010).
4. McMichael, A. & Hanke, T. The quest for an AIDS vaccine: is the CD8+ T-cell approach feasible? *Nat. Rev. Immunol.* **2,** 283–291 (2002).
5. Buchbinder, S. P. *et al.* Efficacy assessment of a cell-mediated immunity HIV-1 vaccine (the Step Study): a double-blind, randomised, placebo-controlled, test-of-concept trial. *Lancet* **372,** 1881–1893 (2008).
6. Rerks-Ngarm, S. *et al.* Vaccination with ALVAC and AIDSVAX to prevent HIV-1 infection in Thailand. *N. Engl. J. Med.* **361,** 2209–2220 (2009).
7. Sattentau, Q. Correlates of antibody-mediated protection against HIV infection. *Curr. Opin. Immunol.* **3,** 368–374 (2008).
8. Scheid, J. F. *et al.* Broad diversity of neutralizing antibodies isolated from memory B cells in HIV-infected individuals. *Nature* **458,** 636–640 (2009).
9. Moir, S. & Fauci, A. S. B cells in HIV infection and disease. *Nat. Rev. Immunol.* **9,** 235–245 (2009).
10. Pantophlet, R. & Burton, D. R. GP120: target for neutralizing HIV-1 antibodies. *Annu. Rev. Immunol.* **24,** 739–769 (2006).
11. Phillips, R. E. *et al.* Human immunodeficiency virus genetic variation that can escape cytotoxic T cell recognition. *Nature* **354,** 453–459 (1991).
12. Wei, X. *et al.* Antibody neutralization and escape by HIV-1. *Nature* **422,** 307–312 (2003).
13. Frost, S. D. *et al.* Neutralizing antibody responses drive the evolution of human immunodeficiency virus type 1 envelope during recent HIV infection. *Proc. Natl Acad. Sci. USA* **102,** 18514–18519 (2005).
14. Richman, D. D., Wrin, T., Little, S. J. & Petropoulos, C. J. Rapid evolution of the neutralizing antibody response to HIV type 1 infection. *Proc. Natl Acad. Sci. USA* **100,** 4144–4149 (2003).
15. Mahalanabis, M. *et al.* Continuous viral escape and selection by autologous neutralizing antibodies in drug-naive human immunodeficiency virus controllers. *J. Virol.* **83,** 662–672 (2009).
16. Burton, D. R. *et al.* Efficient neutralization of primary isolates of HIV-1 by a recombinant human monoclonal antibody. *Science* **266,** 1024–1027 (1994).

© 2010 Macmillan Publishers Limited. All rights reserved.

17. Buchacher, A. *et al.* Generation of human monoclonal antibodies against HIV-1 proteins; electrofusion and Epstein–Barr virus transformation for peripheral blood lymphocyte immortalization. *AIDS Res. Hum. Retroviruses* **10,** 359–369 (1994).
18. Walker, L. M. *et al.* Broad and potent neutralizing antibodies from an African donor reveal a new HIV-1 vaccine target. *Science* **326,** 285–289 (2009).
19. Stiegler, G. *et al.* A potent cross-clade neutralizing human monoclonal antibody against a novel epitope on gp41 of human immunodeficiency virus type 1. *AIDS Res. Hum. Retroviruses* **17,** 1757–1765 (2001).
20. Zhou, T. *et al.* Structural definition of a conserved neutralization epitope on HIV-1 gp120. *Nature* **445,** 732–737 (2007).
21. Braibant, M. *et al.* Antibodies to conserved epitopes of the HIV-1 envelope in sera from long-term non-progressors: prevalence and association with neutralizing activity. *AIDS* **20,** 1923–1930 (2006).
22. Simek, M. D. *et al.* Human immunodeficiency virus type 1 elite neutralizers: individuals with broad and potent neutralizing activity identified by using a high-throughput neutralization assay together with an analytical selection algorithm. *J. Virol.* **83,** 7337–7348 (2009).
23. Virgin, H. W. & Walker, B. D. Immunology and the elusive AIDS vaccine. *Nature* **464,** 224–231.
24. Mease, P. J. B cell-targeted therapy in autoimmune disease: rationale, mechanisms, and clinical application. *J. Rheumatol.* **35,** 1245 (2008).
25. Lim, F. & Abdalla, S. H. Interactions between HIV infection and lymphoplasmacytoid lymphoma. *Leuk. Lymphoma* **47,** 163–166 (2006).
26. Fidler, S. *et al.* Virological and immunological effects of short-course antiretroviral therapy in primary HIV infection. *AIDS* **16,** 2049–2054 (2002).
27. Drummond, A. J. & Rambaut, A. BEAST: Bayesian evolutionary analysis by sampling trees. *BMC Evol. Biol.* **7,** 214 (2007).
28. Kwong, P. D. *et al.* Structure of an HIV gp120 envelope glycoprotein in complex with the CD4 receptor and a neutralizing human antibody. *Nature* **393,** 648–659 (1998).
29. Wu, X. *et al.* Mechanism of human immunodeficiency virus type 1 resistance to monoclonal antibody B12 that effectively targets the site of CD4 attachment. *J. Virol.* **83,** 10892–10907 (2009).
30. Zhang, M. Y. *et al.* Identification and characterization of a new cross-reactive human immunodeficiency virus type 1-neutralizing human monoclonal antibody. *J. Virol.* **78,** 9233–9242 (2004).
31. Duenas-Decamp, M. J., Peters, P. J., Burton, D. & Clapham, P. R. Determinants flanking the CD4 binding loop modulate macrophage tropism of human immunodeficiency virus type 1 R5 envelopes. *J. Virol.* **83,** 2575–2583 (2009).
32. Scanlan, C. N. *et al.* The broadly neutralizing anti-human immunodeficiency virus type 1 antibody 2G12 recognizes a cluster of alpha1→2 mannose residues on the outer face of gp120. *J. Virol.* **76,** 7306–7321 (2002).
33. Liossis, S. N. & Sfikakis, P. P. Rituximab-induced B cell depletion in autoimmune diseases: potential effects on T cells. *Clin. Immunol.* **127,** 280–285 (2008).
34. Garcia-Rodriguez, M. J., Canales, M. A., Hernandez-Maraver, D. & Hernandez-Navarro, F. Late reactivation of resolved hepatitis B virus infection: an increasing complication post rituximab-based regimens treatment? *Am. J. Hematol.* **83,** 673–675 (2008).
35. Schmitz, J. E. *et al.* Effect of humoral immune responses on controlling viremia during primary infection of rhesus monkeys with simian immunodeficiency virus. *J. Virol.* **77,** 2165–2173 (2003).
36. Miller, C. J. *et al.* Antiviral antibodies are necessary for control of simian immunodeficiency virus replication. *J. Virol.* **81,** 5024–5035 (2007).
37. Gaufin, T. *et al.* Effect of B-cell depletion on viral replication and clinical outcome of simian immunodeficiency virus infection in a natural host. *J. Virol.* **83,** 10347–10357 (2009).
38. Aksoy, S. *et al.* Rituximab-related viral infections in lymphoma patients. *Leuk. Lymphoma* **48,** 1307–1312 (2007).
39. Maini, M. K. *et al.* Direct *ex vivo* analysis of hepatitis B virus-specific CD8(+) T cells associated with the control of infection. *Gastroenterology* **117,** 1386–1396 (1999).
40. Sinicco, A. *et al.* Coinfection and superinfection of hepatitis B virus in patients infected with human immunodeficiency virus: no evidence of faster progression to AIDS. *Scand. J. Infect. Dis.* **29,** 111–115 (1997).
41. Rockstroh, J. K. Influence of viral hepatitis on HIV infection. *J. Hepatol.* **44,** S25–27 (2006).
42. Burton, D. R., Stanfield, R. L. & Wilson, I. A. Antibody versus HIV in a clash of evolutionary titans. *Proc. Natl Acad. Sci. USA* **102,** 14943–14948 (2005).
43. Bailey, J. R. *et al.* Neutralizing antibodies do not mediate suppression of human immunodeficiency virus type 1 in elite suppressors or selection of plasma virus variants in patients on highly active antiretroviral therapy. *J. Virol.* **80,** 4758–4770 (2006).
44. Harrer, T. *et al.* Strong cytotoxic T cell and weak neutralizing antibody responses in a subset of persons with stable nonprogressing HIV type 1 infection. *AIDS Res. Hum. Retroviruses* **12,** 585–592 (1996).
45. Hessell, A. J. *et al.* Fc receptor but not complement binding is important in antibody protection against HIV. *Nature* **449,** 101–104 (2007).
46. Hessell, A. J. *et al.* Effective, low-titer antibody protection against low-dose repeated mucosal SHIV challenge in macaques. *Nat. Med.* **15,** 951–954 (2009).
47. Xiao, P. *et al.* Multiple vaccine-elicited nonneutralizing antienvelope antibody activities contribute to protective efficacy by reducing both acute and chronic viremia following simian/human immunodeficiency virus SHIV89.6P challenge in rhesus macaques. *J. Virol.* **84,** 7161–7173.
48. Mascola, J. R. & Montefiori, D. C. The role of antibodies in HIV vaccines. *Annu. Rev. Immunol.* **28,** 413–444.
49. Lewis, G. K. Challenges of antibody-mediated protection against HIV-1. *Expert Rev. Vaccines* **9,** 683–687.
50. Ahuja, A., Anderson, S. M., Khalil, A. & Shlomchik, M. J. Maintenance of the plasma cell pool is independent of memory B cells. *Proc. Natl Acad. Sci. USA* **105,** 4802–4807 (2008).
51. Derdeyn, C. A. *et al.* Envelope-constrained neutralization-sensitive HIV-1 after heterosexual transmission. *Science* **303,** 2019–2022 (2004).
52. Li, M. *et al.* Human immunodeficiency virus type 1 env clones from acute and early subtype B infections for standardized assessments of vaccine-elicited neutralizing antibodies. *J. Virol.* **79,** 10108–10125 (2005).
53. Dorfman, T., Popova, E., Pizzato, M. & Gottlinger, H. G. Nef enhances human immunodeficiency virus type 1 infectivity in the absence of matrix. *J. Virol.* **76,** 6857–6862 (2002).
54. Martin, L. *et al.* Rational design of a CD4 mimic that inhibits HIV-1 entry and exposes cryptic neutralization epitopes. *Nat. Biotechnol.* **21,** 71–76 (2003).
55. Frater, A. J. *et al.* Effective T-cell responses select human immunodeficiency virus mutants and slow disease progression. *J. Virol.* **81,** 6742–6751 (2007).
56. Shankarappa, R. *et al.* Consistent viral evolutionary changes associated with the progression of human immunodeficiency virus type 1 infection. *J. Virol.* **73,** 10489–10502 (1999).
57. Yang, Z. & Nielsen, R. Synonymous and nonsynonymous rate variation in nuclear genes of mammals. *J. Mol. Evol.* **46,** 409–418 (1998).
58. Drummond, A. J., Ho, S. Y., Phillips, M. J. & Rambaut, A. Relaxed phylogenetics and dating with confidence. *PLoS Biol.* **4,** e88 (2006).
59. Drummond, A. J., Rambaut, A., Shapiro, B. & Pybus, O. G. Bayesian coalescent inference of past population dynamics from molecular sequences. *Mol. Biol. Evol.* **22,** 1185–1192 (2005).

Acknowledgments

We thank the Wellcome Trust, NIHR Biomedical Research Programme (Oxford and Imperial College NHS Trust) and the James Martin School for 21st Century for supporting this work. We thank Quentin Sattentau for his advice and support. Antibodies b12 and 4.8d were gifts from Dennis Burton (Scripps research institute) and James Robinson (Tulane University), respectively.

Author contributions

K.H.G.H., A.J.F. and P.J.G. performed the sequence and T-cell analysis. D.B., E.C.T. and M.O.M. performed and interpreted the NAb analysis. A.K. and O.P. performed the bioinformatics analyses. S.J.F., D.M. and J.N.W. performed the clinical studies. G.S.C. and P.K. coordinated the studies in Oxford and London and all authors contributed to the article preparation.

Additional information

Accession numbers: HIV-1 envelope sequences have been deposited in GenBank under accession numbers HQ241073–HQ241186.

Supplementary Information accompanies this paper on http://www.nature.com/naturecommunications

Competing financial interests: The authors declare no competing financial interests.

Reprints and permission information is available online at http://npg.nature.com/reprintsandpermissions/

How to cite this article: Huang, K.-H.G. *et al.* B-cell depletion reveals a role for antibodies in the control of chronic HIV-1 infection. *Nat. Commun.* 1:102 doi: 10.1038/ncomms1100 (2010).

License: This work is licensed under a Creative Commons Attribution-NonCommercial-Share Alike 3.0 Unported License. To view a copy of this license, visit http://creativecommons.org/licenses/by-nc-sa/3.0/

© 2010 Macmillan Publishers Limited. All rights reserved.